LIBRARY
TECHNICAL REPORT SECTION
NAVAL POSTGRADUATE SCHOOL
MONTEREY, CALIFORNIA 93940

AD13269

AGARD-LS-73

AGARD-LS-73

AGARD

ADVISORY GROUP FOR AEROSPACE RESEARCH & DEVELOPMENT

7 RUE ANCELLE 92200 NEUILLY SUR SEINE FRANCE

LECTURE SERIES No. 73

on

Computational Methods for Inviscid and Viscous Two-and-Three-Dimensional Flow Fields

NORTH ATLANTIC TREATY ORGANIZATION

DISTRIBUTION AND AVAILABILITY
ON BACK COVER

NORTH ATLANTIC TREATY ORGANISATION

ADVISORY GROUP FOR AEROSPACE RESEARCH AND DEVELOPMENT

(ORGANISATION DU TRAITE DE L'ATLANTIQUE NORD)

AGARD Lecture Series No.73

COMPUTATIONAL METHODS FOR INVISCID AND VISCOUS TWO-AND-THREE-DIMENSIONAL FLOW FIELDS

The material in this book has been assembled to support a Lecture Series under the joint sponsorship of the Fluid Dynamics Panel and the Consultant and Exchange Programme of AGARD, and the von Kármán Institute for Fluid Dynamics (VKI). The Series was presented on 17–22 February 1975 at the von Kármán Institute, Brussels, Belgium.

THE MISSION OF AGARD

The mission of AGARD is to bring together the leading personalities of the NATO nations in the fields of science and technology relating to aerospace for the following purposes:

- Exchanging of scientific and technical information;
- Continuously stimulating advances in the aerospace sciences relevant to strengthening the common defence posture;
- Improving the co-operation among member nations in aerospace research and development;
- Providing scientific and technical advice and assistance to the North Atlantic Military Committee in the field of aerospace research and development;
- Rendering scientific and technical assistance, as requested, to other NATO bodies and to member nations in connection with research and development problems in the aerospace field;
- Providing assistance to member nations for the purpose of increasing their scientific and technical potential;
- Recommending effective ways for the member nations to use their research and development capabilities for the common benefit of the NATO community.

The highest authority within AGARD is the National Delegates Board consisting of officially appointed senior representatives from each member nation. The mission of AGARD is carried out through the Panels which are composed of experts appointed by the National Delegates, the Consultant and Exchange Program and the Aerospace Applications Studies Program. The results of AGARD work are reported to the member nations and the NATO Authorities through the AGARD series of publications of which this is one.

Participation in AGARD activities is by invitation only and is normally limited to citizens of the NATO nations.

The content of this publication has been reproduced
directly from material supplied by AGARD or the authors.

Published February 1975

Copyright © AGARD 1975

532.516 : 532.526.4

Printed by Technical Editing and Reproduction Ltd
Harford House, 7–9 Charlotte St, London, W1P 1HD

PREFACE

This Lecture Series, jointly sponsored by the Fluid Dynamics Panel, the Consultant Exchange Programme of AGARD and the von Kármán Institute is a follow-up of two other Lecture Series on the same general subject. The aim of this Series is to make fluid dynamicists interested in numerical integration techniques familiar with the latest developments in the field. Although emphasis is placed on application some lectures are on fundamental mathematical aspects.

Experience of the last four years has shown that the joint AGARD-VKI Lecture Series as well as the VKI Courses on Numerical Methods in Fluid Dynamics, held in a bi-annual cycle, have established themselves as an internationally recognised forum for stimulating discussion and sound learning of this rapidly growing field. Each year, more than a hundred participants from various countries in Europe, USA and Canada have attended these Courses. The success of these Lectures is also reflected by the numerous requests received by the National Distribution Centres of AGARD for the previous publications: AGARD Lecture Series 48 (Numerical Methods in Fluid Dynamics) and Lecture Series 64 (Advances in Numerical Fluid Dynamics).

The topics covered in the present Lecture Series comprise numerical stability of hyperbolic partial differential equations, foundation and application of the finite-element method in fluid dynamics; computational methods for laminar and turbulent boundary layers in two-and-three-dimensional flows, numerical solution of the Navier-Stokes equation and separated transonic and supersonic flows at high Reynolds numbers. Finally, it is pointed out that the first results obtained with the new Illiac IV computer for viscous flow simulation are being discussed in this Lecture Series.

Egon KRAUSE
Lecture Series Director

LIST OF SPEAKERS

Lecture Series Director:

Prof. E.Krause
Aerodynamisches Institut
der Rheinisch-Westfalischen
Technischen Hochschule Aachen
51 Aachen
Templergraben 55
Germany

Dr Barrett S.Baldwin
NASA
Ames Research Center
Moffett Field
California 94035
USA

Dr Frederick G.Blottner
Theoretical Fluid Dynamics Division
Sandia Laboratories
Albuquerque
New Mexico 87115
USA

Prof. Heinz-Otto Kreiss
Department of Computer Sciences
University of Uppsala
Sturegatan 4
75223 Uppsala
Sweden

Prof. K.W.Morton
The University of Reading
Reading
Berkshire
UK

Prof. R.Peyret
Université de Paris VI
Mécanique Théorique
Tour 66
4 Place Jussieu
Paris 75230 Cedex 05
France

Dr C.Bellevaux
25 Allée des Côteaux
78470 St Rémy-les-Chevreuses
France

CONTENTS

FLOW ANALYSIS THROUGH NUMERICAL TECHNIQUES

Egon Krause
Aerodynamisches Institut
Rheinisch-Westfälische Technische Hochschule Aachen
Aachen, Germany

SUMMARY

Flow analysis by using numerical techniques is demonstrated in this article. Results obtained from integrations of the governing equations are compared with experimental data of the recent literature. The following problems will be discussed: The inviscid flow about a sphere at supersonic Mach-numbers ranging from $M_\infty = 1.08$ to $M_\infty = 5.0$, calculated with Rusanov's algorithm; incompressible and compressible laminar and turbulent boundary layers on infinite swept wings, calculated with second- and fourth-order accuracy for three different scalar closure assumptions. Hypersonic laminar and turbulent slot injection of frozen flow (He and H_2) and flow in approximated chemical equilibrium (H_2). Finally applications of finite-difference solutions will be discussed for fully viscous flows in bio-fluidmechanical problems.

1. INTRODUCTION

Rapid development of new numerical integration procedures has provided the fluid mechanician with new tools for flow analysis. During the past decade numerical techniques have been applied in all branches of the field with increasing number. A survey recently made in Ref. [1] shows that in the leading scientific engineering journals the number of articles using predominantly numerical methods has increased from one percent in 1963 to 15-20 percent in 1973 of all articles published. It is also interesting that the new methods were immediately used for design purposes. For example, in Ref. [2] a finite-difference solution of the small perturbation form of the potential equation was employed to determine the inviscid surface pressure distribution of the three-dimensional flow about the whole airfoil of the C-141 airplane. This is a remarkable advancement and it is safe to say that in the future design of aircraft and spacecraft will rely more heavily on prediction methods than was possible in the past. Pressure distributions will to a greater extent be determined from numerical integration of the Euler equations as skin-friction coefficients will be obtained from finite-difference solutions of Prandtl's boundary-layer equations for three-dimensional flows. This is of importance since control of the boundary layer on wings and other wetted surfaces can result in substantial drag reduction. Some of the goals which can be achieved in the near future were recently described in Ref. [3]. If it is possible to control the boundary layer to such a degree that a large portion of the flow can be maintained laminar, ten to twenty percent lower operating costs in comparison to the "turbulent" design would result. However, before such predictions become possible, more powerful methods of analysis than those presently in use will have to be developed. For this reason, it will be interesting to see how the fourth computer generation, to be in operation soon, will affect the advancement of numerical techniques. Although the new parallel machines will not cure our stability or convergence problems and although they will force us to develop new methods of solutions and programming techniques, they will cut down computation times by a factor of the order of one hundred, perhaps more. This decrease in computation time will bring a number of problems which could not be tackled until now into our reach.

In this article a few results of recent flow calculations will be described in comparison to experimental data. The purpose of this comparison is twofold: First, to demonstrate the accuracy of presently available finite-difference solutions and secondly, to show the degree of complexity of the flow problems which can be solved. We begin with finite-difference solutions of the Euler equations for supersonic flow about a sphere and continue with a description of complex boundary-layer problems and finally fully viscous incompressible internal flows.

2. THREE-DIMENSIONAL SUPERSONIC INVISCID FLOWS ABOUT BLUNT BODIES

There are several algorithms available through which such flows can be determined. Of the artificial viscosity methods Rusanov's algorithm has often been claimed to be superior in accuracy in comparison to others. The particularities of the method are mainly based on the introduction of artificial flux terms for friction, conduction and diffusion with variable artificial transport coefficients. In addition of more practical importance is the use of different step sizes in the finite-difference formulation. However, the accuracy of Rusanov's method could so far only be achieved in long computation times. Relatively small time steps had to be employed in the integration as the limiting time step derived by Lyubimov and Rusanov from a stability analysis for frozen coefficients appeared to be very restrictiv. In addition a large number of iterations had to be carried out during the transient period. In order to overcome this difficulty, Förster, Roesner and Weiland attempted trial calculations with the aim to detect as to whether or not the stability condition as given by Lyubimov and Rusanov could not be loosened for the first phase of the integration. This attempt proved to be successful as several comparison calculations have shown. In addition the method seems to be well suited for supersonic flow calculations for Mach numbers only

slightly larger than unity. Before we discuss results for such flows we will demonstrate the accuracy of the method for hypersonic Mach numbers: The surface pressure, the density distribution along the z-axis between stagnation point and shock, the shock shape and the sonic line as determined experimentally for a sphere by Sedney and Kahl [4] agree well with the predictions described in Ref. [5][+]. This is shown in Figs. 1 - 3[+], where for a hypersonic Mach number of $M_\infty = 5$, pressure coeffient, non-dimensionalized density shock shape and sonic line are plotted versus normalized coordinates indicated in the Figs. Because of the very satisfactory agreement between measured and calculated pressures, shock shape and sonic line in Figs. 1 and 2, it can be concluded that there are some anomalies in the measured density distribution, in particular the three points in the middle of Fig. 2.

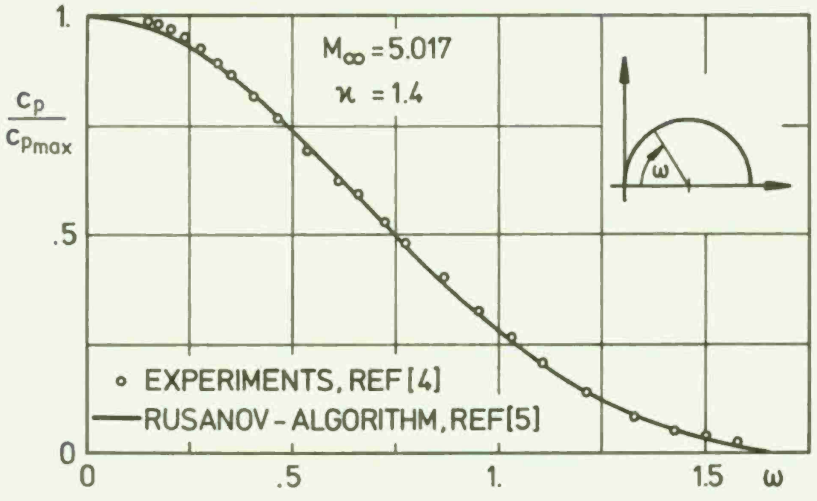

Fig. 1 Surface pressure distribution on a sphere

With decreasing free-stream Mach number the rate of convergence increases markedly. Yet the accuracy of Rusanov's method remains the same as for high supersonic or hypersonic flows. Gooderum's and Wood's density measurements on the surface and along the z-axis of a sphere [6] confirm the accuracy of the results obtained in Ref. [5]. A comparison of calculated and measured data is given in Figs. 4 and 5[+]. The shock shape is equally well predicted (Fig. 6) for $M_\infty = 1.3$. Some further comparisons are shown for even a lower Mach number in Fig. 7. In Ref. [7] Stilp determined experimentally the slope of the front shock of a sphere for free-stream Mach numbers as low as $M_\infty = 1.079$ and $M_\infty = 1.109$. The comparison in Fig. 7[+] shows that Rusanov's method predicts the measured data with sufficient accuracy although the free-stream Mach number of the calculation was not exactly the same as that of the experiments.

In the integration of the transonic flow fields the number of net points varied between 17 and 13 in the direction normal to the surface and between 34 and 27 in the tangential direction. Details of the method of integration are described in [8]. Reduction of computation time was shown to be possible. First results are reported in [9]. By means of a detailed stability analysis in particular of the implicit part of the solution, a substantial increase in the rate of convergence was obtained. These investigations will be published in the near future.

Rusanov's method has in the meantime been applied to flow fields about sphere-cone combinations at angle of attack. It is reported in [5] that the convergence rate is fast as long as the supersonic part of the flow field is kept small.

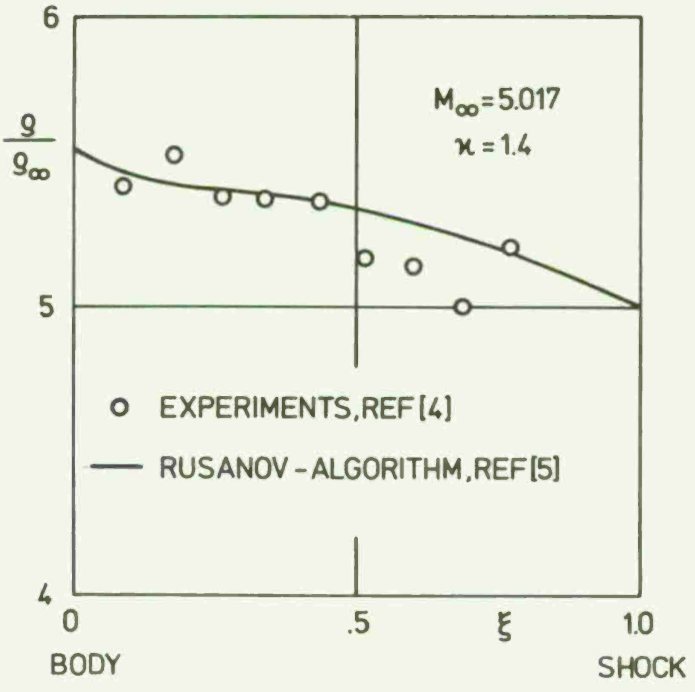

Fig. 2 Density distribution between shock and body of a sphere[+]

3. THREE-DIMENSIONAL BOUNDARY LAYERS

Considerable progress has been made in the development of integration methods for three-dimensional boundary layers. A description of a method adapted to infinite swept wings is given in [10]; a more general method is described in [11] and [12]. Both second-and fourth-order accuracy can be used in implicit, locally linearized difference equations. Eddy viscosity models can easily be incorporated in the integration procedures [10]. Care must, however, be exercised in the calculation of turbulent flows in general and of large cross-flows. Because of large velocity gradients near the wall and large variations of the cross correlations in the outer portion of the boundary layer large numerical errors may occur. These may then falsify the pre-

[+] The data shown in Figs. 2, 3, 5, and 7 were provided by C. Weiland who carried out the details of the integration described in Ref. [5].

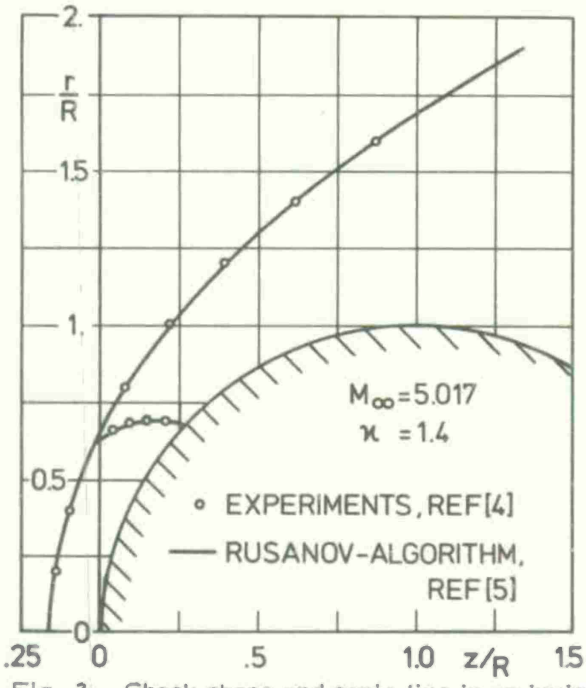

Fig. 3 Shock shape and sonic line in an inviscid flow field about a sphere+)

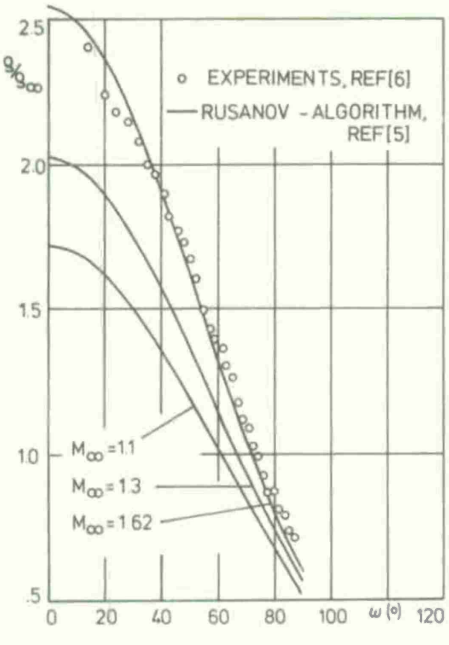

Fig. 4 Surface density distribution on a sphere

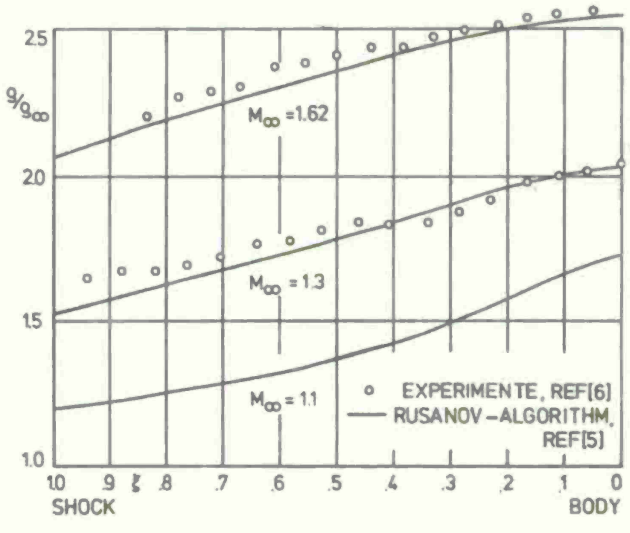

Fig. 5 Density distribution along the z-axis of supersonic flow about a sphere+)

diction considerably and in comparison to experiment wrong conclusions may be drawn for the validity of the closing assumptions. For large crossflows the scalar assumption often employed in eddy viscosity models brakes down.

For laminar flows there are, in general no major difficulties as long as all derivatives are of order unity. Several boundary-layer flows over swept wings with infinite aspect ratio have been analysed with the method of solution described in [10]. The following results were obtained for free-stream Mach numbers $M_\infty = 0.649$, 0.749 and 1.298 and Reynolds numbers of approximately $3 \cdot 10^6$. The sweep angle φ of the wing was assumed to be zero for the first Mach number, 30° for the second and 60° for the third. The pressure distribution was determined experimentally for the upper surface of the wing in [13]. In all three cases considered supersonic flow exists and extends 20 percent of the chord, where a shock can be identified. The pressure coefficient is depicted in the upper part of Fig. 8. The boundary-layer characteristics were determined with an adapted version of the solution for fully three-dimensional flows of [11]. The modification of the solution was carried out by E.H. Hirschel, who also provided the data shown in Fig. 8. The skin friction attains a maximum a short distance downstream from the stagnation line. For $\varphi = 0°$ the maximum is about two and one half times higher than for $\varphi = 60°$. Separation is observed at about 20 percent of the chord. Considerable flow deflection in the boundary layer takes place near the maximum of the shearing stress. For $\varphi = 60°$, the direction of the limiting stream-lines near the wall deviates by some 20° from that of the external flow.

An incompressible boundary layer on a swept wing of infinite aspect ratio was investigated experimentally by Altman and Hayter [14] and more recently by Adams [15], who developed a second-order finite-difference solution for infinite-swept wing conditions. The pressure distribution is that of the NACA 63_1-012 section airfoil at zero angle of attack. In the experiments transition was artificially enforced at 20 percent of the chord for a Reynolds number of $5.4 \cdot 10^6$, zero lift conditions and a sweep angle of $\varphi = 45°$. The skin friction coefficients as calculated with the solution of Ref. [10] are shown in Fig. 9. The integration was carried out by U. Müller of the Aerodynamische Institut with a second-order solution (abbreviated 2.0 in Fig. 9 and subsequent Figs.) together with the closure relations equations (2.18) and (2.19) of Ref. [10], which yield almost the same results except for a short distance downstream from the point where transition was enforced.

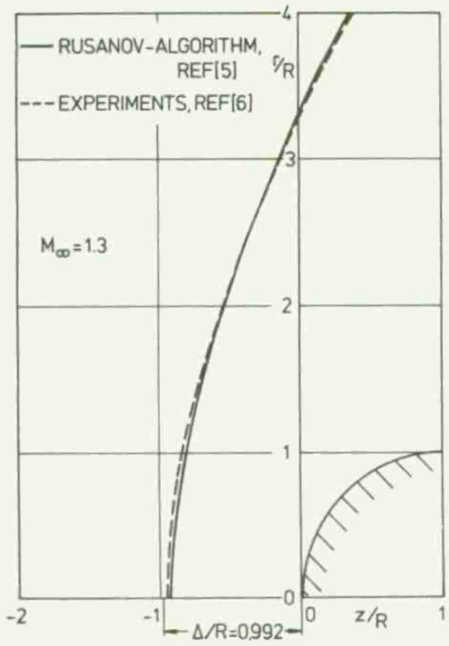

Fig. 6 Shock shape and sonic line in an inviscid flow field about a sphere

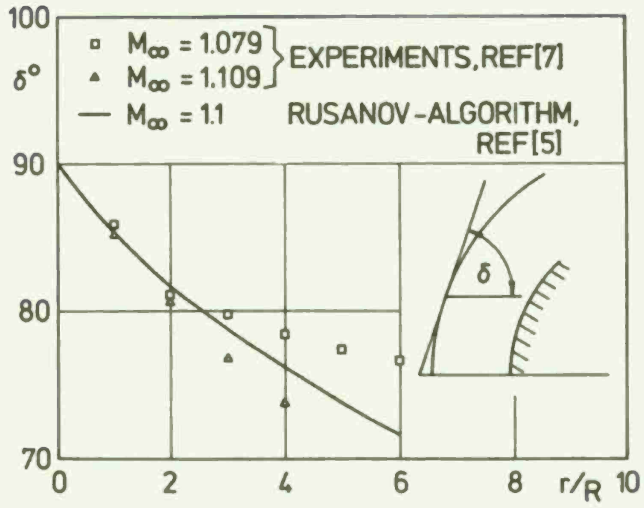

Fig. 7 Angle of the front shock about a sphere near sonic conditions[+)]

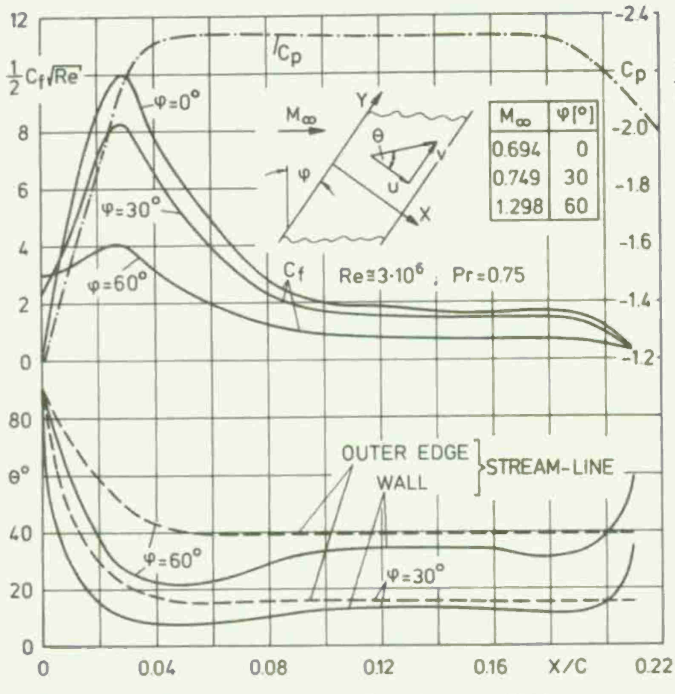

Fig. 8 Pressure-, skin-friction coefficient and flow turning angle in a laminar compressible boundary layer on the upper surface of a swept wing with infinite aspect ratio

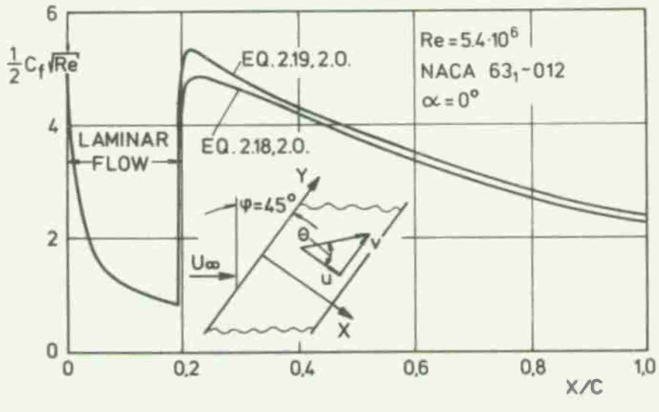

Fig. 9 Skin-friction coefficient calculated with the solution of Ref. [10] for the measurements of Ref. [14]

In Fig. 10 of Ref. [10], the displacement thickness δ^* and momentum thickness θ as calculated with the solution of Ref. [15] and of Ref. [10] are compared with the experimental data, which correspond to those shown in Fig. 9. Deviations from the measured data can be noted immediately downstream from the transition point, but otherwise the accuracy of all three predictions is acceptable. The displacement and the momentum thickness are evaluated for the x-component alone. The small deviations in the predictions are due to the differences in the closure assumptions and can also be noted in the velocity profiles (Fig. 11). At 50 percent chord the predictions obtained with the closure assumptions (2.18) and (2.19) of Ref. [10] show slightly fuller velocity profiles than those of Ref. [15]. Further downstream at x/c = 0.6 all three predictions give virtually the same values; moreover, the agreement with the measurements is indeed good but not surprising since the pressure gradient is very small. The exchange coefficients are then at least approximately the same and the scalar assumption is justified. On the other hand, the comparison in Fig. 11 does not fully confirm the validity of the three closure assumptions for three-dimensional boundary layers. Since the pressure gradient in the y-direction vanishes identically and is small in the x-direction the flow deviates only little from constant pressure conditions in the vicinity of 50 to 60 percent of the chord.

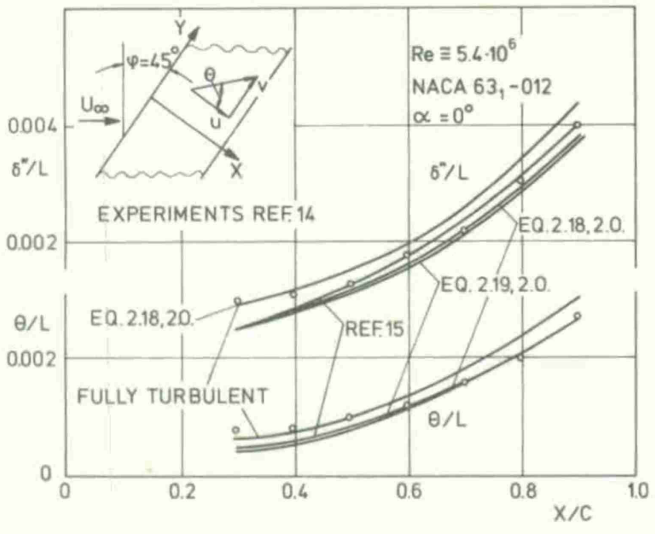

Fig. 10 Comparison of measured displacement and momentum thickness of Ref. [14] with predictions of Ref. [15] and of Ref. [10]

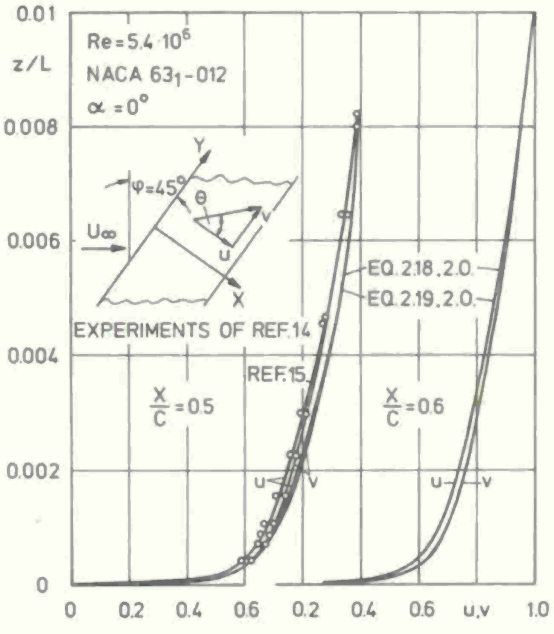

Fig. 11 Comparison of measured velocity profiles of Ref. [14] with predictions of Ref. [15] and of Ref. [10]

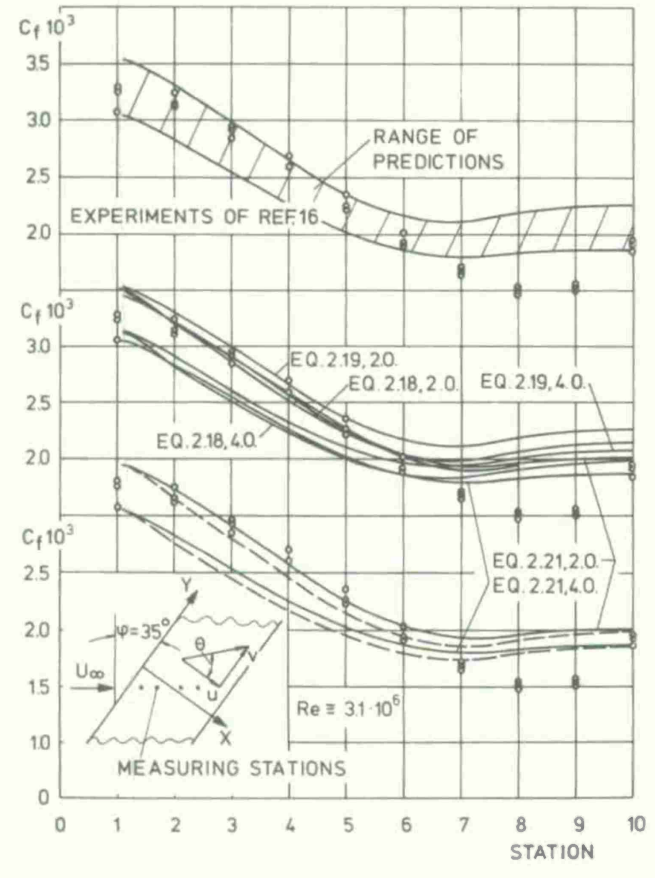

Fig. 12 Comparison of measured skin-friction coefficients with predictions of present second- and fourth-order solution. The curve which ends at point 8 is the prediction of Ref. [17]. The dashed lines give the skin-friction for δ^* based on the u-component of the velocity.

Large pressure gradients in the x-direction were enforced by van den Berg and Elsenaar in their experiment on an infinite swept wing [16]. The oncoming flow of the free-stream is incompressible with a Reynolds number of about $3.1 \cdot 10^6$. The sweep angle is 35° and the pressure gradient is positiv and large enough to lead to separation. W. Kordulla of the Aerodynamische Institut carried out calculations in which all three closure assumptions, equations (2.18), (2.19), and (2.21) of Ref. [10] were employed. Both, second- and fourth-order algorithms were used.

The range of predictions is shown for the shearing stress in the upper part of Fig. 12. Although there is agreement downstream from the leading edge of the wing, the predictions fail near separation. The details of the calculation are shown in the middle of Fig. 12. It is seen that the inclusion of the pressure gradient in the closure assumption (2.21) gives better agreement than equations (2.18) and (2.19) of Ref. [10] which are based on the wall shearing stress alone. It is of importance to point to purely numerical errors. Each calculation was carried out with second-order (2.0) and fourth-order (4.0) truncation errors and substantial differences can be noted. The curve which ends at measuring station 8 represents the prediction of Ref. [17]. These values were obtained after the law of the wall had been modified [17] and adjusted to three-dimensional flows.

In the lower part of Fig. 12 the predictions obtained with the closure assumption (2.21) are replotted for the second- and fourth-order solution. The solid line gives the shearing stress for the case when equation (2.21) is based on a displacement thickness evaluated for both velocity components. The dashed line gives the skin-friction coefficient for a displacement thickness based on the u-component of the velocity alone. Although there is agreement

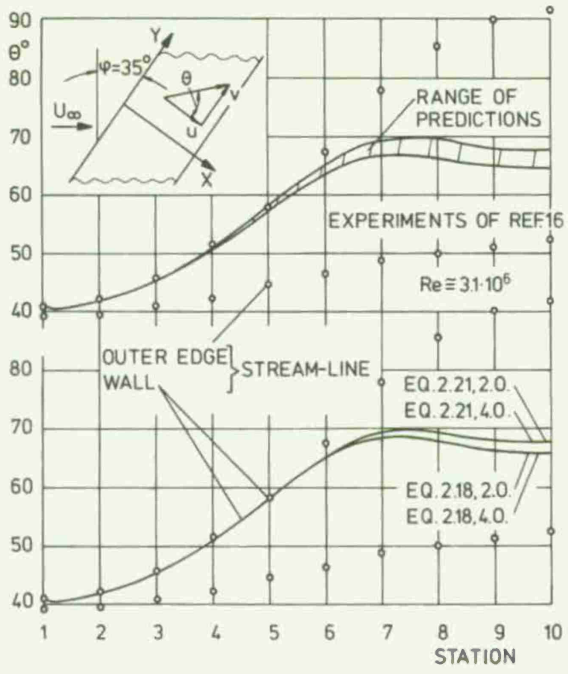

Fig. 13 Calculated and measured (Ref. [16]) flow deflection. Predictions with second- and fourth-order accuracy of Ref. [10].

to investigate the closure assumptions for three-dimensional flows anew and construct more adequate formulations for the outer part of the boundary layer.

It is seen in Fig. 14 that momentum transport is too large in the direction normal to the wall. This is particularly true for the u-component. It is known from experimental investigations that the local shearing stress is not colinear with the velocity vector; this indicates that the eddy viscosity depends on all three coordinates. Near separation, variation of the pressure in the direction normal to the wall influences the variation of the shearing-stress markedly, such that it cannot at the present time be decided, which of the two effects is the dominant one. Investigations are under way at the Aerodynamische Institut in order to determine extermentally shearing-stress distributions in three-dimensional boundary layers. Further investigations are necessary to explain the deviations between second- and fourth-order solutions.

with the experimental data for the second-order solution, there is no justification of adopting the displacement thickness of the u-component for three-dimensional flows.

The flow deflection as measured in the experiment of Ref. [16] and calculated in the solution of Ref. [10] is shown in Fig. 13. Again the assumption of colinearity between local shearing stress and the projection of the velocity vector is found to be invalid near separation.

A comparison of calculated and measured velocity profiles is given in Fig. 14. For the measuring station 4 all six predictions fall almost together and are in agreement with the experiment. It is seen that the difference between second- and fourth-order solution is more pronounced in the shearing stress than in the velocity profiles. Near separation the predicted exchange of momentum is seen to be too large for the x-direction. This is also indicated in Fig. 15 where for the two measuring stations the effective viscosities are plotted versus the coordinate normal to the wall. Large differences can be noted in the outer portion of the boundary layer. Yet, despite the large deviations of equation (2.21) from (2.18) and (2.19) of Ref. [10] the corresponding differences in the velocity profiles are small. For more accurate predictions it is therefore necessary

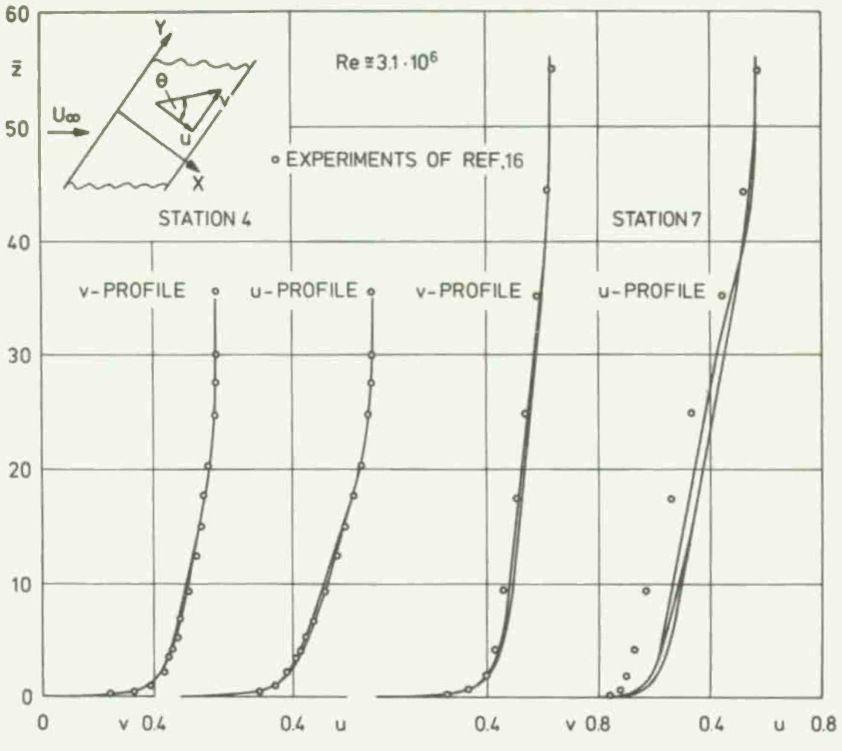

Fig. 14 Measured and calculated velocity profiles. Measurements are of Ref. [13].

4. TANGENTIAL SLOT INJECTION AT HYPERSONIC SPEEDS

Tangential slot injection is of importance for surface cooling and external combustion processes. It has been shown recently, that the cooling effectiveness is large enough for practical application. Theoretical and experimental investigation of injection of foreign gases as He or H_2 has shown that simplification of the description of the diffusion process is not possible [18]. This result was obtained by comparison of a finite-difference solution of Ref. [19] with concentration measurements. The following results of Ref. [19] demonstrate the application of the method for various flow conditions. Fig. 16 shows the calculated concentration decay for laminar and turbulent chmically frozen and approximated

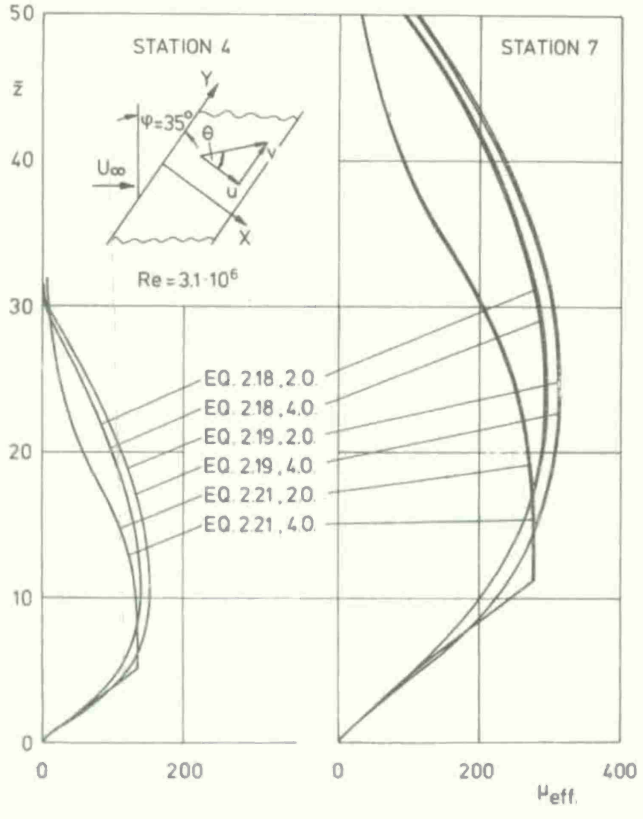

Fig. 15 Evaluation of closure assumptions for the velocity profiles shown in Fig. 14

was shown to vary between 0.4 and 0.8 for free-stream Mach-numbers of $M_\infty = 8$. Constant Prandtl-numbers are often justified in homogeneous flows. This is because the temperature dependence of the dynamic viscosity, the thermal conductivity and the specific heat at constant pressure are nearly compensated in the Prandtl-number. But the dependence of the latter on the concentration is not negligible, resulting in variations of more than 50 percent which in turn may be responsible in marked changes in the concentration profiles. It is also noteworthy that in the description of the transport coefficients from the Chapman-Enskog-theory the billard ball model is not sufficiently accurate to determine viscosity and thermal conductivity. The Lennard-Jones (6, 12)-potential or even more generalized (n, m)-potentials have to be incorporated in the integration procedure.

The second difficulty is introduced by the flame sheet approximation. As the integration of the governing equations for H_2-Air mixtures for the complete reaction mechanism requires large computation times the flame sheet approximation often finds application in fluid mechanical problems. In the present problem the flame sheet separates two adjacent regions in the flow, in which convection and diffusion effects alone chemical equilibrium conditions (flame sheet approximation). It is seen that the decay is rapid, although the turbulent decay is much steeper. Fig. 17 shows the calculated shearing stress distribution at the wall for the conditions of Fig. 16. A minimum can be noticed immediately downstream from the slot. While these calculations were carried out for zero-pressure-gradient-conditions, Fig. 18 shows the influence of positiv and negativ pressure gradients in laminar frozen flow. Separation is obtained in the vicinity of the slot, while in turbulent flows separation cannot be observed. There is a noticeable influence on the wall temperature and on the length of the flame due to non-vanishing pressure gradients. This can be seen in Figs. 19 and 20. In the former the wall temperature is plotted versus the downstream coordinate while the extension of the flame sheet is shown in Fig. 20. According to these results positiv pressure gradients yield shorter and accelerating flows longer flames in comparison to zero-pressure-gradient flows.

The calculations of the results reported here are complicated mainly by three factors. Firstly for laminar frozen flows all diffusion fluxes due to concentration gradients must be taken into account. Comparison calculation of Ref. [18] have shown that assumptions of constant Prandtl-, Lewis- or Schmidt number lead to large deviations in the concentration profiles. For example, the Prandtl-number of the gas mixture

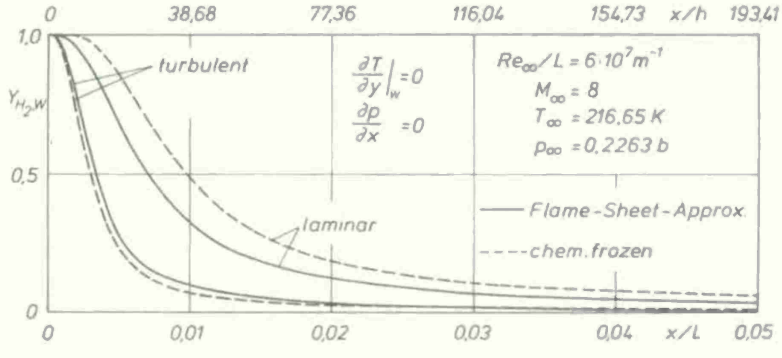

Fig. 16 Concentration decay at the wall for H_2-injection for laminar and turbulent flows

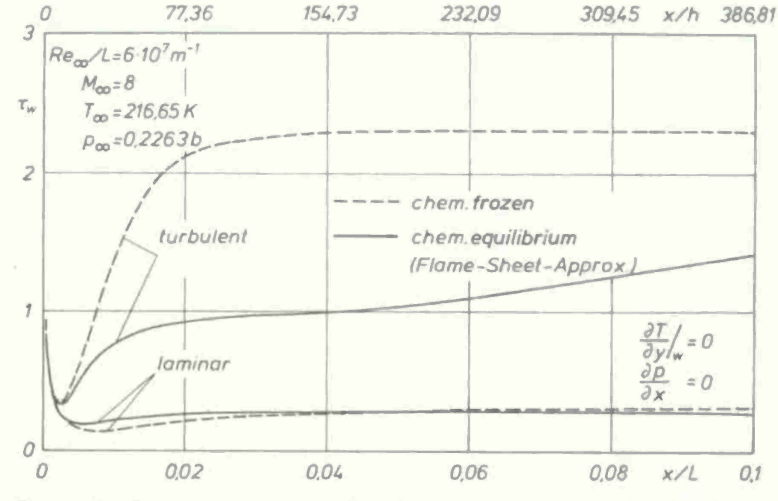

Fig. 17 Shearing-stress distribution at the wall for laminar and turbulent flows

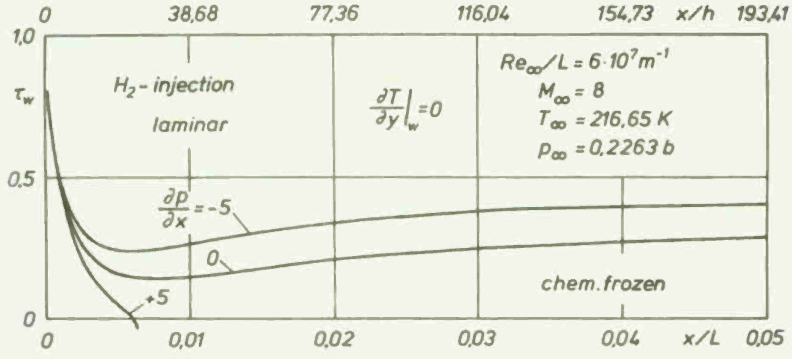

Fig. 18 Shearing-stress distribution for positiv and negativ pressure gradients in laminar flows

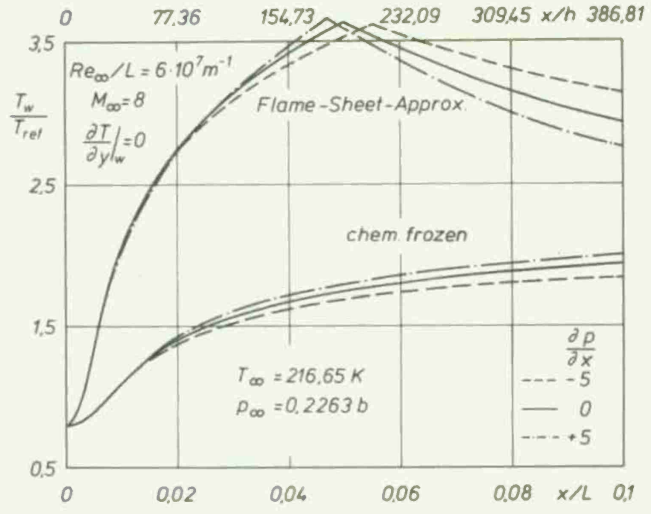

Fig. 19 Wall temperature distribution in turbulent flows for positiv and negativ pressure-distributions

are present. The only reaction product H_2O is generated along the common boundary and in the region close to the wall the molecular O_2-concentration vanishes and in the outer region the H_2-concentration. The flame sheet assumption necessitates the integration of a three-point initial-boundary value problem, in which the location of the internal boundary must be determined. The diffusion fluxes which are discontinous across the flame sheet yield the necessary compatibility condition to ensure continuous concentration profiles.

The third complication is encountered in turbulent flows. Even first-order closure requires very small step sizes, not only because of large velocity gradients near the

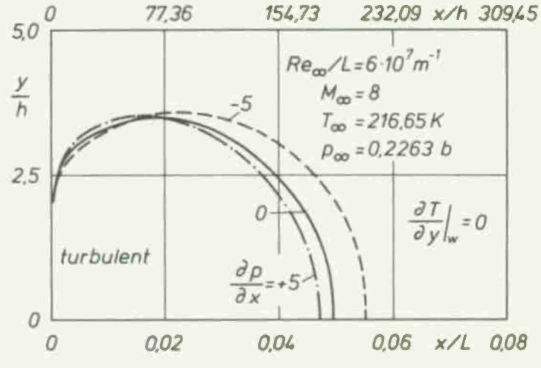

Fig. 20 Influence of pressure gradient on the extent of the flame sheet in turbulent flow

wall but also because of the temperature peak in the outer portion of the boundary layer. Telescoping of the grid in the direction normal to the wall does not serve a useful purpose as the maximum value of the static temperature does not occur at the same location where the cross-correlations attain their maximum. Further details of the integration procedure developed for this problem may be found in Ref. [19].

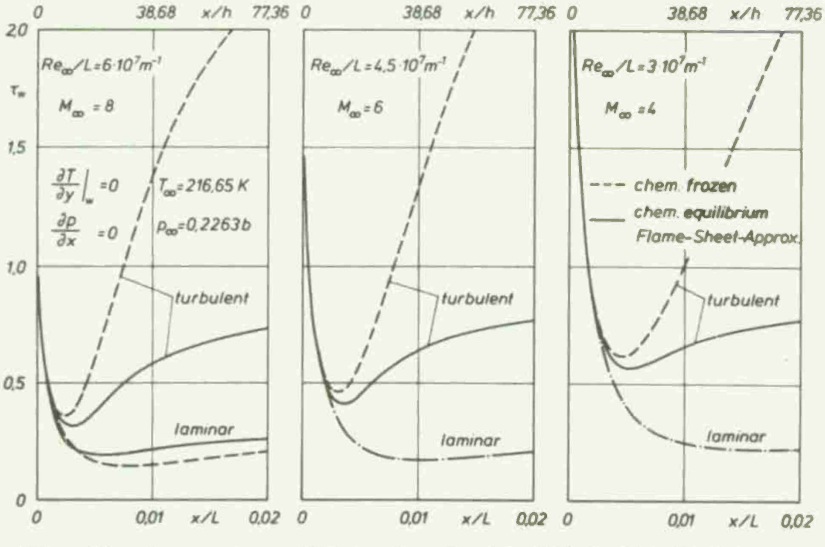

Fig. 21 Comparison of shearing-stress distribution in the vicinity of the slot for different free-stream Mach-numbers. For chemically frozen flows the maximum is reached further downstream.

A large influence on the flow characteristics is exerted by the free-stream Mach number. This is particularly true for the shearing stress and the lines of constant temperature. In Fig. 21 the shearing stress is shown for free-stream Mach numbers 8, 6, and 4. It is seen that the minimum downstream from the slot is shifted to larger x-values and increases with decreasing Mach numbers. For turbulent flows the isotherms of the flows with free-stream Mach numbers as stated above are given in Fig. 22. At $M_\infty = 4$ the flame sheets extends further out into the stream and causes higher temperatures in the outer portion of the boundary layer than at $M_\infty = 8$.

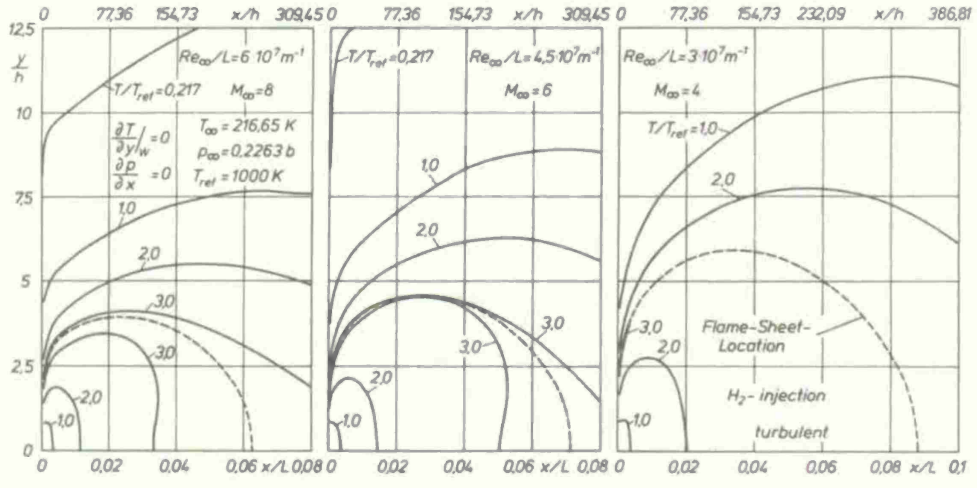

Fig. 22 Lines of constant temperature for chemical equilibrium. Other conditions are the same es in Fig. 21

5. REMARKS ON NUMERICAL SOLUTIONS FOR BIO-FLUIDMECHANICAL PROBLEMS

The implantation of artificial heart valves has almost become a routine operation. Yet heart valves still pose a number of flow problems which are not completely understood. This is not surprising since the flow is extremely complex as it is not only three-dimensional but also unsteady. In particular it is the slow separated flow downstream from the valve which tends to trap various particles of the blood, thereby enhancing the danger of making the recirculating flow thrombogenic. In addition, artificial heart valves are definitely hemolytic and thrombus formation may be caused by the destruction of red blood cells due to high shearing stresses in the flow. It is therefore important to know the detailed structure of the blood flow through artificial valves. So far most investigations have been carried out experimentally using flow visualisation techniques and pressure measurements, as for example Naumann's measurements of the pressure drop in heart valves [20].

An example of vortex formation and recirculating flow behind an open disc-shaped valve is shown in the lower left part of Fig. 23. The experiment was carried out in the water tank of the Aerodynamisches Institut at Reynolds numbers of about 200. The picture in the upper left part of Fig. 21 was obtained through a microscope using a tunnel of 0.3 mm width and a height of 0.16 mm with a new technique deviced by J. Lambert [21]. The flow medium is a mixture of ox-blood and a NaCl solution. The dark spots on the downstream side of the disc indicate the high concentration of red blood cells while the bright spots exhibit much lower concentrations.

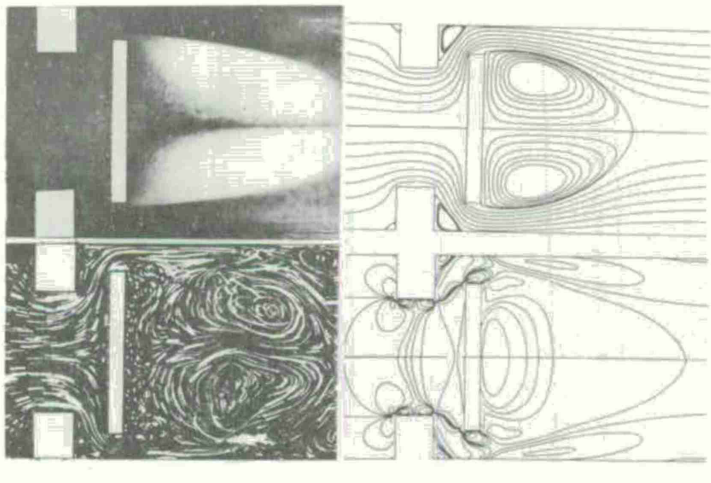

Fig. 23 Flow pattern in idealised heart valve. Computed lines of constant stream function and shearing stress distribution were provided by T. J. Mueller.

The first numerical analysis of this problem was carried out by Mueller and Underwood (Refs. [22], [23], [24]). Integrating the Navier-Stokes equations numerically they obtained the flow pattern shown in the upper right part of Fig. 23. Direct comparison to the flow picture in the lower left part is not possible as the calculation is carried out for steady and axisymmetric flow condition with a Reynolds number of about 200. Although the accuracy of the calculation is not fully explored, shearing stress distributions in the flow can be obtained from the integration. In the lower right part of Fig. 23 lines of constant shearing stress are indicated which at the present time cannot be determined experimentally. It can be expected that with improved accuracy of future calculations our understanding of the flow behaviour in the recirculating region can be much enhanced.

6. CONCLUSIONS

The development of the digital computer has enabled the solution of complex flow problems. Several examples were shown to demonstrate the applicability of numerical solutions. These include three-dimen-

sional supersonic-inviscid flow fields about spheres at transonic free-stream Mach numbers. Two-dimensional laminar incompressible boundary layers can be predicted to any degree of accuracy. The same is true for three-dimensional laminar boundary layers, except that the behaviour of the flow near separation is not fully understood. With the existing models for the Reynolds stresses turbulent flows can also be determined with reasonable accuracy. For small Reynolds numbers separated flows, velocity and pressure distribution have been obtained from numerical solutions of the Navier-Stokes equations. Although laminar and turbulent flows can be simulated little is known about transitional flows and transition or relaminarisation cannot be predicted.

7. LITERATURE

1. Krause, E., Application of numerical techniques in fluid mechanics. The 7th Reynolds-Prandtl lecture. Aeronautical Journal, August 1974, pp. 331-354.
2. Lomax, H., Bailey, F.R. and Ballhaus, W.F., On the numerical simulation of three-dimensional transonic flow with application to the C-141 wing. NASA TND 6933, 1973.
3. Goodmanson, L.T., and Gratzer, L.B., Recent Advances in Aerodynamics for Transport Aircraft. Part II. Astronautics and Aeronautics, January 1974.
4. Sedney, R., and Kahl, G.D., Interferometric Study of the Blunt Body Problem. Ball.Res.Lab., Rep.No. 1100, 1960.
5. Förster, K., Roesner, K., and Weiland, C., The Numerical Solution of Blunt Body Flow Fields Using Rusanov's Method. Paper presented at the fourth International Conference on Numerical Methods in Fluid Dynamics Boulder, USA, June 1974.
6. Gooderum, P.B., and Wood, G.P., Density fields around a sphere at Mach numbers 1.3 and 1.62. NASA TN 2173, 1950.
7. Stilp, A., Strömungsuntersuchungen an Kugeln mit transonischen und supersonischen Geschwindigkeiten in Luft und Frigen-Luft-Gemischen. Ernst-Mach-Institut, Freiburg i.Br., WB Nr. 10165.
8. Lyubimov, A.N., and Rusanov, V.V., Gas flows past blunt bodies. Part I. Calculation Method and Flow Analysis. "Nauka" Press, Moscow 1970. NASA TTF-714, Washington, D.C., February 1974.
9. Weiland, C., Berechnung dreidimensionaler Umströmungen stumpfer Körper im Überschall mit dem Rusanow-Verfahren. Abhandlungen aus dem Aerodynamischen Institut, Heft 21, 1974.
10. Krause, E., Analysis of Viscous Flow over Swept Wings. Paper presented at the 9th Congress of the International Council of the Aeronautical Sciences, Haifa, ICAS PAPER No. 74-20, 1974.
11. Krause, E., Hirschel, E.H., and Kordulla, W., Fourth Order "Mehrstellen"-Integration for Three-Dimensional Turbulent Boundary Layers. AIA-Computational Fluid Dynamics Conference Proceedings, Palm Springs, Cal., 19-20 July 1973.
12. Krause, E., Recent Developments of Finite-Difference Approximations for Boundary-Layer Equations, VKI-Lecture Series to be published in Lecture Notes of Physics by Springer Verlag.
13. Beasley, J.A., Calculation of the Laminar Boundary Layer and the Prediction of Transition on a Sheared Wing. Fluid-Motion-Problems in Wind Tunnel Design, AGARD-Report No. 602, pp. 1-1-1-11, 1973.
14. Altman, J.M., and Hayter, N.F., A Comparison of the Turbulent Boundary-Layer Growth on an Unswept and a Swept Wing. NACA TN 2500, September 1951.
15. Adams, J.C., Jr., Numerical Calculation of the Subsonic and Transonic Turbulent Boundary Layer on an Infinite Yawed Airfoil. AEDC-TR-73-112, July 1973.
16. Van den Berg, B., and Elsenaar, A., Measurements in a Three-Dimensional Incompressible Turbulent Boundary Layer in an Adverse Pressure Gradient Under Infinite Swept Wing Conditions. NLR TR 12092 U, 1972.
17. Fannelop, T.K., and Humphreys, D.A., A Simple Finite-Difference Method for Solving the Three-Dimensional Turbulent Boundary-Layer Equations. AIAA Paper 74-13, AIAA 12th Aerospace Sciences Meeting, Washington D.C., January 30 - February 1, 1974.
18. Kordulla, W., and Will, E., Tangentiales Ausblasen von Helium in laminaren Hyperschallgrenzschichten, ZfW 22, 295-307, 1974.
19. Kordulla, W., Helium- und Wasserstoffwandstrahlen in atmosphärischen Grenzschichten. Doctoral Dissertation Technische Hochschule Aachen 1974.
20. Naumann, A., Strömungsfragen der Medizin. Arbeitsgemeinschaft für Forschung des Landes Nordrhein-Westfalen. Natur-Ingenieur- und Gesellschaftswissenschaften, H.203, 1969.
21. Lambert, J., Eine neue Versuchsanordnung für die direkte mikroskopische Beobachtung des Fließverhaltens von Blut in Modellen natürlicher und künstlicher Gefäßsysteme, to be published in Biomedizinische Technik, Band 20, 1/February 1975.

22. Underwood, F.N. and Mueller, T.J., Numerical studies of the steady axisymmetric flow through a disc-type prosthetic heart valve. Proc. 25th ACEMB, Bal Harbour, Florida, 273, 1972.

23. Mueller, T.J., On the separated flow produced by a fully open disc-type prosthetic heart valve. ASME 1973, Biomechanics Symposium Proceedings, AMD, Vol. 2, pp 97-98, 1973.

24. Mueller, T.J., Numerical and physical experiments in viscous separated flows. Progress in Numerical Fluid Dynamics, Lecture Series 63, 1974.

NUMERICAL TECHNIQUES FOR THE SOLUTION OF THE COMPRESSIBLE NAVIER-STOKES EQUATIONS AND IMPLEMENTATION OF TURBULENCE MODELS

Barrett S. Baldwin,* Robert W. MacCormack,† and George S. Deiwert*
Ames Research Center, NASA, Moffett Field, Calif. 94035, USA

SUMMARY

The time-splitting explicit numerical method of MacCormack is applied to separated turbulent boundary layer flow problems. Modifications of this basic method are developed to counter difficulties associated with complicated geometry and severe numerical resolution requirements of turbulence model equations. The accuracy of solutions is investigated by comparison with exact solutions for several simple cases. Procedures are developed for modifying the basic method to improve the accuracy. Numerical solutions of high-Reynolds-number separated flows over an airfoil and shock-separated flows over a flat plate are obtained. A simple mixing length model of turbulence is used for the transonic flow past an airfoil. A nonorthogonal mesh of arbitrary configuration facilitates the description of the flow field. For the simpler geometry associated with the flat plate, a rectangular mesh is used, and solutions are obtained based on a two-equation differential model of turbulence.

INTRODUCTION

With continuing advances in both computer technology and computational methods, the fluid dynamicist has been able to solve increasingly complex flow problems. Flows governed by the unsteady "compressible Navier-Stokes equations" provide an example. In the recent past (refs. 1 and 2), with computers such as the IBM 360/67 and CDC 6600, we were able to predict two-dimensional shock-separated laminar boundary layer flows at Reynolds numbers of 10^5. Today, with the CDC 7600, STAR, and Burroughs' Illiac IV computers, and with recent advances in turbulence modeling, we are on the threshold of extending our calculations to full-scale-flight Reynolds numbers.

The field of turbulence modeling has received an impetus from increasing computer capabilities. Even if the quest for a universal turbulence model (refs. 3-5) eventually proves to be illusory, models tailored to particular flows will undoubtedly continue to be important in engineering applications. The degree of complexity that can be tolerated is increasing with the gains in computer speed and capacity. Three-dimensional time-dependent solutions of the conservation relations, with enough resolution to compute the important turbulent eddies (ref. 6), may become commonplace in the future. Turbulence modeling will still be needed for the subgrid scales and near walls. There is a need for more experiments to test the adequacy of the turbulence models that are evolving. Development of new experimental techniques such as the laser doppler velocimeter (ref. 7) are making essentially disturbance-free measurements possible. Numerical solutions of the type described here can aid in the design and interpretation of the experiments.

This paper presents results from several investigations that have been previously published (refs. 8-11). The turbulence model equations pose a more severe numerical resolution requirement than the Navier-Stokes equations. To counter this difficulty, a procedure that utilizes flux correction factors to improve the accuracy of the numerical solution was developed. In the first part of this paper, the ideas leading to that concept are described and simple examples demonstrating the principle are presented.

Only modest progress was made toward the basic goal of testing the adequacy of turbulence models. However, knowledge was gained that should be useful in the design of future experiments and to improve the efficiency of later calculations. It was found that the viscous sublayer of a turbulent boundary layer near a separation point is insensitive to the use of the boundary layer approximation, although this approximation may be invalid for the entire boundary layer, depending on pressure gradients.

Most of the effort in these investigations has gone into development of machine codes that can generate solutions of the time-averaged conservation relations coupled to turbulence model equations. Numerical solutions of transonic separated flows over a thick airfoil are presented. These solutions are designed to provide insight into the Reynolds-number dependence of such flows. Numerical solutions of shock-separated hypersonic turbulent boundary layer flows, based on either a simple mixing-length model or a two-equation differential model of turbulence, were obtained. An extreme case (high Mach number and strong shock wave) was chosen in the hope that techniques would be developed capable of treating the range of conditions at which experimental data will become available.

NUMERICAL METHODS

Preliminary Considerations

The two-dimensional mean-flow equations and turbulence model equations to be considered in this paper can be written as

$$\frac{\partial U}{\partial t} + \frac{\partial F}{\partial x} + \frac{\partial G}{\partial y} = E \ , \tag{1}$$

where U is a column vector of conserved quantities per unit volume (mass, momentum, energy, turbulent energy, etc.). The fluxes F and G are column vectors that contain convection and diffusion terms. The components of the source vector E associated with the mean-flow equations are zero. However, nonzero source terms appear in the turbulence model equations; for example, those representing production and dissipation of turbulent energy. The fluxes and sources are functions of auxiliary variables such as the

*Research Scientist.
†Assistant Chief, Computational Fluid Dynamics Branch.

x component of velocity u and the first derivatives of these variables. The auxiliary variables are algebraic functions of the conserved quantities. The specific relationships implied in these statements are listed in later sections. The quantities appearing explicitly in equation (1), or linear combinations of them, are often smoothly varying compared to the auxiliary variables, a fact which has not been fully exploited in numerical solutions. Knowledge of the behavior of the fluxes and sources from a numerical solution can sometimes be used to tailor the numerical procedure to obtain a more accurate solution. In some cases, it can be shown that use of exact values of the fluxes can produce exact numerical solutions.

Basic Numerical Method

To accomplish the goal of computing shock separated turbulent flows, a numerical method is needed that can treat shock waves in the inviscid regions and also treat the compressible viscous flow equations. MacCormack's (ref. 12) explicit two-step second-order method (a Lax-Wendroff variant) has been widely used and has been found to perform reliably in the computation of a variety of inviscid and viscous flows.

The two-dimensional time-dependent calculations in this paper are based on MacCormack's (ref. 1) time-splitting method for solution of the Navier-Stokes equations. The conserved quantity U in equation (1) is advanced by a time step Δt_x as though the $\partial G/\partial y$ and E terms were absent, and then by a time step Δt_y in which $\partial F/\partial x$ is omitted. The source term, when it is present, is included with $\partial G/\partial y$ because a sensitive balance develops between E and $\partial G/\partial y$ in the solution of turbulence model equations. The finite-difference operation utilizes a predictor and corrector sequence. The predictor step in the advancement Δt_x can be denoted by

$$\bar{U}_{ij}(t_x + \Delta t_x, t_y) = U_{ij}(t_x, t_y) - \frac{\Delta t_x}{\Delta x}\left[F_{ij}(t_x, t_y) - F_{i-1,j}(t_x, t_y)\right] \tag{2}$$

and the corrector by

$$U_{ij}(t_x + \Delta t_x, t_y) = \frac{1}{2}\left\{U_{ij}(t_x, t_y) + \bar{U}_{ij}(t_x + \Delta t_x, t_y) - \frac{\Delta t_x}{\Delta x}\left[\bar{F}_{i+1,j}(t_x + \Delta t_x, t_y) - \bar{F}_{i,j}(t_x + \Delta t_x, t_y)\right]\right\} . \tag{3}$$

The bar on $\bar{F}$ indicates that predicted quantities $\bar{U}$ are to be used in the evaluation of fluxes. The elements of F represent fluxes (or stresses) that are evaluated in such a manner as to achieve second-order accuracy after the predictor-corrector sequence is completed. For example, at the cell surface lying midway between mesh points i and i+1, the flux value u is evaluated as u_i in the predictor and as u_{i+1} in the corrector. The stress derivative of u is evaluated as $(u_{i+1} - u_i)/\Delta x$ in both predictor and corrector. The corresponding relations for the advancement Δt_y are

$$\bar{U}_{ij}(t_x, t_y + \Delta t_y) = U_{ij}(t_x, t_y) - \frac{\Delta t_y}{\Delta y}\left[G_{ij}(t_x, t_y) - G_{i,j-1}(t_x, t_y)\right] + \Delta t_y E_{ij}(t_x, t_y) \tag{4}$$

and

$$U_{ij}(t_x, t_y + \Delta t_y) = \frac{1}{2}\left\{U_{ij}(t_x, t_y) + \bar{U}_{ij}(t_x, t_y + \Delta t_y) - \frac{\Delta t_y}{\Delta y}\left[\bar{G}_{i,j+1}(t_x, t_y + \Delta t_y) - \bar{G}_{i,j}(t_x, t_y + \Delta t_y)\right] + \Delta t_y \bar{E}_{ij}(t_x, t_y + \Delta t_y)\right\} . \tag{5}$$

The source terms E, when present, are evaluated at the center of the cell being advanced in both predictor and corrector.

Let $L_x(\Delta t_x)$ denote the pair of operations by which $U_{ij}(t_x + \Delta t_x, t_y)$ is obtained from $U_{ij}(t_x, t_y)$ and let $L_y(\Delta t_y)$ denote the analogous determination of $U_{ij}(t_x, t_y + \Delta t_y)$ from $U_{ij}(t_x, t_y)$. MacCormack (ref. 1) has shown that, although the sequence $L_x(\Delta t)L_y(\Delta t)$ is accurate only to first order in Δx and Δy, symmetrical sequences such as $L_y(\Delta t/2)L_x(\Delta t)L_y(\Delta t/2)$ retain second-order accuracy. Computational efficiency is enhanced by the use of operator sequences of the form

$$L(\Delta t) = \left[L_y\left(\frac{\Delta t}{2n}\right)L_x\left(\frac{\Delta t}{n}\right)L_y\left(\frac{\Delta t}{2n}\right)\right]^n ,$$

where n is an integer representing the number of operations $L_yL_xL_y$ that are to be applied in one time step Δt. When mesh Reynolds numbers $(\rho u \Delta x/\mu)$ are greater than 2, the maximum time step for which the calculations will be stable is determined by the CFL (Courant-Friedrichs-Lewy) conditions (ref. 1)

$$\Delta t \leq \frac{2n\Delta y}{(v+c)_{max}} \text{ and } \frac{n\Delta x}{(u+c)_{max}} .$$

In regions of coarse mesh, n is set equal to 1 and large values of n (up to 100 in this paper) are used in fine mesh regions. Most of the computing time is then spent in the finest mesh, which constitutes a small fraction of the total number of computation points. Cumulative values of fluxes at the last cell face between meshes are stored during operation in the fine mesh. These values are used to obtain average fluxes to be applied during operation in the adjacent coarser mesh.

Inviscid Burgers Equation

For purposes of illustrating the use of knowledge of the solution to improve the accuracy of the finite-difference procedure, numerical solutions of the equation

$$\frac{\partial u}{\partial t} + \frac{\partial}{\partial x}\left(\frac{1}{2} u^2\right) = 0 \tag{6}$$

have been obtained. Kutler (ref. 13) has investigated the ability of several differencing techniques to capture the propagating discontinuity that results from the initial conditions

$$u(o,x) = 1.0 - S_F(x - x_1) \tag{7}$$

and the boundary conditions

$$u(t,0) = 1.0 \ , \tag{8}$$

$$u(t,x_2) = 0 \quad . \tag{9}$$

The function $S_F(x - x_1)$ is the unit step function

$$S_F(x - x_1) = \begin{cases} 0, \text{ for } x < x_1 \\ 1, \text{ for } x_1 < x \end{cases} . \tag{10}$$

The exact solution of equations (6)-(9) is

$$u(t,x) = 1 - S_F\left(x - \frac{1}{2} t\right) . \tag{11}$$

Kutler found that MacCormack's method accurately predicts the position of the discontinuity as a function of time, but smears it over several mesh points. The smearing was greatly reduced with CFL numbers (CFL $\equiv u_{max}\Delta t/\Delta x$) near 1.0. Since CFL numbers well below 1.0 are used in this paper, it is of interest to note the performance of MacCormack's method in such cases.

The differencing used in this paper corresponds to evaluation of the flux at cell faces between the mesh points. Evaluation of F according to the relations

$$F_{i+(1/2)} = \frac{1}{2} u_i^2 \ , \text{ for predictor,} \tag{12}$$

and

$$\bar{F}_{i+(1/2)} = \frac{1}{2} \bar{u}_{i+1}^2 \ , \text{ for corrector,} \tag{13}$$

leads to second-order accuracy, since, after the predictor and corrector steps are completed, the effect is approximately equivalent to averaging the fluxes at i and $i+1$ to obtain the value at $i+(1/2)$. For solution of equation (6) a uniform mesh with $\Delta x = 0.1$ was used.

Figure 1 shows a comparison with the exact solution of numerical results obtained at a CFL number equal to 0.1. At $t = 10$, the solution has settled essentially into the cyclic behavior shown, which repeats itself as the wave front progresses past each mesh point. The position of the wave front, which can be deduced from the numerical solution, remains accurate.

If the exact fluxes at the cell faces between computation points

$$F_{i+(1/2)} = \frac{1}{2}\left[1 - S_F\left(x_{i+(1/2)} - \frac{1}{2} t\right)\right]^2 = \frac{1}{2}\left[1 - S_F\left(x_{i+(1/2)} - \frac{1}{2} t\right)\right] \tag{14}$$

are used in both predictor and corrector, the numerical solution is exact except at the computation point nearest the wave front. The value of u at that point increases from zero linearly with time so that the position of the wave front between mesh points can be accurately inferred. The accuracy of the numerical solution can be improved by any modification of the basic method that results in the use of accurate values of the fluxes at the cell faces. For example, the flux can be computed in both predictor and corrector according to the relation

$$F_{i+(1/2)} = \begin{cases} \frac{1}{2} u_i^2 \ , \text{ if } 1 < (u_i + u_{i+1}) < 1.9 \\ \frac{1}{2} u_{i+1}^2 \ , \text{ if } 0.1 < (u_i + u_{i+1}) < 1 \end{cases} \tag{15}$$

and can be computed according to the basic method from equations (12) and (13), if $u_i + u_{i+1}$ is in neither of the above specified ranges. The results in figure 2 were computed by this means with a CFL number equal to 0.1. Essentially the same accurate solution can also be obtained from the unmodified basic method with a CFL number close to 1.0.

Linear Viscous Equation

A more useful modification of the basic method results from a study of the linear equation

$$\frac{\partial u}{\partial t} + \frac{\partial}{\partial x}\left(cu - \nu \frac{\partial u}{\partial x}\right) = 0 \ . \tag{16}$$

In complicated flow problems, time-dependent solutions are often used as a means of arriving at a final steady-state solution that is of primary interest. The steady-state solution of equation (16) that is approached as $t \to \infty$ is obtained by setting the flux equal to a constant

$$cu - \nu \frac{\partial u}{\partial x} = -\tau_0 \ . \tag{17}$$

With the boundary conditions

$$u(t,0) = 0 \tag{18}$$

and

$$u(t,1) = 1 \ , \tag{19}$$

the steady-state solution is

$$u(\infty,x) = \frac{1 - \exp(cx/\nu)}{1 - \exp(c/\nu)} \ . \tag{20}$$

With

$$c = -1 \tag{21}$$

and

$$\nu = 0.05 \ , \tag{22}$$

the solution resembles a viscous boundary layer.

For numerical solutions the initial conditions

$$u(o,x) = \begin{cases} 0 \ , \text{ for } x = 0 \\ 1.0, \text{ for } x > 0 \end{cases} \tag{23}$$

are used. In the basic numerical method, the flux $F = (cu - \nu \partial u/\partial x)$ is evaluated at cell faces between mesh points according to the relations

$$F_{i+(1/2)} = cu_i + \nu\left(\frac{u_{i+1} - u_i}{\Delta x}\right) \ , \text{ for predictor,} \tag{24}$$

and

$$\bar{F}_{i+(1/2)} = c\bar{u}_{i+1} + \nu\left(\frac{\bar{u}_{i+1} - \bar{u}_i}{\Delta x}\right), \text{ for corrector.} \tag{25}$$

The same formula for the stress derivative is used in both predictor and corrector, since the finite difference is properly centered about the cell face between mesh points, as required for second-order accuracy.

It is instructive to estimate the truncation error of the numerical solution according to the modified equation approach developed by Warming and Hyett (ref. 14). With MacCormack's differencing technique, the numerical solution of equation (16) would satisfy exactly the modified differential equation

$$\frac{\partial u}{\partial t} + \frac{\partial}{\partial x}\left(cu - \nu \frac{\partial u}{\partial x}\right) + \frac{c}{6}\left(\Delta x^2 - c^2 \Delta t^2\right) \frac{\partial^3 u}{\partial x^3} + \text{higher-order terms} = 0 \ , \tag{26}$$

which is obtained by Taylor series expansion of solutions of the finite-difference equation. Thus Δt and Δx must be chosen such that the truncation error, the third term in equation (17), does not swamp the viscous term that we intend to compute. The requirements for numerical stability are

$$\Delta t < \frac{\Delta x}{c} \text{ and } \frac{1}{2}\frac{\Delta x^2}{\nu} \ . \tag{27}$$

It is apparent from equation (20) that, with $c = -1$ and $\nu = 0.05$, $\Delta x \tilde{<} 0.1$ is required for adequate resolution of the boundary layer. In that case, the second condition in equation (27) is more restrictive than the first, and $\Delta t^2 << \Delta x^2$. The requirement that the truncation error in equation (26) be small compared to the viscous term is then

$$\left|\frac{c\Delta x^2}{6} \frac{\partial^3 u}{\partial x^3}\right| << \left|\nu \frac{\partial^2 u}{\partial x^2}\right| \ .$$

Evaluation of these derivatives from equation (20) leads to

$$\frac{c^2 \Delta x^2}{\nu^2} << 6 \ . \tag{28}$$

Therefore the mesh Reynolds number $|c|\Delta x/\nu$ must be small compared to $\sqrt{6}$.

A numerical solution of equation (16) has been obtained with the boundary conditions in equations (18) and (19), constant values in equations (21) and (22), and initial conditions represented by equation (23). A mesh spacing $\Delta x = 0.1$ was used. In figure 3, the numerical solution is compared to the exact

solution represented by equation (20). Since it is often expensive to refine the mesh in practical fluid-flow problems, it is of interest to investigate the possibility of improving the accuracy of the numerical solution by modifying the numerical method. If we are primarily interested in the final steady-state solution, it is not necessary to impose accurate values of the fluxes at all states of the time-dependent calculation. The steady-state solution is approximately

$$u - 1 \approx - \exp\left(- \frac{x}{\nu}\right) \quad \text{as} \quad t \to \infty ,$$

showing that the variation of $u - 1$ with x can be accurately represented by an exponential. In the interval $x_i \leq x \leq x_{i+1}$, the exponential variation that passes through u_i at x_i and u_{i+1} at x_{i+1} can be written

$$u - 1 = (u_i - 1)\exp\left[\left(\frac{x - x_i}{\Delta x}\right)\ell n\left(\frac{u_{i+1} - 1}{u_i - 1}\right)\right] . \tag{29}$$

Evaluation at a cell face halfway between mesh points yields

$$u_{i+(1/2)} = 1 - \sqrt{(u_i - 1)(u_{i+1} - 1)} , \tag{30}$$

and differentiation of equation (29) leads to

$$\left(\frac{\partial u}{\partial x}\right)_{i+(1/2)} = \left[\frac{u_{i+(1/2)} - 1}{\Delta x}\right]\ell n\left(\frac{u_{i+1} - 1}{u_i - 1}\right) . \tag{31}$$

Accordingly, the flux $F = cu - \nu(\partial u/\partial x)$ in equation (16) would be

$$F_{i+(1/2)} = c - \sqrt{(u_i - 1)(u_{i+1} - 1)}\left[c - \frac{\nu}{\Delta x}\ell n\left(\frac{u_{i+1} - 1}{u_i - 1}\right)\right] . \tag{32}$$

To use equation (32) in a machine code, it is necessary to avoid the singular behavior that occurs when u_i or u_{i+1} approaches 1 too closely. This can be accomplished by replacing the 1's in equation (32) with 1.01. Use of equation (32) in a numerical solution of equation (16) virtually reproduces the exact steady-state solution, as shown in figure 4. This remains true even when the condition for small truncation error of the basic method, in equation (28), is violated. In addition, the skin friction

$$\tau_0 = \nu\left(\frac{\partial u}{\partial x}\right)_{x \to 0}$$

can still be computed accurately by evaluating the derivative from equation (29) at a point near $x = 0$.

Several additional steps can be taken to make the results of the foregoing study more general and more useful. Knowledge of the exact solution was used in choosing the 1's for equations (29)-(31), but this can be avoided. Without specifying the form of the flux F, which can be a nonlinear function of u and $\partial u/\partial x$, suppose variations in the interval $x_{i-1} < x < x_{i+1}$ are of the form

$$u - A = (u_i - A)\exp\left[\frac{(x - x_i)}{\Delta x}\ell n\left(\frac{u_{i+1} - A}{u_i - A}\right)\right] . \tag{33}$$

Evaluation at $x = x_{i-1}$ and rearrangement leads to

$$A = \frac{(u_{i+1}u_{i-1} - u_i^2)}{u_{i+1} - 2u_i + u_{i+1}} . \tag{34}$$

To avoid a zero in the denominator of this expression, the condition

$$|u_{i+1} - 2u_i + u_{i-1}| > \varepsilon_0(|u_{i+1}| + |u_i|) \tag{35}$$

is imposed with $\varepsilon_0 \sim 10^{-3}$. Violation of this condition is an indication that the variation of u is nearly linear and the basic numerical method is adequate and needs no modification in the interval $x_{i-1} < x < x_{i+1}$. However, if inequality (35) is satisfied, A can be computed from equation (34). To avoid singular behavior of the logarithm in equation (33), the condition

$$(u_{i+1} - A)(u_i - A) > \varepsilon_0^2(u_{i+1}^2 + u_i^2) \tag{36}$$

is imposed. Violation of this condition is an indication that u is nearly constant in the interval $x_i < x < x_{i+1}$ and again the basic numerical method would generate accurate values of fluxes at the cell face between x_i and x_{i+1}. However, if inequality (36) is satisfied, no singular behavior will occur in the computation of the relations

$$u_{i+(1/2)} = A + \text{sgn}(u_i - A)\sqrt{(u_{i+1} - A)(u_i - A)} \tag{37}$$

and

$$\left(\frac{\partial u}{\partial x}\right)_{i+(1/2)} = \frac{[u_{i+(1/2)} - A]}{\Delta x} \ell n\left(\frac{u_{i+1} - A}{u_i - A}\right) . \tag{38}$$

Expansion of u_i and u_{i+1} about $(u_{i+1} + u_i)/2$ in these relations shows that they differ from the basic method in equations (24) and (25) by terms of the order $(u_{i+1} - u_i)^2$. Numerical solutions from the basic method are accurate to the second order in Δx, and are exact if the variations are polynomials of the second degree or less. Numerical solutions based on equations (37) and (38) are also accurate to the second order in Δx and are exact if the variations are exponential. When the variations are not exponential, the latter method produces an effect akin to a transformation in which the logarithms are computed rather than the original variables. It is shown in a later section that this feature is useful for the numerical solution of turbulence model equations in boundary layers where the turbulence quantities vary through many orders of magnitude.

For more complicated flow problems, nonuniform meshes are essential to minimize both the required storage space and the computation time. When the mesh spacing is not uniform, a procedure different from the foregoing is needed, as follows: If variations are of the form

$$u - A = B \exp(\alpha_o x) \tag{39}$$

in the interval $x_{i-1} < x < x_{i+1}$, it follows that

$$u_{i+1} - A = B \exp(\alpha_o x_{i+1}) , \tag{40a}$$

$$u_i - A = B \exp(\alpha_o x_i) , \tag{40b}$$

$$u_{i-1} - A = B \exp(\alpha_o x_{i-1}) . \tag{40c}$$

Elimination of A leads to

$$u_{i+1} - u_i = B[\exp(\alpha_o x_{i+1}) - \exp(\alpha_o x_i)] \tag{41a}$$

and

$$u_i - u_{i-1} = B[\exp(\alpha_o x_i) - \exp(\alpha_o x_{i-1})] . \tag{41b}$$

The ratio of these relations can then be written

$$\frac{u_{i+1} - u_i}{u_i - u_{i-1}} = \exp[\alpha_o(x_i - x_{i-1})]\left\{\frac{1 - \exp[\alpha_o(x_{i+1} - x_i)]}{1 - \exp[\alpha_o(x_i - x_{i-1})]}\right\}$$

or

$$\alpha_o = \frac{\ell n\left(\frac{u_{i+1} - u_i}{u_i - u_{i-1}}\right) - \ell n\left\{\frac{1 - \exp[\alpha_o(x_{i+1} - x_i)]}{1 - \exp[\alpha_o(x_i - x_{i-1})]}\right\}}{x_i - x_{i-1}} \tag{42}$$

The inequalities

$$|u_i - u_{i-1}| > \varepsilon_o(|u_{i+1}| + |u_i| + |u_{i-1}|) \tag{43}$$

and

$$(u_{i+1} - u_i)(u_i - u_{i-1}) > \varepsilon_o{}^2(u_{i+1}^2 + u_i{}^2 + u_{i-1}^2) \tag{44a}$$

are imposed to avoid singular behavior ($\varepsilon_o \sim 10^{-3}$). If these inequalities are not satisfied, the variations are linear or not monotonic and the basic numerical method (see section on basic numerical method) should be used. However, if inequalities (43) and (44a) are satisfied, α_o can be computed (by iteration) from equation (42), with the added restriction

$$|\alpha_o|(x_i - x_{i-1}) \geq \varepsilon_o , \tag{44b}$$

which is also needed to avoid singular behavior in evaluation of the right side of equation (42). If the equality in equation (44b) is the only solution allowed by this restriction, use of that value will produce an effect in the following formulas (equations (45)-(49)) that is equivalent to the basic method. Once a value of α_o has been arrived at that satisfies inequality (44b), B can be computed using equation (41b) and A evaluated from equation (40b). Then, according to equation (39), we obtain

$$u_{i+(1/2)} = A + B \exp\left[\alpha_o x_{i+(1/2)}\right] \tag{45}$$

and, by differentiation of equation (39), we have

$$\left(\frac{\partial u}{\partial x}\right)_{i+(1/2)} = \alpha_o\left[u_{i+(1/2)} - A\right] . \tag{46}$$

With as much complication as is represented by the use of equations (42)-(46), one might wonder whether refining the mesh would entail less computer time in a compute-bound-flow problem. However, if the final steady-state solution is of primary interest, it is not necessary to solve the foregoing equations at every time step. Instead, correction factors for $u_{i+(1/2)}(\partial u/\partial x)_{i+(1/2)}$ can be evaluated periodically and used to correct the fluxes computed according to the basic method, from equations (24) and (25), at intervening time steps. The correction factors are

$$C_{U,i+(1/2)} = \frac{u_{i+(1/2)}}{u_i} , \text{ predictor,} \tag{47}$$

$$\bar{C}_{U,i+(1/2)} = \frac{u_{i+(1/2)}}{u_{i+1}} , \text{ corrector,} \tag{48}$$

$$C_{DU,i+(1/2)} = \frac{(x_{i+1} - x_i)\left(\frac{\partial u}{\partial x}\right)_{i+(1/2)}}{(u_{i+1} - u_i)} , \text{ predictor and corrector,} \tag{49}$$

with $u_{i+(1/2)}$ and $(\partial u/\partial x)_{i+(1/2)}$ evaluated according to equations (40)-(46) and u_i, u_{i+1} obtained from the numerical solution at the same timestep. The initial values and default values — failure of inequalities or zero denominators in equations (47)-(49) — of the correction factors are 1.0.

Application of the flux correction factors in the problem presently under discussion consists of replacing equations (24) and (25) with the respective relations

$$F_{i+(1/2)} = cu_i C_{U,i+(1/2)} + \nu\left(\frac{u_{i+1} - u_i}{\Delta x}\right) C_{DU,i+(1/2)}$$

and

$$\bar{F}_{i+(1/2)} = c\bar{u}_{i+1}\bar{C}_{U,i+(1/2)} + \nu\left(\frac{\bar{u}_{i+1} - \bar{u}_i}{\Delta x}\right) C_{DU,i+(1/2)}$$

Numerical solution of equation (16) with correction factors computed every tenth timestep produced the same accurate steady-state solution obtained by the earlier modification of the basic method but without significant increase in computer time relative to the basic method.

It is important to note that flux correction factors resulting from any other procedure based on the properties of the numerical solution could be used similarly to improve the accuracy of the steady-state solution. For example, correction factors from higher-order methods that are evaluated infrequently rather than at every timestep may enhance the efficiency of a machine code to be used in a compute-bound-flow problem. Alternatively, a refined mesh could be used infrequently in critical regions to evaluate flux correction factors that would produce accurate steady-state solutions on a coarser mesh.

Simplified Turbulence Model Equations

In the viscous sublayer of a turbulent boundary layer, quantities for which differential equations are provided by turbulence models vary through several orders of magnitude, thereby posing a severe numerical resolution requirement. Complete turbulence model equations are listed in a later section of this paper. It is instructive to investigate the properties of a simplified version of the Saffman-Wilcox (ref. 5) turbulence model represented by the relations

$$\frac{\partial \zeta}{\partial \tau} + \frac{\partial}{\partial \eta}\left(-\frac{\partial \zeta}{\partial \eta}\right) = -20\zeta^{3/2} \tag{50}$$

$$\frac{\partial e_s}{\partial \tau} + \frac{\partial}{\partial \eta}\left(-\frac{\partial e_s}{\partial \eta}\right) = -10\sqrt{\zeta}\, e_s \tag{51}$$

The quantity ζ represents the square of pseudovorticity (or rate of dissipation) normalized with respect to the value at the wall. The quantity e_s represents the turbulent energy per unit mass of fluid. The time τ and distance from the wall η have been normalized in a way that simplifies the constant coefficients. In the section on turbulence models, equations (50) and (51) are shown to be applicable in a portion of the viscous sublayer where the eddy viscosity is small compared to the molecular viscosity and the gas density and temperature are approximately constant.

With the boundary conditions

$$\zeta(t,0) = 1 , \tag{52}$$

$$e_s(t,0) = 0 , \tag{53}$$

$$\zeta(t,\eta_{11}) = \zeta_{11} , \tag{54}$$

$$e_s(t,\eta_{11}) = e_{s_{11}} , \tag{55}$$

the exact steady-state solution is

$$\zeta(\infty,\eta) = (\zeta_{11}^{-1/4} - \eta_{11} + \eta)^{-4} \tag{56}$$

and

$$e_s(\infty,\eta) = \left[\frac{(\zeta_{11}^{-1/4} - \eta_{11} + \eta)^m - (\zeta_{11}^{-1/4} - \eta_{11} + \eta)^{(1-m)}}{\zeta_{11}^{(-m/4)} - \zeta_{11}^{-(1-m)/4}}\right] e_{s_{11}} , \tag{57}$$

where

$$m = \frac{1}{2}(1 + \sqrt{41}). \tag{58}$$

For simplicity, ζ_{11} and $e_{s_{11}}$ have been chosen to be

$$\zeta_{11} = (1 + \eta_{11})^{-4} \tag{59}$$

and

$$e_{s_{11}} = 1 , \tag{60}$$

so that equation (56) becomes

$$\zeta(\infty,\eta) = (1 + \eta)^{-4} \tag{61}$$

and equation (57) becomes

$$e_s(\infty,\eta) = \frac{(1 + \eta)^m - (1 + \eta)^{1-m}}{(1 + \eta_{11})^m - (1 + \eta_{11})^{(1-m)}} . \tag{62}$$

Suitable initial conditions for time dependent numerical solution of equations (50) and (51), respectively, are

$$\zeta(0,\eta) = \begin{cases} 1 , & \text{for } \eta = 0 \\ (1 + \eta_{11})^{-4}, & \text{for } \eta > 0 \end{cases} \tag{63}$$

and

$$e_s(0,\eta) = \begin{cases} 0 , & \text{for } \eta = 0 \\ 1 , & \text{for } \eta > 0 \end{cases} . \tag{64}$$

The variable η in equations (50) and (51) is a dimensionless version of the y coordinate. For numerical solution of these equations by the basic method (see section on basic numerical method), the fluxes G in equation (1) are evaluated at the cell face between uniformly spaced mesh points according to the relations

$$G_{\zeta,j+(1/2)} = \left(\frac{\partial \zeta}{\partial \eta}\right)_{j+(1/2)} = \frac{\zeta_{j+1} - \zeta_j}{\Delta\eta} \tag{65}$$

and

$$G_{es,j+(1/2)} = \left(\frac{\partial e_s}{\partial \eta}\right)_{j+(1/2)} = \frac{e_{sj+1} - e_{sj}}{\Delta\eta} , \tag{66}$$

and the source terms E are evaluated at the cell centers

$$E_{\zeta,j} = -20\zeta_j^{3/2} \tag{67}$$

and

$$E_{es,j} = -10\sqrt{\zeta_j}\, e_{sj} . \tag{68}$$

Equations (65)-(68) apply to the predictor. In the present case, the formulas for the corrector are identical with unbarred quantities replaced by their counterparts containing bar overscripts. In figure 5, a comparison is shown between the resulting steady-state numerical solution according to the basic method and the exact solution. The ratio $e_s/\sqrt{\zeta}$ is proportional to the eddy viscosity. A comparison of this quantity with the exact values is also shown in figure 5.

In an effort to improve the accuracy of the solution without refining the mesh, the modification of the basic method described in the previous section can be used to compute the fluxes. In addition, it is necessary to compute the source terms on the right sides of equations (50) and (51) more accurately. For this purpose, the source term in equation (50), for example, can be expressed as a flux in the form

$$-20\zeta^{3/2} = \frac{\partial}{\partial\eta}\int -20\zeta^{3/2}\, d\eta \ .$$

The appropriate finite difference expression of this relationship is

$$E_{\zeta,j} = \frac{1}{\Delta\eta}\int_{\eta_{j-(1/2)}}^{\eta_{j+(1/2)}} -20\zeta^{3/2}\, d\eta \ . \tag{69}$$

For the purpose of demonstrating the usefulness of flux- and source-correction factors, such factors are first derived from the exact solution for ζ, as was done in the section on the inviscid Burgers equation. The exact solution for ζ in equation (61) can be used in equation (69) to compute a source-term correction factor to be applied in the finite-difference solution, namely,

$$C_{E\zeta,j} = \frac{\int_{\eta_{j-(1/2)}}^{\eta_{j+(1/2)}} \zeta^{3/2} d\eta}{\Delta\eta\zeta_j^{3/2}} = \frac{(1+\eta_j)^4}{3\Delta\eta}\left\{\frac{1}{[1+\eta_{j-(1/2)}]^3} - \frac{1}{[1+\eta_{j+(1/2)}]^3}\right\} . \tag{70}$$

Also from the exact solution of equation (61), the flux correction factor is

$$C_{G\zeta,j+(1/2)} = \frac{4\Delta\eta}{[1+\eta_{j+(1/2)}]^5\left[\frac{1}{(1+\eta_j)^4} - \frac{1}{(1+\eta_{j+1})^4}\right]} . \tag{71}$$

If the basic numerical method represented by equations (65) and (67) is modified according to the relations

$$G_{\zeta,j+(1/2)} = \frac{C_{G\zeta,j+(1/2)}(\zeta_{j+1} - \zeta_j)}{\Delta\eta} \tag{72}$$

and

$$E_{\zeta,j} = C_{E\zeta,j}(-20\zeta_j^{3/2}) \ , \tag{73}$$

the resulting steady-state numerical solution is exact except for roundoff errors. Thus, if flux and source correction factors can be found by means other than through a thorough knowledge of the exact solution, the accuracy of the numerical solution can be improved without refining the mesh. One way to accomplish this is by assuming that the variations are exponential, as in the previous section. This leads to correction factors that will produce an effect roughly equivalent to a transformation in which differential equations for the logarithms of the variables are solved numerically rather than solving the original equations, although no such transformation is actually carried out. If the mesh is uniform, the procedure for the flux correction factor is given by equations (34)-(38) and (47)-(49). For a nonuniform mesh, equations (40)-(46) replace (34)-(38). It should be reemphasized that it is not necessary to compute the flux correction factors at every timestep if only the steady-state solution is of interest.

The source correction factor corresponding to exponential variations requires further development. If the variation of E is of the form

$$E = A + B\exp(\alpha_o\eta) \tag{74}$$

in the interval $\eta_{j-(1/2)} \le \eta \le \eta_{j+(1/2)}$, it follows, by integration, that

$$\int_{\eta_{j-(1/2)}}^{\eta_{j+(1/2)}} E\, d\eta = A\left[\eta_{j+(1/2)} - \eta_{j-(1/2)}\right] + \frac{B}{\alpha_o}\left\{\exp\left[\alpha_o\eta_{j+(1/2)}\right] - \exp\left[\alpha_o\eta_{j-(1/2)}\right]\right\} ,$$

and the source correction factor becomes

$$C_{E,j} = \frac{A}{E_j} + \frac{B\left\{\exp\left[\alpha_o\eta_{j+(1/2)}\right] - \exp\left[\alpha_o\eta_{j-(1/2)}\right]\right\}}{\alpha_o\left[\eta_{j+(1/2)} - \eta_{j-(1/2)}\right]E_j} , \tag{75}$$

with the constants α_o, B, A determined in terms of E_{j+1}, E_j, E_{j-1} by the procedure represented by equations (40)-(44). If the mesh is uniform, A is determined by equations (34)-(36) and

$$\alpha_o = \frac{\ln\left(\frac{E_{j+1} - A}{E_j - A}\right)}{\Delta\eta} \ , \text{ for uniform mesh,} \tag{76}$$

and

$$B = \frac{E_j - A}{\exp(\alpha_o\eta_j)} \ , \text{ for uniform mesh.} \tag{77}$$

The initial value and default value of C_{Ej} is 1.0. Application of the correction factors is the same as in equations (72) and (73).

In figure 6, results from a numerical solution obtained, according to equations (49) and (75), by computing flux- and source-correction factors every tenth timestep are compared with the exact solution. It is apparent that this modification greatly improves the accuracy of the solution in comparison with results from the basic numerical method (fig. 5), even though the variations with η are not exponential. Such gains in accuracy are to be expected when there are large variations of dependent variables between mesh points that are not well represented by second-degree polynomials.

COMPRESSIBLE MEAN-FLOW EQUATIONS

Basis of Equations

Time-dependent solutions of the conservation relations for viscous compressible flows that are coupled to turbulence model equations are presented in a later section. Turbulence effects in compressible flows are incorporated by means of the "time averaged" viscous flow equations cast in terms of "mass averaged" variables. The effects of turbulence on the flow are expressed in terms of a scalar eddy-viscosity coefficient. A useful derivation of the mean equations of motion and the Reynolds stress equations in terms of mass-averaged variables has been given by Rubesin and Rose (ref. 15). A proliferation of explicit mean-product fluctuation terms arising from compressibility is avoided by this technique. The resulting mean-flow equations are formally the same as their laminar flow counterparts, except for the addition of the Reynolds stress tensor and additional mean-dissipation terms. The mass-averaged Reynolds stress equations correspond, term by term, to the constant property equation of Rotta (ref. 16) and the turbulence kinetic energy equation is consistent with Rotta's and Townsend's (ref. 17) constant property equations. Consequently, turbulence models that have evolved from Reynolds stress equations for incompressible flows can be applied to compressible flows (albeit the constants may change due to compressibility).

The turbulence models employed in this paper express the Reynolds stress tensor in terms of an eddy viscosity ε. A Reynolds analogy is used for the Reynolds heat flux and a laminar analogy for the mean-dissipation tensor. Thus the vectors U, F, G, E in equation (1), which correspond to the mean-flow equations, can be expressed in the form

$$U = \begin{pmatrix} \rho \\ \rho u \\ \rho v \\ e \end{pmatrix}, \quad F = \begin{pmatrix} \rho u \\ \rho uu + \sigma_x \\ \rho vu + \tau_{xy} \\ (e + \sigma_x)u + \tau_{xy} + q_x \end{pmatrix}, \quad G = \begin{pmatrix} \rho v \\ \rho uv + \tau_{xy} \\ \rho v^2 + \sigma_y \\ (e + \sigma_y)v + \tau_{xy}u + q_y \end{pmatrix}, \quad E = \begin{pmatrix} 0 \\ 0 \\ 0 \\ 0 \end{pmatrix}. \tag{78}$$

The density ρ is a mean value and the velocities u, v are mass-averaged values. The bulk viscosity in the viscous terms is taken to be zero. Thus the stresses are

$$\sigma_x = p + \frac{2}{3}(\mu + \varepsilon)\left(\frac{\partial u}{\partial x} + \frac{\partial v}{\partial y}\right) - 2(\mu + \varepsilon)\frac{\partial u}{\partial x} + \frac{2}{3}\rho e_s , \tag{79}$$

$$\tau_{xy} = \tau_{yx} = -(\mu + \varepsilon)\left(\frac{\partial u}{\partial y} + \frac{\partial v}{\partial x}\right) , \tag{80}$$

$$\sigma_y = p + \frac{2}{3}(\mu + \varepsilon)\left(\frac{\partial u}{\partial x} + \frac{\partial v}{\partial y}\right) - 2(\mu + \varepsilon)\frac{\partial v}{\partial y} + \frac{2}{3}\rho e_s , \tag{81}$$

and the heat-flux components are

$$q_x = -\left(\frac{\mu}{P_R} + \frac{\varepsilon}{P_{RT}}\right)\gamma\frac{\partial e_i}{\partial x} , \tag{82}$$

and

$$q_y = -\left(\frac{\mu}{P_R} + \frac{\varepsilon}{P_{RT}}\right)\gamma\frac{\partial e_i}{\partial y} . \tag{83}$$

The last term in equations (79) and (81) arises from the definition of static pressure as the mean of the three normal stresses (including Reynolds stresses). The quantity e_s is the turbulent energy per unit mass of fluid. The mass-averaged specific internal energy e_i is related to the mean total energy per unit volume e, as in laminar flow, by

$$e_i = \frac{e}{\rho} - \frac{u^2 + v^2}{2} . \tag{84}$$

Equations of state relate the mean pressure p and temperature T to ρ and e_i. The perfect gas relations

$$p = (\gamma - 1)\rho e_i \tag{85}$$

and

$$T = \frac{e_i}{C_v} \tag{86}$$

and the Sutherland viscosity relation

$$\mu = \frac{C_1 T^{3/2}}{C_2 + T} \tag{87}$$

are valid approximations at the conditions of experiments referred to in this paper. In these relations the ratio of specific heats γ is equal to 1.4 and C_v is equal to 4290 ft lb/slug °R (717.53 in MKS units). The constant C_1 is 2.27×10^{-8} slug °R/ft sec (1.4582×10^{6} MKS) and C_2 is 198.6 °R (110.333 MKS).

Differencing Method for Rectangular Mesh

As discussed in the section on numerical methods, the fluxes and stresses are evaluated at cell faces between the computation points in such a manner as to achieve second-order accuracy after the predictor-corrector sequence is concluded. It is sufficient to describe the technique for the L_x operator, since the procedure is the same for the L_y operator with (x,y), (u,v), and (i,j) interchanged. The L_x operator requires evaluation of the terms of F in equation (78) at cell faces $[i + (1/2)]$ between computation points i and i+1, which are at the centers of the cells. Treatment of quantities appearing in F that do not entail derivatives is exemplified by the notation

$$\rho_{i+(1/2)} = \begin{cases} \rho_i & \text{, for predictor} \\ \rho_{i+1} & \text{, for corrector .} \end{cases} \tag{88}$$

However, there is one exception to this rule. To avoid a nonlinear instability that arises when u changes from negative to positive within a cell, the u that multiplies ρ, ρu, ρv, and $(e + \sigma_x)$ is modified according to the relation

$$u_{i+(1/2)} = \frac{1}{2}(u_{i+1} + u_i), \text{ if } (u_{i+1} - u_i) > 0 \text{ and } (3u_{i+1} - u_i)(3u_i - u_{i+1}) < 0 , \tag{89}$$

in both predictor and corrector (ref. 1). The j subscript has been omitted in equations (88) and (89) since the center of the cell face lies at the same value of y as the center of the cell in a rectangular mesh. Also, for simplicity, the bar overscript representing predicted quantities is omitted here and in subsequent relations.

Treatment of derivatives appearing in F is according to the notation

$$\left(\frac{\partial u}{\partial x}\right)_{i+(1/2),j} = \frac{u_{i+1,j} - u_{i,j}}{x_{i+1} - x_i} \text{ , for predictor and corrector ,} \tag{90}$$

and

$$\left(\frac{\partial u}{\partial y}\right)_{i+(1/2),j} = \begin{cases} \dfrac{u_{i,j+1} - u_{i,j-1}}{y_{j+1} - y_{j-1}} & \text{, for predictor} \\ \dfrac{u_{i+1,j+1} - u_{i+1,j-1}}{y_{j+1} - y_{j-1}} & \text{, for corrector .} \end{cases} \tag{91}$$

Integral Form For Nonorthogonal Mesh

When the boundaries of the flow field under investigation are not aligned with a rectangular mesh, many computational problems are avoided by the use of a nonorthogonal mesh that does fit the boundaries. In the absence of source terms, integration of equation (1) over a volume element converts equation (1) into the following form:

$$\frac{\partial}{\partial t}\int_{vol} U \, d\,vol + \int_S \vec{H}\cdot\vec{n}\, ds = 0 , \tag{92}$$

where

$$U \equiv \begin{pmatrix} \rho \\ \rho u \\ \rho v \\ e \end{pmatrix} , \quad \vec{H} \equiv \begin{pmatrix} \rho\vec{q} \\ \rho u\vec{q} + \ddot{\tau}\cdot\vec{e}_x \\ \rho v\vec{q} + \ddot{\tau}\cdot\vec{e}_y \\ e\vec{q} + \ddot{\tau}\cdot\vec{q} - k\vec{\nabla}T \end{pmatrix} . \tag{93}$$

The velocity vector $\vec{q}$ and stress tensor $\ddot{\tau}$ can be expressed, respectively, as

$$\vec{q} \equiv u\vec{e}_x + v\vec{e}_y ,$$

$$\vec{\vec{\tau}} \equiv \sigma_x \vec{e}_x\vec{e}_x + \tau_{xy}\vec{e}_x\vec{e}_y + \tau_{yx}\vec{e}_y\vec{e}_x + \sigma_y\vec{e}_y\vec{e}_y ,$$

where $\vec{e}_x$, $\vec{e}_y$ are unit vectors, $\vec{n}$ is a unit vector normal to the surface of the computation cell, and σ_x, τ_{xy}, σ_y are defined in equations (79)-(81). These equations can be solved in the Cartesian x,y coordinate system for an arbitrary quadrilateral volume element (sketch a).

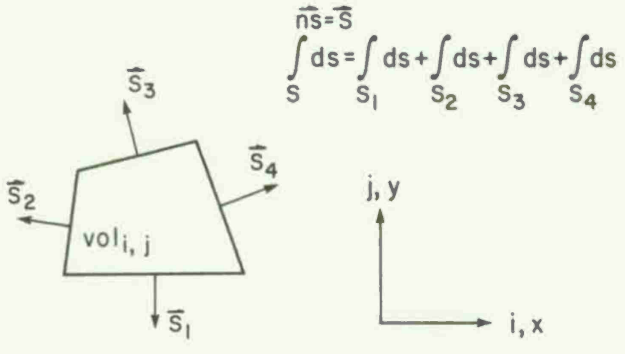

Sketch a. Quadrilateral volume element.

According to MacCormack (ref. 18), equations (4) and (5) in the L_y operator are replaced by

$$\left.\begin{aligned} \text{predictor:}\quad & \overline{U^{n+(1/2)}_{i,j}} = U^{n}_{i,j} - \frac{\Delta t}{vol_{i,j}}\left(\vec{H}^{n}_{i,j}\cdot\vec{S}_3 + \vec{H}^{n}_{i,j-1}\cdot\vec{S}_1\right) \\ \text{corrector:}\quad & U^{n+(1/2)}_{i,j} = \frac{1}{2}\left\{U^{n}_{i,j} + \overline{U^{n+(1/2)}_{i,j}} - \frac{\Delta t}{vol_{i,j}}\left[\vec{H}^{\overline{n+(1/2)}}_{i,j+1}\cdot\vec{S}_3 + \vec{H}^{\overline{n+(1/2)}}_{i,j}\cdot\vec{S}_1\right]\right\} \end{aligned}\right\} \qquad (94)$$

where superscript n is a timestep index and $\vec{S}_1 \ldots \vec{S}_4$ are area vectors for the volume element $vol_{i,j}$, and the L_x operator becomes

$$\left.\begin{aligned} \text{predictor:}\quad & \overline{U^{n+1}_{i,j}} = U^{n+(1/2)}_{i,j} - \frac{\Delta t}{vol_{i,j}}\left[\vec{H}^{n+(1/2)}_{i,j}\cdot\vec{S}_4 + \vec{H}^{n+(1/2)}_{i-1,j}\cdot\vec{S}_2\right] \\ \text{corrector:}\quad & U^{n+1}_{i,j} = \frac{1}{2}\left[U^{n+(1/2)}_{i,j} + \overline{U^{n+1}_{i,j}} - \frac{\Delta t}{vol_{i,j}}\left(\vec{H}^{\overline{n+1}}_{i+1,j}\cdot\vec{S}_4 + \vec{H}^{\overline{n+1}}_{i,j}\cdot\vec{S}_2\right)\right] \end{aligned}\right\} \qquad (95)$$

The solution can be advanced more frequently with smaller timesteps in regions of fine mesh as mentioned in the discussion that follows equation (5). To evaluate the viscous derivatives for a nonorthogonal mesh, the following transformation is appropriate:

$$\frac{\partial\phi}{\partial x} = \frac{\partial\phi}{\partial\xi}\frac{\partial\xi}{\partial x} + \frac{\partial\phi}{\partial\eta}\frac{\partial\eta}{\partial x} , \quad \frac{\partial\phi}{\partial y} = \frac{\partial\phi}{\partial\xi}\frac{\partial\xi}{\partial y} + \frac{\partial\phi}{\partial\eta}\frac{\partial\eta}{\partial y} , \qquad (96)$$

where ϕ is a dummy dependent variable and (ξ,η) are the local coordinates of the nonorthogonal mesh (sketch b). The derivatives are differenced according to the relations

$$\frac{\partial\phi}{\partial x} = \frac{\Delta\phi_\xi\Delta y_\eta - \Delta\phi_\eta\Delta y_\xi}{\Delta x_\xi\Delta y_\eta - \Delta x_\eta\Delta y_\xi} , \quad \frac{\partial\phi}{\partial y} = \frac{\Delta\phi_\xi\Delta x_\eta - \Delta\phi_\eta\Delta x_\xi}{\Delta y_\xi\Delta x_\eta - \Delta y_\eta\Delta x_\xi} , \qquad (97)$$

where (for surfaces S_3 and S_4)

$$\Delta\phi_\xi = \phi_{i+1,jj} - \phi_{im,jj} , \quad \Delta\phi_\eta = \phi_{ii,j+1} - \phi_{ii,jm} , \qquad (98)$$

$$\Delta x_\xi = x_{i+1,jj} - x_{im,jj} , \quad \Delta x_\eta = x_{ii,j+1} - x_{ii,jm} , \qquad (99)$$

$$\Delta y_\xi = y_{i+1,jj} - y_{im,jj} , \quad \Delta y_\eta = y_{ii,j+1} - y_{ii,jm} , \qquad (100)$$

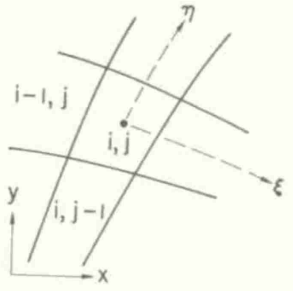

Sketch b. Nonorthogonal mesh notation.

and

$$im = \begin{cases} i & \text{for Lx} \\ i-1 & \text{for Ly} \end{cases}, \quad ii = \begin{cases} i \\ i+1 & \text{for Lx corrector} \end{cases}, \tag{101}$$

$$jm = \begin{cases} j-1 & \text{for Lx} \\ j & \text{for Ly} \end{cases}, \quad jj = \begin{cases} j \\ j+1 & \text{for Ly corrector} \end{cases}. \tag{102}$$

This treatment of the viscous derivatives always results in centered differences, maintains the second-order accuracy obtained by symmetric ordering of the L_x and L_y operators, and provides consistent treatment of discontinuous boundary conditions (such as at the leading and trailing edges of airfoils). The algorithm represented by equation (89) is again necessary to avoid a nonlinear instability associated with an expansion in which the velocity changes sign.

TURBULENCE MODELS

Mixing Length Model

A simple mixing-length model (ref. 3) was used by Deiwert (refs. 9, 11) to treat turbulence for the calculation of separated flow over a thick airfoil. Detailed solutions are discussed in a later section. Using this mixing-length model, the eddy viscosity ε, in the neighborhood of the wall, is defined as

$$\varepsilon = \rho \ell^2 \left| \frac{\partial u}{\partial y} + \frac{\partial v}{\partial x} \right| , \tag{103}$$

where

$$\ell = 0.4\, y \left[1 - \exp\left(-y \sqrt{\left| \frac{\rho}{\mu} \frac{\partial u}{\partial y} \right|_w} \Big/ 26 \right) \right] \tag{104}$$

until the following value of ℓ is reached and subsequently used:

$$\ell = 0.07\delta$$

where δ is determined by an arbitrary cutoff criterion based on the vorticity. For the wake region,

$$\varepsilon = 0.001176 \rho \delta \left| u_\delta - u_{\mathfrak{L}} \right| , \tag{105}$$

where u_δ and $u_{\mathfrak{L}}$ are the velocities at the edge of the wake and its centerline, respectively.

While ultimately it will be necessary to resort to more advanced turbulence models for separated flows, the above model should provide some insight into the influence of Reynolds numbers on such flows, as well as provide an instrument for the development of the requisite numerical methods.

Two-Equation Turbulence Model

Calculations have been carried out by Baldwin and MacCormack (ref. 8) for the shock-separated hypersonic turbulent boundary layer based on either the simple mixing-length model or on the Saffman-Wilcox (ref. 5) model. In the two-equation turbulence model, the eddy viscosity is assumed to be a function of local properties of the turbulence. The properties selected are the specific turbulent energy e_s and the pseudovorticity (or rate of dissipation) Ω, which satisfy equation (1) with

$$U = \begin{pmatrix} \rho e_s \\ \rho\Omega^2 \end{pmatrix}, \qquad F = \begin{pmatrix} \rho e_s u + e_x \\ \rho\Omega^2 u + \omega_x \end{pmatrix},$$

$$G = \begin{pmatrix} \rho e_s v + e_y \\ \rho\Omega^2 v + \omega_y \end{pmatrix}, \quad E = \begin{pmatrix} e_e \\ e_\omega \end{pmatrix}, \tag{106}$$

where

$$e_x = -(\mu + \sigma^* \varepsilon) \frac{\partial e_s}{\partial x},$$

$$e_y = -(\mu + \sigma^* \varepsilon) \frac{\partial e_s}{\partial y},$$

$$\omega_x = -(\mu + \sigma \varepsilon) \frac{\partial \Omega^2}{\partial x},$$

$$\omega_y = -(\mu + \sigma \varepsilon) \frac{\partial \Omega^2}{\partial y}, \tag{107}$$

$$e_e = \left[\alpha^* \sqrt{\left(\frac{\partial u}{\partial y} + \frac{\partial v}{\partial x}\right)^2 + 2\left(\frac{\partial u}{\partial x}\right)^2 + 2\left(\frac{\partial v}{\partial y}\right)^2} - \beta^* \rho\Omega - \xi_s \left(\frac{\partial u}{\partial x} + \frac{\partial v}{\partial y}\right) \right] \rho e_s,$$

$$e_\omega = \left[\alpha \sqrt{\left(\frac{\partial u}{\partial x}\right)^2 + \left(\frac{\partial u}{\partial y}\right)^2 + \left(\frac{\partial v}{\partial x}\right)^2 + \left(\frac{\partial v}{\partial y}\right)^2} - \beta \rho\Omega \right] \rho\Omega^2 .$$

The values of the constants σ^*, σ, α^*, α, β^*, β, ξ_s are 0.5, 0.5, 0.3, 0.2638, 0.09, 0.18, and 2.5, respectively. The eddy viscosity ε appearing in the above relations, as well as in the mean-flow equations, is given by

$$\varepsilon = \frac{e_s}{\Omega} \tag{108}$$

Saffman (ref. 19), Wilcox and Alber (ref. 20), and other authors have demonstrated a wide range of applicability of the above model for incompressible and compressible flows. More recently, Saffman and Wilcox (ref. 5) have shown that the model provides reasonable predictions of viscous sublayers in turbulent boundary layers and reproduces the law of the wall, which has been observed experimentally. For this application, the appropriate boundary conditions with a wall at $y = 0$ are

$$(e_s)_{y=0} = 0 \tag{109}$$

$$(\Omega)_{y=0} = \frac{\tau_w}{\alpha^* \rho_w \mu_w} S\left(z_0 \frac{\sqrt{\tau_w \rho_w}}{\mu_w}\right) \tag{110}$$

where the subscript w refers to conditions in the gas at the wall. The function S is assumed to be a universal function of its argument, which includes as a factor the wall roughness height z_0. By comparison of calculations with measurements in incompressible flows, Saffman and Wilcox (ref. 5) have found the approximate variation of S in the entire range from rough to smooth walls. In particular, S equal to 100 or greater corresponds to smooth walls, as in the present application. In the far outer inviscid flow, following Wilcox (ref. 21), e_s and Ω are given constant values that correspond approximately to wind-tunnel turbulence and produce a negligible value of eddy viscosity.

Equations (50) and (51), used earlier to demonstrate numerical techniques, are derived from equations (1), (106), and (107) by retention of the dominant terms e_y and ω_y in G, retention of $-\beta^* \rho\Omega \rho e_s$ in e_e, and deletion of all terms except $-\beta \rho\Omega \rho\Omega^2$ in e_ω. Further, ε is neglected compared to μ, which is approximated by μ_w, the value at the wall, and ρ approximated by ρ_w. These are valid approximations in the viscous sublayer. Finally, equations (50) and (51) follow from the transformation $\zeta = (\Omega/\Omega_w)^2$, $\tau = (C/20)t$, $\eta = \sqrt{C/20}\, y$, where $C = \beta \rho_w^2 \Omega_w / \mu_w$.

The differencing technique for the turbulence model equations according to the basic numerical method used in this investigation is the same as for the mean-flow equations.

RESULTS

Separated Transonic Flow over an Airfoil

High Reynolds-number transonic flows exhibit several features that are important to aerodynamic design. Flow past an airfoil in a high Mach-number subsonic freestream contains a supersonic region somewhere between leading and trailing edges. The supersonic flow becomes subsonic by passing through a standing shock. If the shock strength is large enough, boundary-layer separation will occur. Depending on the airfoil configuration, there may be separation at the trailing edge, as well as the shock-induced

separation, and the two regions may coalesce. To further complicate the analysis of such flows, the boundary layer is generally turbulent, and its response to adverse pressure gradients may depend on the Reynolds number.

To develop techniques for the investigation of such flow fields and assess the influence of the Reynolds number, the flow over a two-dimensional 18-percent-thick biconvex airfoil at zero angle-of-attack is simulated for chord Reynolds numbers of 1, 2, 4, and 6.67×10^6 and a freestream Mach number of 0.775. The numerical method used is described in the section on the integral form for nonorthogonal mesh. The turbulence is represented by the mixing-length model defined in equations (103)-(105).

The airfoil, initially at rest, is impulsively started at time zero at the final freestream Mach number and pressure. Figure 7 shows the control volume within which the flow field development is followed in time. At a sufficient distance upstream of the leading edge (in this case, 6 chord lengths), the flow is assumed uniform at the freestream conditions ($u = U_\infty$, $v = 0$) as it is along the far transverse boundary (again, 6 chord lengths away). The downstream boundary is positioned far enough downstream of the trailing edge (9 chord lengths) that all gradients in the flow direction can be assumed negligible. The surface of the airfoil is impermeable and no-slip boundary conditions are imposed ($u = v = 0$). The airfoil is assumed adiabatic ($\vec{\nabla}T\cdot\vec{n} = 0$) and the normal surface pressure gradient taken to be zero ($\partial p/\partial n = 0$). Ahead of and behind the airfoil the flow is symmetric. To simulate boundary-layer separation reliably, it is necessary to resolve the boundary layer all the way into the viscous sublayer. As a rule of thumb, a first mesh spacing of $\Delta y_{min} = (2/3)c/\sqrt{Re_c}$ is adequate.

The mesh shown in figure 8 contains 50 by 38 computation points. In the x direction, the mesh is uniform over the airfoil (20 stations) and is exponentially stretched ahead (10 stations) and behind (20 stations). In the y direction, a coarse mesh of 26 points is exponentially stretched away from the airfoil. The innermost region is further subdivided into a medium mesh of 10 exponentially stretched points, and the innermost of these is divided into a fine mesh of 4 uniformly spaced points. The operator sequence $(L_yL_xL_y)^n$ (see discussion following eq. (5)) is used with different timesteps in the fine, medium, and coarse meshes according to the relation

$$\Delta t = \left[\frac{h}{|v| + a + \frac{\alpha_1}{h}(\mu + \varepsilon)/\rho}\right]_{min},$$

where h is the mesh spacing, v is the appropriate velocity, a the local speed of sound, and α_1 a function of the mesh aspect ratio. All solutions were carried out for a time corresponding to the motion of a fluid particle through 7.5 chord lengths in the mean flow. Convergence to a steady state was determined by monitoring the stress tensor on the body surface and in the near wake.

Figure 9 shows the variations of pressure coefficient over the airfoil surface ($C_p = 2(p - p_\infty)/\rho_\infty u_\infty^2$). The inviscid pressure coefficient is included for comparison. All of the viscous solutions lie to the left of the inviscid solution because of boundary-layer displacement effects. Of the features affected by viscosity, the shock location is most affected as a result of flow separation that is present in the viscous solutions. At the trailing edge, the viscous flow pressure distributions show a plateau in the region of a long separation bubble extending into the wake. As the Reynolds number is decreased, the shock strength is diminished and the shock location moves upstream. This results from the thickening of the boundary layer and decrease in momentum, which increases the susceptibility to separation. A decrease in Reynolds number is also accompanied by a decrease in pressure recovery behind the shock, indicating larger displacement effects in the separated region. For the particular geometry under consideration, the influence of the Reynolds number on surface pressure distribution is not great, but is in the directions to be expected. For the range of Reynolds numbers considered, the shock is centered ($c_p = c_p^*$) between the 73- and 75-percent chord.

Figure 10 shows the skin-friction variation over the airfoil surface ($c_f = 2\tau_w/\rho_\infty u_\infty^2$). Ahead of the shock, as the Reynolds number is decreased, the skin-friction coefficient is increased. Separation occurs farther upstream at the lower Reynolds numbers, and, for the four Reynolds numbers considered, begins between the 69- and 72-percent chord, some 3-percent chord ahead of the shock location indicated from the pressure plots. Aft of the shock-induced separation region, the flow tends to reattach, but merges with the trailing edge separation. The skin-friction coefficient distribution for the lowest Reynolds number exhibits the widest variation in the combined separation region and, in fact, almost reattaches. This tendency becomes less pronounced with increasing Reynolds number.

Figures 11(a) and 11(b) show variations of displacement and momentum thicknesses, respectively. Both thickness parameters increase with decreasing Reynolds number and vary by more than three orders of magnitude over the length of the airfoil. Immediately ahead of the shock-induced separation region, both thickness parameters begin increasing dramatically over the separation bubble. This thickening is due to the reverse flow near the airfoil surface.

Typical boundary-layer profiles ahead of the shock are compared in figure 12 with the "law of the wall." The symbols represent the numerical solution and are at values of y^+ that correspond to the centers of the computation cells. The profiles each have one point in the viscous sublayer where u^+ varies linearly with y^+ so that accurate values of skin friction can be computed. It can be seen that resolution through the wall and wake-flow regions of the boundary layer is adequate for attainment of realistic solutions.

Velocity profiles in the separation region are shown in figure 13. These variations over the aft portion of the airfoil and in the wake are plotted in terms of physical coordinates. The first separated profile is at 0.725 chord, indicating separation somewhat ahead of that station. The shock location is immediately downstream at about 0.740 chord. The reattachment point is nearly 0.2-chord downstream of the trailing edge. Figure 13 also shows the dividing streamline within which the net mass flow is zero. Details of the solutions in the separated region are similar for the other cases at higher Reynolds number.

Figure 14 is a Mach-number contour plot near the surface of the airfoil. Contours are shown for $0 \leq M \leq 1.4$ in increments of 0.02. Thickening of the boundary layer as it progresses down the airfoil is clearly indicated. At a station near 70-percent chord, the shock impinges on the boundary layer and the flow separates, resulting in large displacement effects. Large transverse gradients in the boundary layer gradually die out in the wake. Inside the separation bubble, the gradients are much smaller than in the boundary layer or near wake, indicating a lower speed and nearly constant density flow.

Figure 15(a) shows isobars and 15(b) Mach-number contours from the calculation at the highest Reynolds number $Re_c = 6.67 \times 10^6$. These plots clearly indicate the position of the standing shock, and, in figure 15(b), the boundary layer, wake, and separation bubble off the trailing edge are apparent. The isobars are at $0.46 \leq p/p_\infty \leq 1.32$ in increments of 0.02. The Mach-number contours in figure 15(b) cover a different range than those in figure 14, namely, $0.40 \leq M \leq 1.40$ in increments of 0.02. Because both the forward and rearward stagnation regions of the separation bubble are surrounded by contours of decreasing pressure, they are clearly discernible in the isobar plots.

Shock Induced Separation of a Hypersonic Turbulent Boundary Layer

The flow field investigated is depicted in figure 16. Air flowing from left to right forms a turbulent boundary layer on a flat plate. The shock-wave incident on the boundary layer produces a separation bubble within which there is reversed flow. Deflection of descending streamlines by the plate aft of reattachment gives rise to a reflected shock wave. Calculations of primary interest are confined to the neighborhood of the interaction region within the boundaries of the rectangle BCGF. Flow quantities are held fixed along BC and CG. Zero slip and a constant wall temperature T_w are imposed as boundary conditions along the flat plate. Since the flow equations are either nearly hyperbolic or parabolic along FG, there is little upstream influence, and the flow quantities at the last column of mesh points are equated to the values computed at the next-to-last column of points in each timestep. A calculation starts from a uniform flow, except for the imposed values along BC and CG. The turbulent boundary layer and shock wave grow with time and, eventually, a steady-state solution is achieved. Calculations have been made based on either the mixing-length model of reference (22) or the two-equation turbulence model described by equations (106)-(110).

It was not known at the outset whether the bow wave from formation of the boundary layer would cause significant effects. Consequently, calculations have also been made using the same machine code within the boundaries ABDE. The boundary layer profiles along BD and skin friction and heat transfer computed at B agreed within 10 percent with calculations obtained from a machine code developed by Marvin and Sheaffer (ref. 23) based on the boundary-layer approximation.

The experiment used for comparison was conducted by Holden (ref. 24). Measurements were made of pressure, skin friction, and heat transfer along the flat plate in the interaction region. The case selected for comparison is at Mach number 8.47 and Reynolds number 22.5×10^6 based on freestream conditions and distance from leading edge to shock impingement. The pressure rises by a factor of 83 across incident and reflected shocks. In the calculations, the shock strength is adjusted to match this ratio. The position of the shock is adjusted to match the measured pressure distribution as closely as possible. Figure 17 contains a Schlieren photograph of the experimental flow field in the interaction region.

The computational mesh employed is shown in figure 18. Spacing in the x direction is uniform with $\Delta x = 0.0102$ ft. Mesh spacing in the y direction is also uniform within each of four regions. In the outer inviscid region, which contains 10 rows of points, $\Delta y = 0.0096$ ft. The finest mesh near the wall contains 5 rows of points with $\Delta y = 5 \times 10^{-5}$ ft. Two intermediate regions containing 6 and 10 rows of points are spaced at intervals of $\Delta y = 4 \times 10^{-4}$ and 3.2×10^{-3} ft, respectively.

Figure 19 contains a plot of a velocity profile in terms of universal coordinates showing the degree of resolution achieved. The symbols are at the computational mesh points. The viscous sublayer is well resolved at this station in the initial turbulent boundary layer ahead of the interaction. The departure from the law of the wall in outer regions is due to density variations in this highly cooled boundary layer. An incompressible version of universal coordinates u^+, y^+ was used for simplicity, since a check on resolution of the viscous sublayer was of primary interest.

In regions near the wall, the turbulence model equations pose a more severe resolution problem than the mean-flow equations. This results from steep gradients, which are themselves relatively slowly varying. The aforementioned method that produces exponential accuracy, equations (33)-(38), was used in the L_y operator in the finest mesh. This procedure is particularly suited to boundary layers, which are quasi-one-dimensional. Figure 20 contains plots showing the computed variations of turbulence quantities according to the Saffman-Wilcox model. These profiles are at a station in the initial boundary layer ahead of the interaction. The quantities are nondimensionalized in a way that produces the same variations in the viscous sublayer at all upstream stations except near the leading edge. The peak value of ε/μ_w may appear to be low because values of μ near the peak are a factor of 4 below μ_w. The 3.7 power variation of e_s^+ and -2 power variation of Ω^+ near the wall are in agreement with the exact solution of the simplified model given in equations (61) and (62). The basic numerical method produced entirely different variations. The modification that produces exponential accuracy is essential in this application. The number of mesh points required for comparable results from the basic method would entail prohibitive computation times.

In the region aft of reattachment, the viscous sublayer becomes an order of magnitude thinner than in the boundary layer ahead of the interaction. Straightforward application of the basic numerical method would again require prohibitive computation times in a mesh fine enough to resolve the viscous sublayer. Therefore, we have developed a procedure that utilizes iterative solutions of the steady-state boundary layer approximation near the wall. Periodically, the boundary layer equations are solved iteratively to find the values of τ_w, q_w, $(\partial e_s/\partial y)_w$, and $(\partial \Omega^2/\partial y)_w$ that provide an inner solution matching the values of u_{ij}, $(e_i)_{ij}$, $(e_s)_{ij}$, and Ω_{ij} at the third row of mesh points from the wall. The inner solution then provides values of all variables at the second row of mesh points to be used in succeeding timesteps of the

finite-difference solution. The inner solution is repeated often enough to retain time accuracy of the calculation.

Figure 21 contains a velocity profile obtained by the foregoing technique. At this station, in the compressed region aft of reattachment, the finest mesh of the finite difference solution (square symbols) does not resolve the viscous sublayer. The inner solution described above is represented by circles. It can be seen that the inner solution, extended beyond the region in which it is used (out to J = 3) continues to match the finite difference solution farther out. Calculations were made with and without the use of the inner solution in the separated region where the viscous sublayer is adequately resolved in the finite-difference mesh. The results were insensitive to the use of the boundary-layer approximation within the viscous sublayer, although it is known that the boundary-layer approximation may fail if it is used through the entire viscous region near a separation point with appreciable pressure gradients normal to the wall. Figure 22 contains reversed flow velocity profiles in the separated region. It is apparent that the viscous sublayer must be resolved near the separation point. Departures from the law of the wall are large in this region.

Preliminary calculations were in gross disagreement with the experimental measurements of Holden (ref. 24) in the separated region. The computed pressure rise was much steeper than indicated by the measurements. Errors from the numerical method would be expected to produce a discrepancy in the opposite direction. It was found that this discrepancy in pressure distributions could be removed by introducing a momentum defect in the freestream outside the turbulent boundary layer ahead of the interaction in a manner to be discussed shortly. The calculations indicate that the entropy layer due to the bow wave produced by formation of the boundary layer ahead of the interaction is not of sufficient strength to produce the momentum defect needed. It is possible that intermittent shock waves caused by turbulent eddies do produce an entropy layer of the strength needed. Since we are not equipped to compute such effects, the flow quantities were readjusted at the upstream boundary by the amounts needed for agreement with the experimental pressure distribution. The readjustments were made at constant pressure and constant total temperature as though the momentum defect were produced by shock waves in the flow ahead.

Figure 23 shows the computed and assumed mass-flux profiles ahead of the interaction. The computed profiles are from the machine code of Marvin and Sheaffer (ref. 23), which is based on the boundary-layer approximation. They are also nearly the same as results from the machine code of this investigation applied in the region from the leading edge to the upstream boundary for computation in the interaction region (station BC in fig. 16). In figure 24, comparisons are shown between the measured and computed pressure distributions with and without the assumed momentum defect. The hypersonic pressure coefficient $\tilde{C}_p = 2p/\rho_\infty u_\infty^2$ is used here. Figure 25 shows computed streamlines. Although the assumed momentum defect has only a small effect on the computed skin friction and heat transfer ahead of the interaction, it has a profound effect on the flow in the interaction region. The modification of initial profiles doubles the size of the separation bubble both along the flat plate and normal to it. The remainder of results in this paper are based on the assumed initial profiles that produce agreement with the measured pressure distribution.

Figure 26 contains a plot of skin-friction coefficient showing the real time for a solution to reach a steady state. This is a calculation based on the Saffman-Wilcox model. The solution is started from a converged solution of the mixing-length model. The field of computation extends over a distance of about 0.4 ft (0.12192 m) and includes the interaction region. The plot shows the variation of skin-friction coefficient at the downstream end of the computation field versus time. This result is indicative of the minimum time that a wind tunnel should be operated to reach a state corresponding to arbitrarily longer times. Since the entire flow field of interest, starting at the leading edge of the flat plate is roughly six times as long as the computation field, presumably wind-tunnel operating times should be six times as long as that indicated in the figure. The time required to reach steady state according to the mixing-length model was about the same as in this figure.

In figure 27, comparisons are shown between computed and measured skin friction and heat transfer in the interaction region. The skin friction coefficient is defined as $C_f = 2\tau w/\rho_\infty u_\infty^2$ and the heat transfer coefficient as $C_H = q_w/\gamma(C_v T_{st} - e_{iw})\rho_\infty u_\infty$. The magnitudes of variations in the forward- and reversed-flow regions predicted by both turbulence models are consistent with the measurements. However, the extent of the reversed flow from both calculations exceeds that indicated by the measurements. The levels of skin friction and heat transfer predicted by the mixing-length model aft of reattachment are well below the measured values. The Saffman-Wilcox model prediction of skin friction is in better agreement with the measurements, but still low. Additional calculations were made to estimate the degree of wall roughness that would be required to elevate the computed skin friction to the level indicated by the experiment. It was found that wall roughness heights less than 10^{-5} ft (3.048×10^{-6} m) would not be effective. Information from Holden (ref. 24) indicates that the flat plate itself was an order of magnitude smoother than this. However, the skin-friction-element mountings did present discontinuities of that order to the flow. It may be difficult to make measurements that do not disturb the flow in viscous sublayers as thin as that which develops at the conditions of this experiment.

Differences in the predictions from the simpler (mixing length) and more advanced turbulence models will be discussed presently. The reason for overestimation of the heat transfer aft of reattachment by the Saffman-Wilcox model is not known. The rapid rise of C_H in the neighborhood of reattachment can be attributed to two factors. A high level of turbulent energy is generated over the separation bubble. This turbulence is convected by descending streamlines to a region near the reattachment point. At the same time, the pseudovorticity at the wall goes to zero when τ_w is zero and a finite value of S = 100 is imposed in the boundary condition (eq. (110)). Consequently, the eddy viscosity assumes relatively large values near the reattachment point, compared to values somewhat removed at the same distance from the wall. This is illustrated in figure 28, which contains plots of the ratio of eddy viscosity to molecular velocity at the wall. This anomaly will probably be removed by later versions of the boundary condition on pseudovorticity.

Profiles of the model variables at a station near the downstream end of the computation field are shown in figure 29. The levels of eddy viscosity aft of reattachment according to the Saffman-Wilcox

model are everywhere larger than those from the mixing-length model. This difference can be attributed to lags in adjustments along streamlines, not accounted for by the mixing-length model. According to the Saffman-Wilcox model, turbulence generated over the separation bubble persists downstream and diffuses toward the wall. This effect can be illustrated by defining an equilibrium turbulent energy $(e_s)_{eq}$ as that which would be present if the production and dissipation of turbulent energy were equal with negligible contributions from convection and diffusion. Setting e_e equal to zero in equation (107), neglecting all velocity derivatives except $|\partial u/\partial y|$, and multiplying terms inside the bracket by $\varepsilon = e_s/\Omega$ leads to the relation

$$(e_s)_{eq} = \frac{\alpha^*}{\beta^*} \frac{\varepsilon}{\rho} \left| \frac{\partial u}{\partial y} \right| \tag{111}$$

This is equivalent to Townsend's (ref. 25) definition of equilibrium turbulent energy (with the same numerical constant). In attached boundary layers with zero pressure gradient, e_s assumes values close to $(e_s)_{eq}$, except near the wall. Figure 30 contains plots of the ratio $e_s/(e_s)_{eq}$ from the foregoing numerical solution. The behavior at a station ahead of the interaction is typical of attached boundary layers. The large increase near the wall results from inward diffusion of turbulence, which is destroyed by enhanced degradation and viscous dissipation. However, the peaks in the ratio at downstream stations arise from rapid changes in flow quantities along streamlines. The Saffman-Wilcox model calculation indicates that appreciable departure from equilibrium persists aft of reattachment through the remainder of the computation field.

Calculations of the type described can aid in the design of experiments for the purpose of testing the turbulence models that are evolving. Sensitivity of the flow to experimental practices as well as to computational approximations can be found. Prediction of the required wind-tunnel residence time to establish the flow was insensitive to approximations in the calculations. An unexpected sensitivity of the separated flow field to conditions in the oncoming stream ahead of the interaction was predicted by both turbulence models. The height of permissible roughness on instrumentation that would not disturb the flow in an unknown manner was not greatly different according to the two models for which calculations were made. The calculations were insensitive to use of the boundary-layer approximation within the viscous sublayer, although this approximation may fail if applied farther out in the presence of appreciable pressure gradients normal to the wall. Hopefully, future interaction between experiment and calculation will produce measurements of the needed profiles outside the boundary layer ahead of the interaction.

REFERENCES

1. MacCormack, R. W.: Numerical Solution of the Interaction of a Shock Wave with a Laminar Boundary Layer, Lecture Notes in Physics, vol. 8, New York, Springer-Verlag, 1971, p. 151.

2. Carter, J. E.: Numerical Solutions of the Supersonic Laminar Flow Over a Two-Dimensional Compression Corner, Lecture Notes in Physics, vol. 19, New York, Springer-Verlag, 1973, p. 69.

3. Launder, B. E. and Spalding, D. B.: Lectures in Mathematical Models of Turbulence, New York, Academic Press, 1972.

4. Donaldson, C. du P.: Calculation of Turbulent Shear Flows for Atmospheric and Vortex Motions, AIAA Paper 71-217, presented at AIAA 9th Aerospace Sciences Meeting in New York, Jan. 25-27, 1971.

5. Saffman, P. G. and Wilcox, D. C.: Turbulence Model Predictions for Turbulent Boundary Layers, AIAA Journal, vol. 12, no. 4, 1974.

6. Deardorff, J. W.: A Numerical Study of Three-Dimensional Turbulent Channel Flow at Large Reynolds Numbers, J. Fluid Mech., vol. 41, 1970, p. 453.

7. Yanta, W. J.: Turbulence Measurements with a Laser Doppler Velocimeter, May 1973, Naval Ord. Lab., TR 73-94.

8. Baldwin, B. S. and MacCormack, R. W.: Numerical Solution of the Interaction of a Strong Shock Wave with a Hypersonic Turbulent Boundary Layer, AIAA Paper 74-558, presented at AIAA 7th Fluid and Plasma Dynamics Conference in Palo Alto, June 17-19, 1974.

9. Deiwert, G. S.: Numerical Simulation of High Reynolds Number Transonic Flows, AIAA Paper 74-603, presented at AIAA 7th Fluid and Plasma Dynamics Conference in Palo Alto, June 17-19, 1974.

10. Baldwin, B. S. and MacCormack, R. W.: Interaction of Strong Shock Wave with Turbulent Boundary Layer, Proceedings of 4th International Conference on Numerical Methods at Boulder, Col., July 1974 (to be published).

11. Deiwert, G. S.: High Reynolds Number Transonic Flow Simulation, Proceedings of 4th International Conference on Numerical Methods at Boulder, Col., July 1974 (to be published).

12. MacCormack, R. W.: The Effect of Viscosity in Hypervelocity Impact Cratering, 1969, AIAA Paper 69-354.

13. Kutler, Paul: Computation of Three-Dimensional Inviscid Supersonic Flows, Lecture Notes in Physics, New York, Springer-Verlag, 1974 (to be published).

14. Warming, R. F. and Hyett, B. J.: The Modified Equation Approach to the Stability and Accuracy Analysis of Finite-Difference Methods, J. Comp. Phys., vol. 14, no. 2, Feb. 1974.

15. Rubesin, M. W. and Rose, W. C.: The Turbulent Mean-Flow Reynolds-Stress, and Heat-Flux Equations in Mass-Averaged Dependent Variables, March 1973, NASA TM X-62,248.

16. Rotta, J.: Statistical Theory of Inhomogeneous Turbulence, Part 1, translation (NASA TTF-14,560) of "Statistische Theorie nichthomogener Turbulentz, 1, Mitteilung," Z. Physik, vol. 129, 1951, pp. 547-572.

17. Townsend, A. A.: The Structure of Turbulent Shear Flow, Cambridge University Press, 1956.

18. MacCormack, R. W. and Paullay, A. J.: Computational Efficiency Achieved by Time Splitting of Finite Difference Operators, 1972, AIAA Paper 72-154.

19. Saffman, P. G.: A Model for Inhomogeneous Turbulent Flow, Proc. Roy. Soc. Lond., Series A, vol. 317, 1970, pp. 417-433.

20. Wilcox, D. C. and Alber, I. E.: A Turbulence Model for High Speeds, Proceedings of the 1972 Heat Transfer and Fluid Mechanics Institute, June 1972, Stanford Univ. Press.

21. Wilcox, D. C.: Calculation of Turbulent Boundary Layer Shock Wave Interaction, AIAA Journal, vol. 11, no. 4, 1973, pp. 1592, 1594.

22. Inouye, M.; Marvin, J. G.; and Sheaffer, Y. S.: Turbulent-Wake Calculations with an Eddy-Viscosity Model, AIAA Journal, vol. 10, no. 2, Feb. 1972, pp. 216-217.

23. Marvin, J. G. and Sheaffer, Y. S.: A Method for Solving the Nonsimilar Laminar Boundary-Layer Equations Including Foreign Gas Injection, Nov. 1969, NASA TN D-5516.

24. Holden, M. S.: Shock Wave-Turbulent Boundary Layer Interaction in Hypersonic Flow, AIAA Paper 72-74, presented at AIAA 10th Aerospace Sciences Meeting, San Diego, Jan. 1972 (supplemental data included in private communication).

25. Townsend, A. A.: Equilibrium Layers and Wall Turbulence, J. Fluid Mech., vol. 11, 1961, pp. 97-120.

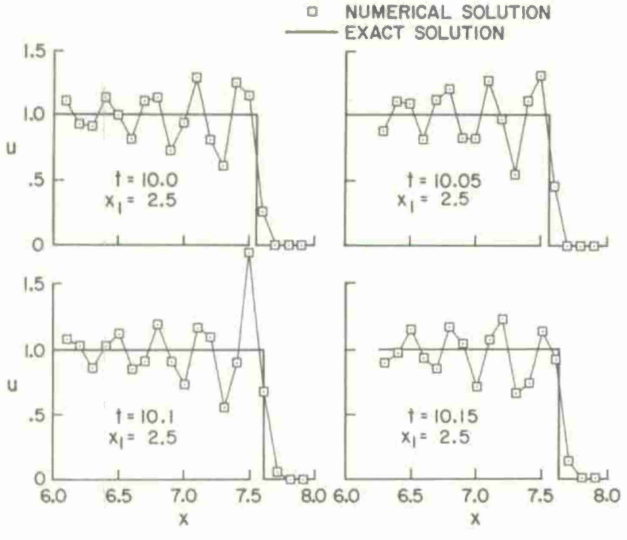

Fig. 1 Solution of Burger's equation (basic method, CFL = 0.1).

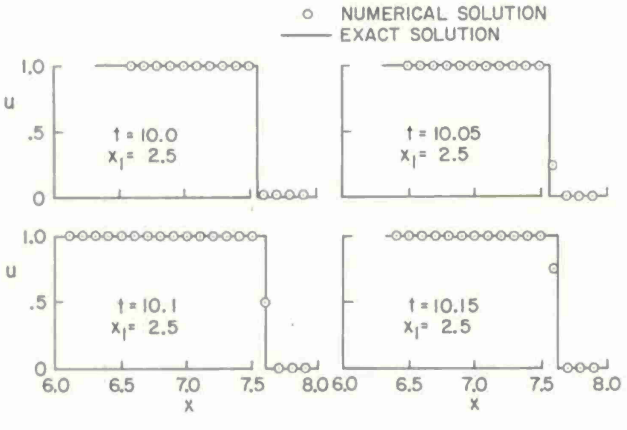

Fig. 2 Solution of Burger's equation (modified method, CFL = 0.1).

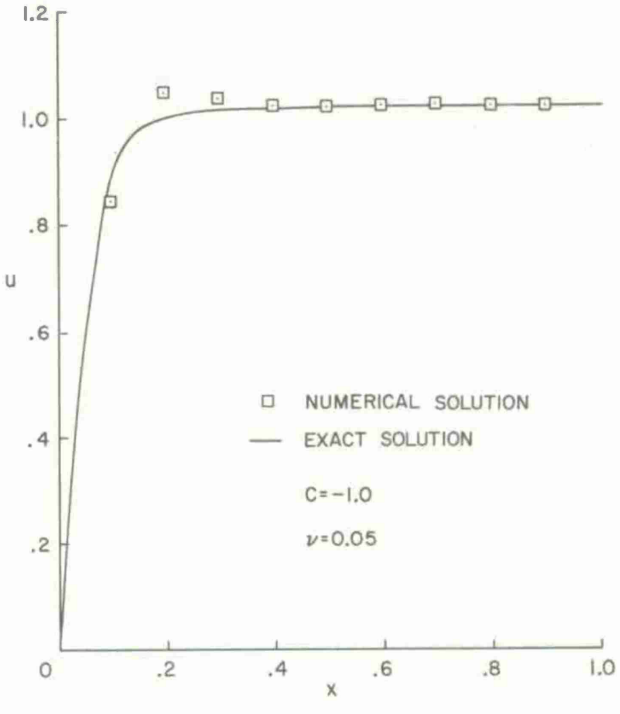

Fig. 3 Linear viscous equation (basic method).

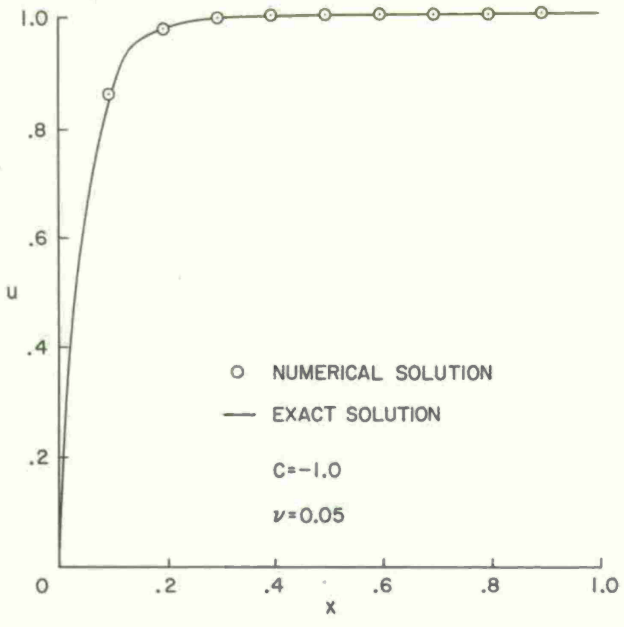

Fig. 4 Linear viscous equation (exponential flux factor).

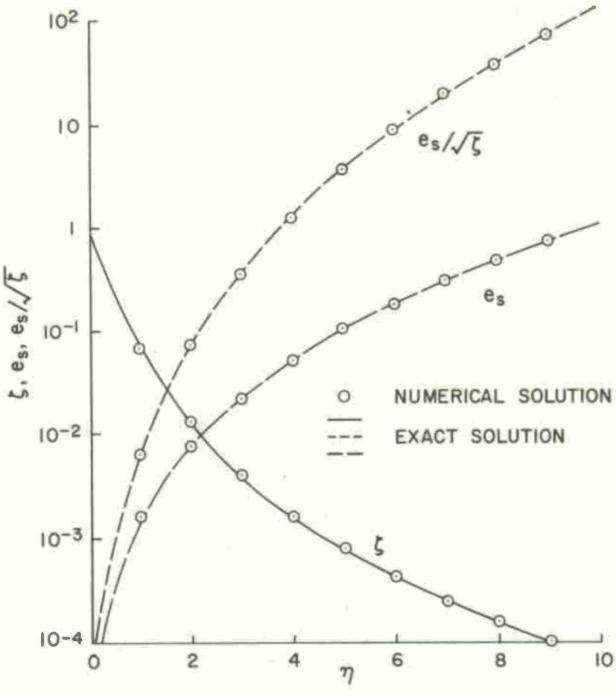

Fig. 6 Simplified turbulence model (exponential accuracy).

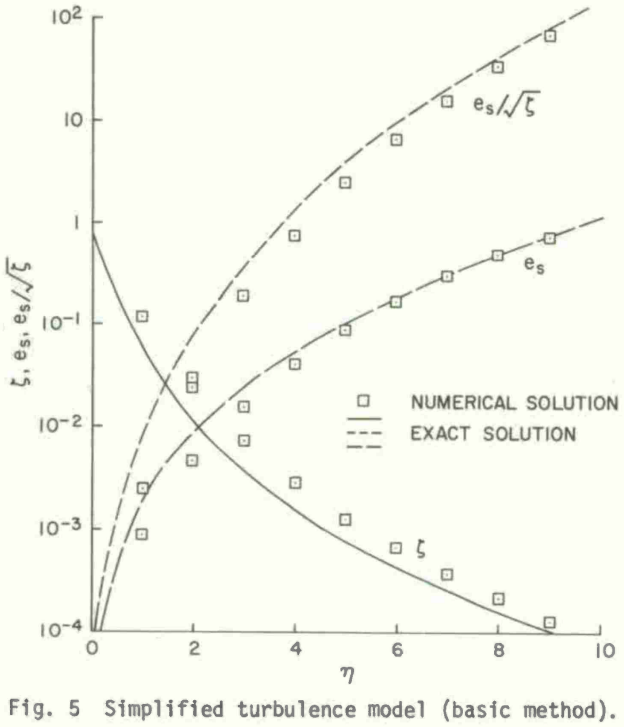

Fig. 5 Simplified turbulence model (basic method).

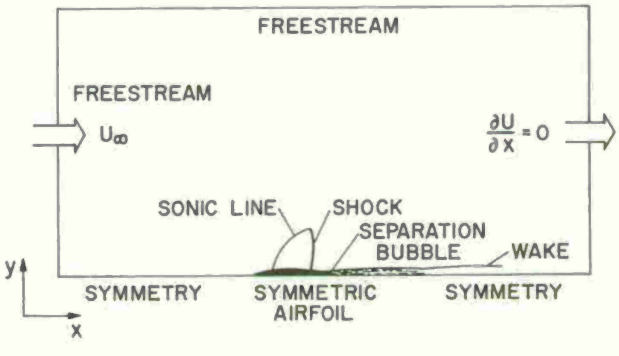

Fig. 7 Computational control volume (flow over airfoil).

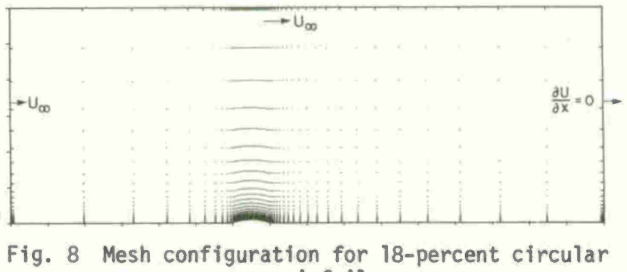

Fig. 8 Mesh configuration for 18-percent circular arc airfoil.

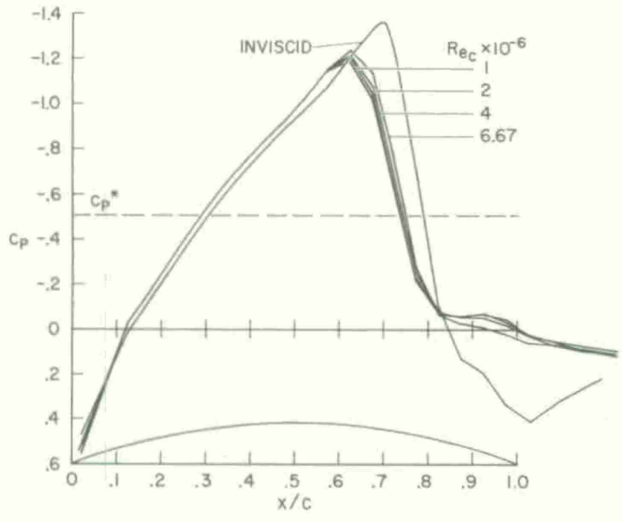

Fig. 9 Pressure distribution over 18-percent circular arc (M_∞ = 0.775).

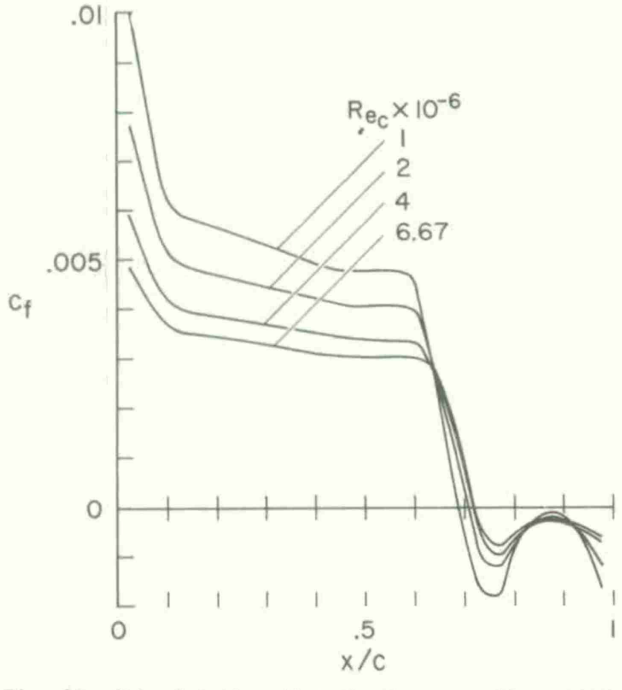

Fig. 10 Skin-friction distribution over 18-percent circular arc (M_∞ = 0.775).

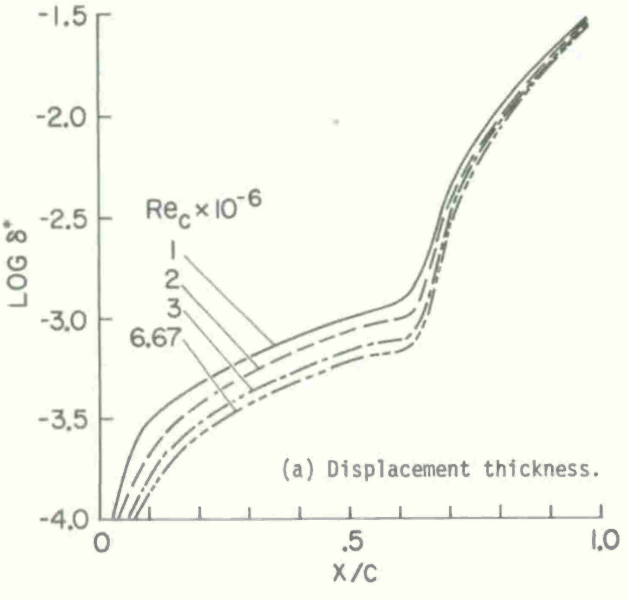

Fig. 11 Thickness parameters on 18-percent circular arc (M_∞ = 0.775).

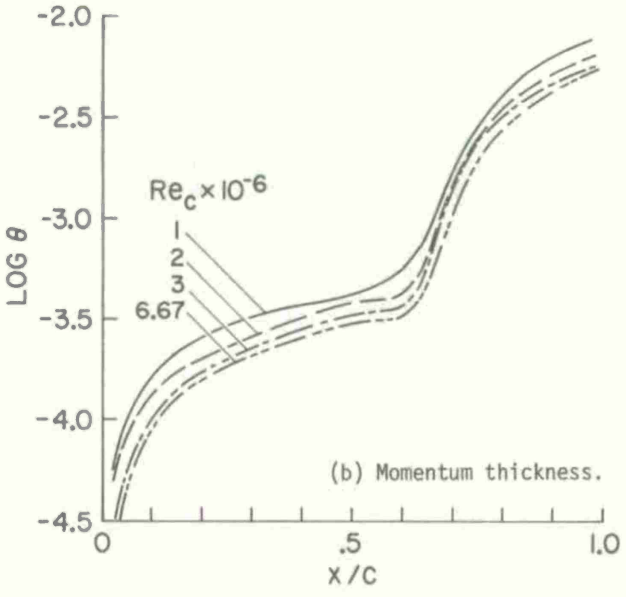

Fig. 11 Concluded.

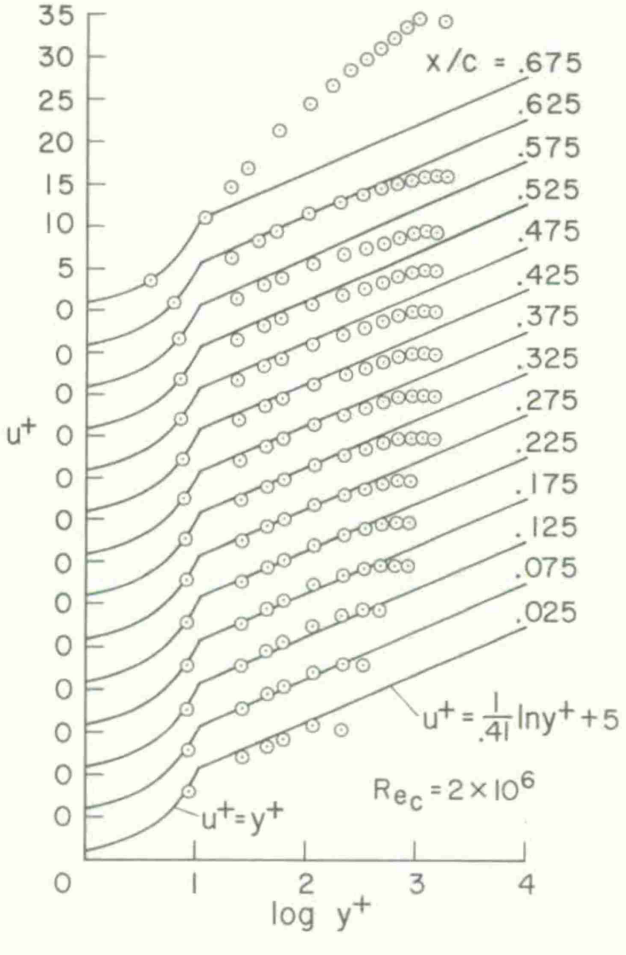

Fig. 12 Velocity profiles ahead of shock.

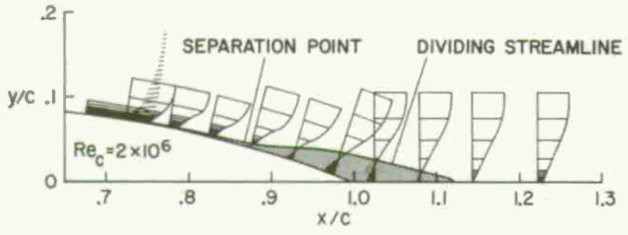

Fig. 13 Separation velocity profiles on 18-percent circular arc (M_∞ = 0.775).

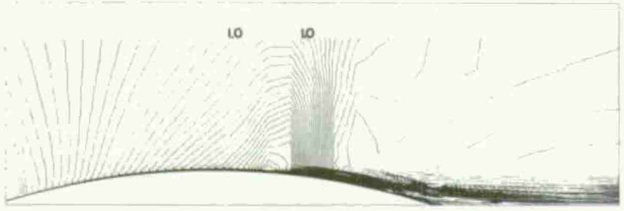

Fig. 14 Mach-number contours (M_∞ = 0.775, Re_c = 4×10^6).

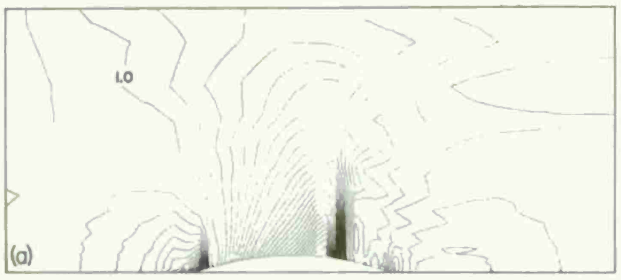

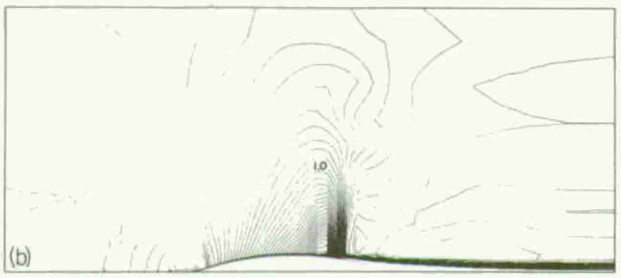

Fig. 15 Flow-field contours (M_∞ = 0.775, Re_c = 6.67×10^6). (a) Isobars. (b) Mach-number contours.

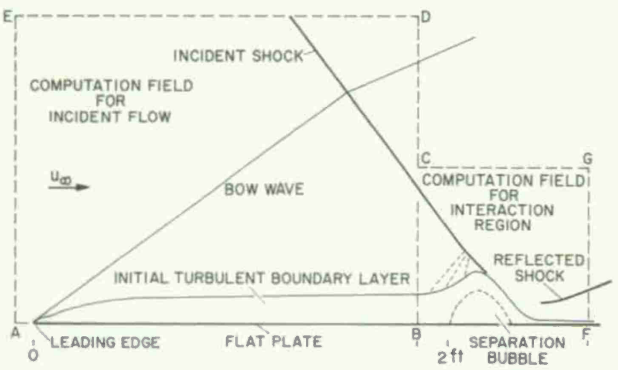

Fig. 16 Shock-induced, separated turbulent flow.

Fig. 17 Schlieren photograph of interaction region.

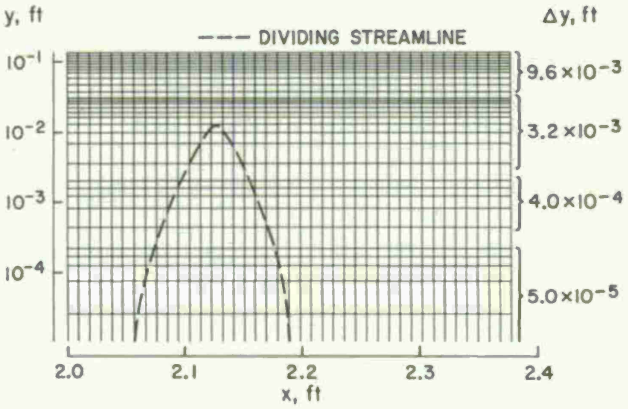

Fig. 18 Computational mesh.

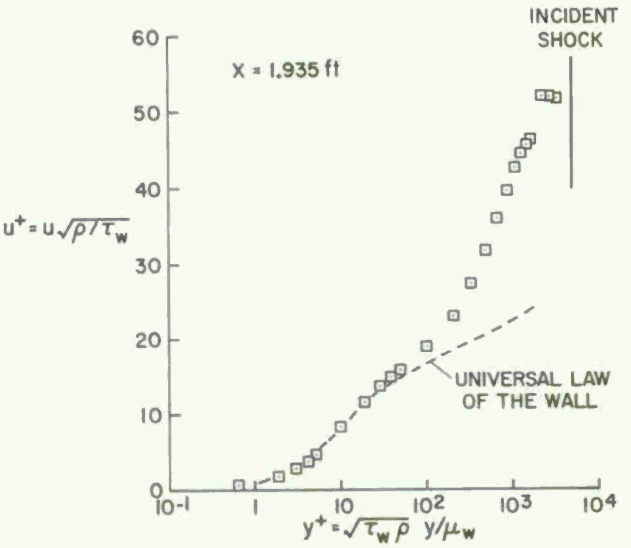

Fig. 19 Velocity profile ahead of interaction.

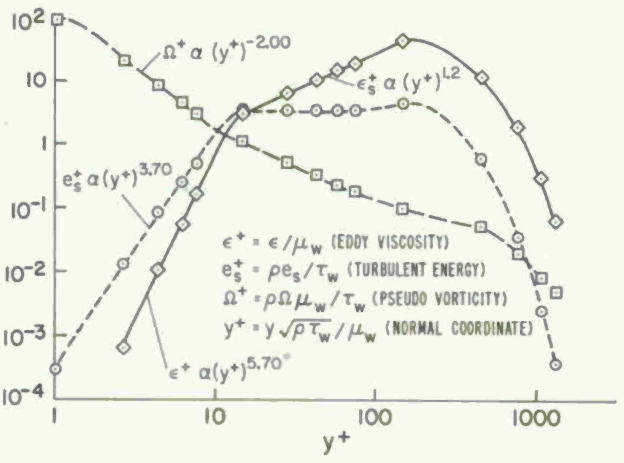

Fig. 20 Turbulence model variations ahead of interaction.

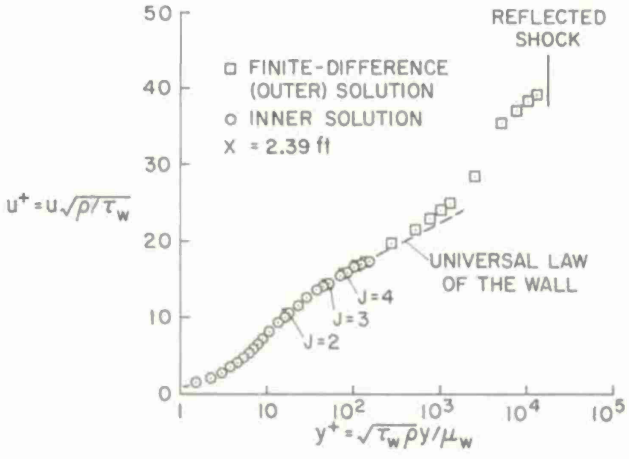

Fig. 21 Velocity profile aft of reattachment.

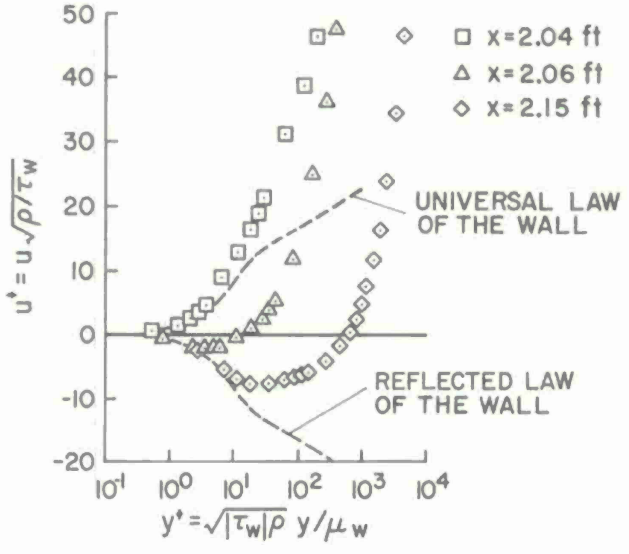

Fig. 22 Velocity profiles in interaction region.

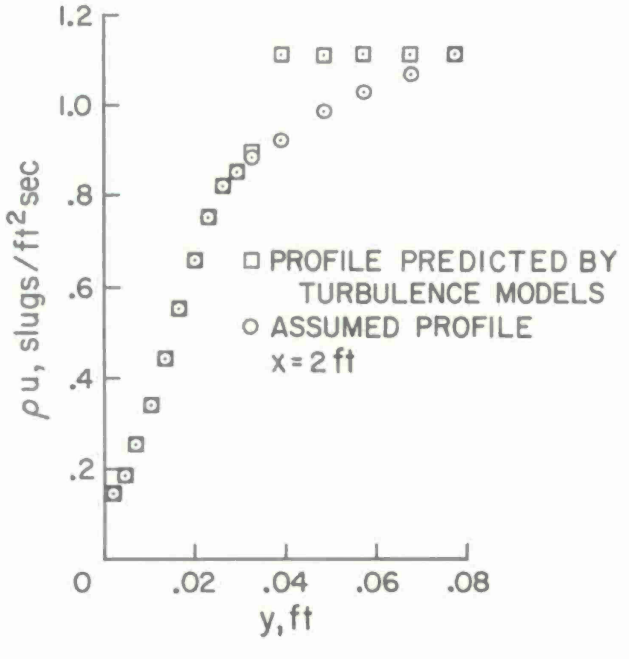

Fig. 23 Mass-flux profiles.

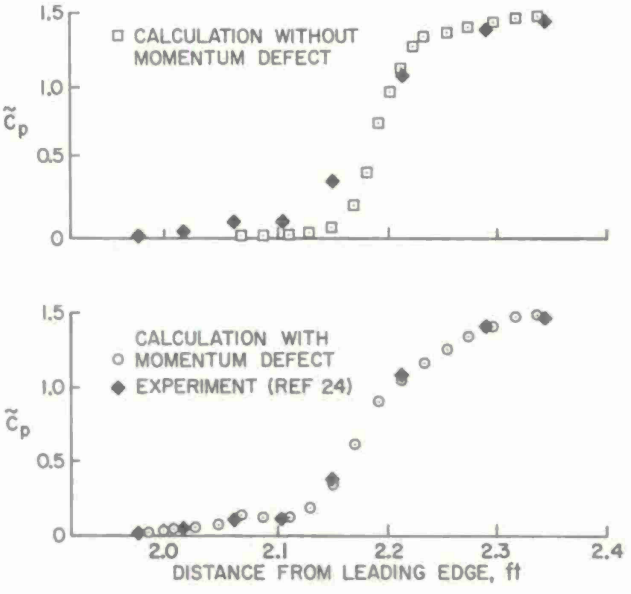

Fig. 24 Pressure distributions.

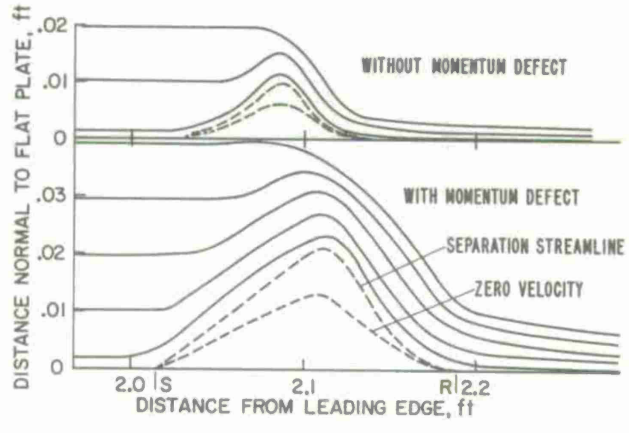

Fig. 25 Computed streamlines.

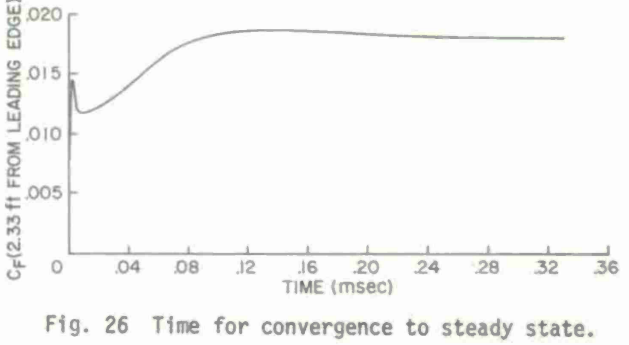

Fig. 26 Time for convergence to steady state.

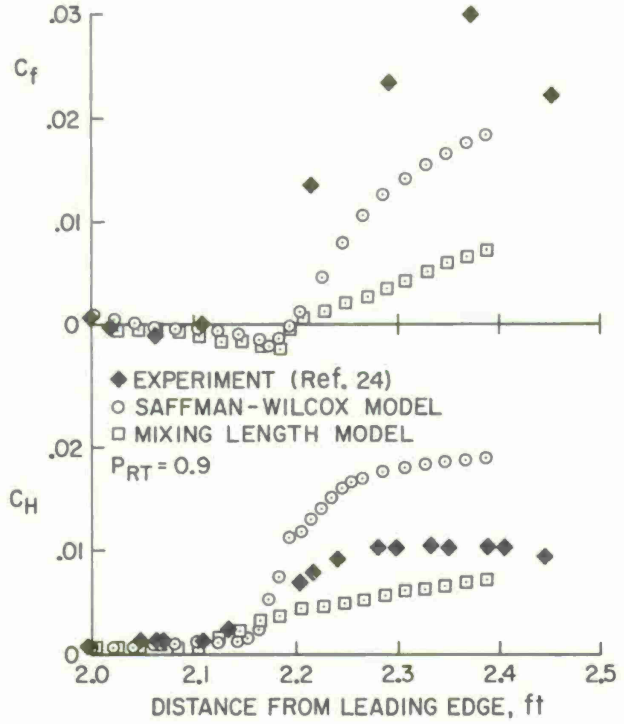

Fig. 27 Comparison with experiment.

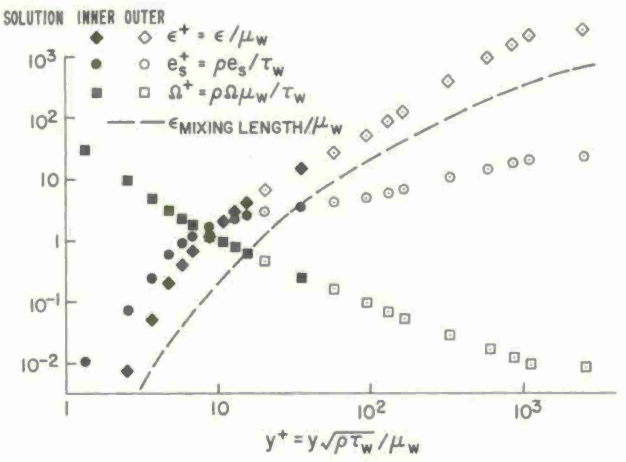

Fig. 29 Turbulence model variations aft of reattachment.

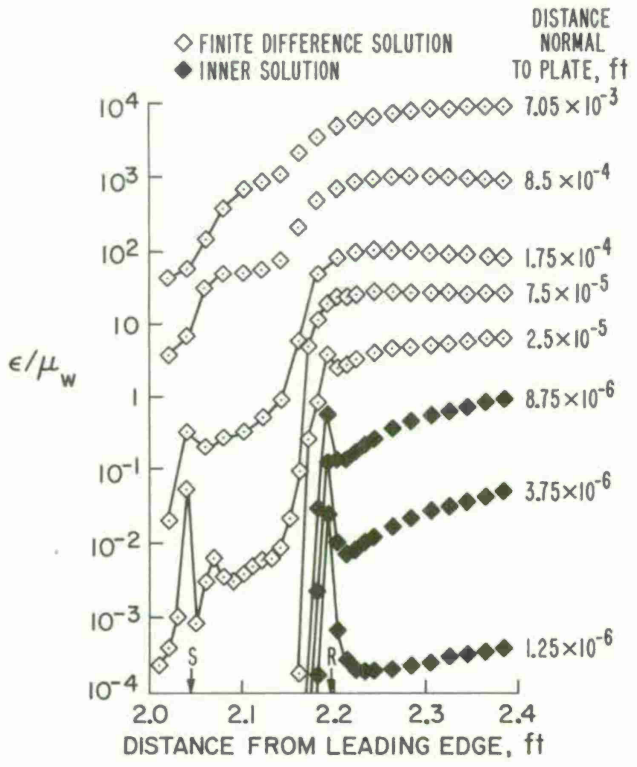

Fig. 28 Variations of eddy viscosity.

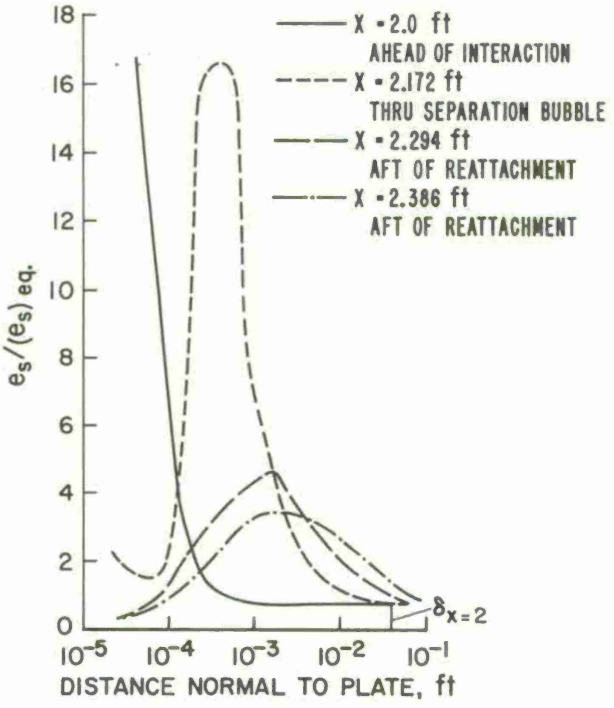

Fig. 30 Departure of turbulent energy from equilibrium.

COMPUTATIONAL TECHNIQUES FOR BOUNDARY LAYERS†

by
F. G. Blottner
Sandia Laboratories
Albuquerque, New Mexico 87115
United States

SUMMARY

The present status of the numerical computation of boundary layers is given for two- and three-dimensional flows. The appropriate transformations to apply to the governing equations are considered, and the possible solution procedures are discussed. The emphasis of this paper is on the finite-difference procedures which are illustrated for the two-dimensional, incompressible flows. For compressible flows the Crank-Nicolson technique is given. The changes which are needed to this approach, when the flow is turbulent, are presented. The finite-difference procedures utilized for unsteady flows are given. Solution techniques for three-dimensional flows are described and the features which are different from two-dimensional flows are emphasized.

1. INTRODUCTION

There have been several survey papers concerned with the solution of the boundary-layer equations. Paskonov and Chudov[1] have reviewed papers concerned with finite-difference methods of solution of the boundary-layer equations. A similar type of review has been given by Blottner,[2] and also presented is a technique for solving the boundary-layer equations for a multicomponent gas mixture. A general survey on boundary-layer research has been made by Smith[3] where a brief review is given of solution techniques. Also, several books are available on some of the methods. An implicit finite-difference procedure is given in the book by Patankar and Spalding[4] and is applied to two-dimensional laminar and turbulent flows. A complete description of the differential-difference method of Smith and colleagues has been published by Jaffe and Smith.[5] A limited account of solution techniques for three-dimensional, turbulent boundary layers is presented by Nash and Patel.[6] Also, a forthcoming book by Cebeci and Smith[7] is concerned with the solution of the turbulent boundary-layer equations with the Keller box scheme.

The purpose of this paper is to give a description of the methodology of the numerical solution techniques for boundary layers and to present one method of solution in detail where it is applied to the various boundary-layer problems. This paper is not intended to include all the solution techniques that have been applied to the boundary-layer equations. The emphasis will be on finite-difference procedures with the method of weighted residuals and the matrix-integral method being only briefly mentioned. This neglect mainly results from the author's lack of first-hand experience with these procedures and not that one approach is better than the other. An adequate evaluation has not been made of these methods, although an initial attempt was made as reported by Lewis.[8] Also, there is a need to be aware of the various techniques which have been proposed, as some of these methods were perhaps before their time. For example, one approach results in a system of stiff ordinary differential equations and when this method was originally investigated, a good computer program for the solution of these equations was not available. The second objective of the paper is to present a good method for solving boundary-layer flows. The method chosen is the Crank-Nicolson finite-difference scheme with which the author has had first-hand experience. This is one reason it is chosen, but, in addition, this type of numerical procedure has proven to be a good technique for solving the boundary-layer equations by many people. Also, most of the other methods have received rather complete coverage by other authors while the Crank-Nicolson method has not been discussed in detail for various boundary-layer flows in a unified manner. There have been some recent developments in this method which are just becoming available in the literature. Therefore, the present formulation of the Crank-Nicolson scheme is relatively new and results in a second-order accurate scheme in both coordinates.

There are a number of subjects and items that are related to the numerical solution of the boundary-layer equations that have not been included. Such things as higher order boundary-layer theory, real gas flows, various boundary conditions, and other boundary-layer-like flows have been neglected. The use of higher order boundary-layer theory has not been included as it has not proven to be a useful approach, as yet. The introduction of real gas effects into the governing equation introduces at least one significant problem if finite-chemical reactions are considered. The production terms make the governing species equations "stiff" and the numerical procedure must take this into account. One approach has been given by Blottner[2] for a first-order scheme in the flow direction where the equations are handled in an uncoupled manner. For higher order schemes, coupling of the governing equations is probably required, but this has not been established. The use of wall boundary conditions or inviscid edge flow conditions has generally very little influence on the numerical solution technique. There is perhaps one exception, the case of massive blowing at the surface. Libby[9] has indicated that some of the numerical methods fail for this case, and he has used an asymptotic analysis. As the title of this paper indicates, only boundary-layer flows are considered. However, the techniques presented in this paper can be applied to other fluid flows. For example, Hornbeck[10] has presented finite-difference solution techniques for boundary layers, jets, free convection, channel flow, and tube flow. There have been many people who have used the established numerical solution techniques for various boundary-layer flows. These papers have not been referred to in most cases, although there might have been some improvement in the numerical schemes. If the author has overlooked something of importance, it is not intentional, but is due to limitation of time and the large number of papers that have appeared.

---

† This work was supported by the U. S. Atomic Energy Commission.

The paper is divided into a number of sections with the governing equations for a laminar, three-dimensional, unsteady boundary-layer flow given in Section 2. The numerical solution of various forms of these equations will be considered. For turbulent flows, the governing equations depend on the closure model. Therefore, the special equations used to illustrate the solution of turbulent flow will be discussed in that section. Since a large class of boundary-layer problems is included with the two-dimensional and axisymmetric steady equations and transformations of these equations have been developed, Section 3 presents these governing equations. Then a review is given of the transformations that have been used with numerical solutions. The governing equations in terms of Levy-Lees variables are presented, and this form of the equations are used for the subsequent numerical solutions. In Section 4 the solution techniques for solving the similar boundary-layer equations are given. It is necessary to solve these equations in order to obtain initial profiles of the dependent variables which gives the initial conditions for the solution along the surface. The solution techniques for these two-point boundary-value, ordinary differential equations are extremely important as they can be utilized in the two- and three-dimensional problems. A review of solution procedures that have been used is given. Then a finite-difference procedure which uses Newton-Raphson linearization is presented. The method keeps the finite-difference equations for the continuity and momentum equations coupled, which is shown later to be significant for solutions along the surface. Also, the Keller midpoint scheme is illustrated in this section.

A review of many of the difference methods for solving the non-similar, two-dimensional and axisymmetric boundary-layer equations is given in Section 5. These are illustrated with the Levy-Lees form of the incompressible, boundary-layer equations. The procedure considered best for solving the incompressible equations is described in detail in Section 6. The convergence of the iteration procedures used to solve the nonlinear, finite-difference equations required for a second-order scheme is discussed. Also, a procedure of judging the accuracy and order of a scheme is presented. The incompressible, finite-difference scheme is extended to the compressible boundary-layer equations in Section 7. The difficulties of even knowing the governing equations for a turbulent boundary are indicated in Section 8. For turbulent flow, the major numerical problem results from the large gradients which occur near the surface and the resulting need for a large number of grid points across the layer. A variable grid scheme is presented which is used with the Crank-Nicolson scheme and gives a second-order accurate solution.

In Section 9 the extension of numerical techniques for steady boundary layers to the unsteady case is reviewed. The Crank-Nicolson scheme can be readily used for this problem if there is no reverse flow. The formulation of the boundary conditions and initial conditions appears to be the major difficulty.

The solution techniques for solving three-dimensional boundary layers are described in Section 10. The features which make the three-dimensional problem different from the two-dimensional flow are described. The selection of the coordinate system is considered, and a description of the finite-difference schemes are given.

The final section, 11, is a summary of the status of computational techniques for solving boundary layers.

2. BOUNDARY-LAYER EQUATIONS

The general form of the governing laminar equations is now considered, and the notation is chosen to give the time-honored form of the two-dimensional, boundary-layer equations as suggested by Van Dyke.[11] Since unsteady flows and three-dimensional flows will be investigated, the form needed was originally derived by Hayes[12] and can also be found in the books by Stewartson[13] and Moore.[14] An orthogonal system of curvilinear coordinates (x_1, y, x_3) is employed on the surface over which the boundary layer is flowing. The coordinate normal to the surface is y with y = 0 being the surface. The lines x_1 = constant and x_3 = constant give a system of orthogonal coordinates on the surface. The square of the element of arc $d\ell$ on the surface is

$$d\ell^2 = h_1^2 dx_1^2 + h_3^2 dx_3^2 \tag{2-1}$$

where h_1 and h_3 are metric coefficients and a function of x_1 and x_3. Since the boundary layer is assumed thin, the metric coefficient in the y direction is assumed to be one which gives for the square of the element of arc in the boundary layer the following relation

$$ds^2 = h_1^2 dx_1^2 + dy^2 + h_3^2 dx_3^2 \tag{2-2}$$

It is assumed that the local boundary-layer thickness is small compared with the principal radii of curvature of the surface. The resulting equations are referred to as the thin or first-order boundary-layer equations.

The substantial derivative for the above coordinate system is

$$\frac{D}{Dt} = \frac{\partial}{\partial t} + \frac{u}{h_1}\frac{\partial}{\partial x_1} + v\frac{\partial}{\partial y} + \frac{w}{h_3}\frac{\partial}{\partial x_3} \tag{2-3}$$

where t is time, and u, v, w are the velocity components in the directions of the x_1, y, x_3 axes, respectively. The boundary-layer equations for an unsteady compressible perfect gas flow with constant specific heats, c_p, and constant Prandtl number, Pr, are

Continuity

$$\frac{\partial \rho}{\partial t} + \frac{1}{h_1 h_3}\left[\frac{\partial}{\partial x_1}(h_3\,\rho u) + \frac{\partial}{\partial y}(h_1 h_3\,\rho v) + \frac{\partial}{\partial x_3}(h_1\,\rho w)\right] = 0 \tag{2-4}$$

x_1 - Momentum

$$\frac{Du}{Dt} + uwK_1 - w^2K_3 = -\frac{1}{\rho h_1}\frac{\partial p}{\partial x_1} + \frac{1}{\rho}\frac{\partial}{\partial y}\left(\mu\frac{\partial u}{\partial y}\right) \tag{2-5}$$

y - Momentum

$$\frac{\partial p}{\partial y} = 0 \tag{2-6}$$

x_3 - Momentum

$$\frac{Dw}{Dt} - u^2K_1 + uwK_3 = -\frac{1}{\rho h_3}\frac{\partial p}{\partial x_3} + \frac{1}{\rho}\frac{\partial}{\partial y}\left(\mu\frac{\partial w}{\partial y}\right) \tag{2-7}$$

Energy

$$\rho c_p\frac{DT}{Dt} = \frac{Dp}{Dt} + \frac{\partial}{\partial y}\left(\frac{\mu c_p}{Pr}\frac{\partial T}{\partial y}\right) + \mu\left(\frac{\partial u}{\partial y}\right)^2 + \mu\left(\frac{\partial w}{\partial y}\right)^2 \tag{2-8}$$

The geodesic curvatures of the surface coordinate lines have been introduced and are given by

$$K_1 = \frac{1}{h_1 h_3}\frac{\partial h_1}{\partial x_3} \quad \text{for } x_3 = \text{constant} \tag{2-9a}$$

$$K_3 = \frac{1}{h_1 h_3}\frac{\partial h_3}{\partial x_1} \quad \text{for } x_1 = \text{constant} \tag{2-9b}$$

the other notation in the above equations, (2-4) to (2-8), is the density ρ, the viscosity μ, the temperature T, and the pressure p, which is constant across the boundary layer as Eq. (2-6) shows.

The governing equations are completed with the equation of state

$$p = \rho RT \tag{2-10}$$

and a viscosity law

$$\mu = \mu(T) \tag{2-11}$$

The foregoing boundary-layer equations are solved with the boundary and initial conditions which will now be described. If the usual no-slip condition is used, then the velocity components at the surface (y = 0) are

$$u = v = w = 0 \tag{2-12a}$$

With mass transfer at the surface, the velocity component v is specified. Also, the velocity component w can be non-zero with a specified value for a body of resolution with spin. The final surface boundary condition is the wall temperature or heat transfer is prescribed which gives

$$T = T_w(t, x_1, x_3) \quad \text{or} \quad \frac{\partial T}{\partial y} = q_w(t, x_1, x_3) \tag{2-12b}$$

At the outer edge of the boundary layer ($y \to \infty$) the classical approach is followed where the velocity components and the temperature are set equal to the inviscid flow quantities at the surface. These boundary conditions are expressed as

$$u = u_e(t, x_1, x_3) \tag{2-13a}$$

$$w = w_e(t, x_1, x_3) \tag{2-13b}$$

$$T = T_e(t, x_1, x_3) \tag{2-13c}$$

The governing equations for the inviscid flow at the surface where $v_e = 0$ are

$$\frac{\partial u_e}{\partial t} + \frac{u_e}{h_1}\frac{\partial u_e}{\partial x_1} + \frac{w_e}{h_3}\frac{\partial u_e}{\partial x_3} + u_e w_e K_1 - w_e^2 K_3 = -\frac{1}{\rho_e h_1}\frac{\partial p}{\partial x_1} \tag{2-14a}$$

$$\frac{\partial w_e}{\partial t} + \frac{u_e}{h_1}\frac{\partial w_e}{\partial x_1} + \frac{w_e}{h_3}\frac{\partial w_e}{\partial x_3} - u_e^2 K_1 + u_e w_e K_3 = -\frac{1}{\rho_e h_3}\frac{\partial p}{\partial x_3} \tag{2-14b}$$

$$\rho_e c_p \left(\frac{\partial T_e}{\partial t} + \frac{u_e}{h_1}\frac{\partial T_e}{\partial x_1} + \frac{w_e}{h_3}\frac{\partial T_e}{\partial x_3}\right) = \frac{\partial p}{\partial t} + \frac{u_e}{h_1}\frac{\partial p}{\partial x_1} + \frac{w_e}{h_3}\frac{\partial p}{\partial x_3} \tag{2-14c}$$

where the subscript e indicates the quantities are the conditions at the edge of the boundary layer. The pressure gradients required in the boundary-layer equations, (2-5), (2-7), and (2-8), are determined from Eqs. (2-14) with the boundary conditions (2-13) employed. Another approach is to specify the pressure as a function of t, x_1, and x_3 and then with the appropriate boundary and initial conditions to solve the partial differential equations, (2-14), for the velocity components u_e and w_e and the temperature T_e.

If sufficient initial conditions are provided in a plane perpendicular to the surface, the boundary-layer equations can be solved in a region downstream if the zones of influence and dependence are properly taken into account. These zones have been discussed by Der and Raetz[15] and Wang.[16] The sufficient conditions to start the solution of the boundary-layer equations has been considered by Ting.[17] These topics will be discussed further when the various problems are considered.

3. TRANSFORMATION OF THE TWO-DIMENSIONAL AND AXISYMMETRIC STEADY EQUATIONS

The governing equations for these two cases are written with the use of the parameter j which is 0 for two-dimensional flow and 1 for axisymmetric flow. The surface curvilinear coordinates and the metric coefficients become

$$x_1 = x \quad \text{and} \quad h_1 = 1 \tag{3-1a}$$

$$x_3 = \begin{cases} z & \text{two-dimensional} \\ \varphi & \text{axisymmetric} \end{cases} \qquad \text{and } h_3 = r_b^j(x) \tag{3-1b}$$

where x is the distance along the body surface measured from the tip or the stagnation point; z is the distance in the direction normal to the two-dimensional plane, and r_b is the radius of the body of revolution. The boundary-layer equations, (2-4) to (2-8), for this case have $\partial/\partial x_3 = 0$ and $w = 0$ which gives

Continuity

$$\frac{\partial}{\partial x}(r_b^j \rho u) + \frac{\partial}{\partial y}(r_b^j \rho v) = 0 \tag{3-2}$$

x - Momentum

$$\rho u \frac{\partial u}{\partial x} + \rho v \frac{\partial u}{\partial y} = -\frac{\partial p}{\partial x} + \frac{\partial}{\partial y}\left(\mu \frac{\partial u}{\partial y}\right) \tag{3-3}$$

Energy

$$\rho c_p u \frac{\partial T}{\partial x} + \rho c_p v \frac{\partial T}{\partial y} = u \frac{\partial p}{\partial x} + \frac{\partial}{\partial y}\left(\frac{\mu c_p}{Pr}\frac{\partial T}{\partial y}\right) + \mu\left(\frac{\partial u}{\partial y}\right)^2 \tag{3-4}$$

where the pressure is constant across the boundary layer. These equations are completed with the equation of state, (2-10), and the viscosity law, (2-11).

In the development of boundary-layer theory there has been a number of transformations applied to the governing equations. For the numerical solution of the boundary-layer equations a finite-difference procedure could be applied directly to the physical coordinate, Eqs. (3-2)-(3-4). However, there are several difficulties when this form of the equations is used, such as: (1) the boundary-layer thickness usually increases downstream, (2) for bodies with a sharp tip or leading edge there is a singularity at this location, and (3) for hypersonic flows, the tangential velocity has a large gradient near the outer edge. The solution of the equations in physical coordinates has been used in the work of Flügge-Lotz and Yu,[18], Brailovskaya and Chudov,[19] Paskonov,[20] and Blottner and Flügge-Lotz.[21]

The von Mises form of the equations has been used by Mitchell and Thomson,[22] Mitchell,[23] and Patankar and Spalding.[24] For these equations the independent variable is x and the stream function is ψ, which satisfies the continuity equation. The governing equations become the transformed momentum and energy equations. However, the momentum equation has a singularity at the wall which makes the von Mises form of the equations difficult to solve numerically. This singularity has been overcome by Mitchell and Thomson with an expansion for the velocity in the vicinity of the wall.

In much of the early work in solving the boundary-layer equations, for example, Flügge-Lotz,[25] Flügge-Lotz and Baxter,[26] Baxter and Flügge-Lotz,[27] and Kramer and Lieberstein,[28] the Crocco form of the equations is employed. In this transformation the independent variables x and y are replaced by x and u and the dependent variable is the viscous shearing stress τ. The continuity and momentum equations are combined with this transformation. With this form of the governing equations, the range of the independent variable u is finite and the outer edge is well defined. However, there are several disadvantages with this transformation as there is a singularity at the outer edge of the boundary layer. For the case with velocity overshoot, it is difficult to apply the Crocco form as quantities are double valued as a function of u.

Other transformations such as the Dorodnitsyn-Howarth have been used by Wu[29] and Blottner and Flügge-Lotz.[21] This transformation removes the density from the formal equations by introducing a new normal coordinate which is a function of the density. Sills[30] has transformed the semi-infinite boundary layer normal coordinate into a finite interval before obtaining a finite-difference solution.

One of the problems with all of the previous methods is the starting of the solution of the equations. For sharp bodies, one would want to start the solution at the tip, whereas for a blunt body the solution should start at the stagnation point. At the tip of a sharp body, the boundary-layer thickness is zero and the solution in physical coordinates is inappropriate. If the boundary-layer equations are transformed into similarity variables, then in the transformed plane the boundary layer is nearly of uniform thickness for many flow situations. Also, the partial differential equations reduce to ordinary differential equations at the tip of a body or at a stagnation point. The foregoing transformations can be placed in similarity form, but the transformation that has been generally employed is the Levy-Lees.[31] This form of the equations was used by Blottner[32] for a binary gas mixture and will now be applied to the governing equations, (3-2) to (3-4). The new independent variables are

$$\eta(x, y) = u_e r_b^j \sqrt{\frac{\mathscr{K}}{2\xi}} \int_0^y \rho \, dy \tag{3-5a}$$

$$\xi(x) = \mathscr{K} \int_0^x (\rho\mu)_r \, u_e r_b^{2j} \, dx \tag{3-5b}$$

where $\mathscr{K}$ is a constant and the derivatives become

$$\frac{\partial}{\partial x} = \mathscr{K} \, (\rho\mu)_r \, u_e r_b^{2j} \frac{\partial}{\partial \xi} + \frac{\partial \eta}{\partial x} \frac{\partial}{\partial \eta} \tag{3-6a}$$

$$\frac{\partial}{\partial y} = \rho u_e \, r_b^j \sqrt{\frac{\mathscr{K}}{2\xi}} \frac{\partial}{\partial \eta} \tag{3-6b}$$

The new dependent variables are

$$F = u/u_e \tag{3-7a}$$

$$\theta = h/h_e = T/T_e \tag{3-7b}$$

$$V = 2\xi(F \, \partial\eta/\partial x + \rho v \, r_b^j/\sqrt{2\xi/\mathscr{K}})/[\mathscr{K}(\rho\mu)_r \, u_e \, r_b^{2j}] \tag{3-7c}$$

The governing equations become

Continuity

$$2\xi \, \partial F/\partial \xi + \partial V/\partial \eta + F = 0 \tag{3-8a}$$

x - Momentum

$$2\xi F \, \partial F/\partial \xi + V \, \partial F/\partial \eta + \beta(F^2 - \theta) - \partial(\ell \, \partial F/\partial \eta)/\partial \eta = 0 \tag{3-8b}$$

Energy

$$2\xi F \, \partial\theta/\partial\xi + V \, \partial\theta/\partial\eta - \alpha\ell(\partial F/\partial\eta)^2 - (1/Pr) \, \partial(\ell \, \partial\theta/\partial\eta)/\partial\eta = 0 \tag{3-8c}$$

where the following notation is introduced

$$\ell = \rho\mu/(\rho\mu)_r \tag{3-9a}$$

$$\beta = (2\xi/u_e)\, du_e/d\xi \tag{3-9b}$$

$$\alpha = u_e^2/(c_p T_e) \tag{3-9c}$$

The above Eqs. (3-8) can be written without the continuity equation which is automatically satisfied with the introduction of the stream function $\psi = f\sqrt{2\xi/\mathcal{K}}$. The velocity components become

$$\rho u\, r_b^j = \partial\psi/\partial y = \rho\, u_e\, r_b^j\, \partial f/\partial\eta \tag{3-10a}$$

$$\rho v\, r_b^j = -\,\partial\psi/\partial x = \sqrt{2\xi/\mathcal{K}}\left\{\mathcal{K}(\rho\mu)_r\, u_e\, r_b^j \left(2\xi\,\frac{\partial f}{\partial\xi} + f\right)/(2\xi) - (\partial\eta/\partial x)(\partial f/\partial\eta)\right\} \tag{3-10b}$$

With $F = \partial f/\partial\eta$ and the definition of V, the following is obtained

$$V = -\,(2\xi\,\partial f/\partial\xi + f) \tag{3-11}$$

The governing equations become

x - Momentum

$$2\xi\left(\frac{\partial f}{\partial\eta}\frac{\partial^2 f}{\partial\xi\partial\eta} - \frac{\partial f}{\partial\xi}\frac{\partial^2 f}{\partial\eta^2}\right) = \frac{\partial}{\partial\eta}\left(\ell\,\frac{\partial^2 f}{\partial\eta^2}\right) + f\frac{\partial^2 f}{\partial\eta^2} + \beta\left[\theta - \left(\frac{\partial f}{\partial\eta}\right)^2\right] \tag{3-12a}$$

Energy

$$2\xi\left(\frac{\partial f}{\partial\eta}\frac{\partial\theta}{\partial\xi} - \frac{\partial f}{\partial\xi}\frac{\partial\theta}{\partial\eta}\right) = \frac{1}{Pr}\frac{\partial}{\partial\eta}\left(\ell\,\frac{\partial\theta}{\partial\eta}\right) + f\,\frac{\partial\theta}{\partial\eta} + \alpha\ell\left(\frac{\partial^2 f}{\partial\eta^2}\right)^2 \tag{3-12b}$$

The boundary conditions for the foregoing equations are as follows:

At wall (without mass transfer and specified wall temperature)

$$\eta = 0 \;:\quad F = V = f = 0 \text{ and } \theta = \theta_w \tag{3-13}$$

At outer edge

$$\eta = \eta_e \;:\quad F = \theta = \partial f/\partial\eta = 1 \tag{3-14}$$

To complete the governing equations initial conditions can be obtained at $\xi = 0$ from Eqs. (3-8) or (3-12) which become ordinary differential equations.

4. SIMILAR SOLUTIONS

4.1 Similar Boundary-Layer Equations

The partial differential equations for the boundary layer can be reduced to ordinary differential equations when $\xi = 0$ or when the ξ-derivatives are zero. At the tip of a sharp body or at a stagnation point, $\xi = 0$. The flow along a flat plate and incompressible wedge flow have the ξ-derivatives zero. Also, the assumption of local similarity (ξ-derivatives zero) can be used to obtain approximate solutions to some flows. The usefulness of similar solutions is of limited value now that complete two-dimensional flow solutions can be readily obtained. However, there is the need to obtain profiles of the dependent variable in order to have the initial conditions for the two-dimensional solutions. These profiles are obtained from the similar form of the governing equation which for Eqs. (3-8) become

$$\partial V/\partial\eta + F = 0 \tag{4-1a}$$

$$\partial(\ell\,\partial F/\partial\eta)/\partial\eta - V\,\partial F/\partial\eta + \beta(\theta - F^2) = 0 \tag{4-1b}$$

$$\partial(\ell\,\partial\theta/\partial\eta)/\partial\eta - Pr\,V\,\partial\theta/\partial\eta + Pr\,\alpha\ell\,(\partial F/\partial\eta)^2 = 0 \tag{4-1c}$$

while Eqs. (3-12) become

$$\frac{\partial}{\partial\eta}\left(\ell\,\frac{\partial^2 f}{\partial\eta^2}\right) + f\,\frac{\partial^2 f}{\partial\eta^2} + \beta\,[\theta - (\partial f/\partial\eta)^2] = 0 \tag{4-2a}$$

$$\frac{\partial}{\partial\eta}\left(\ell\,\frac{\partial\theta}{\partial\eta}\right) + Pr\,f\,\frac{\partial\theta}{\partial\eta} + Pr\,\alpha\ell\,(\partial^2 f/\partial\eta^2)^2 = 0 \tag{4-2b}$$

For the similar form V = -f. The similar equations constitute a system of nonlinear, ordinary differential equations and are of the two-point boundary value form with the boundary conditions previously given in Eqs. (3-13) and (3-14). At present, there are no computer library subroutines for solving this type of problem, but a variety of techniques have been used and some will be described in the next sections. A more complete study of numerical methods for solving two-point boundary-value problems is given by Keller,[33] for example.

4.2 Initial Value Methods (Shooting)

This procedure changes the boundary-value problem into an initial-value problem. New boundary conditions are assumed at one end of the interval of integration such that sufficient initial conditions are available to start the solution. The assumed boundary conditions are changed until the integrated equations satisfy the original boundary conditions at the other end of the interval. The similar boundary-layer equations are usually written as a system of first-order ordinary differential equations which then allows any of the standard integration procedures to be employed. Then a Newton-Raphson technique is used to iterate on the boundary conditions that have to be determined as initial conditions. This type of procedure has been applied to the compressible boundary layer for a perfect gas by Reshotko and Beckwith[34] and for a real multicomponent air mixture by Lenard.[35] For the more complicated problem, there can be as many as seven boundary conditions that must be assumed and iterated on until the outer edge conditions are satisfied. Not only does the initial-value method rapidly become exceedingly difficult to apply to boundary-layer problems with complex flows, it is also difficult or impossible to make the procedure converge. The nature of the last problem has been illustrated by Fay and Kaye[36] for a linearized equation. For this example the solutions consist of exponentials and if the guessed initial condition is not correct, an extraneous part of the solution grows exponentially and will dominate the initial-value solution.

Other initial-value methods have been used to improve the convergence of the Newton-Raphson method. Nachtsheim and Swigert[37] have used a least-squares convergence criterion method which introduces additional perturbation, ordinary-differential equations. Another idea of integrating initially to a value of the independent variable less than the desired value has been investigated by Roberts and Shipman.[38] The boundary conditions can be satisfied for a smaller than desired value of the independent variable. With this procedure repeated several times, the solution can possibly be extended to the end of the desired interval. A similar method has been investigated by Keller[33] where the interval is divided into several subintervals.

Perhaps the most successful initial-value approach uses a Newton-Raphson technique to linearize the governing equations. Then the linear equations are used to obtain a particular solution and a homogeneous solution for each boundary condition. The particular and homogeneous solutions are then combined such that all of the boundary conditions are satisfied. This approach was first suggested for boundary-value problems by Hestenes[39] and was later developed further by Bellman and Kalaba[40] and referred to as quasi-linearization. This technique has been used by Radbill[41] to solve the Falkner-Skan equation and has been investigated further by Libby and Chen[42] where the question of uniqueness is considered. It should be noticed that the shooting method with quasilinearization can encounter difficulties if the initial-values solutions grow exponentially and become very large over the interval of integration.

A parametric differentiation technique has been applied to the solution of nonlinear flow problems by Rubbert and Landahl.[43] This method is appropriate for a problem with a parameter in the governing equations and where a solution exists for one value of the parameter. The technique then proceeds to find the solution away from the known solution with changing values of the parameter. The Falkner-Skan equation has been solved with β being the parameter and the resulting differential equations being solved with the Runge-Kutta integration method. Although the initial value method was used, for this problem the methods of the next section could also be utilized.

4.3 Finite-Difference Methods

In this approach the derivatives in the governing equations are replaced with finite-difference relations and the resulting equations are solved such that all the boundary conditions are satisfied. For nonlinear ordinary differential equations such as the boundary-layer equations, the finite-difference method results in a system of nonlinear algebraic equations. In all of the methods the governing equations or the differential equation must be linearized in order to obtain a system of linear algebraic equations which can be solved readily. With this procedure it is necessary to assume an initial guess for the dependent variables. Then an iteration process is required until the guessed variables match the calculated variables from the solution of the linear algebraic equations. The manner in which the linearization is performed on the differential or difference equations is very important. The method of nonlinear simulataneous displacements has been used by Lew[44] to solve the Falkner-Skan system of nonlinear difference equations. With this approach only one dependent variable at one grid point is assumed unknown in each difference equation with the remaining variables assumed known from a previous iteration. If the one dependent variable appears in a nonlinear manner, Newton-Raphson linearization is applied to give a linear equation. This method requires the solution of explicit algebraic equations for the dependent variables which are relatively easy to solve. However, the convergence of this method is not as rapid as the methods which are described subsequently. Another approach is to uncouple the governing equations by considering only one dependent variable is unknown in each equation. When that variable appears in a nonlinear form in the equation, some convenient linear form is used to replace these terms. The resulting equations will be of tridiagonal form for each governing equation. This type of procedure has been used by Varzhanskaya, Obroskova and Starova,[45] Holt,[46] and Fay and Kaye.[36] Another method to linearize the equations is to use a Newton-Raphson or quasilinearization approach. With this method the nonlinear terms are evaluated with a truncated Taylor's series. The resulting equations will be coupled and the finite-difference equations will be of block tridiagonal form. This approach has been used by Casaccio[47] (called method of linear corrections) and Sylvester and Meyer,[48] Keller and Cebeci[49] and Werle and Bertke.[50] The previous linearization considered above usually results in a simpler system of difference equation to be solved but requires more iteration to obtain a converged solution. The Newton-Raphson approach results in more complex difference equations but requires fewer iterations to converge. This

procedure also appears in general to have a better chance of converging.

To illustrate the finite-difference method with Newton-Raphson linearization, the incompressible boundary-layer (Falkner-Skan) equations are considered. For this case $\ell = 1$ and $\theta = 1$. The present approach was suggested by Davis and used by Werle and Bertke.[50] The continuity equation, (4-1a), is evaluated at the point $(j - \frac{1}{2})$ with the terms in the equation evaluated with second-order accuracy (truncation error of the difference equation is of the order of the step-size squared) which gives

$$(\partial V/\partial \eta)_{j-\frac{1}{2}} = (V_j - V_{j-1})/\Delta\eta + O(\Delta\eta^2) \tag{4-3a}$$

$$F_{j-\frac{1}{2}} = (F_j + F_{j-1})/2 + O(\Delta\eta^2) \tag{4-3b}$$

where $\Delta\eta = (\eta_j - \eta_{j-1})$. The resulting expression for the continuity equation becomes

$$V_j = V_{j-1} - (1/2)\,\Delta\eta(F_j + F_{j-1}) \tag{4-4}$$

The nonlinear terms in the momentum equation, (4-1b), are linearized with the Newton-Raphson procedure which gives

$$F^2 = 2\bar{F}F - \bar{F}^2 \tag{4-5a}$$

$$V\,\partial F/\partial\eta = -\bar{V}\,\partial\bar{F}/\partial\eta + \bar{V}\,\partial F/\partial\eta + V\,\partial\bar{F}/\partial\eta \tag{4-5b}$$

where all quantities are evaluated at j and quantities with a bar are determined from a previous iteration. The terms in Eq. (4-1b) are written in finite-difference form at the point j with the use of Eq. (4-5) to obtain

$$\partial^2 F/\partial\eta^2 = (F_{j+1} - 2F_j + F_{j-1})/\Delta\eta^2 \tag{4-6a}$$

$$V\,\partial F/\partial\eta = \left[-\bar{V}_j(\bar{F}_{j+1} - \bar{F}_{j-1}) + \bar{V}_j(F_{j+1} - F_{j-1}) + V_j(\bar{F}_{j+1} - \bar{F}_{j-1})\right]/2\Delta\eta \tag{4-6b}$$

The momentum equation, (4-1b) becomes the following finite-difference equation with the use of relations (4-5a) and (4-6) and all terms have been multiplied by $(-\Delta\eta^2/2)$:

$$-A_j F_{j-1} + B_j F_j - C_j F_{j+1} + a_j V_j = D_j \qquad j = 2,3,\cdots J-1 \tag{4-7}$$

where

$$A_j = (1 + \bar{V}_j\,\Delta\eta/2)/2 \tag{4-8a}$$

$$B_j = 1 + \Delta\eta^2\,\beta\bar{F}_j \tag{4-8b}$$

$$C_j = (1 - \bar{V}_j\,\Delta\eta/2)/2 \tag{4-8c}$$

$$D_j = (\Delta\eta^2/2)\left[\beta + \beta\bar{F}_j^2 + \bar{V}_j(\bar{F}_{j+1} - \bar{F}_{j-1})/(2\Delta\eta)\right] \tag{4-8d}$$

$$a_j = (\bar{F}_{j+1} - \bar{F}_{j-1})\,\Delta\eta/4 \tag{4-8e}$$

The wall boundary conditions are located at the point $j = 1$ where $F_1 = V_1 = 0$ while outer edge boundary conditions are located at the point $j = J$ where $F_J = 1$. The finite-difference equations, (4-4) and (4-7), are coupled and are used along with boundary conditions to determine the two unknowns V_j and F_j, at the grid points $j = 1, 2, \cdots J$. The coefficients of Eq. (4-7) depend on the variables $\bar{V}_j$ and $\bar{F}_j$ which are known from an initial guess or the previous iteration. For the initial guess, the present approach sets $\bar{F}_j = 1.0$ everywhere except $\bar{F}_1 = 0$ and then $\bar{V}_j$ is determined from Eq. (4-4). The difference equations, (4-4) and (4-7), are readily solved with a modified tridiagonal algorithm developed by Davis as reported in Werle and Bertke. An extended version of this method is given in Appendix A. Although this method only looks slightly more complex than the usual Thomas algorithm which is given in Appendix B, the modified version requires approximately twice the computer time. In order to uncouple the difference equation, many authors assume that the term $a_j V_j$ in Eq. (4-7) is known. With this procedure Eq. (4-7) is of the usual tridiagonal form and F_j is obtained with the Thomas algorithm. Then V_j is obtained from Eq. (4-4) and an iteration procedure is performed until F_j and V_j are known to the desired accuracy. This approach converges slower than the Davis coupled method which uses Newton-Raphson linearization and has quadratic convergence (*). For the Blasius equation and the same criterion for convergence, the coupled method requires 4 iterations while the uncoupled method requires 13 iterations.

* If $\delta^{(i)}$ is the error in the computed solution for the ith iteration, then $\delta^{(i+1)} = K[\delta^{(i)}]^2$ where K is a constant.

If the approaches are employed with a large step-size $\Delta\eta$ or the maximum η is very large, there will be an oscillation of the results with each grid point location. If V is assumed known and Eq. (4-7) is taken as the difference equation, then Keller[33] has shown there is a unique solution if the following condition is satisfied for the step-size:

$$\Delta\eta \leq 2/|V| \tag{4-9}$$

With $\eta_e = 6$, $V = -4.78$ which gives $\Delta\eta \leq 0.42$. Since V increases with η, then with η_e large the step-size $\Delta\eta$ must be much smaller. Also, Greenspan[51] states that the solution of the tridiagonal equations, (4-7), (with V known) exists and is unique if the system is diagonally dominant ($B_j > |A_j| + |C_j|$). If $\beta > 0$, then diagonal dominance is assumed if relation (4-9) is satisfied. Price, Varga, and Warren[52] have obtained relation (4-9) as a necessary and sufficient condition for non-oscillatory solution of Eq. (4-7) with V a constant and $\beta = 0$.

Another finite-difference method for solving the boundary-layer equations has been developed by Keller and Cebeci[49] which uses the Keller[53] midpoint scheme. The method writes the governing equations as a system of first-order equations which for the incompressible equation, (4-2a), gives

$$\partial f/\partial\eta = u \tag{4-10a}$$

$$\partial u/\partial\eta = v \tag{4-10b}$$

$$\partial v/\partial\eta = -fv - \beta(1 - u^2) \tag{4-10c}$$

with the boundary conditions

$$f(o) = 0 \; ; \quad u(o) = 0 \quad \text{and} \quad u(\infty) = 1 \tag{4-11}$$

With the midpoint, second-order accurate finite-difference approximation, the governing equations become

$$(f_j - f_{j-1})/\Delta\eta = (u_j + u_{j-1})/2 \tag{4-12a}$$

$$(u_j - u_{j-1})/\Delta\eta = (v_j + v_{j-1})/2 \tag{4-12b}$$

$$(v_j - v_{j-1})/\Delta\eta = -(fv)_{j-\frac{1}{2}} - \beta + \beta u^2_{j-\frac{1}{2}} \tag{4-12c}$$

Equation (4-12c) is linearized by Keller and Cebeci by first writing:

$$f = \bar{f} + \delta f \tag{4-13a}$$

$$u = \bar{u} + \delta u \tag{4-13b}$$

$$v = \bar{v} + \delta v \tag{4-13c}$$

These quantities are substituted into Eq. (4-12c) and quadratic terms in δf, δu, and δv are neglected. Again, the quantities with a bar are obtained from the previous iteration, and f, u, and v are the results from the iteration. In the work of Keller and Cebeci, the difference equations are written with δf, δu, and δv as the unknowns being determined. The approach developed here will be to use f, u, and v as the unknowns which is similar to that developed in the previous method, Eqs. (4-4) and (4-7). Equation (4-12c) is linearized with the relations

$$fv = -\bar{f}\bar{v} + \bar{v}f + \bar{f}v \tag{4-14a}$$

$$u^2 = 2\bar{u}u - \bar{u}^2 \tag{4-14b}$$

and quantities at $j-\frac{1}{2}$ are evaluated with

$$W_{j-\frac{1}{2}} = (W_j + W_{j-1})/2 \tag{4-15}$$

where W represents f, u, or v. When the above relations are utilized in Eq. (4-12c), the linear form becomes

$$a_j f_j - \tilde{a}_j f_{j-1} + b_j u_j - \tilde{b}_j u_{j-1} + c_j v_j - \tilde{c}_j v_{j-1} = S_j \tag{4-16}$$

where

$$a_j = \frac{1}{2}\,\Delta\eta\,\bar{v}_{j-\frac{1}{2}}$$

$$\tilde{a}_j = -\frac{1}{2}\,\Delta\eta\,\bar{v}_{j-\frac{1}{2}}$$

$$b_j = -\Delta\eta\,\beta\,\bar{u}_{j-\frac{1}{2}}$$

$$\tilde{b}_j = \Delta\eta\,\beta\,\bar{u}_{j-\frac{1}{2}}$$

$$c_j = 1 + \frac{1}{2}\,\Delta\eta\,\bar{f}_{j-\frac{1}{2}}$$

$$\tilde{c}_j = 1 - \frac{1}{2}\,\Delta\eta\,\bar{f}_{j-\frac{1}{2}}$$

$$S_j = \Delta\eta(\bar{f}\bar{v})_{j-\frac{1}{2}} - \Delta\eta\,\beta(1 + \bar{u}^2_{j-\frac{1}{2}})$$

The difference equations for the present scheme are Eqs. (4-12a), (4-12b), and (4-16) with $j = 2,3,4,\cdots J$. As Keller has shown, these equations can be written as a system of block-tridiagonal equations. The boundary conditions (4-11) and the difference equations are written as the following system of equations where Eq. (4-12b) with $j = 2$ is written as if it is a boundary condition:

$$f_1 = 0 \tag{4-17a}$$

$$u_1 = 0 \tag{4-17b}$$

$$u_2 - \frac{1}{2}\,\Delta\eta(v_2 + v_1) = 0 \tag{4-17c}$$

In the following, $j = 2, 3, 4, \cdots, J - 1$

$$f_j - f_{j-1} - \frac{1}{2}\,\Delta\eta(u_j + u_{j-1}) = 0 \tag{4-17d}$$

$$a_j f_j - \tilde{a}_j f_{j-1} + b_j u_j - \tilde{b}_j u_{j-1} + c_j v_j - \tilde{c}_j v_{j-1} = S_j \tag{4-17e}$$

$$u_{j+1} - u_j - \frac{1}{2}\,\Delta\eta(v_{j+1} + v_j) = 0 \tag{4-17f}$$

while the remaining equations give

$$f_J - f_{J-1} - \frac{1}{2}\,\Delta\eta\,u_{J-1} = \frac{1}{2}\,\Delta\eta \tag{4-17g}$$

$$\tilde{a}_J f_J - \tilde{a}_J f_{J-1} - \tilde{b}_J u_{J-1} + c_J v_J - \tilde{c}_J v_{J-1} = S_J - b_J \tag{4-17h}$$

$$u_J = 1 \tag{4-17i}$$

The above Eqs. (4-17) are written in matrix form as

$$B_1 W_1 - C_1 W_2 = D_1 \tag{4-18a}$$

$$-A_j W_{j-1} + B_j W_j - C_j W_{j+1} = D_j \qquad j = 2,3,\cdots, J - 1 \tag{4-18b}$$

$$-A_J W_{J-1} + B_J W_J = D_J \tag{4-18c}$$

where the various terms are

$$W_j = \begin{vmatrix} f_j \\ u_j \\ v_j \end{vmatrix} \qquad B_1 = \begin{vmatrix} 1 & 0 & 0 \\ 0 & 1 & 0 \\ 0 & 0 & -\Delta\eta/2 \end{vmatrix}$$

$$C_1 = \begin{vmatrix} 0 & 0 & 0 \\ 0 & 0 & 0 \\ 0 & -1 & \Delta\eta/2 \end{vmatrix} \qquad D_1 = \begin{vmatrix} 0 \\ 0 \\ 0 \end{vmatrix}$$

$$A_j = \begin{vmatrix} 1 & \Delta\eta/2 & 0 \\ \tilde{a}_j & \tilde{b}_j & \tilde{c}_j \\ 0 & 0 & 0 \end{vmatrix} \qquad B_j = \begin{vmatrix} 1 & -\Delta\eta/2 & 0 \\ a_j & b_j & c_j \\ 0 & -1 & -\Delta\eta/2 \end{vmatrix}$$

$$C_j = \begin{vmatrix} 0 & 0 & 0 \\ 0 & 0 & 0 \\ 0 & -1 & \Delta\eta/2 \end{vmatrix} \qquad D_j = \begin{vmatrix} 0 \\ S_j \\ 0 \end{vmatrix}$$

$$A_J = \begin{vmatrix} 1 & \Delta\eta/2 & 0 \\ \tilde{a}_J & \tilde{b}_J & \tilde{c}_J \\ 0 & 0 & 0 \end{vmatrix} \qquad B_J = \begin{vmatrix} 1 & 0 & 0 \\ a_J & 0 & c_J \\ 0 & 1 & 0 \end{vmatrix}$$

$$D_J = \begin{vmatrix} \Delta\eta/2 \\ S_J - b_J \\ 1 \end{vmatrix}$$

The above Eqs. (4-18) are solved with the block-tridiagonal method which is described in Appendix B. The midpoint scheme has rapid convergence of the iteration procedure as in the Davis coupled method, but the solution requires the use of the more time-consuming block-tridiagonal difference equations.

The foregoing midpoint, finite-difference scheme has been utilized in a method to obtain Falkner-Skan solutions with reverse flow by Keller and Cebeci.[54] Also, the previously described Davis coupled scheme has been used to obtain reverse flows by Werle and Bertke.[50]

5. NON-SIMILAR SOLUTION TECHNIQUES

5.1 Introduction

Some of the various numerical techniques that have been employed to solve the two-dimensional boundary-layer equations along a surface are presented. A complete description is not intended but only the basic ideas of the methods will be given. In order to illustrate the various techniques, the incompressible equations are employed and are obtained from Eqs. (3-8) where $\theta = 1$ and $\ell = 1$ which gives

$$2\xi\, \partial F/\partial\xi + \partial V/\partial\eta + F = 0 \tag{5-1a}$$

$$2\xi F\, \partial F/\partial\xi + V\, \partial F/\partial\eta + \beta(F^2 - 1) - \partial^2 F/\partial\eta^2 = 0 \tag{5-1b}$$

or Eq. (3-12a) becomes

$$2\xi\left(\frac{\partial f}{\partial\eta}\frac{\partial^2 f}{\partial\xi\partial\eta} - \frac{\partial f}{\partial\xi}\frac{\partial^2 f}{\partial\eta^2}\right) = \frac{\partial^3 f}{\partial\eta^3} + f\frac{\partial^2 f}{\partial\eta^2} + \beta\left[1 - \left(\frac{\partial f}{\partial\eta}\right)^2\right] \tag{5-2}$$

The boundary conditions have been given previously by Eqs. (3-13) and (3-14).

In the description of the various finite-difference schemes a uniform grid will be employed. The grid point locations are given by $\eta_{j+1} = \eta_j + \Delta\eta$ where $\eta_1 = 0$ and $j = 1, 2, 3, \cdots, J$ and $\xi_{i+1} = \xi_i + \Delta\xi$ where $\xi_1 = 0$ and $i = 1, 2, 3, \cdots, I$.

Also, many of the non-similar techniques reduce to the similar solution problem and an understanding of the previous section is necessary to understand this section.

5.2 Semi-Discrete Method (Boundary Value)

This approach was originated by Hartree and Womersley[55] as a technique to change partial differential equations into ordinary differential equations for solution on a mechanical differential analyzer. The main feature of this method for two independent variables is that derivatives with respect to one of the variables are replaced with finite-differences. The resulting equations are ordinary differential equations. In the present case the derivatives in the flow direction are replaced with finite-differences and the resulting equations are of the boundary-value type. This approach is also referred to as a differential-difference scheme and the method of lines in the Russian literature which has been reviewed by Liskovets.[58] The method was first applied to the boundary-layer equations by Leight[57] and later by Manohar.[56] The method has been developed further and applied to a variety of problems by Smith and colleagues. This work is described in the review article by Jaffe and Smith.[5]

There have been three formulations of this procedure as follows:

(a) Point method - The governing equations are evaluated at the point (i+1) with the ξ-derivative utilizing the independent variable at the point (i+1) and one or more

values which have been determined previously. The derivative is expressed as

$$(\partial F/\partial \xi)_{i+1} = aF_{i+1} + bF_i + cF_{i-1} + \cdots \tag{5-3}$$

where the coefficients a, b, c, $\cdots$ depend on the choice of the distribution of the grid system. The resulting ordinary differential equations will have F_{i+1} and V_{i+1} as the independent variables with all other quantities known. If coefficients a and b are non-zero, the method will be first order in the ξ direction. With the coefficients a, b, and c non-zero, the method becomes second order.

(b) Mean method - The governing equations are evaluated at the point $(i+\frac{1}{2})$ where the simplest formulation uses the trapezoidal rule which results in the following for the derivative:

$$(\partial F/\partial \xi)_{i+\frac{1}{2}} = (F_{i+1} - F_i)/\Delta\xi \tag{5-4a}$$

All the other terms in the governing equation are evaluated, for example, as

$$F_{i+\frac{1}{2}} = \frac{1}{2}(F_{i+1} + F_i) \tag{5-4b}$$

where F can represent a derivative. The product terms can be written in two forms with the following chosen:

$$(V\ \partial F/\partial \eta)_{i+\frac{1}{2}} = V_{i+\frac{1}{2}}\ (\partial F/\partial \eta)_{i+\frac{1}{2}} \tag{5-4c}$$

(c) Least-Squares method - This method has been utilized to damp out initial profile errors when the solution is started far downstream with a small step-size. The ξ-derivative is approximated with a least-squares method where, for example, a quadratic curve is used with four grid points.

When any of the above procedures are applied to the boundary layer Eqs. (5-1) or (5-2), the resulting equations are two-point boundary-value, ordinary differential equations. Therefore, the equations are nearly the same as the similar equations given in Eqs. (4-1) and (4-2) and any of the solution techniques described in Section 4 can be utilized. In the work of Smith and colleagues a shooting method was employed to obtain the solution while a better approach would be to use the finite-difference method of Section 4.3. When the mean method formulation is utilized with the finite-difference method, the resulting difference equations are the same as the Crank-Nicolson method which will be described subsequently in Section 5.4.4.

In order to improve the accuracy of the solution in the direction normal to the surface, Peters[59, 60] has used a Hermitian finite-difference procedure. The partial differential equations are reduced to a two-point boundary-value problem with the use of the difference relation (5-3). The velocity F is approximated between three grid points with the fourth-order polynomial

$$F(\eta) = \frac{1}{2}F_{j+1}(t^2 + t) + F_j(1 - t^2) + \frac{1}{2}F_{j-1}(t^2 - t) + \alpha t(1 - t^2) + \beta t^2(1 - t^2) \tag{5-5}$$

where $t = (\eta - \eta_j)/\Delta\eta$ and t = 1, 0, and -1 which gives F_{j+1}, F_j, and F_{j-1}, respectively. The derivatives of F become

$$\frac{\partial F}{\partial \eta} = \left[\frac{1}{2}F_{j+1}(2t + 1) - 2F_j t + \frac{1}{2}F_{j-1}(2t - 1) + \alpha(1 - 3t^2) + \beta(2t - 4t^3)\right]/\Delta\eta \tag{5-6a}$$

$$\frac{\partial^2 F}{\partial \eta^2} = \left[F_{j+1} - 2F_j + F_{j-1} - 6\alpha t + \beta(2 - 12t^2)\right]/\Delta\eta^2 \tag{5-6b}$$

The above derivatives, (5-3) and (5-6), and the function, (5-5), are used to evaluate the terms in the momentum equation, (5-1b). This finite-difference equation is evaluated at the three points t = 1, t = 0, and t = -1 which gives the following three equations:

$$L_{11}F_{j+1} + L_{12}F_j + L_{13}F_{j-1} + L_{14}\alpha + L_{15}\beta = d_{j+1} \tag{5-7a}$$

$$L_{21}F_{j+1} + L_{22}F_j + L_{23}F_{j-1} + L_{24}\alpha + L_{25}\beta = d_j \tag{5-7b}$$

$$L_{31}F_{j+1} + L_{32}F_j + L_{33}F_{j-1} + L_{34}\alpha + L_{35}\beta = d_{j-1} \tag{5-7c}$$

where the coefficients have been given by Peters. These equations are used to eliminate the unknowns α and β which give the tridiagonal equations

$$-A_j F_{j-1} + B_j F_j - C_j F_{j+1} = D_j \tag{5-8}$$

which is solved with the procedure given in Appendix B. The dependent variable V is obtained from Eq. (5-1a) with the use of Simpson's integration formula. Since the governing equation, (5-1b), has been linearized to obtain the linear difference Eqs. (5-7), an iteration between the solution of Eq. (5-8) and the solution for V is required. Since a Newton-Raphson linearization has not been used, the convergence of the iteration is probably slow and one would question if 4th order accuracy has been achieved. This procedure has also been used by Krause[81] for solving boundary-layer flow, and he refers to it as the "mehrsteller"-integration technique.

5.3 Semi-Discrete Method (Initial Value)

This method is the same as the previous method except the derivatives across the boundary layer in this case are replaced with finite differences. The resulting equations will be first order and of the initial value type. Steiger and Sepri[82] used this method to solve the von Mises form of the boundary-layer equations. The scheme was not successful as the resulting ordinary differential equations are stiff and were not readily solved with a Runge-Kutta integration procedure. Lubard and Schetz[83] used the semi-discrete method and applied it to the boundary-layer equations in physical coordinates. This paper indicates the method is very successful as the modified Runge-Kutta integration scheme of Treanor[84] was used. When this procedure is applied to Eqs. (5-1), the resulting ordinary differential equations become

$$2\xi F_j \frac{\partial F_j}{\partial \xi} = - V_j (F_{j+1} - F_{j-1})/(2\Delta\eta) - \beta(F_j^2 - 1) + (F_{j+1} - 2F_j + F_{j-1})/\Delta\eta^2 \quad j = 2,3,\cdots, J-1 \quad (5\text{-}9)$$

where

$$V_j = V_1 - \int_0^{\eta_j} \left(2\xi \frac{\partial F}{\partial \xi} + F\right) d\eta \quad (5\text{-}10)$$

The trapezoidal rule is used to evaluate the integral and with the boundary condition $F_1 = 0$ the above becomes

$$V_j = V_1 - \frac{1}{2}\left(2\xi \frac{\partial F_j}{\partial \xi} + F_j\right) - \Delta\eta \sum_{n=2}^{j-1} \left(2\xi \frac{\partial F_n}{\partial \xi} + F_n\right) \quad (5\text{-}11)$$

Equation (5-11) is substituted into Eq. (5-9) to obtain a system of J-2 nonlinear, ordinary differential equations of the form

$$\frac{\partial F_j}{\partial \xi} = f\left(\xi, F_{j-1}, F_j, F_{j+1}, \frac{\partial F_n}{\partial \xi}\right) \quad \begin{cases} n = 2,3,\cdots, j-1 \\ j = 2,3,\cdots, J-1 \end{cases} \quad (5\text{-}12)$$

This is not the standard form for integration subroutines but with additional algebra can be written in the usual form without the derivative appearing on the right side of Eq. (5-12). Since these equations are stiff, one of the recently developed computer programs, such as the Gear[85] method, should be used. These computer programs feature variable order methods, automatic step and error control, and are capable of effectively solving stiff, ordinary differential equations.

5.4 Finite-Difference Methods

5.4.1 Explicit (Binder[86]-Schmidt[87]) - As early as 1938 Prandtl[88] proposed an explicit finite-difference method for solving the boundary-layer equations. A new impetus was provided in 1955 when Flügge-Lotz[26] applied an explicit scheme to the Crocco form of the boundary-layer equations. A method for handling the boundary-layer equations in physical coordinates was developed by Wu[89] where the proper form of the continuity equation was determined. When this scheme is applied to Eqs. (5-1), the resulting difference equation for the momentum equation is

$$2\xi_i F_{i,j} (F_{\underline{i+1}} - F_i)_j/\Delta\xi + V_{i,j}(F_{j+1} - F_{j-1})_i/(2\Delta\eta) + \beta(F_{i,j}^2 - 1) - (F_{j+1} - 2F_j + F_{j-1})_i/\Delta\eta^2 = 0 \quad (5\text{-}13a)$$

and the continuity equation is

$$\xi_{i+1}(F_{i+1} - F_i)_j/\Delta\xi + \xi_{i+1}(F_{i+1} - F_i)_{j-1}/\Delta\xi + (\underline{V_j} - V_{j-1})_{i+1}/\Delta\eta + \frac{1}{2}(F_j + F_{j-1})_{i+1} = 0 \quad (5\text{-}13b)$$

The unknown quantities in each equation are underlined where F's at (i+1) and various grid points j across the layer are first determined from Eq. (5-13a). Then Eq. (5-13b) is used to determine the V's at (i+1) and the grid points j. The boundary condition $V_1 = 0$ is used to obtain the solution of Eq. (5-13b) and the boundary conditions $F_1 = 0$ and $F_J = 1$ are used to obtain the complete solution of F at (i+1).

This method is second-order accurate in the direction across the boundary layer and first-order accurate in the flow direction. Wu has given the following restriction on the step-size for a flat plate incompressible flow as a sufficient condition for stability of the difference scheme:

$$\Delta x < (\Delta y^2 u/2\nu) \tag{5-14a}$$

which becomes in the present coordinates

$$\Delta\xi < \xi F \Delta\eta^2 \tag{5-14b}$$

He has also given the following restriction

$$\Delta y < 2\psi/v \tag{5-15}$$

and this resembles the previous condition, (4-9), for the similar solutions.

5.4.2 DuFort-Frankel[89] - This explicit method was first used by Raetz[70] for solving the three-dimensional boundary-layer equations. More recently it has been employed by Pletcher[71] for solving turbulent boundary layers. The advantage of this scheme over the usual explicit scheme is that the DuFort-Frankel scheme is stable without restrictions on the step-sizes. However, there are disadvantages which will be discussed after the method has been described. The present formulation follows that of Pletcher, but he applied it to the boundary-layer equations in physical coordinates. The momentum equation is evaluated at the point (i,j) as follows:

$$\xi_i F_{i,j} \underline{(F_{i+1} - F_{i-1})_j}/\Delta\xi + V_{i,j}(F_{j+1} - F_{j-1})_i/(2\Delta\eta)$$

$$+ \beta(F_{i,j}^2 - 1) - \left[(F_{j+1} + F_{j-1})_i - \underline{(F_{i+1} + F_{i-1})_j}\right]/\Delta\eta^2 = 0 \tag{5-16a}$$

while the continuity equation is evaluated at the point $(i+1, j-\frac{1}{2})$ and becomes

$$\xi_{i+1}\left[(F_{i+1} - F_{i-1})_j + (F_{i+1} - F_{i-1})_{j-1}\right]/(2\Delta\xi) + \underline{(V_j - V_{j-1})_{i+1}}/\Delta\eta + \tfrac{1}{2}(F_j + F_{j-1})_{i+1} = 0 \tag{5-16b}$$

Again, the unknowns are underlined and after the F's have been obtained, the V's are then calculated. In this method three levels of information in the ξ-direction have been used. The continuity equation is first order in the ξ-direction and second order in the η-direction while the momentum equation has the following truncation error:

$$(\Delta\xi/\Delta\eta)^2\, \partial^2 F/\partial\xi^2 + O(\Delta\xi^2) + O(\Delta\eta^2)$$

Since in boundary-layer theory $\partial^2 F/\partial\xi^2$ is assumed zero, the first term in the truncation error should be small. This unpleasant feature of the truncation error of the DuFort-Frankel method does not appear to be a problem for the boundary-layer equations, but the step-sizes should be chosen to keep this term small. The present formulation is first order in the ξ-direction and requires two initial profiles of data to extend the solution downstream. In the work of Pletcher the initial profile of data is used with an explicit-difference scheme to generate the second initial profile of data. Again, this limits the method to a first-order scheme in the flow direction.

5.4.3 Implicit - The use of an implicit-difference scheme was first applied to the boundary-layer equations in physical coordinates by Rouleau and Osterle.[72] This scheme has the property of being stable and is first order in the flow direction. The difference equations in this case are

$$2\xi_{ij}(F_{i+1} - F_{ij})/\Delta\xi + V_{i,j}(F_{j+1} - F_{j-1})_{i+1}/(2\Delta\eta)$$

$$+ \beta\left[(F_{i+1}F_i)_j - 1\right] - (F_{j+1} - 2F_j + F_{j-1})/\Delta\eta^2 = 0 \tag{5-17a}$$

and

$$2\xi_{i+1}(F_{i+1} - F_i)_j/\Delta\xi + (V_j - V_{j-1})_{i+1}/\Delta\eta + \tfrac{1}{2}(F_j + F_{j-1})_{i+1} = 0 \tag{5-17b}$$

The unknowns in the momentum equation, (5-17a), are F_{j-1}, F_j, and F_{j+1} at (i+1). Rouleau and Osterle used a relaxation procedure to solve these simultaneous difference equations. The appropriate approach is to use the tridiagonal solution technique described in Appendix B. After the F's have been obtained, the continuity equation, (5-17b), is used to obtain the V's across the boundary layer.

5.4.4 Crank-Nicolson[73] - The initial application of this method was made by Kramer and Lieberstein[28] to the Crocco form of the boundary-layer equations. Later at about the same time Brailoskaya and Chudov[19] in Russia and Blottner and Flügge-Lotz[21] in the United States developed this approach for physical coordinates. In all of these methods the finite-difference equations are written such that the unknowns appear as linear terms. The momentum equation, (5-1b), is written as

$$2\xi_{i+\frac{1}{2}} F_{i+\frac{1}{2},j} \left(F_{i+1} - F_i\right)_j/\Delta\xi + V_{i+\frac{1}{2},j} \left[\left(F_{j+1} - F_{j-1}\right)_{i+1} + \left(F_{j+1} - F_{j-1}\right)_i\right]/(4\Delta\eta)$$

$$+ \beta\left(F_{i,j}\, F_{i+1,j} - 1\right) - \left[\left(F_{j+1} - 2F_j + F_{j-1}\right)_{i+1} + \left(F_{j+1} - 2F_j + F_{j-1}\right)_i\right]/(2\Delta\eta^2) = 0 \quad (5\text{-}18a)$$

and the continuity equation, (5-1a), becomes

$$\xi_{i+\frac{1}{2}} \left[\left(F_{i+1} - F_i\right)_j + \left(F_{i+1} - F_i\right)_{j-1}\right]/\Delta\xi + \left(V_j - V_{j-1}\right)_{i+\frac{1}{2}}/\Delta\eta + \frac{1}{4}\left[\left(F_{i+1} + F_i\right)_j + \left(F_{i+1} + F_i\right)_{j-1}\right] = 0 \quad (5\text{-}18b)$$

When Eq. (5-18a) is rearranged, it is the tridiagonal form

$$-A_j\, F_{j-1} + B_j F_j - C_j\, F_{j+1} = D_j \quad (5\text{-}19)$$

and the F's can be determined with the alogrithm described in Appendix B. Then Eq. (5-18b) is used to solve for $V_{i+\frac{1}{2},j}$ and the solution is started at the wall where $V_1 = 0$. This method and the following implicit schemes are stable without any restrictions on the step sizes.

If this method is to be a true Crank-Nicolson scheme, then the terms $F_{i+\frac{1}{2},j}$ and $V_{i+\frac{1}{2},j}$ cannot be approximated at a previous grid point where they are known as is usually done. An iteration could be performed where these terms are evaluated as follows:

$$F_{i+\frac{1}{2},j} = \frac{1}{2}\left(F_{i+1} + F_i\right)_j$$

with a similar expression for V. It will be shown later that this approach is not the best; the convergence rate for this type of iteration procedure is slow. Although the Crank-Nicolson scheme can be second-order accurate in the flow direction, most procedures in practice are first-order accurate and iteration should not be performed with this solution technique.

The Crank-Nicolson scheme has been applied to the combined continuity-momentum, Eq. (5-2), by Fussell and Hellums.[74] The nonlinear terms are linearized (not Newton-Raphson) and an iteration procedure is employed. Although the authors claim rapid convergence, the number of iterations is not given and the same objections as discussed above also apply to this approach. Since a third-order derivative appears in Eq. (5-2), the derivative is evaluated with five grid points and the resulting implicit difference equations are of the penta-diagonal type. This requires a more complex solution algorithm than the usual Crank-Nicolson schemes described previously.

Fannelop[75] has also solved the continuity-momentum equation, (5-2), with a Crank-Nicolson scheme. In this approach Eq. (5-2) is rewritten as

$$2\xi\left(F\frac{\partial F}{\partial \xi} - \frac{\partial f}{\partial \xi}\frac{\partial F}{\partial \eta}\right) = \frac{\partial^2 F}{\partial \eta^2} + f\frac{\partial F}{\partial \eta} + \beta\left(1 - F^2\right) \quad (5\text{-}20a)$$

and

$$f = f_0(\xi, 0) + \int_0^{\eta} F\, d\eta \quad (5\text{-}20b)$$

The Crank-Nicolson differences are used to replace the various terms in Eq. (5-20a) where the terms are linearized such that the unknowns appear linearly. Equation (5-20b) is then used to determine the f's across the boundary layer. Then an iteration procedure is used to reevaluate the terms that were linearized such that all terms are centered properly. In this method the term $(\partial f/\partial \xi)_{i+\frac{1}{2},j}$ is initially set equal to $(\partial f/\partial \xi)_{i-\frac{1}{2},j}$ to start the iteration procedure. Again, this method has not used Newton-Raphson linearization, and it is questionable if one should iterate to obtain a second-order scheme.

5.4.5 Box Scheme - The basic idea for this approach was presented in Section 4.3 for the Keller midpoint scheme. The box scheme was developed by Keller[78] and has been applied to the boundary-layer equations by Keller and Cebeci.[49] The governing equation, (5-2), is written as a system of first-order equations by introducing two new unknowns, u and v, which give

$$\partial f/\partial \eta = u \quad (5\text{-}21a)$$

$$\partial u/\partial \eta = v \quad (5\text{-}21b)$$

$$\partial v/\partial\eta + fv + \beta(1 - u^2) + 2\xi\left(-u\frac{\partial u}{\partial\xi} + v\frac{\partial f}{\partial\xi}\right) = 0 \qquad (5\text{-}21c)$$

The first two equations, (5-21a) and (5-21b), are evaluated at the point $(i+1, j-\frac{1}{2})$ which gives

$$(f_j - f_{j-1})_{i+1}/\Delta\eta = \frac{1}{2}(u_j + u_{j-1})_{i+1} \qquad (5\text{-}22a)$$

$$(u_j - u_{j-1})_{i+1}/\Delta\eta = \frac{1}{2}(v_j + v_{j-1})_{i+1} \qquad (5\text{-}22b)$$

Equation (5-21c) is evaluated at the center of the box which is the point $(i+\frac{1}{2}, j-\frac{1}{2})$. The various terms in this equation are written in finite-difference form as follows:

$$\partial v/\partial\eta = \left[(v_j - v_{j-1})_{i+1} + (v_j - v_{j-1})_i\right]/(2\Delta\eta) \qquad (5\text{-}23a)$$

$$fv = \frac{1}{2}\left[(fv)_{i+1} + (fv)_i\right]_{j-\frac{1}{2}} \qquad (5\text{-}23b)$$

$$\beta = \frac{1}{2}(\beta_{i+1} + \beta_i) \qquad (5\text{-}23c)$$

$$\beta u^2 = \frac{1}{2}\left[(\beta u^2)_{i+1} + (\beta u^2)_i\right] \qquad (5\text{-}23d)$$

$$2\xi u\,\partial u/\partial\xi = \xi_{i+\frac{1}{2}}(u_{i+1} + u_i)_{j-\frac{1}{2}}(u_{i+1} - u_i)_{j-\frac{1}{2}}/\Delta\xi \qquad (5\text{-}23e)$$

$$2\xi v\,\partial f/\partial\xi = \xi_{i+\frac{1}{2}}(v_{i+1} + v_i)_{j-\frac{1}{2}}(f_{i+1} - f_i)_{j-\frac{1}{2}}/\Delta\xi \qquad (5\text{-}23f)$$

When the above relations, (5-23), are substituted into Eq. (5-21c), the nonlinear terms are linearized with the Newton-Raphson relations, (4-14), and terms at $(j-\frac{1}{2})$ are evaluated with Eq. (4-15); the resulting difference equation is

$$a_j f_j - \tilde{a}_j f_{j-1} + b_j u_j - \tilde{b}_j u_{j-1} + c_j v_j - \tilde{c}_j v_{j-1} = s_j \qquad (5\text{-}24)$$

This equation is the same form as Eq. (4-16), but the coefficients in the above equation are much more complex than those in Eq. (4-16), and are given by Blottner.[77] Equations (5-22) are also the same as Eqs. (4-12a) and (4-12b). Therefore, the present equations are the same as Eqs. (4-18) except new relations must be introduced for the coefficients a_j, $\tilde{a}_j$, b_j, $\tilde{b}_j$, c_j, and $\tilde{c}_j$. The solution then proceeds as described previously with the block-diagonal method.

As this method is implicit, it is stable like the Crank-Nicolson scheme without any restrictions on the step-sizes.

5.4.6 Petukhov Method[78] - This method was devised to avoid oscillations which can occur with a Crank-Nicolson scheme for problems with large local gradients in the flow direction. To illustrate this method consider the partial-differential equation which is expressed as

$$\partial F/\partial\xi = L[F] \qquad (5\text{-}25a)$$

where

$$L[F] = a_0\,\partial^2 F/\partial\eta^2 + a_1\,\partial F/\partial\eta + a_2 F + a_3 \qquad (5\text{-}25b)$$

Two steps are taken to advance the solution from (i) to (i+1) and these two steps are repeated in an iterative manner. The finite-difference equations for the two steps are

$$(F_{i+\frac{1}{2}} - F_i)/(\tfrac{1}{2}\Delta\xi) = L[F_{i+\frac{1}{2}}] - \frac{1}{4}\Delta\xi\,\partial^2 F/\partial\xi^2 + O(\Delta\xi^2) \qquad (5\text{-}26a)$$

$$(F_{i+1} - F_{i+\frac{1}{2}})/(\tfrac{1}{2}\Delta\xi) = L[F_{i+1}] - \frac{1}{4}\Delta\xi\,\partial^2 F/\partial\xi^2 + O(\Delta\xi^2) \qquad (5\text{-}26b)$$

where

$$\partial^2 F/\partial\xi^2 = (\bar{F}_{i+1} - 2\bar{F}_{i+\frac{1}{2}} + F_i)/(\tfrac{1}{2}\Delta\xi)^2 \qquad (5\text{-}26c)$$

The quantities with a bar are evaluated from a previous iteration. Since the coefficients in Eq. (5-25b) can depend on F, they would be evaluated with $\bar{F}$ from the previous iteration.

To investigate the characteristics of this finite-difference scheme, Blottner[79] represented the right side of Eq. (5-25) as

$$L[F] = (P - QF)/\epsilon \tag{5-27}$$

where the quantities ϵ and Q are assumed positive to make the equation inherently stable. The η-derivatives have been neglected in Eq. (5-25b) and this results in a linear, ordinary-differential equation for (5-25). The exact solution to this equation is

$$F(\xi_i) = C\Lambda^i + P/Q \tag{5-28}$$

where $\Lambda = \exp(-\varphi)$ and $\varphi = \Delta\xi Q/\epsilon$. The solutions of this equation with the Petukhov method is the same as Eq. (5-28) except

$$\Lambda = (1 - \tfrac{1}{4}\varphi)/(1 + \tfrac{3}{4}\varphi + \tfrac{1}{4}\varphi^2) \tag{5-29}$$

while the Crank-Nicolson scheme gives

$$\Lambda = (1 - \tfrac{1}{2}\varphi)/(1 + \tfrac{1}{2}\varphi) \tag{5-30}$$

For small values of φ, both the Petukhov and Crank-Nicolson methods are second-order accurate and are a good approximation to the exact exponential solution. For large values of φ, the Petukhov method has the appropriate asymptotic behavior of Λ approaching zero while the Crank-Nicolson method Λ approaches -1. This indicates why the Crank-Nicolson method might slowly damp-out an error with an oscillating value.

The complete details of how the boundary-layer equations are written in finite-difference form is not given by Petukhov. It is stated that two iterations of the equations for each step $\Delta\xi$ is reasonable. This requires six evaluations of L[F] for each step $\Delta\xi$ while the Crank-Nicolson scheme described in Section 6 requires two evaluations. The Petukhov method requires more computer time than the Crank-Nicolson scheme when the same step sizes are used, but should give more accurate results for some problems.

5.4.7 Multi-level Method - With the semi-discrete method of the boundary-value type (Section 5.2), it was indicated by Eq. (5-3) that the ξ-derivative could involve several levels of values of the dependent variable in the marching direction. Davis and Flügge-Lotz[50] have used a three-level scheme where the derivative at (i+1) is expressed as

$$\partial F/\partial\xi = (3F_{i+1} - 4F_i + F_{i-1})/(2\Delta\xi) + O(\Delta\xi^2) \tag{5-31}$$

The η-derivatives are evaluated at (i+1) with central differences. Terms, which should be evaluated at (i+1) but would give a nonlinear difference equation, are approximated with extrapolated values where the dependent variables at (i) and (i-1) are used.

This type of method cannot be used to start the solution away from the initial profiles or when the ξ-derivative is discontinuous. The method is second-order accurate without iteration and no stability problems were encountered. A second-order scheme must be used to start the solution in order to obtain a second-order accurate solution downstream with a uniform grid $\Delta\xi$. Since the starting method could be used to continue the solution downstream, the multi-level method loses much of its appeal.

5.5 Integral-Control Volume Method

With this method, the governing equations are integrated over a small control volume and the integral is evaluated by assuming linear or quadratic variation of the variables between the grid points. This approach has been used by Shchennikov[81] and Patankar and Spalding.[4] The control volume is taken from i to i+1 and from $j-\frac{1}{2}$ to $j+\frac{1}{2}$ which is the same as used by Patankar and Spalding. With the linear variation, the first term in Eq. (5-1b) becomes

$$2\xi F\,\partial F/\partial\xi = \int_{\xi_i}^{\xi_{i+1}}\int_{\eta_{j-\frac{1}{2}}}^{\eta_{j+\frac{1}{2}}} \xi\,\frac{\partial F^2}{\partial\xi}\,d\eta\,d\xi/(\Delta\xi\,\Delta\eta) = \frac{1}{8}\,\frac{\xi_{i+\frac{1}{2}}}{\Delta\xi}\Big[(F_{i+1} + F_i)_{j+1}\,(F_{i+1} - F_i)_{j+1}$$

$$+ 6(F_{i+1} + F_i)_j\,(F_{i+1} - F_i)_j + (F_{i+1} + F_i)_{j-1}\,(F_{i+1} - F_i)_{j-1}\Big] \tag{5-32}$$

The other terms in the momentum and continuity equations can be evaluated in a similar manner. The resulting momentum difference equation is nonlinear and is linearized with terms assumed known from a previous iteration to obtain the usual tridiagonal system of Eqs. (5-19). In the two references, the continuity equation has been eliminated with the use of von Mises variables or with the use of Eq. (5-2). In the work of Patankar and Spalding, a linear variation of the variables is assumed and the method is second-order accurate in the direction normal to the surface. Byrkin and Shchennikov[82] have used quadratic variation of the variables and the method is fourth-order accurate in the η-direction.

In the paper by Shchennikov the boundary-layer equations are also written in divergence form and then are evaluated with the gauss formula which gives for each conservation equation ($k = 1,2,\cdots$)

$$\nabla \cdot \bar{\Psi}_k = \left(\oint_L \Psi_{x_k}\, dy + \oint_L \Psi_{y_k}\, dx\right)/\Delta x\, \Delta y = 0 \qquad (5\text{-}33)$$

where L is the contour of the elementary volume $\Delta x \cdot \Delta y$. The quantities Ψ_{x_k} and Ψ_{y_k} are the projection of the vector $\bar{\Psi}_k$ on the x and y axes, respectively. The integrals in (5-33) are evaluated with the trapezoidal rule and the derivatives in the normal direction y are replaced with central differences. The resulting difference equations are nonlinear and of second-order accuracy in both directions if the complete equations are solved.

5.6 Other Methods

Although the intention has been to consider finite-difference methods for solving the boundary-layer equations, it is worthwhile to at least mention some of the other useful methods. Dorodnitsyn[83] introduced the method of integral relations and applied it to the boundary-layer equations. Pallone[84] later used the strip-integral method. The general method of weighted residuals for solving the boundary-layer equations has been thoroughly explored by Bethel[85] and developed further by Bossel.[86] In all of these methods the partial-differential equations are reduced to a system of first-order ordinary differential equations of the initial-value type.

Another approach which has proved very useful is the matrix-integral method developed by Kendall and Bartlett.[87] The boundary-layer equation, (5-2), is used and is integrated across strips from j to j+1. The dependent variable f is approximated with a spline function over the interval and derivatives in the flow direction are replaced with finite-differences. The resulting system of nonlinear, equations are solved by Newton-Raphson iteration. The order of this method has not been determined, and all of the numerical results indicate no stability limitations.

The finite-element method has recently been used by Baker[88] and Oden and Wellford[89] for solving the boundary-layer equation. The usefulness of this approach for boundary-layer flow at this time is an open question.

6. INCOMPRESSIBLE BOUNDARY-LAYER PROCEDURE

6.1 Davis Coupled Scheme

The purpose of this section is to present in detail a good numerical method for solving the incompressible boundary-layer equations. The method chosen is a Crank-Nicolson scheme which has coupling between the continuity and momentum equations. This method was suggested by Davis and used by Werle and Bertke.[50] An investigation of the accuracy of this scheme and several others has been made by Blottner.[77] Of the second-order accurate approaches, this method has simplicity and for example, is faster than the Keller box scheme. In the future, the use of higher order methods could prove to be better than the present scheme, but further work needs to be performed on this subject.

Rather than solving the incompressible equations, (5-1), the compressible form, (3-8), will be used where $\theta = 1$ and $\ell = 1$ for the present case. The momentum equation, (3-8b), is evaluated at the location $(i+\frac{1}{2},j)$ with the ξ-derivative written as

$$F\, \partial F/\partial \xi = \frac{1}{2}\,(F_{i+1} + F_i)_j\,(F_{i+1} - F_i)_j/\Delta\xi = \frac{1}{2}\,(F^2_{i+1} - F^2_i)_j/\Delta\xi \qquad (6\text{-}1)$$

The other terms in the equation are averaged between (i) and (i+1) and are at the position j which gives

$$V\, \partial F/\partial \eta = \frac{1}{2}\,(V\, \partial F/\partial \eta)_{i+1} + \frac{1}{2}\,(V\, \partial F/\partial \eta)_i \qquad (6\text{-}2a)$$

$$\beta(F^2 - \theta) = \frac{1}{2}\,[\beta(F^2 - \theta)]_{i+1} + \frac{1}{2}\,[\beta(F^2 - \theta)]_i \qquad (6\text{-}2b)$$

$$\partial(\ell\, \partial F/\partial \eta)/\partial \eta = \frac{1}{2}\,[\partial(\ell\, \partial F/\partial \eta)/\partial \eta]_{i+1} + \frac{1}{2}\,[\partial(\ell\, \partial F/\partial \eta)/\partial \eta]_i \qquad (6\text{-}2c)$$

The nonlinear terms are linearized with the Newton-Raphson procedure where the required relations are given in Eqs. (4-5). The derivatives are then evaluated with central differences which are

$$(\partial F/\partial \eta)_{i,j} = (F_{j+1} - F_{j-1})_i/(2\Delta\eta) \qquad (6\text{-}3a)$$

$$[\partial(\ell\, \partial F/\partial \eta)/\partial \eta]_{i,j} = [\ell_{j+\frac{1}{2}}\,(F_{j+1} - F_j) - \ell_{j-\frac{1}{2}}\,(F_j - F_{j-1})]_i/\Delta\eta^2 \qquad (6\text{-}3b)$$

The resulting difference equation for the momentum equation becomes

$$(-A_j F_{j-1} + B_j F_j - C_j F_{j+1})_{i+1} + (aV)_{i+1,j} = D_{i+1,j} \qquad j = 2,3,\cdots J-1 \qquad (6\text{-}4)$$

where

$$A_{i+1,j} = (\ell_{j-\frac{1}{2}} + \bar{V}_j \, \Delta\eta/2)_{i+1}/2 \qquad (6\text{-}5a)$$

$$B_{i+1,j} = (\ell_{j+\frac{1}{2}} + \ell_{j-\frac{1}{2}})_{i+1}/2 + \Delta\eta^2 \left[\beta_{i+1} + (\xi_{i+1} + \xi_i)/\Delta\xi\right] \bar{F}_{i+1,j} \qquad (6\text{-}5b)$$

$$C_{i+1,j} = (\ell_{j+\frac{1}{2}} - \bar{V}_j \, \Delta\eta/2)_{i+1}/2 \qquad (6\text{-}5c)$$

$$a_{i+1,j} = (\bar{F}_{j+1} - \bar{F}_{j-1})_{i+1} \, \Delta\eta/4 \qquad (6\text{-}5d)$$

$$D_{i+1,j} = A_{i,j} F_{i,j-1} + C_{i,j} F_{i,j+1} - \left[(\ell_{j+\frac{1}{2}} + \ell_{j-\frac{1}{2}}) + \Delta\eta^2 \beta F_j\right]_i F_{i,j}/2$$

$$+ \Delta\eta^2 \left[(\theta_j \beta)_{i+1} + (\theta_j \beta)_i\right]/2 + \frac{1}{2} \Delta\eta^2 \left\{(\xi_i + \xi_{i+1}) (F_i^2 + \bar{F}_{i+1}^2)_j/\Delta\xi \right.$$

$$\left. + \left[\bar{V}_j (\bar{F}_{j+1} - \bar{F}_{j-1})/(2\Delta\eta) + \beta \bar{F}_j^2\right]_{i+1}\right\} \qquad (6\text{-}5e)$$

Quantities with a bar are evaluated from a previous iteration or are evaluated initially at (i) rather than (i+1). The continuity equation, (3-8a), is evaluated at the point $(i+\frac{1}{2}, j-\frac{1}{2})$ where the various terms are replaced with the following relations:

$$\partial F/\partial\xi = \left[(F_{i+1} - F_i)_j + (F_{i+1} - F_i)_{j-1}\right]/(2\Delta\xi) \qquad (6\text{-}6a)$$

$$\partial V/\partial\eta = \left[(V_j - V_{j-1})_{i+1} + (V_j - V_{j-1})_i\right]/(2\Delta\eta) \qquad (6\text{-}6b)$$

$$F = \left[(F_j + F_{j-1})_{i+1} + (F_j + F_{j-1})_i\right]/4 \qquad (6\text{-}6c)$$

The resulting difference relation is

$$V_{i+1,j} = V_{i+1,j-1} - c_j (F_j + F_{j-1})_{i+1} + d_j \qquad j = 2,3,\cdots J \qquad (6\text{-}7)$$

where

$$c_j = 2 \, \Delta\eta \, (\tfrac{1}{4} + \xi_{i+\frac{1}{2}}/\Delta\xi)$$

$$d_j = -2 \, \Delta\eta \, (\tfrac{1}{4} - \xi_{i+\frac{1}{2}}/\Delta\xi)(F_j + F_{j-1})_i - (V_j - V_{j-1})_i$$

The two difference equations, (6-4) and (6-7), are coupled and are readily solved with the modified tridiagonal algorithm given in Appendix A. In the solution of these equations the boundary conditions are required and are obtained from Eqs. (3-13) and (3-14) which are expressed as

$$V_{i+1,1} = 0, \quad F_{i+1,1} = 0, \text{ and } F_{i+1,J} = 1 \qquad (6\text{-}8)$$

At $\xi = 0$, the partial-differential equations become the similar equation, (4-1), and provide the necessary initial conditions for the solution along the surface. The coefficients for Eq. (6-4) remain the same as those given by Eqs. (6-5) except for the following:

$$B_j = (\ell_{j+\frac{1}{2}} + \ell_{j-\frac{1}{2}})/2 + \Delta\eta^2 \, \beta \, \bar{F}_j \qquad (6\text{-}9a)$$

$$D_j = \frac{1}{2} \Delta\eta^2 \left[\beta + \bar{V}_j (\bar{F}_{j+1} - \bar{F}_{j-1})/(2\Delta\eta) + \beta \, \bar{F}_j^2\right] \qquad (6\text{-}9b)$$

The subscripts (i+1) are neglected when the initial profiles are being obtained. These coefficients are the same as given previously by Eqs. (4-8) with $\ell = 1$. The continuity equation, (6-7), at $\xi = 0$ has $c_j = \Delta\eta/2$ and $d_j = 0$ and is the same as Eq. (4-4).

6.2 Edge Conditions and Location

In order to obtain the boundary-layer solution, the inviscid flow velocity must be given, and for a body of revolution r_b must be specified. With the velocity known, the pressure gradient parameter β is determined from Eq. (3-9b) and the transformed coordinate ξ is obtained from Eq. (3-5b). For example, for the Howarth problem of linearly retarded velocity field, the edge velocity varies as

$$u_e/U_\infty = (1 - x/L) \tag{6-10}$$

where L is a reference length and U_∞ is the free-stream velocity. The transformed coordinate ξ becomes the following when $(\rho\mu)_r = (\rho\mu)_\infty$, $\mathscr{K} = 1/(\rho\mu U)_\infty$ and $r_b^{2j} = 1$:

$$\xi = x[1 - x/(2L)] \tag{6-11}$$

The physical coordinate x in terms of ξ is

$$x/L = 1 - \sqrt{1 - 2\xi/L} \tag{6-12}$$

The pressure gradient parameter becomes

$$\beta = (2\xi/L)/[(2\xi/L) - 1] \tag{6-13}$$

For the Howarth problem analytical expressions can be determined for all of the above relations; however, in general these quantities have to be determined numerically. In addition, the location of the edge of the boundary layer must be specified. For many flows the edge can be taken at $\eta_e = 6$ and constant along the surface. This approach is appropriate for the Howarth problem except near separation where there is a rapid increase in the thickness of the boundary layer. If the boundary layer is growing, grid points can be added as suggested by Blottner and Flügge-Lotz.[41] Patankar and Spalding[84] have also developed a technique which adds points to the grid across the boundary layer as needed. The transformation (3-5a) has been modified by Beckwith and Bushnell [30] to account for the growth of turbulent boundary layers as follows:

$$\eta = u_e\, r_b^j \frac{\sqrt{\mathscr{K}}}{(2\xi)^n} \int_0^y \rho dy \tag{6-14}$$

In their work $j = 0$, $\mathscr{K} = 1/\mu^2$ and ρ = constant. For laminar flow $n = \frac{1}{2}$ while $n \approx 0.8$ to 1.0 for turbulent flows. Another modification of the transformation has been utilized by Blottner, Johnson, and Ellis[91] which is

$$\eta = \frac{u_e\, r_b^j}{\eta_e} \sqrt{\frac{\mathscr{K}}{2\xi}} \int_0^y \rho dy \tag{6-15}$$

In this case one has to specify how η_e varies along the surface which is not known in many cases until the problem is solved. This same approach has been used by Kendall and Bartlett[87] except the parameter η_e is determined as part of the solution. At a certain η the velocity is specified to have a given value and η_e becomes an unknown in the problem. The approach of adding grid points for turbulent boundary layers with the Keller box scheme is described by Keller and Cebeci.[92]

6.3 Convergence of Iteration Procedure

Since several of the quantities in the coefficient relations (6-5) need to be evaluated from a previous iteration, the required number of iterations of the difference equations, (6-4) and (6-7), must be assessed. This has been investigated by Blottner,[77] and it has been shown that only one iteration is necessary to achieve a second-order accurate difference scheme in the ξ-direction. This is illustrated in Fig. 1 where the error of the velocity gradient at the wall is shown as a function of the step size $\Delta\xi$ for the Howarth problem at $\xi = 0.8$. The method of determining the error will be described in the next section. For the smaller step sizes the slope is approaching a value of two which it should have as a second-order accurate scheme.

The significant difference between the present scheme and other Crank-Nicolson schemes is the convergence rate of the iteration process to the desired second-order accurate result. If the momentum-difference equation is linearized and uncoupled from the continuity equation, the resulting process converges very slowly. This type of scheme was described in Section 5.4.4 and is obtained from Eq. (6-4) by assuming that $V_{i+1,j}$ is known from a previous iteration or grid point. With one iteration this method appears to be a first-order scheme as shown in Fig. 1. The results with 19 iterations show the proper second-order behavior with a slope of 2. Even with 9 iterations the solution does not have second-order behavior.

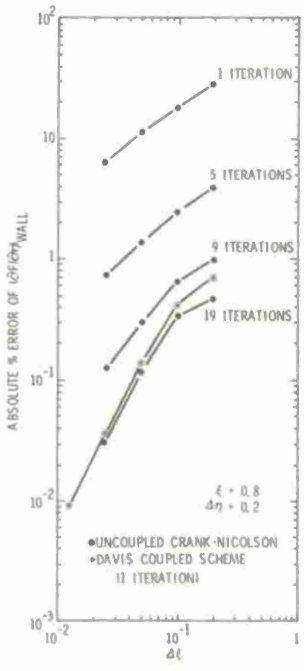

Figure 1. Accuracy of Crank-Nicolson scheme with various $\Delta\xi$ for Howarth problem.

In both the uncoupled and coupled schemes, the results are second-order accurate in the η-direction which is independent of the number of iterations performed.

6.4 Accuracy of Solutions

The only quantities that remain to be specified are the step-sizes $\Delta\xi$ and $\Delta\eta$ which will determine the accuracy of the results. At present there are no boundary-layer codes which automatically determine the step-sizes based on some desired accuracy of the results. The usual procedure is to obtain solutions with several different step-sizes and if the solution does not change much, it is then assumed that an adequate solution has been obtained. A better procedure has been developed by Blottner where Richardson extrapolation is utilized to obtain an "exact" solution. For the present Crank-Nicolson scheme, the method is second-order accurate in both coordinate directions and if W represents the solution at some location, then the following relation exists:

$$W_c = W_E + a\Delta\xi^2 + b\Delta\eta^2 + \cdots \tag{6-16}$$

where a and b are constants, W_c is the computed solution, and W_E is the exact solution when the step-sizes go to zero. If solutions are obtained with $\Delta\eta$ = constant and $\Delta\xi = \Delta\xi_0$ and $\Delta\xi = \frac{1}{2}\Delta\xi_0$, then Eq. (6-16) is used to obtain the "exact" solution with $\Delta\xi \to 0$ but with a finite value of $\Delta\eta$ which is

$$W_{\Delta\xi\to 0} = W_E + b\Delta\eta^2 = W_c\left(\tfrac{1}{2}\Delta\xi_0\right) + \frac{1}{3}\left[W_c\left(\tfrac{1}{2}\Delta\xi_0\right) - W_c\left(\Delta\xi_0\right)\right] + \cdots \tag{6-17}$$

where $W_c(\Delta\xi_0)$ is the solution obtained with step-size $\Delta\xi_0$. The "exact" solution $W_{\Delta\xi\to 0}$ is used to judge the accuracy of the solutions with step-size $\Delta\xi_0$ as follows:

$$\%\ \text{Error of } W(\Delta\xi_0) = \left[W_c(\Delta\xi_0) - W_{\Delta\xi\to 0}\right]/W_{\Delta\xi\to 0} \tag{6-18}$$

A similar equation is used for solutions with other step-sizes. At least three different step-sizes should be used to be sure the error is behaving as indicated in Eq. (6-16). Equations similar to (6-17) and (6-18) are used to evaluate the accuracy of the solution with various $\Delta\eta$.

The accuracy of the wall velocity gradient for various step-sizes $\Delta\xi$ has already been considered in Fig. 1. With the Davis coupled scheme, the wall velocity gradient for the Howarth problem has an error less than 1% at $\xi = 0.8$ (separation is at $\xi \approx 0.090$) with 8 steps taken along the surface. The effect of $\Delta\eta$ on the accuracy of the wall velocity gradient is shown in Fig. 2. As the solution proceeds downstream, more steps are required across the boundary layer if the accuracy is to be maintained. These results indicate that approximately 50 intervals across the flow are required in order to have 1% accuracy for the wall velocity gradient.

The modified tridiagonal algorithm requires approximately twice as much computer time as the standard tridiagonal algorithm. However, the uncoupled scheme requires many iterations and its total computer time is larger than the coupled scheme when a second-order accurate method is desired. If only a first-order scheme is adequate, the uncoupled scheme requires less overall computer time. When

the difference in computer times for the methods in Fig. 1 is taken into account, there is a considerable saving in computer time if a second-order method is used rather than a first-order method when accurate wall shear stress results ($\approx 1\%$) are desired. If very accurate results are desired, it would probably be advantageous to go to even a higher order method.

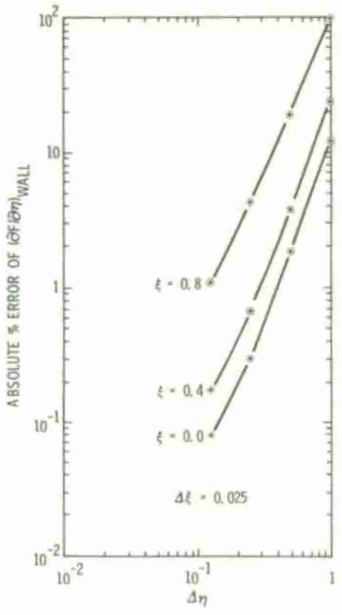

Figure 2. Accuracy of Crank-Nicolson scheme with various $\Delta\eta$ for Howarth problem.

7. COMPRESSIBLE, BOUNDARY-LAYER PROCEDURE

The Davis coupled version of the Crank-Nicolson scheme is now extended to the compressible boundary layers, Eqs. (3-8), for two-dimensional and axisymmetric steady flows. In Section 6 the technique was developed for the compressible continuity and x-momentum equations. Therefore, the energy equation must now be written in finite-difference form. Although there is coupling between the x-momentum and energy equations, these equations will be handled in an uncoupled manner. This has been shown by Blottner[7] to be a reasonable approach for the problems that were investigated.

The energy equations, (3-8c), is evaluated at the point $(i+\frac{1}{2},j)$ where the ξ-derivative is written as

$$2\xi F\,\partial\theta/\partial\xi = \left[(\xi F)_{i+1} + (\xi F)_i\right]_j (\theta_{i+1} - \theta_i)_j /\Delta\xi \qquad (7\text{-}1)$$

The other terms are first averaged between (i) and (i+1) as done in Eqs. (6-2) and then the nonlinear terms are linearized with the Newton-Raphson procedure, (4-5). The derivatives are evaluated with central difference relation as given by Eqs. (6-3). The energy equation becomes the following finite-difference equation:

$$(-A_j\theta_{j-1} + B_j\theta_j - C_j\theta_{j+1})_{i+1} = D_j \qquad j = 2,3,\cdots J-1 \qquad (7\text{-}2)$$

where

$$A_{i+1,j} = \left(\ell_{j-\frac{1}{2}}/Pr + V_j\,\Delta\eta/2\right)_{i+1}/2$$

$$B_{i+1,j} = \left(\ell_{j+\frac{1}{2}} + \ell_{j-\frac{1}{2}}\right)_{i+1}/(2Pr) + \Delta\eta^2\left[(\xi F)_{i+1} + (\xi F)_i\right]_j/\Delta\xi$$

$$C_{i+1,j} = \left(\ell_{j+\frac{1}{2}}/Pr - V_j\,\Delta\eta/2\right)_{i+1}/2$$

$$D_j = A_{i,j}\theta_{i,j-1} + C_{i,j}\theta_{i,j+1} + \left\{\left[\alpha\ell(\partial F/\partial\eta)^2\right]_{i+1} + \left[\alpha\ell(\partial F/\partial\eta)^2\right]_i\right\}_j \Delta\eta/2$$

$$- \theta_{i,j}\left\{\left(\ell_{j+\frac{1}{2}} + \ell_{j-\frac{1}{2}}\right)_i/(2Pr) - \Delta\eta^2\left[(\xi F)_{i+1} + (\xi F)_i\right]_j/\Delta\xi\right\}$$

The initial profile of θ at $\xi = 0$ is obtained from Eq. (7-2) with the coefficients simplified by setting all terms at (i) to zero and setting $\xi_i = \xi_{i+1} = 0$. The finite-difference equations, (7-2), are of the tridiagonal form and are solved with the Thomas algorithm given in Appendix B. The boundary conditions have been given by Eqs. (3-13) and (3-14) which are expressed as

$$\theta_1 = \theta_W = T_W/T_e \tag{7-3a}$$

$$\theta_J = 1 \tag{7-3b}$$

In the incompressible case $\ell = 1$, while for compressible flow Eq. (3-9a) is used to determine the value of ℓ. If $(\rho\mu)_r = (\rho\mu)_\infty$ and a linear viscosity law ($\mu = CT$) is used, then ℓ becomes with the use of the equation of state, (2-10), the following:

$$\ell = p_e/p_\infty \tag{7-4}$$

The pressure across the boundary layer is assumed constant. The parameter α is also required and is defined by Eq. (3-9c) which gives

$$\alpha = (\gamma - 1)\, M_\infty^2\, (u_e/U_\infty)^2/(T_e/T_\infty) \tag{7-5}$$

In order to evaluate Eqs. (7-4) and (7-5) the inviscid flow quantities at the edge of the boundary layer are required. The classical approach is followed where it is assumed that the inviscid flow along the surface provides the boundary-layer edge conditions. If the inviscid flow velocity at the surface is assumed known, then the isentropic flow relations for a perfect gas give

$$T_e/T_\infty = 1 + \frac{1}{2}(\gamma - 1)\, M_\infty^2\left[1 - (u_e/U_\infty)^2\right] \tag{7-6}$$

$$p_e/p_\infty = (T_e/T_\infty)^{\frac{\gamma}{\gamma-1}} \tag{7-7}$$

If the inviscid surface pressure is known, then the velocity is determined from

$$u_e/U_\infty = \left\{1 + \left[1 - (p_e/p_\infty)^{\frac{\gamma-1}{\gamma}}\right]\Big/\left(\frac{\gamma - 1}{2}\, M_\infty^2\right)\right\}^{1/2} \tag{7-8}$$

and the temperature ratio is determined from Eq. (7-6). In either case, with the velocity or the pressure specified along the surface; the parameters ℓ and α can be determined from Eqs. (7-4) and (7-5), respectively.

For the compressible case the wall boundary conditions remain the same except an additional condition must be provided for the energy equation. As Eq. (7-3a) indicates, one possible condition is to specify the wall temperature T_W.

The convergence of the iteration procedure at each step and the accuracy of the foregoing scheme has been investigated by Blottner.[77] The linearly retarded edge velocity problem was solved for the case with $M_\infty = 4$, $T_W = T_\infty$, and $\eta_e = 8$ which has also been solved by Fitzhugh.[93] The results show that the finite-difference scheme is second-order accurate with the energy equation uncoupled and with one iteration at each ξ-step. The procedure described in Section 6.4 has been utilized to judge the accuracy of this problem. The accuracy of the wall velocity gradient at $\xi = 0.1$ for various $\Delta\xi$ with $\Delta\eta = 0.2$ and various $\Delta\eta$ with $\Delta\xi = 0.0025$ is given in Fig. 3. The curves have a slope of approximately 2 which shows that the method is second-order accurate. These results were obtained with one iteration at each ξ-step along the surface. The results with the present scheme are compared with other numerical solutions which are given by Fitzhugh in Fig. 4. There are significant differences between the results which should be due to truncation errors as a result of too large step-sizes being used. The solution of Blottner (labeled present study) are "exact" as far as the figure is concerned. The linearly retarded free-stream velocity problem has also been investigated by Werle and Senechal[94] and their results show similar differences when compared to the solutions of Fitzhugh. The present finite-difference scheme has been used to solve a problem investigated by Werle and Senechal and the results are in excellent agreement except near separation where there appears to be a slight difference. The accuracy of the present finite-difference scheme results for the skin friction parameters are tabulated below:

ξ	% Error of $C_f\sqrt{Re}$
0	0.042
0.004	0.059
0.008	0.077
0.012	0.097
0.016	0.13
0.020	0.17
0.024	0.25
0.028	0.40
0.032	0.86
0.034	1.72
0.036	26.0

The results show that the accuracy has deteriorated significantly near the separation point.

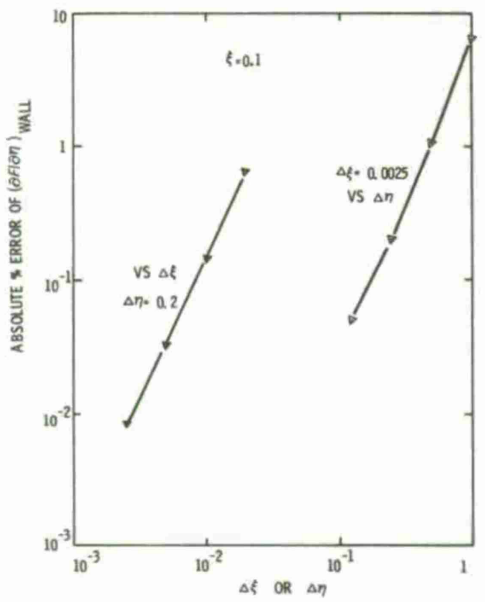

Figure 3. Accuracy of the Finite-Difference procedure for the linearly retarded flow at $M_\infty = 4$ and $T_W = T_\infty$.

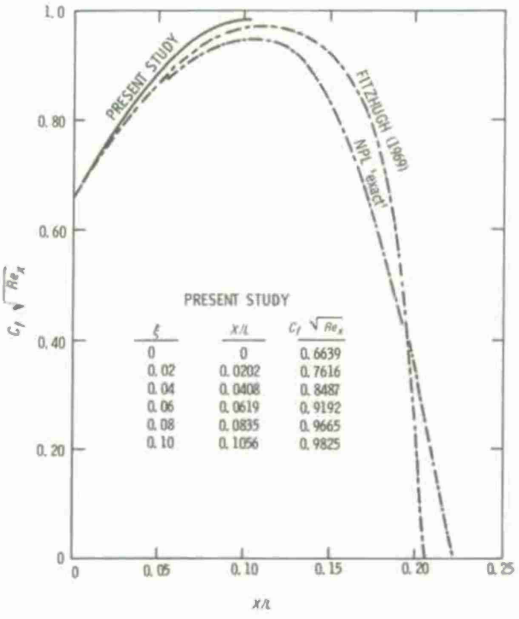

Figure 4. Results of present finite-difference scheme compared to other numerical solutions for linearly retarded flow at $M_\infty = 4$ and $T_W = T_\infty$.

8. TURBULENT BOUNDARY-LAYER FLOWS

It would appear difficult to describe computational techniques for solving turbulent flows when the governing equations are not a unique system. Even the type of the partial differential equations can change depending on the closure model used to determine the Reynolds stresses. The turbulent energy equation approach by Bradshaw, Ferriss, and Atwell[96] results in a system of hyperbolic equations. The method of characteristics was used to obtain the numerical solution. Nash[98] has used an explicit finite-difference scheme for the same type of turbulence model. As the governing equations are not appropriate near a surface, an inner solution of the viscous sublayer is matched to the outer numerical solution in both of these papers. All of the other closure models as described below result in parabolic partial-differential equations. In the initial work on the prediction of turbulent boundary layers the mean-velocity-field closure has been employed by Mellor,[97] Patankar and Spalding,[4] and Smith and Cebeci.[98] In the first of these papers the solution is obtained completely across the boundary layer. Mellor used the Hartree-Womersley semi-discrete method for solving the governing equations where the ordinary differential equations are solved across the layer with a Runge-Kutta integration procedure. Patankar and Spalding used a Crank-Nicolson type of finite-difference scheme which is not applied to the wall. A wall-function is introduced that gives the flow quantities at the wall as a function of quantities at the first grid point away from the wall. Smith and Cebeci first use a Levy-Lees transformation of the governing equations and then use an implicit finite-difference scheme to obtain the solution across the complete boundary layer. Due to the large gradients that occur near the surface, a variable grid system is employed. A more complex closure approach with the mean turbulent energy closure scheme was initially investigated by Glushko,[99] Beckwith and Bushnell,[100] and Mellor and Herring.[101] This approach introduces a transport equation for the turbulent kinetic energy and for boundary-layer flows this is a parabolic partial differential equation. An even more complex closure approach is the mean Reynolds stress model which results in a system of equations for the Reynolds stresses. Donaldson and Rosenbaum[102] have used this approach with the most recent work being reported by Varma, et.al.[103] In this last paper the governing equations consist of nine coupled parabolic partial-differential equations. The numerical solution is obtained with a forward-time and centered-space, fully implicit, finite-difference scheme.

There are many other papers concerned with the numerical solution of the turbulent boundary-layer equations. With the exception of the work of Bradshaw et. al. and Nash and the distribution function approaches, the turbulent boundary-layer equations are a system of parabolic partial-differential equations for the various closure models. The number of equations depends on the closure model employed. Therefore, the numerical techniques developed for laminar flows are also appropriate for turbulent flows. However, there is one significant difference which has been indicated above and has been illustrated by Blottner[104] and is shown in Fig. 5. For a turbulent boundary-layer flow, an excessive number of grid points are required normal to the surface to obtain 1% accuracy of the wall shear stress, τ_W, if a uniform grid spacing is used. The introduction of the following nonuniform grid has been used by Smith and Cebeci:[98]

$$\Delta\eta_{j+\frac{1}{2}} = K\,\Delta\eta_{j-\frac{1}{2}} \qquad j = 2,3,\cdots,(J-1) \tag{8-1}$$

where $\eta_{j+1} = \eta_j + \Delta\eta_{j+\frac{1}{2}}$ and $\eta_1 = 0$. This grid spacing has been used by several authors with a slowly varying grid ($K \approx 1.02$) which requires several hundred intervals across the boundary layer. The Keller box scheme has been used by Keller and Cebeci[94] with a rapidly varying grid ($K = 1.82$) with several tens of intervals across the boundary layer. A transformation of the independent variable can also be introduced as has been done by Roberts.[106] Another approach has been used by Davis[108] where the Crocco form of the boundary-layer equations are used. The large gradients in the dependent variables near the surface are eliminated which allows a uniform grid system to be applied. The problems with this transformation for the laminar boundary layer have been discussed in Section 3.

Following the format of the previous sections, we will now illustrate how the Crank-Nicolson scheme can be applied to a turbulent boundary layer flow. The variable grid scheme of Blottner[107] will be applied to the incompressible form of the equations where a mean-velocity-field closure model is used. The eddy-viscosity formulation of Keller and Cebeci[94] has been used in the paper by Blottner and will be used for any results presented in this section. The governing equations are given by (3-8) with $\theta = 1$ and $\ell = 1 + \epsilon/\nu$ where ϵ is the eddy viscosity.

The variable grid scheme is interpreted in terms of a coordinate stretching approach. A new coordinate N is introduced where a uniform interval ΔN is used and is related to the original coordinate η by a relation of the form

$$\eta = \eta(N) \tag{8-2}$$

The η-derivatives are transformed into the new coordinate system and central differences are employed to obtain

$$\left(\frac{\partial W}{\partial \eta}\right)_j = \left(\frac{\partial W}{\partial N}\Big/\frac{\partial \eta}{\partial N}\right)_j = (W_{j+1} - W_{j-1})\Big/\left[2\Delta N(d\eta/dN)_j\right] + O(\Delta N^2) \tag{8-3a}$$

and

$$\frac{\partial}{\partial \eta}\left(\ell\,\frac{\partial W}{\partial \eta}\right)_j = \frac{\partial}{\partial N}\left(\ell\,\frac{\partial W}{\partial N}\Big/\frac{d\eta}{dN}\right)_j \Big/\left(\frac{d\eta}{dN}\right)_j = \left(\frac{d\eta}{dN}\right)_j^{-1}\left[\left(\ell\Big/\frac{d\eta}{dN}\right)_{j+\frac{1}{2}}\left(\frac{W_{j+1} - W_j}{\Delta\eta}\right) - \left(\ell\Big/\frac{d\eta}{dN}\right)_{j-\frac{1}{2}}\left(\frac{W_j - W_{j-1}}{\Delta\eta}\right)\right] + O(\Delta N^2) \tag{8-3b}$$

The present approach replaces the coordinate derivatives with finite-differences to obtain

$$\eta'_j = (d\eta/dN)_j = (\eta_{j+1} - \eta_{j-1})/(2\Delta N) + O(\Delta N^2) \tag{8-4a}$$

$$\eta'_{j+\frac{1}{2}} = (d\eta/dN)_{j+\frac{1}{2}} = (\eta_{j+1} - \eta_j)/\Delta N + O(\Delta N^2) \tag{8-4b}$$

When these relations (8-4) are employed in Eqs. (8-3), the resulting difference equations for the derivatives are

$$(\partial W/\partial\eta)_j = (W_{j+1} - W_{j-1})/(\eta_{j+1} - \eta_{j-1}) + O(\Delta N^2) \tag{8-5a}$$

$$\left[\partial(\ell\,\partial W/\partial\eta)/\partial\eta\right]_j = 2\left[\ell_{j+\frac{1}{2}}(W_{j+1} - W_j)/(\eta_{j+1} - \eta_j) - \ell_{j-\frac{1}{2}}(W_j - W_{j-1})/(\eta_j - \eta_{j-1})\right]/(\eta_{j+1} - \eta_{j-1}) + O(\Delta N^2) \tag{8-5b}$$

The above derivatives are second-order accurate in terms of ΔN when a relation of the form of Eq. (8-2) is used to specify the grid points. For example, the grid spacing with the relation of Smith and Cebeci as given in Eq. (8-1) becomes

$$\eta_j = \eta_J\left(K^{N_j/\Delta N_0} - 1\right)\Big/\left(K^{1/\Delta N_0} - 1\right) \qquad j = 1,2,3,\cdots J \tag{8-6}$$

where $N_j = (j - 1)\Delta N$ and $N_J = 1$. The values of K and ΔN_0 are two parameters which are chosen to give the desired grid spacing.

The finite-difference equation for the momentum equation, (3-8b), is obtained as described in Section 6.1 except the derivatives (6-3) are replaced with the derivatives (8-5). The resulting difference equation is

$$(-A_jF_{j-1} + B_jF_j - C_jF_{j+1})_{i+1} + (aV)_{i+1,j} = D_{i+1,j} \qquad j = 2,3,\cdots, J - 1 \tag{8-7}$$

where

$$A_{i+1,j} = \left[(\ell/\eta')_{j-\frac{1}{2}} + \bar{V}_j \Delta N/2\right]_{i+1} /2 \tag{8-8a}$$

$$B_{i+1,j} = \tilde{B}_{i+1,j} + \Delta N^2 \eta_j' \, (\xi_i + \xi_{i+1}) \, \bar{F}_{i+1,j}/\Delta\xi \tag{8-8b}$$

$$C_{i+1,j} = \left[(\ell/\eta')_{j+\frac{1}{2}} - \bar{V}_j \Delta N/2\right]_{i+1} /2 \tag{8-8c}$$

$$D_{i+1,j} = \tilde{D}_{i+1,j} + \left(A_j F_{j-1} - \tilde{B}_j F_j + C_j F_{j+1}\right)_i - (a\bar{V})_{i,j} + \tilde{D}_{i,j}$$

$$+ \Delta N^2 \eta_j' \, (\xi_i + \xi_{i+1})(\bar{F}^2_{i+1} + F^2_i)_j/(2\Delta\xi) \tag{8-8d}$$

$$\tilde{B}_{i+1,j} = \left[(\ell/\eta')_{j+\frac{1}{2}} + (\ell/\eta')_{j-\frac{1}{2}}\right]_{i+1} \Big/ 2 + \Delta N^2 \eta_j' (\beta \, \bar{F}_j)_{i+1} \tag{8-8e}$$

$$\tilde{D}_{i+1,j} = (a\bar{V})_{i+1,j} + \frac{1}{2} \Delta N^2 \eta_j' \beta_{i+1} (1 + \bar{F}^2_{i+1,j}) \tag{8-8f}$$

$$a_{i+1,j} = (\bar{F}_{j+1} - \bar{F}_{j-1})_{i+1} \, \Delta N/4 \tag{8-8g}$$

Where $\bar{V}$ or $\bar{F}$ have a subscript (i), the bar on these quantities is neglected as these quantities are known. If $\eta_j' = 1$ and $\theta_j = 1$ at all grid points, then the coefficients (8-8) are identical to the ones previously presented in Eqs. (6-5) for the incompressible, laminar boundary layer. At $\xi = 0$, the coefficients (8-8) remain the same with the subscripts (i+1) ignored, except the following two coefficients become:

$$B_{i+1,j} = \tilde{B}_j \tag{8-9a}$$

$$D_{i+1,j} = \tilde{D}_j \tag{8-9b}$$

The difference equation for the continuity equation, (3-8a), is the same as previously given in Eq. (6-7) except $\Delta\eta = \Delta\eta_{j-\frac{1}{2}} = (\eta_j - \eta_{j-1})$ in the coefficients for c_j and d_j. Also, it should be noticed that $\Delta\xi$ which appears in the coefficients (8-8) can change as the solution steps along the surface. The governing equations, (8-7) and (6-7), for the incompressible, turbulent boundary layer are solved as described in Section 6.1.

Although it has been implied that the nonlinear difference equations have been linearized with the Newton-Raphson method, this is not completely true. The eddy viscosity ϵ is a function of the velocity F and its gradient, but in the linearization procedure ϵ is treated as a known quantity. Therefore, the eddy viscosity is evaluated from the solution at the previous step or iteration. The convergence properties of the iteration procedure and the accuracy of the variable grid scheme have been investigated by Blottner.[107] The laminar-to-turbulent flow along a flat plate (turbulence model included everywhere except at leading edge) was obtained where the edge Reynolds number, $Re_x = u_e x/\nu$, at the last step is 1.88×10^6. The solution was obtained with various number of iterations at each step and different number of intervals along and across the boundary layer. The grid spacing across the layer is specified by Eq. (8-6) with $K = 1.82$, $\Delta N_0 = 0.1$ and $\eta_e = 24.2538$. The wall skin friction parameter $C_f = \sqrt{2/\xi} \, (\partial F/\partial\eta)_w$ is used to judge the accuracy and behavior of the results. The accuracy of the solution is illustrated in Fig. 6 for various number of intervals across the boundary layer. These solutions were obtained with 15 intervals along the flat plate and the skin friction error is for the last step. The results presented were obtained with 3 iterations while solutions with only one iteration are nearly the same and also have second-order behavior. Also shown in Fig. 6 is the accuracy of the Keller box scheme for the same problem. The variable grid scheme approach has about the same accuracy in the η-direction as the Keller box scheme for this example. The accuracy of the variable grid scheme for various number of intervals in the ξ-direction and 80 intervals across the boundary layer is illustrated in Fig. 7. With one iteration at each step in ξ, the method shows second-order behavior except when 15 intervals are used. With 19 iterations, second-order behavior is obtained for all intervals investigated. However, even with this many iterations the solutions have not converged (difference in the dependent variables between successive iterations is greater than 10^{-8} at a point half-way across the layer). For the laminar flow case, the solution converges with 4 or 5 iterations. For the turbulent case, the slow convergence is attributed to the lack of complete Newton-Raphson linearization. However, the present linearization is adequate and one iteration at each ξ step is sufficient.

The use of several grid spacing relations (8-2) has been investigated by Blottner[104] for turbulent boundary layers. The method of Smith and Cebeci works as well as any of those considered. An optimal node distribution technique has been developed by Denny and Landis[108] for two-point boundary-value problems. The grid point locations are adjusted in an iterative process such that the local truncation errors of the finite-difference equation are minimized. This or a similar type procedure might be useful to extend to the partial differential equations governing the turbulent boundary layer.

Another problem that generally does not occur with laminar boundary-layer flows, is the change in thickness of the turbulent boundary layer in the η coordinate system. This is illustrated for the laminar-to-turbulent flow along a flat plate problem in Fig. 8. The value of η at the location where $F = 0.99$ is shown at various distances or Re_x's along the plate. Cebeci and Smith [109] state that for $Re_x = 10^9$, the η at the edge of the boundary layer has a value of 150. Therefore, some method must be used to take these large changes in thicknesses into account. Several approaches that have been utilized are discussed in Section 6.2.

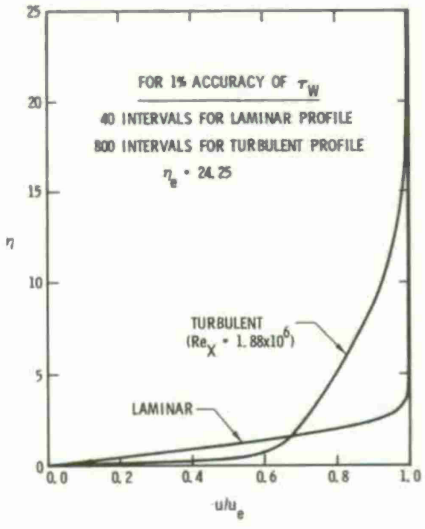

Figure 5. Laminar and turbulent velocity profiles.

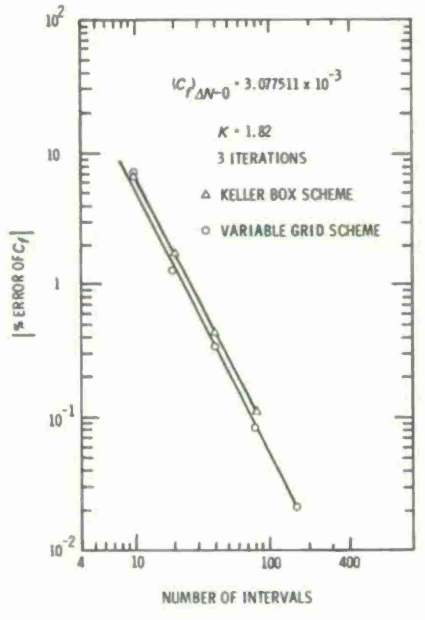

Figure 6. Accuracy of skin friction for turbulent boundary layer at $Re_x = 1.88 \times 10^6$ with various number of intervals in η-direction.

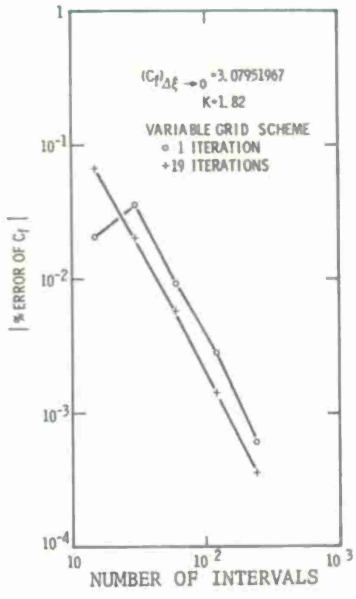

Figure 7. Accuracy of skin friction for turbulent boundary layer at $Re_x = 1.88 \times 10^6$ with various number of intervals in ξ-direction.

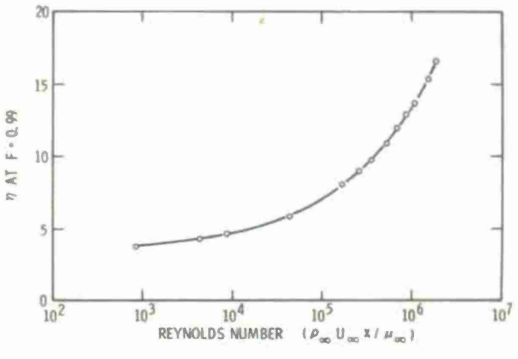

Figure 8. Growth of turbulent boundary layer on a flat plate.

9. UNSTEADY BOUNDARY-LAYER FLOWS

Rather than consider the general three-dimensional, unsteady problem defined by Eqs. (2-4) to (2-8), the present discussion will be limited to the two-dimensional, incompressible boundary-layer equations. Since the techniques developed for steady flows can be extended to the unsteady case, the numerical techniques can readily be demonstrated with these simplified governing equations. Many of the techniques developed for steady compressible, turbulent, or three-dimensional boundary layers have been applied to the unsteady case.

With Eqs. (3-1) employed, $\partial/\partial x_3 = 0$, $w = 0$, ρ = constant, and $j = 0$; the governing Eqs. (2-4) and (2-5) become

$$\partial u/\partial x + \partial v/\partial y = 0 \tag{9-1a}$$

$$\partial u/\partial t + u\, \partial u/\partial x + v\, \partial u/\partial y = -(\partial p/\partial x)/\rho + \nu\, \partial^2 u/\partial y^2 \tag{9-1b}$$

The boundary conditions for the surface and for the outer edge of the boundary layer are

$$y = 0, \quad u = v = 0 \tag{9-2a}$$

$$y \to \infty, \quad u = u_e(x,t) \tag{9-2b}$$

If there is no reverse flow, the solution of Eqs. (9-1) can be obtained for various x's with t held constant or for various t's with x held constant. However, to proceed with such a solution, initial conditions are required at the initial time, t_i, for the variables everywhere and at some upstream location, x_0, the variables are specified for later times. This is expressed as follows where the solution is obtained from position x_0 to x_1 and from time t_i to t_f:

$$\text{For } t = t_i \text{ and } x_0 \le x \le x_f, \qquad u = u_i(x,y) \tag{9-3a}$$

$$\text{For } x = x_0 \text{ and } t_i \le t \le t_f, \qquad u = u_0(t,y) \tag{9-3b}$$

The velocity $v_i(x,y)$ is obtained from the continuity equation, (9-1a), while $v_o(t,y)$ is obtained from a compatibility equation which results from eliminating $\partial u/\partial x$ from the governing equations, (9-1). The specification of the initial conditions can be a problem unless a steady, boundary-layer solution can be used at t_i and an unsteady similar solution at x_o. For the impulsive motion of a body, the boundary-layer thickness is initially zero and a numerical problem is introduced if physical variables are used. Some of the transformations employed will be considered subsequently.

Much of the work on unsteady boundary layers has been concerned with incompressible, two-dimensional flows. The initial numerical techniques were applied to the governing equations in physical coordinates. The first use of a finite-difference scheme for solving the unsteady boundary-layer equations was made by Paskonov and Rabin'kina.[110] The compressible form of the governing equations were investigated where the Crank-Nicolson scheme of Paskonov[20] for the steady equations was extended to the unsteady equations. The flow variables are assumed known at (n) and are solved for at (n+1) with $\Delta t = t^{n+1} - t^n$ and the subscript n indicating the time coordinate location. The derivatives for the momentum equation are evaluated at $(n+\frac{1}{2}, i+\frac{1}{2}, j)$ as follows with a uniform grid:

$$\partial u/\partial t = (u^{n+1} - u^n)_{i+1,j}/(2\Delta t) + (u^{n+1} - u^n)_{i,j}/(2\Delta t) \tag{9-4}$$

$$\partial u/\partial x = (u_{i+1} - u_i)^{n+1}_j/(2\Delta x) + (u_{i+1} - u_i)^n_j/(2\Delta x) \tag{9-5}$$

With W representing either $\partial u/\partial y$ or $\partial^2 u/\partial y^2$, these derivatives are written as

$$W = \frac{1}{4}\left(W^{n+1}_{i,j} + W^{n+1}_{i+1,j} + W^n_{i,j} + W^n_{i+1,j}\right) \tag{9-6}$$

where central differences are used to evaluate the η-derivatives as follows:

$$(\partial u/\partial y)^n_{i,j} = (u_{j+1} - u_{j-1})^n_i/(2\Delta y) \tag{9-7}$$

$$(\partial^2 u/\partial y^2)^n_{i,j} = (u_{j+1} - 2u_j + u_{j-1})^n_i/\Delta y^2 \tag{9-8}$$

When the above derivatives are substituted in the momentum equation, (9-1b), the resulting difference equation will be of the form

$$(-A_j F_{j-1} + B_j F_j - C_j F_{j+1})^{n+1}_{i+1} = D^{n+1}_{i+1,j} \tag{9-10}$$

The coefficient u in the momentum equation, (9-1b), is evaluated with Eq. (9-6) where W represents u. Initially, it is assumed that the coefficient is known which requires that $W^{n+1}_{i+1,j}$ be set to $W^n_{i+1,j}$. Then an iteration is performed with this term evaluated from the previous iteration. As the Newton-Raphson iteration is not used, the convergence is probably slow and a second-order accurate scheme is difficult to obtain with this approach. The coefficient v is evaluated at $i+\frac{1}{2}$ with the use of the continuity equation.

The continuity equation, (9-1a), is evaluated at the point $(n+\frac{1}{2}, i+\frac{1}{2}, j-\frac{1}{2})$ with the same approach used in the Crank-Nicolson scheme. The derivatives are written as

$$\partial u/\partial x = \frac{1}{4}\left[(\partial u/\partial x)^{n+1}_j + (\partial u/\partial x)^{n+1}_{j-1} + (\partial u/\partial x)^n_j + (\partial u/\partial x)^n_{j-1}\right]_{i+\frac{1}{2}} \tag{9-11a}$$

where

$$(\partial u/\partial x)^n_{i+\frac{1}{2},j} = (u_{i+1} - u_i)^n_j/\Delta x$$

and

$$\partial v/\partial y = (v_j - v_{j-1})^{n+1}_{i+\frac{1}{2}}/(2\Delta y) + (v_j - v_{j-1})^n_{i+\frac{1}{2}}/(2\Delta y) \tag{9-11b}$$

When these relations are substituted into the continuity equation, the resulting relation can be used to determine $v^{n+1}_{i+\frac{1}{2},j}$ across the boundary layer after Eq. (9-10) has been solved. An iteration

procedure is used to improve the accuracy of the solution of the momentum and continuity difference equations.

This type of Crank-Nicolson scheme has also been independently developed by Dwyer[111] and Hall.[112] In this last paper it is stated that von Neuman's criterion for numerical stability indicates that the method is unconditionally stable. It needs to be added that the velocity u must be positive. An explicit finite-difference scheme was investigated by Farne and Arpaci[113] which is an extension of the two-dimensional explicit scheme (Section 5.4.1). This is a first-order method and the step-size Δt is restricted in size to insure numerical stability. Oleinik[114] proposed this explicit scheme also and in addition, she proposed a first-order accurate implicit scheme. This scheme is an extension of the two-dimensional implicit scheme (Section 5.4.3) and is a first-order accurate method. The unsteady boundary layer at the stagnation point of an infinite plane wall with impulsively started external flow was investigated by Katagiri.[115] This flow is an unsteady, one-dimensional (space) problem and was solved with the difference-differential method which was described in Section 5.2. The Keller box scheme (Section 5.4.5) has been extended to the unsteady equations by Phillips and Ackerberg.[116] Newton-Raphson iterations are used to solve the nonlinear finite-difference equations, and this method is second-order accurate. The solution procedure with the block tridiagonal method as described in Appendix B is not used, but the difference equations are combined such that the modified tridiagonal method of Appendix A is used. This type of modification of the Keller box scheme for steady, two-dimensional flow has been made by Blottner.[77] A change of the box scheme is introduced by Phillips and Ackerberg when there is backflow which allows stable solutions to be obtained. Unsteady flows with reverse flow have also been considered by Telionis, Tsahalis and Werle.[117] The zig-zag derivative introduced by Krause[116] for three-dimensional steady boundary layers was used to evaluate the following derivative at $(n+\frac{1}{2}, i, j)$

$$\partial u/\partial x = (u_i - u_{i-1})_j^{n+1}/(2\Delta x) + (u_{i+1} - u_i)_j^n/(2\Delta x) \tag{9-12}$$

The other derivatives in the governing equations are evaluated as follows:

$$\partial u/\partial t = (u^{n+1} - u^n)_{i,j}/\Delta t \tag{9-13a}$$

$$W = (W^{n+1} + W^n)_{i,j}/2 \tag{9-13b}$$

where W represents the η-derivatives which are evaluated with Eqs. (9-7) and (9-8). With reverse flow, the use of the above procedure requires downstream boundary conditions or one mesh point in the x-direction is lost with each step in time.

Other numerical solution techniques have been applied to the unsteady boundary-layer equations. Bartlett, Anderson, and Kendall[119] have used the integral matrix method for solving the governing equations for a gas in chemical equilibrium with the flow either laminar or turbulent. Koob and Abbott[120] have used the method of weighted residuals and the method of lines to solve the time-dependent, two-dimensional incompressible equations.

The solution of unsteady turbulent flows have been investigated by Patel and Nash[121] with an explicit finite-difference scheme. This is a modification of a method used previously for steady, three-dimensional flows. Cebeci and Keller[142] have used the box scheme (Section 5.4.5) to solve the unsteady turbulent flow on an infinite plate which results in a problem with one space dimension.

The solution of unsteady and three-dimensional boundary-layer flows has been investigated by Dwyer.[123] Two implicit, first-order accurate finite-difference schemes have been used to obtain the results. The significant difficulties encountered in this investigation were the determination of the initial conditions and how to handle reverse flow.

Several types of transformations are used with the unsteady boundary-layer equations. For impulsive flow toward an infinite plane wall, Katagiri introduces the new independent variables.

$$\tau = 2\sqrt{at} \tag{9-14a}$$

$$\eta = y/(2\sqrt{\nu t}) \tag{9-14b}$$

where the velocity at the edge of the boundary layer for $t > 0$ is $u_e = ax$. At $\tau = 0$, the transformed governing equation becomes an ordinary differential equation in η which can be solved to provide the initial conditions for the problem. The physical boundary layer has zero thickness at $\tau = 0$, but in the transformed plane a finite thickness is obtained. This procedure gives a result similar to the Levy-Lees transformation for the steady flow over a semi-infinite flat plate at the leading edge.

For the incompressible, two-dimensional boundary-layer equations with an unsteady exterior flow, the following type of transformations have been used with the authors indicated:

$$\left.\begin{aligned} \xi(x) &= x \\ \eta(x,y,t) &= \sqrt{u_e(x,t)/(2\nu x)}\ y \\ \tau &= t \end{aligned}\right\} \qquad \text{Dwyer} \qquad (9\text{-}15)$$

$$\left.\begin{aligned} \xi(x,t) &= \int_0^x u_e(x,t)\,dx \\ \eta(x,y,t) &= \left[u_e(x,t)/\sqrt{2\xi}\right]y \\ \tau &= t \end{aligned}\right\} \qquad \text{Telionis, et.al.} \qquad (9\text{-}16)$$

$$\left.\begin{aligned} \xi(x) &= \int_0^x u_{e_m}(x)\,dx \\ \eta(x,y) &= \left[u_{e_m}(x)/\sqrt{2\xi}\right]y \\ \tau &= t \end{aligned}\right\} \qquad \text{Tsahalis \& Telionis}^{124} \qquad (9\text{-}17)$$

Dwyer gives the following reasons for using the transformation (9-15) before the numerical solution: (1) possible leading edge singularities along the plane $x = 0$ are removed; (2) equations to determine the initial conditions along $\xi = 0$ may be obtained by taking the limit $\xi \to 0$; (3) the boundary-layer thickness is very nearly constant in terms of the transformed coordinate η; and (4) the derivatives of the independent variables are stretched so that high accuracy may be obtained with relatively large step-sizes. The transformation of Telionis, et.al. (9-16) was used for calculating transient flows while the transformation (9-17) was used for oscillatory flows. For the unsteady form of the compressible governing equations, (3-2) to (3-4), Bartlett, et. al. used a modified Levy-Lees coordinate system. There have been several transformations utilized with the unsteady equations, but there does not appear to be any clear choice of the one to use. Further investigation of the appropriate transformations to use needs to be performed.

Although the box scheme is an adequate finite-difference approach for solving the unsteady boundary-layer equations, the Crank-Nicolson scheme as used by Paskonov and Rabin'kina is preferred. The appropriate formulation of this scheme with Newton-Raphson linearization has not been done, but is an easy extension of the scheme described in Section 6.1. Before this is done, the transformed form of the governing equations needs to be decided.

10. THREE-DIMENSIONAL BOUNDARY-LAYER FLOWS

10.1 Introduction

Solution techniques for the governing equations, (2-4) to (2-11), for steady flow will be considered in this section. A general method for solving three-dimensional flows is not available. At present, a limited number of flow problems have been solved with special techniques for each problem. For two-dimensional and axisymmetric boundary-layer flows, very general codes have been developed. For two-dimensional flows these codes are independent of the body geometry while for axisymmetric bodies the radius must be specified and for both cases one coordinate system is used. For three-dimensional flows, there is no unique coordinate system and many different ones have been employed. With a coordinate system chosen, the geometry of the body or the inviscid streamlines is necessary to determine the metric coefficients. The inviscid flow for three-dimensional flows are not readily available either from analytical or numerical results. These results when available are a function of two independent variables and this introduces significantly more complexity than occurs in the two-dimensional case.

As a result of the difficulties of the solution of the complete three-dimensional problem, many authors have investigated approximate techniques or special cases. The small crossflow approximation of Hayes[12] has been developed by Fannelop[125] by means of a systematic perturbation procedure. Although such procedures are important, the present concern is with "exact" solutions of the governing equations with numerical techniques. The simplest exact solution of the three-dimensional boundary-layer equations is the flow at a stagnation point as considered by Howarth.[126] The governing equations are reduced to ordinary, differential equations and can be solved with techniques developed for similar solutions. There are three special flows that reduce to the two-dimensional or axisymmetric governing equations (slightly changed) plus the x_3-momentum equation where there are only two independent variables, x_1 and y. The first case is the flow over a yawed infinite cylinder where for laminar flow the x_3-momentum equation is uncoupled. This problem has been investigated by Reshotko and Beckwith[127] when the external flow is of the Falkner-Skan type and the governing equations are reduced to similar form. For turbulent flows, the x_3-momentum equation is coupled to the two-dimensional equations, and the non-similar numerical solution has been obtained by Cebeci.[128] The second example is the flow over a spinning

body of revolution at zero incidence. The governing equations consist of the axisymmetric equations which are slightly modified plus the x_3-momentum equation. The finite-difference solution of this problem for incompressible flow has been obtained by Koh and Price[129] while Muraca[130] considered the compressible case. The third case is the flow in the plane of symmetry. Again, a system of governing equations is obtained which involves two space dimensions. The solution of these equations has generally used exterior flows which give similar solutions. The flow on a sharp cone at incidence was first considered by Moore[131] and the more recent results are given by Wu and Libby.[132] Nonsimilar symmetry-plane solutions with finite-differences have been obtained by Seliverstov[133] on a spherical segment and by Wang[134] on a ellipsoid at incidence in incompressible flow. Another special case is the supersonic flow over a cone at incidence where it was shown by Moore[135] that a similar transformation in the x_1 direction exists of the form $\eta \sim y/\sqrt{x_1}$. The governing equations become partial differential equations involving the independent variables η and x_3. This two-dimensional problem for circular cones was solved with a finite-difference scheme initially by Cooke[136] and Vvedenskaya[137] and later by Dwyer[138] and Boericke.[139] The boundary layer on elliptic cones in supersonic flow has been solved numerically by Bashkin[140] for the case of zero incidence and by McGowan and Davis[141] for the case with angle of attack. Although the foregoing solutions result from simplified forms of the three-dimensional equations, some of these results are a necessary part of the complete solution. The stagnation point and the similar cone solutions provide initial conditions for the complete solution over blunt and sharp bodies, respectively. The plane of symmetry results can be used as boundary conditions.

The properties of the three-dimensional boundary-layer equations were first investigated by Raetz[142] where he introduced the "influence principle." The influence of the solution at any point is transferred to other points first by conduction along the straight line paralleling the y-axis and passing through that point and then by convection downstream along all streamlines through that line. This zone of influence is the region bounded by the body surface and the edge of the boundary layer and the outer and inner characteristic envelopes and is illustrated in Fig. 9. The characteristic envelopes are the surfaces normal to the body surface with the outer one containing the inviscid streamline while the inner one contains the surface streamline. Raetz also states that the solution at a given point depends only on the solution within another distinct zone, called the "dependence zone."

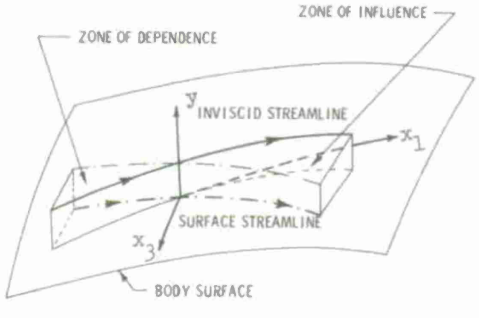

Figure 9. Region of influence and dependence.

This zone is formed by the region bounded by the body surface and the edge of the boundary layer, the outer and inner characteristic envelopes passing through the solution point and an upstream initial-value surface which nowhere coincides with a characteristic envelope. There must be unidirectional flow across the initial-value surface. Such a zone has the important property: Appropriate data on the initial-value surface and boundary conditions at the body surface and edge of the boundary layer determines a unique solution of the three-dimensional boundary-layer equations everywhere within and only within the zone of dependence. The appropriate initial conditions for a compressible gas as given by Ting[17] are the density profile, the velocity component u and a third quantity which is a combination of the initial profile of ρ, u, v, and w. The zones of influence and dependence for three-dimensional boundary-layer equations have been re-examined by Wang[16] from the point of view of subcharacteristics which are the streamlines of the flow.

For the numerical solution of the three-dimensional boundary-layer equations, the finite-difference scheme must take into account the zone of dependence. The stability of the schemes and where the solution can be calculated on a surface with given initial conditions are determined by the zone of dependence. In two-dimensional calculations the zone of dependence is automatically taken into account. For three-dimensional solutions the marching direction specification is a function of the problem being solved and introduces another complexity to the numerical solution procedure. The boundary-layer solution regions are also limited to flows without separation phenomena. As used by Eichelbrenner,[143] we call "separated" a region that is inaccessible to the viscous flow coming from infinity upstream. He also introduced the term "clash phenomena" to describe the coming together of two boundary layers. This phenomena gives a boundary region where the governing equations, (2-4) to (2-11), are not valid. Again, more complexity results in determining the three-dimensional solution due to separation and clash phenomena.

10.2 Coordinate Systems

With the governing equations in terms of an orthogonal coordinate system, the surface coordinates must be defined and the metric coefficients determined. The selection of a coordinate system in the past has meant a choice which results in a simplification of the governing equations and boundary conditions. When numerical solutions are being obtained, this consideration is not important. A coordinate system which allows the solution to start from the initial conditions and proceed in a logical manner over the surface is more important. Since at present there appears to be no superior coordinate system, the types of coordinates used by various authors will be reviewed.

A coordinate system coinciding with the inviscid streamlines was discussed by Hayes[12] and has been used mainly for approximate solutions, for example Fannelop.[135] Most authors have used coordinates related to the geometry of the surface. The simplest case is Cartesian coordinates where $h_1 = h_3 = 1$, and this can be used on developable surfaces (bending a plane without stretching or shrinking). For these flows, the boundary conditions at the wall or at the edge of the boundary layer have been used to generate the three-dimensional boundary-layer flow. A geodesic coordinate system has been used by Moore[136] where the metric coefficients are $h_1 = 1$ and $h_3 = r(x_1, x_3)$. For the case of a body of revolution, this system is the same as that given by Eq. (3-1) for axisymmetric flows where $r = r_b(x_1)$. For a conical body, x_1 is measured along rays from the apex and $r(x_1)$ is a linear function of x_1 giving the scale change of the noncircular cross section. This is the coordinate system used by McGowan and Davis[141] for conical bodies in supersonic flow at incidence. Moore[144] also states that the geodesic coordinate system can be formulated in any surface where x_1 is measured along the surface geodesics (line joining two points on the surface to give the shortest distance). The surface contour $x_1 = 0$ is chosen anywhere except it must be orthogonal to the geodesics and the coordinate system will be orthogonal. Wang[145] has used an ellipsoidal coordinate system for the three-dimensional flow over an ellipsoid at incidence. For the same body at zero incidence, Der and Raetz[15] have used as one coordinate the line of intersection of the body surface and a meridian plane. The other coordinate on the surface are lines perpendicular to the first set of lines of intersection and is illustrated in Fig. 10. Der[148] indicates that a numerical method of calculating this type of orthogonal coordinate

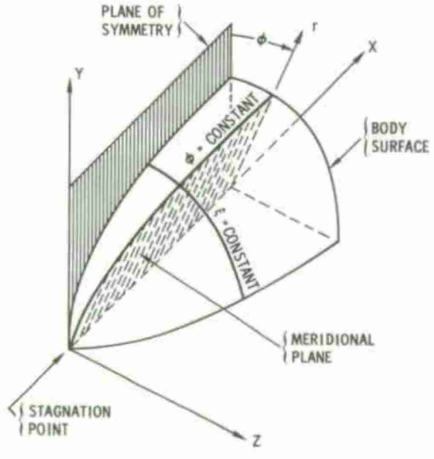

Figure 10. Surface coordinate system.

system on a general body configuration has been developed. This same type of coordinate system has been used by Blottner and Ellis[147] for blunt bodies at incidence. An improved procedure for finding the surface coordinates is given. Rather than the origin at the nose of the body, the origin of the coordinate system is located at the stagnation point which allows the solution to proceed away from this point in a systematic manner.

The analysis in this paper has been limited to orthogonal coordinate systems, but this is not necessary. Shevelev[148] has used a non-orthogonal coordinate system to obtain the incompressible boundary-layer flow over an ellipsoid at incidence. The coordinate system employed is similar to that illustrated in Fig. 10 with meridional planes about an axis which goes through the stagnation point and the center of the ellipsoid. The intersection of these planes with the body surface gives one coordinate. The other coordinate is obtained from the intersection of parallel planes with the body surface. The parallel planes are perpendicular to the plane of symmetry and are parallel to the plane tangent to the body surface at the stagnation point. There does not appear to be any advantage to use the non-orthogonal coordinate system for this problem. However, nonorthogonal coordinates would be useful if the boundary-layer results are made available in a more natural coordinate system of the body being considered. Also, Rizzi, et.al.[149] have used a non-orthogonal curvilinear system to obtain the supersonic inviscid flow on blunt bodies and it would be beneficial to use the same system for the boundary-layer solution.

10.3 Transformation of Governing Equations

In order to have the three-dimensional boundary layer of more uniform thickness in the computational coordinates and to obtain ordinary, differential equations at a stagnation line, stagnation point, and tip of bodies, a similar transformation of the equations is employed. No single approach has been adopted to transform the governing equations; therefore, some of the approaches that have been used will be given.

In order to obtain similar solutions, Fong[150] introduced the new independent variables

$$\xi = \int_0^{x_1} (\rho\mu)_r \, dx_1 \tag{10-1a}$$

$$\eta = \sqrt{u_e/(2\xi)} \int_0^y \rho \, dy \tag{10-1b}$$

$$\omega = \int_0^{x_3} (\rho\mu)_r \, h_3 \, dx_3 \tag{10-1c}$$

Two stream functions are used to satisfy the continuity equation. The governing equations for the flow about yawed infinite cylindrical surfaces have been transformed with the Levy-Lees type variables by Zemlyanskii.[151] The independent variables become

$$\xi = \int_0^{x_1} (\rho\mu)_e \, u_e h_3^2 h_1 \, dx_1 \tag{10-2a}$$

$$\eta = \left(u_e h_3/\sqrt{2\xi}\right) \int_0^y \rho \, dy \tag{10-2b}$$

$$\omega = x_3 \tag{10-2c}$$

and the velocities are written as

$$u = u_e \, \partial f/\partial\eta = u_e \, F \tag{10-3a}$$

$$w = w_e \, \partial g/\partial\eta = w_e \, G \tag{10-3b}$$

For Cartesian coordinates ($h_1 = h_3 = 1$) the following transformation has been used by Dwyer and McCroskey,[152] Fillo and Burbank,[153] and Cebeci[154] for incompressible flows:

$$\xi = x_1 \tag{10-4a}$$

$$\eta = \sqrt{u_e/(2\nu\xi)} \, y \tag{10-4b}$$

$$\omega = x_3 \tag{10-4c}$$

The factor of 2 in Eq. (10-4b) does not appear in the paper of Cebeci while the same new independent variables with 2 in the numerator have been used by Blottner and Ellis[147] for blunt body incompressible flows. Dwyer and McCroskey introduce the new dependent variables

$$F = u/u_e \tag{10-5a}$$

$$V = v\sqrt{x/(2\nu u_e)} + F(\beta_\xi - 1)/2 + (w/u_e)\,\eta\,\beta_\omega/2 \tag{10-5b}$$

where

$$\beta_\xi = (\xi/u_e)\,\partial u_e/\partial\xi$$

$$\beta_\omega = (\xi/u_e)\,\partial u_e/\partial\omega$$

The resulting governing equations are second-order partial differential equations. In the work of Fillo and Burbank, and Cebeci, two stream functions are introduced to satisfy the continuity equation which gives

$$u = \partial\psi/\partial y \tag{10-6a}$$

$$v = -\partial\psi/\partial x_1 - \partial\varphi/\partial x_3 \tag{10-6b}$$

$$w = \partial\varphi/\partial y \tag{10-6c}$$

where

$$\psi = \sqrt{2\nu x u_e}\, f(\xi,\eta,\omega) \tag{10-7a}$$

$$\varphi = w_e\sqrt{2\nu x/u_e}\, g(\xi,\eta,\omega) \tag{10-7b}$$

This approach has been used previously by Moore[144] for the compressible, three-dimensional boundary-layer equations. Fillo and Burbank introduce $F = \partial f/\partial\eta = u/u_e$ and $G = \partial g/\partial\eta = w/w_e$ which makes the governing equations second-order while Cebeci uses f and g as the independent variables and has third-order equations. The approach of Fillo and Burbank is the same as that used by Fannelop for the two-dimensional equations (see Section 5.4.4). For the blunt body solutions of Blottner and Ellis, the new dependent variables are the following:

$$F = u/u_e \tag{10-8a}$$

$$G = w/W_e \tag{10-8b}$$

$$V = \frac{1}{2}\,\xi\left[v\sqrt{2/u_e\nu\xi} + (F/h_1)\,\partial\eta/\partial x_1 + (W_e G/u_e h_3)\,\partial\eta/\partial x_3\right] \tag{10-8c}$$

where W_e is a reference velocity which can be w_e or u_e. The resulting governing equations in this case are second order.

For the compressible flow on sharp cones at incidence, and with and without spin; Dwyer[138] and Watkins[165] have used nearly the same new independent variables. The method of Watkins is presented and it is appropriate for any sharp body of revolution. The metric coefficients are $h_1 = 1$ and $h_3 = r_b$ and the new variables are

$$\xi = \int_0^{x_1} (\rho\mu)_r\, r_b^2\, dx_1 \tag{10-9a}$$

$$\eta = \sqrt{u_e/(2\xi)}\, r_b \int_0^y \rho\, dy \tag{10-9b}$$

$$\omega = x_3 = \varphi \tag{10-0c}$$

The new dependent variables are

$$F = u/u_e \tag{10-10a}$$

$$G = w/u_e \tag{10-10b}$$

$$\theta = T/T_e \tag{10-10c}$$

$$V = \sqrt{2\xi/u_e}\,\rho v/[r_b(\rho\mu)_r] + 2\xi\,[F\, r_b\,\partial\eta/\partial x_1 + G\,\partial\eta/\partial x_3]/[r_b^3(\rho\mu)_r] \tag{10-10d}$$

The governing equations are of second-order and are a more general form of the two-dimensional equation given in Eqs. (3-8). Vatsa and Davis[168] have used Levy-Lees variables for the compressible flow on a sphere-cone at incidence and with geodesic coordinates. The solution is restricted to the downstream region of the body. The new independent variables are

$$\xi = x_1 \tag{10-11a}$$

$$\eta = u_e h_3/\sqrt{2\xi}\int_0^y \rho\, dy \tag{10-11b}$$

$$\omega = x_3 \tag{10-11c}$$

where

$$\Phi = \Phi_0 + \int_{\xi_0}^{\xi} \rho_e \mu_e u_e h_3^2 \, d\xi$$

The new dependent variables are introduced as follows:

$$F = u/u_e$$

$$G = w/w_e$$

$$\theta = T/T_e$$

and a velocity-like term V is defined which satisfies the continuity equation.

The three-dimensional boundary-layer equations have also been transformed with the Crocco variables by McGowan and Davis,[141] Mayne,[157] and Popinski and Davis.[158] Another type of transformation has been used by Der and Raetz[16] and Warsi[159] where the normal coordinate y is replaced with $\eta = \sqrt{1 - F}$ and a shear coefficient is introduced as an unknown.

10.4 Inviscid Flow

One of the major problems with solving the three-dimensional boundary-layer equations is the determination of the inviscid flow. The purpose of this section is to indicate the problems that have been solved and what information was used for the inviscid flow. The following three-dimensional flows have been investigated:

1. Ellipsoid at Incidence - For incompressible flow the potential flow solution is used. (Shevelev,[146] Blottner and Ellis,[147] and Wang[148])

2. Flat Plate with Attached Cylinder - The incompressible flow around the cylinder is obtained from potential theory. (Dwyer,[160] Fillo and Burbank,[163] and Cebeci[154])

3. Parabolic Flow over a Flat Plate - The inviscid velocities are specified and for incompressible flow the governing equations reduce to a similar solution. This inviscid flow has been used to investigate the influence of a wall hot spot on the three-dimensional flow (Krause and Hirschel[161]).

4. Jet Against a Wall - The inviscid flow for this problem is obtained from potential flow theory for two impinging jets. (East and Pierce[162] and Cebeci[154])

5. Rotating Blades - An extension of a result of Sears which relates the steady potential flow past a nonlifting blade in a uniform, two-dimensional stream to the desired flow is used. (Dwyer and McCroskey[164])

6. Conical Flow - The inviscid flow over circular cones at incidence has been obtained numerically by several authors and these results are used for the inviscid flow on spinning cones. These solutions are only a function of x_3 and can be used in tabulated or curve fit form. Usually the pressure is taken from the numerical solution and the remaining edge properties are obtained from the inviscid flow equations. (Watkins[165] and Dwyer and Sanders[163]) The effect of the swallowing of the inviscid flow has also been taken into account on circular cones. (Mayne[157] and Popinski-Davis[158])

7. Blunt Bodies - Several solutions have been obtained for the supersonic and hypersonic flow over blunt bodies. A Newtonian type of pressure distribution has been used to generate the inviscid flow conditions on a sphere-cone. (Der[148]) The other inviscid flows have been obtained from numerical solutions and the configurations that have been considered are sphere-cones, ellipsoid, and segmental body (sphere-reverse cone) at incidence. Curve fit relations have been used to represent the complete numerical data in some cases (Andreev and Shevelev[154]) while in other papers only the pressure is treated in this manner with the other inviscid flow conditions calculated. (Vvedenskaya,[166] Shevelev,[146] Vatsa-Davis,[156] and Popinski-Davis[158])

8. Flow over Sphere with Interference - The inviscid flow for this problem was obtained from experimental measurements. (Karabelas and Hanratty[167])

The approximate techniques for solving three-dimensional boundary-layer flows of Fannelop[126] and DeJarnette and Hamilton[168] have generated procedures for obtaining the inviscid flow and this work should be considered as a possible approach. Also, there have been no direct finite-difference solutions of the inviscid surface equations, (2-14), where the pressure is specified and is obtained from a complete numerical solution.

There appears to be considerable difficulties with handling the inviscid flow data and problems are encountered with obtaining smooth distributions of the flow quantities. The swallowing of the inviscid flow on blunt bodies has not been investigated and this phenomena introduces a significantly more complex data handling problem than the case with constant entropy on the body.

10.5 Finite-Difference Methods

There have been various schemes proposed for solving the three-dimensional steady boundary-layer equations, (2-4) to (2-8). Both explicit and implicit methods have been used and these methods are stable for two-dimensional flows. However, for three-dimensional flows there are restrictions on the allowable step-sizes to maintain numerical stability as pointed out by Krause, et.al.[169] Since the three-dimensional boundary layer has zones of influence and dependence, the numerical scheme must take these into account. Krause, et.al. have shown that the following stability parameter γ must satisfy certain inequalities:

$$\gamma = (h_1 \, w \, \Delta x_1)/(h_3 \, u \, \Delta x_3) \tag{10-12}$$

The restrictions on γ will be indicated for the various schemes which will show that many schemes are unstable with a reverse crossflow. The other interesting property of the various schemes is the initial and boundary conditions which are required to continue the solution downstream without dropping grid points.

The governing equations for momentum and energy conservation in either physical or transformed coordinates contain first derivatives in the three coordinate directions and second derivatives only in the direction normal to the surface. Rather than writing all the difference relations for each scheme, sketches will be used to illustrate the various methods. The grid system and notation employed is given in Fig. 11, where the y-coordinate is coming out of the paper and all grid points shown are at the location (j). The unknown grid points in all cases are at the location (i,k).

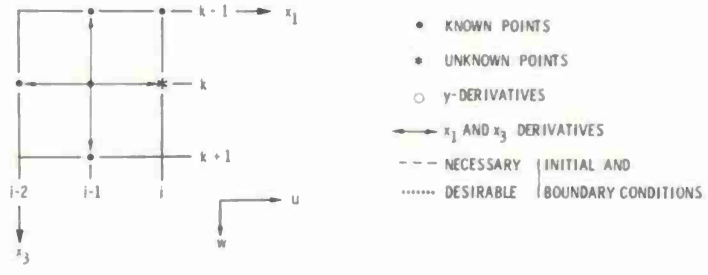

Figure 11. Grid System and Notation.

The y-derivatives are evaluated with central differences as follows unless indicated otherwise:

$$(\partial W/\partial y)_{i,j,k} = (W_{j+1} - W_{j-1})_{i,k}/(2\Delta y) \tag{10-13}$$

$$(\partial^2 W/\partial y^2)_{i,j,k} = (W_{j+1} - 2W_j + W_{j-1})_{i,k}/\Delta y^2 \tag{10-14}$$

The first derivatives in the x_1 and x_3 directions are evaluated with the points at the arrowheads. For the illustrated case in Fig. 11, these derivatives are

$$(\partial W/\partial x_1)_{i-1,j,k} = (W_i - W_{i-2})_{j,k}/(2\Delta x_1) \tag{10-15}$$

$$(\partial W/\partial x_3)_{i-1,j,k} = (W_{k+1} - W_{k-1})_{i-1,j}/(2\Delta x_3) \tag{10-16}$$

The location of necessary initial and boundary conditions required for each method will be shown with a dashed line. If the desirable boundary conditions, which are indicated with the dotted line, are not available, then a grid point is dropped as the calculation proceeds in the x_1-direction.

If the continuity equation has been retained as one of the governing equations, then it needs to be handled differently than the other conservation equations. The continuity equation in either the physical or transformed coordinates contains only first derivatives in the three coordinate directions and these derivatives are evaluated as follows:

$$(\partial W/\partial y)_{i,j-\frac{1}{2},k} = (W_j - W_{j-1})_{i,k}/\Delta y \tag{10-17a}$$

$$\partial W/\partial x_1 = \left|(\partial W/\partial x_1)_j + (\partial W/\partial x_1)_{j-1}\right|/2 \qquad (10\text{-}17b)$$

$$\partial W/\partial x_3 = \left|(\partial W/\partial x_3)_j + (\partial W/\partial x_3)_{j-1}\right|/2 \qquad (10\text{-}17c)$$

The y-derivative is evaluated at the (i,k) points as indicated by the circle in the sketches for the various schemes. The first derivatives in the x_1 and x_3 directions in Eqs. (10-17) are evaluated with the (i,k) points shown by the arrows in the sketches.

The finite-difference schemes are grouped according to the type of solution procedure used to solve the resulting difference equations. The three groups that result are explicit, implicit, and cube scheme which are now described.

10.5.1 Explicit - An extension of the two-dimensional DuFort-Frankel scheme, which was described in Section 5.4.2, has been applied to the three-dimensional equations by Der and Raetz[15] and East and Pierce[162] but these schemes are different. The second derivative in these schemes is handled in a special manner and is written as

$$(\partial^2 W/\partial y^2)_{i-1,j,k} = \left[(W_{j+1} + W_{j-1})_{i-1} - (W_i + W_{i-2})_j\right]_k \Big/ \Delta y^2 \qquad (10\text{-}18)$$

The two variations are shown in Fig. 12. For the Der and Raetz scheme, two forms of the initial data can be used. One case is shown with the heavy dashed lines and the other with the light dashed lines. For the second case, information is required at the two levels (i-1) and (i-2) and thus a

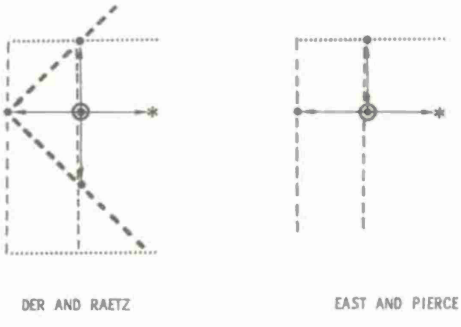

Figure 12. Explicit schemes.

starting procedure is required for this method. The same is true for the East and Pierce scheme. The authors imply that these methods are stable, but no stability analysis has been performed. One would guess for the Der and Raetz scheme that the condition required is $-1 \le \gamma \le 1$ while for the East and Pierce scheme the condition is $0 \le \gamma \le \infty$. This indicates that the Der and Raetz scheme can be stable for a reverse crossflow while the East and Pierce scheme would be unstable. For both of these methods the only unknown in the difference equations are quantities at the one grid point (i,j,k) which can be solved explicitly. The Der and Raetz scheme is a second-order method while the East and Pierce scheme is first order.

10.5.2 Implicit - These schemes are related to the implicit and Crank-Nicolson schemes for two-dimensional flows. The implicit methods result in difference equations with the unknown dependent variables appearing at the three grid points, j+1, j, and j-1, with the other locations for the points being (i) and (k). The various schemes that have been proposed and the restrictions on γ are presented in Fig. 13. The derivatives are evaluated as the notation in Fig. 11 indicates. The evaluation of the x_3-derivative in the Krause[169] zig-zag scheme is special and is written as

$$(\partial W/\partial x_3)_{i-\frac{1}{2},j,k} = \left[(W_{k+1} - W_k)_{i-1,j} + (W_k - W_{k-1})_{i,j}\right]/(2\Delta x_3) \qquad (10\text{-}19)$$

The results for the stability parameter are taken from Krause, et.al.[169] and Dwyer and Sanders.[163] Although no stability analysis has been performed for the Shevelev[148] scheme, one would expect the requirement to be $0 \le \gamma \le \infty$. Shevelev indicated that a Crank-Nicolson scheme should be used and Dwyer[160] also utilized the same type of scheme where the y-derivatives are evaluated at the four corners of the box. Krause[118] pointed out that the y-derivatives only have to be evaluated at the two corners as shown in Fig. 13. All of these schemes become unstable if there is a reverse crossflow. The methods shown in the lower part of Fig. 13 are stable with reverse crossflow if the step-sizes satisfy the stability parameter restriction. The method of Hall[170] requires two levels of initial data to start the solution unless initial data are specified along the heavy dashed lines. The Krause[169] zig-zag scheme requires initial and boundary conditions along the two perpendicular directions as shown in Fig. 13. The Shevelev, Shevelev-Dwyer, and Krause (1969) schemes require the same type of initial and boundary conditions. The Dwyer-Sanders[163] scheme is the only method which

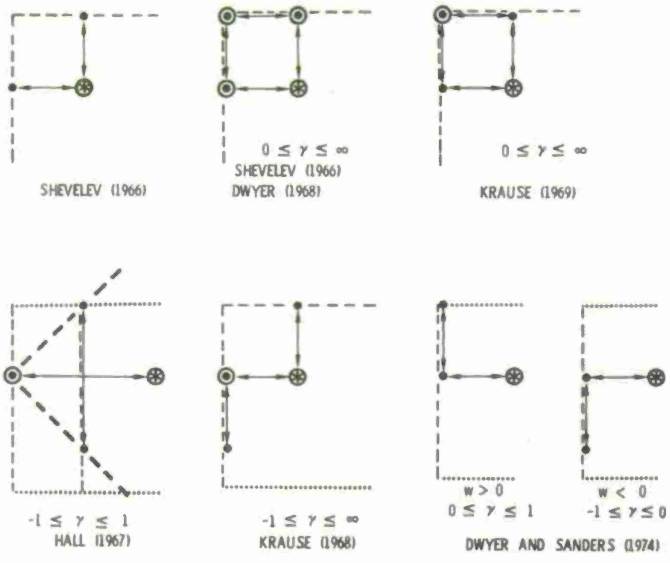

Figure 13. Implicit schemes.

can calculate the solution downstream from a plane of initial data. If additional boundary conditions are not given as shown in Fig. 13, then grid points are dropped as the solution proceeds. This also occurs with the Hall and Krause (1968) schemes. All of these methods can be second-order accurate except the Shevelev and Dwyer-Sanders schemes which are first order. Blottner and Ellis[147] suggested that a two-step Lax-Wendroff scheme might be adopted to the advection terms to give a second-order method when starting with initial data on a plane.

Since the finite-difference equations for the three-dimensional boundary layer are nonlinear, a linearization is performed. The resulting equations are uncoupled and of the form of Eq. (5-19) which are solved with the method of Appendix B. The continuity equation is of special form and gives an explicit solution for v (or related quantity) in terms of the other dependent variables. As shown for the two-dimensional boundary layer in Section 6, this type of linearization and iteration converges very slowly. This appears to be the reason that Blottner and Ellis[147] did not obtain second-order accurate results as an insufficient number of iterations were performed. The coupling of the difference equations with complete Newton-Raphson linearization has not been performed. The resulting difference equations will require the block-tridiagonal procedure of Appendix B. The blocks will be 3 x 3 for the incompressible boundary-layer equations while 4 x 4 for the compressible case if the energy equation is coupled.

10.5.3 Cube Scheme - This method is an extension of the box scheme for two-dimensional flow described in Section 5.4.5. The governing equations are written as a system of first-order equations before they are written in finite-difference form. This scheme is similar to that of Shevelev and Dwyer which is illustrated in Fig. 13. Since the equations are first-order, the y-derivatives at the corners are evaluated as follows:

$$(\partial W/\partial y)_{i,j-\frac{1}{2},k} = (W_j - W_{j-1})_{i,k}/\Delta y \tag{10-20}$$

Also, the first-order derivatives in the x_1 and x_3 directions are averaged between the values at (j) and (j-1) as follows:

$$(\partial W/\partial x_1)_{j-\frac{1}{2}} = \left[(\partial W/\partial x_1)_j + (\partial W/\partial x_1)_{j-1}\right]/2 \tag{10-21a}$$

$$(\partial W/\partial x_3)_{j-\frac{1}{2}} = \left[(\partial W/\partial x_3)_j + (\partial W/\partial x_3)_{j-1}\right]/2 \tag{10-21b}$$

The evaluation of the x_1 and x_3 derivatives are then obtained as the arrows indicate in Fig. 13 for the Shevelev and Dwyer scheme. This method is second-order accurate and Newton-Raphson linearization has been used. Therefore, converged solutions should be obtained after a few iterations. This method uses the block-tridiagonal procedure of Appendix B for the solution of the difference equations and for incompressible flow the block are 6 x 6. The stability of this method has not been stated, but it should be unstable for reverse crossflow.

10.6 Solutions and Limitations

The previous discussion has indicated the type of three-dimensional boundary layers that have been solved. These results generally require the finite-difference solution of three separate problems as follows:

(1) Tip, Stagnation Point or Leading Edge - The governing equations are a function of the transformed normal coordinate and x_3. A two-dimensional finite-difference scheme is required and the solution is started where the crossflow zero is zero.

(2) Plane of Symmetry - The governing equations are a function of the normal coordinate and x_1. A two-dimensional, finite-difference scheme is required and the solution is started at the leading edge, tip, or stagnation point.

(3) Three-Dimensional Flow - Depending on the initial and boundary conditions available, one of the three-dimensional, finite-difference schemes of Section 10.5 is employed.

If a code is to have any general use, there must be several of the schemes included in order that a stable solution may be obtained and allow the solution to continue depending on the local initial and boundary condition available. Flexibility of the use of various schemes and choice of where the solutions are performed is required. When regions of separated flow or clash lines are encountered, the marching procedure must be such that these regions can be excluded or taken into account properly. The automations of these choices would be very desirable.

Most of the three-dimensional solutions have been for laminar flows, but the extension to turbulent flows does not appear to add any new difficulties not already encountered with two-dimensional flows. Turbulent solutions have been obtained by East and Pierce,[162] Cebeci,[154] and Harris and Morris.[171]

The extension of the three-dimensional numerical techniques to unsteady flows has only been performed by Dwyer.[163] There appears to be no new problems introduced unless flow reversals occur.

11. STATUS OF BOUNDARY-LAYER COMPUTATIONAL TECHNIQUES

Although significant progress has been made in developing numerical techniques for solving the boundary-layer equations, there is the need for more efficient procedures. When one is confronted with the task of solving a three-dimensional flow, a complex reacting gas flow, or a turbulent flow with complex governing equations; prohibitive computing times can occur. In the earlier work on solution techniques, the main concern was developing a procedure which was stable and provided reasonably accurate results when needed. Recently, the interest has been in obtaining more accurate procedures and solving the more complex flows.

Adequate second-order accurate, finite-difference schemes exist for solving two-dimensional and axisymmetric perfect gas flows. The method of weighted residuals and the matrix integral method need to be investigated and the accuracy assessed. Also, higher-order, finite-difference schemes need further study. For solutions with the same accuracy, the computer time required for the various schemes needs to be evaluated. Hopefully, a better idea can be obtained on when higher-order schemes should be used and which methods should be pursued in the future. Automatic techniques should be developed for keeping the error within certain bounds by changing step-sizes and the order of the method. For turbulent flows, there is a need to find better ways to specify the grid spacing such that accurate results are obtained with the minimum number of grid points. As more efficient techniques are developed for the two-dimensional boundary-layer equations, they can be utilized in the solution procedures for unsteady, three-dimensional or real gas flows.

For unsteady, two-dimensional boundary-layer flows, there has been a limited amount of work performed. The two-dimensional techniques have been extended to the unsteady case, and three-dimensional steady schemes have been utilized when there is reverse flow. If there is reverse flow, further study is needed to determine the validity of the use of the boundary-layer equations. Additional work on the appropriate transformation to use with the unsteady boundary-layer equations is needed.

For steady, three-dimensional flows, difference schemes have been developed for various initial and boundary conditions and a limited number of problems have been solved. One problem appears to be the development of a general code for solving a variety of three-dimensional flows. This requires further evaluation of coordinate systems, transformations, and more accurate and better ways of handling the inviscid flow data needed. Also, more flexibility needs to be added into the codes such that the various difference schemes can be used as needed to satisfy the zones of dependence. The interaction of the boundary layer with the inviscid flow is a difficult problem that has only been handled for the sharp cone at incidence. One of the significant problems is knowing when or where to utilize the boundary-layer approach for a problem. For boundary-layer flows with boundary regions and significant interaction with the inviscid flow, perhaps the parabolic approach or the complete Navier-Stokes equations should be used for these flow situations.

APPENDIX A

SOLUTION OF MODIFIED TRIDIAGONAL EQUATIONS

A method is presented for solving the following coupled, finite-difference equations

$$-A_j F_{j-1} + B_j F_j - C_j F_{j+1} + a_j V_j + b_j V_{j-1} = D_j$$

$$V_j = V_{j-1} - c_j (F_j + F_{j-1}) + d_j$$

These equations are a particular form of the block-tridiagonal equations and a special form of the solution procedure of Appendix B.

The following parameters are first determined:

$$\left.\begin{aligned} E_J &= 0 \\ G_J &= 0 \\ e_J &= 1 \end{aligned}\right\} \quad \text{Obtained with boundary conditions at outer edge}$$

$$\left.\begin{aligned} E_j &= \left[A_j - c_j \left(C_j G_{j+1} - a_j\right)\right] / \mathcal{D} \\ G_j &= \left(C_j G_{j+1} - a_j - b_j\right) / \mathcal{D} \\ e_j &= \left[D_j + \left(C_j G_{j+1} - a_j\right) d_j + C_j e_{j+1}\right] / \mathcal{D} \end{aligned}\right\} \quad j = (J-1), (J-2), \cdots$$

where

$$\mathcal{D} = B_j - C_j E_{j+1} + c_j \left(C_j G_{j+1} - a_j\right)$$

Then the solution is obtained from

$$\left.\begin{aligned} F_1 &= 0 \\ V_1 &= 0 \end{aligned}\right\} \quad \text{Boundary conditions at wall}$$

$$\left.\begin{aligned} F_j &= E_j F_{j-1} + G_j V_{j-1} + e_j \\ V_j &= V_{j-1} - c_j (F_j + F_{j-1}) + d_j \end{aligned}\right\} \quad j = 2,3,4,\cdots J$$

APPENDIX B

SOLUTION OF TRIDIAGONAL AND BLOCK-TRIDIAGONAL EQUATIONS

Finite-difference relations of the form of Eqs. (4-18) are solved efficiently with the procedure we will describe. For tridiagonal equations, all of the quantities in Eqs. (4-18) are scalars while for block-tridiagonal equations the quantities are matrices and vectors. The Gaussian elimination process given below has been called the Thomas[172] algorithm and apparently was discovered independently by many others. For additional details of the block-triangular decomposition see, for example, Isaacson and Keller[173] and for explicit relations for blocks up to 3 x 3 see von Rosenberg.[174] A comparison of the block-tridiagonal factorization method with the band matrix method has been made by Varah.[175]

The solution is started by first determining the following quantities:

$$E_1 = B_1^{-1} C_1$$

$$e_1 = B_1^{-1} D_1$$

$$\left.\begin{aligned} E_j &= \left(B_j - A_j E_{j-1}\right)^{-1} C_j \\ e_j &= \left(B_j - A_j E_{j-1}\right)^{-1} \left(D_j + A_j e_{j-1}\right) \end{aligned}\right\} \quad j = 2,3,\cdots(J-1)$$

The solution is then completed with the use of the following relations:

$$W_J = \left(B_J - A_J E_{J-1}\right)^{-1} \left(D_J + A_J e_{J-1}\right) = e_J$$

$$W_j = E_j W_{j+1} + e_j \qquad j = (J-1), (J-2), \cdots 2,1$$

If the boundary conditions for the tridiagonal equations are

$$W_1 = W_w$$

$$W_J = 1$$

then

$$\left.\begin{aligned} B_1 &= 1 \\ C_1 &= 0 \\ D_1 &= W_w \end{aligned}\right\} \quad \begin{aligned} E_1 &= 0 \\ e_1 &= W_w \end{aligned}$$

$$\left.\begin{aligned} A_J &= 0 \\ B_J &= 1 \\ D_J &= 1 \end{aligned}\right\} \quad e_J = 1$$

For the block-tridiagonal equation, the boundary conditions give the above terms and are matrices as shown in Eqs. (4-18).

Greater efficiency is attained in this solution procedure for the block-tridiagonal case if the equation for E_j and e_j are solved with Gaussian elimination rather than with the use of the inverse matrix.

1. Paskonov, V. M. and Chudov, L. A.,"Difference Methods of Computing the Flow in the Boundary Layer," Vychisl. Metody i Programmirovanie, No. 11, Moscow Univ. Press, 1968, pp. 55-74.

2. Blottner, F. G., "Finite Difference Methods of Solution of the Boundary-Layer Equations," AIAA Jnl. Vol. 8, No. 3, Feb. 1970, pp. 193-205.

3. Smith, A. M. O., "A Decade of Boundary-Layer Research," Appl. Mech. Rev., Vol. 23, No. 1, Jan. 1970, pp. 1-9.

4. Patankar, S. V. and Spalding, D. B., Heat and Mass Transfer in Boundary Layers, London, Morgan-Grompian Book Ltd, 1967.

5. Jaffe, N. A. and Smith, A. M. O., "Calculation of Laminar Boundary Layers by Means of a Differential-Difference Method," pp. 49-212 in Progress in Aerospace Sciences, Vol. 12, Ed. D. Küchemann, New York, Pergamon Press, 1972.

6. Nash, J. F. and Patel, V. C., Three-Dimensional Turbulent Boundary Layers, Atlanta, Georgia, Scientific and Business Consultants, Inc., 1972.

7. Cebeci, T. and Smith, A. M. O., Analysis of Turbulent Boundary Layers, New York, Academic Press, 1974.

8. Lewis, C. H., "Numerical Methods for Nonreacting and Chemically Reacting Laminar Flows - Tests and Comparisons," Jnl Spacecr. & Rockets, Vol. 8, No. 2, Feb. 1971, pp. 117-122.

9. Libby, P. A., "Numerical Analysis of Stagnation Point Flows with Massive Blowing," AIAA Jnl., Vol. 8, No. 11, Nov. 1970, pp. 2095-2096.

10. Hornbeck, R. W., National Aeronautics and Space Administration, Numerical Marching Techniques for Fluid Flows with Heat Transfer, 1973, NASA SP-297.

11. Van Dyke, M., "Review of Laminar Boundary Layers," J. Fluid Mech., Vol. 18, 1964, pp. 477-480.

12. Hayes, W. D., U. S. Naval Ordnance Test Station, China Lake, California, The Three-Dimensional Boundary Layer, 1951, NAVORD Rept. 1313.

13. Stewartson, K., The Theory of Laminar Boundary Layers in Compressible Fluids, London, Oxford University Press, 1964.

14. Moore, F. K. (Ed.), Theory of Laminar Flows, Vol. 14, Princeton, New Jersey, Princeton University Press, 1964, pp. 286-394.

15. Der, J. and Raetz, G. S., Institute of the Aerospace Sciences, Solution of General Three-Dimensional Laminar Boundary-Layer Problems by an Exact Numerical Method, 1962, Paper No. 62-70.

16. Wang, K. C., "On the Determination of the Zones of Influence and Dependence for Three-Dimensional Boundary Layer Equations," J. Fluid Mech., Vol. 48 , No. 2, July 1971, pp. 397-404.

17. Ting, L., "On the Initial Conditions for Boundary Layer Equations," J. Math. Phys., Vol. XLIV, No. 4, Dec. 1965, pp. 353-367.

18. Flügge-Lotz, I. and Yu, E., Division of Engineering Mechanics, Stanford University, Development of a Finite Difference Method for Computing a Compressible Laminar Boundary Layer with Interaction, May 1960, TR 127.

19. Brailovskaya, I. Yu and Chudov, L. A., "The Solution of Boundary Layer Equations by a Difference Method," Vychisl. Metody i Progr., Moscow University, No. 1, 1962.

20. Paskonov, V. M., A Standard Program for the Solution of Boundary Layer Problems in Numerical Methods in Gas Dynamics, edited by G. S. Roslyakov and L. A. Chudov, Moscow, Moscow University Press, 1963.

21. Blottner, F. G. and Flügge-Lotz, I., "Finite-difference Computation of the Boundary Layer with Displacement Thickness Iteration," Journal de Mecanique, Vol. II, No. 4, Dec. 1963, pp. 397-423.

22. Mitchell, A. R. and Thomson, J. Y., "Finite Difference Methods of Solution of the von Mises Boundary Layer Equations with Special References to Conditions near a Singularity," Z. angew. Math. Phys., Vol. 9, 1958, pp. 26-37.

23. Mitchell, A. R., "Solution of the von Mises Boundary Layer Equation using a High-Speed Computer," Math. of Computn. Vol. 15, No. 75, July 1961, pp. 238-242.

24. Patankar, S. V. and Spalding, D. B., "A Finite-Difference Procedure for Solving the Equations of the Two-Dimensional Boundary Layer," Int. J. Heat Mass Trans., Vol. 10, 1967, pp. 1389-1411.

25. Flügge-Lotz, I., A Difference Method for the Computation of the Laminar Compressible Boundary Layer, 50 Jahre Grenzschichtforschung, Friedr. Vieweg und Sohn, Braunschweig, 1955, pp. 393-406.

26. Flügge-Lotz, I. and Baxter, D. C., Division of Engineering Mechanics, Stanford University, The Solution of Compressible Laminar Boundary Layer Problems by a Finite Difference Method, Part 1: Description of the Method, September 1956, TR 103.

27. Baxter, D. C. and Flügge-Lotz, I., "Compressible Laminar Boundary Layer Behavior Studied by a Finite Difference Methods," Z. angew. Math. Phys., Vol. XIb, pp. 81-96.

28. Kramer, R. F. and Lieberstein, H. M., "Numerical Solution of the Boundary-Layer Equations without Similarity Assumptions," J. Aerospace Sci., Vol. 26, No. 8, Aug. 1959, pp. 508-514.

29. Wu, J. C., "On the Finite-Difference Solution of Laminar Boundary Layer Problems," Proceedings of the 1961 Heat Transfer and Fluid Mechanics Institute, Stanford,California, Stanford University Press, June 1961.

30. Sills, J. A., "Transformations for Infinite Regions and Their Application to Flow Problems," AIAA Jnl., Vol. 7, No. 1, Jan. 1969, pp. 117-123.

31. Lees, L., "Laminar Heat Transfer Over Blunt-Nosed Bodies at Hypersonic Flight Speeds," Jet Propulsion, Vol. 26, No. 4, April 1956, pp. 259-269.

32. Blottner, F. G., "Chemical Non-Equilibrium Boundary Layer," AIAA Jnl., Vol. 2, No. 2, February 1964, pp. 232-240.

33. Keller, H. B., Numerical Methods for Two-Point Boundary-Value Problems, Waltham, Mass., Blaisdell Publishing Co., 1968.

34. Reshotko, E. and Beckwith, I. E., National Aeronautics and Space Administration, Compressible Laminar Boundary Layer over a Yawed Infinite Cylinder with Heat Transfer and Arbitrary Prandtl Number, 1958, NACA Report 1379.

35. Lenard, M., General Electric Space Sciences Laboratory, Philadelphia, Pennsylvania, Chemically Reacting Boundary Layer, March 1964, TIS R64SD14.

36. Fay, J. A. and Kaye, H., "Finite Difference Solution of Nonequilibrium Boundary Layers," AIAA Jnl., Vol. 5, No. 11, Nov. 1967, pp. 1949-1954.

37. Nachtsheim, P. R. and Swigert, P., National Aeronautics and Space Administration, Satisfaction of Asymptotic Boundary Conditions in Numerical Solution of Systems of Nonlinear Equations of Boundary-Layer Type, October 1965, NASA TN D-3004.

38. Roberts, S. M. and Shipman, J. S., "Continuation in Shooting Methods for Two-Point Boundary Value Problems," Jnl. math. Analys. Applic., Vol. 18, 1967, pp. 45-58.

39. Hestenes, M. R., Rand Corporation, Santa Monica, California, Numerical Methods of Obtaining Solutions of Fixed End Point Problems in the Calculus of Variation, August 1949, Rept. RM-102.

40. Bellman, R. E. and Kalaba, R. E., Quasilinearization and Nonlinear Boundary-Value Problems, New York, American Elsevier Publishing Co., Inc., 1965.

41. Radbill, J. R., "Application of Quasilinearization to Boundary-Layer Equations," AIAA Jnl., Vol. 2, No. 10, Oct. 1964, pp. 1860-1862.

42. Libby, P. A. and Chen, K. K., "Remarks on Quasilinearization Applied in Boundary-Layer Calculations," AIAA Jnl., Vol. 4, No. 5, May 1966, pp. 937-938.

43. Rubbert, P. E. and Landahl, M., "Solution of Nonlinear Flow Problems through Parametric Differentiation," Phys. Fluids, Vol. 10, No. 4, April 1967, pp. 831-835.

44. Lew, H. G., "Method of Accelerated Successive Replacement Applied to Boundary-Layer Equations," AIAA Jnl., Vol. 6, No. 5, May 1968, pp. 929-931.

45. Varzhanskaya, T. S., Obroskova, E. I., and Starova, E. N., "Boundary Layer Near the Critical Point," Numerical Methods in Gas Dynamics, G. S. Roslyakov and L. A. Chudov, editors, Moscow, Moscow University Press, 1963.

46. Holt, J. F., "Numerical Solution of Nonlinear Two-Point Boundary Problems by Finite Difference Methods," J. Ass. Comput. Mach., Vol. 7, 1964, pp. 366-373.

47. Casaccio, A., "Similar Solutions for the Laminar Mixing of Reactive Gases," AIAA Jnl., Vol. 2, No. 8, Aug. 1964, pp. 1403-1409.

48. Sylvester, R. J. and Meyer, F., "Two-Point Boundary Problems by Quasilinearization," J. Soc. ind. appl. Math. Vol. 13, No. 2, June 1965, pp. 586-602.

49. Keller, H. B. and Cebeci, T., "Accurate Numerical Methods for Boundary Layer Flow I: Two-Dimensional Laminar Flows," Lecture Notes in Physics, Proceedings of Second International Conference on Numerical Methods in Fluid Dynamics, Berlin, Springer-Verlag, 1971.

50. Werle, M. J. and Bertke, S. D., "A Finite-Difference Method for Boundary Layers with Reverse Flow," AIAA Jnl. Vol. 10, No. 9, Septempber 1972, pp. 1250-1252.

51. Greenspan, D., Discrete Numerical Methods in Physics and Engineering, New York, Academic Press, Inc., 1974.

52. Price, H. S., Varga, R. S., and Warren, J. E., "Application of Oscillation Matrices to Diffusion-Convection Equations," J. Math & Phys., Vol. 45, 1966, pp. 301-311.

53. Keller, H. B., "Accurate Difference Methods for Linear Ordinary Differential Systems Subject to Linear Constraints," SIAM Jnl. Numer. Analysis, Vol. 6, No. 1, March 1969, pp. 8-30.

54. Keller, H. B. and Cebeci, T., "An Inverse Problem in Boundary-Layer Flows: Numerical Determination of Pressure Gradient for a Given Wall Shear," Jnl. Comput. Phys., Vol. 10, 1972, pp. 151-161.

55. Hartree, D. R. and Womersley, J. R., "A Method for the Numerical or Mechanical Solution of Certain Types of Partial Differential Equations," Proc. Royal Soc. Series A, Vol. 161, 1937, pp. 353-366.

56. Liskovets, O. A., "The Method of Lines (Review)," Differential Equations, Vol. 1, 1965, pp. 1308-1323.

57. Leight, D. C. F., "The Laminar Boundary-Layer Equation: A Method of Solution by Means of an Automatic Computer," Proc. Camb. Phil. Soc., Vol. 51, 1955, pp. 320-332.

58. Manohar, R., "A Characteristic Difference Method for the Calculation of Steady Boundary-Layer Flow," Proceedings of the 4th Congress on Theoretical and Applied Mechanics, Indian Society of Theoretical and Applied Mechanics, Kharagpur, 1958, pp. 135-144.

59. Peters, Norbert, "Solution of Boundary Layer Equations for Chemically Reacting Gases with a Multi-point Method," Ph.D. Dissertation, Technische Universität, Berlin, Germany, 1971.

60. Peters, Norbert, "Boundary Layer Calculation by a Hermition Finite Difference Method," Fourth International Conference on Numerical Methods in Fluid Dynamics, Boulder, Colorado, June, 1974.

61. Krause, E., Hirschel, E. H., and Kordulla, W., "Fourth Order 'Mehrstellen'-Integration for Three-Dimensional Turbulent Boundary Layers," Proceedings AIAA Computational Fluid Dynamics Conference, July 19-20, 1973.

62. Steiger, M. H. and Sepri, P., Polytechnic Institute of Brooklyn, New York, On the Solution of Initial-Valued Boundary Layer Flows, May 1965, PIBAL Rept. 872.

63. Lubard, S. C. and Schetz, J. A.,"The Numerical Solution of Boundary Layer Problems," Proc. 1968 Heat Transfer and Fluid Mech. Institute, Edited by A. F. Emery and C. A. Depew, Stanford, California, Stanford University Press, June 1968.

64. Treanor, C. E., "A Method for the Numerical Integration of Coupled First-order Differential Equations with Greatly Different Time Constants," Math. of Computn., Vol. 20, Jan. 1966, p. 93.

65. Gear, C. W., Numerical Initial Value Problems in Ordinary Differential Equations, Englewood Cliffs, Prentice-Hall, 1971.

66. Binder, L., Doctoral Dissertation of the Technische Hochschule, München, Wilhelm, Knapp, Halle, 1911.

67. Schmidt, E., Föppl's Festschrift, Berlin, Julius Springer, 1924, p. 179.

68. Prandtl, L., "Zur Berechnung der Grenzschichten," Z. angew. Math. Mech., Vol. 18, 1938, pp. 77-82, (Translated as Note on the Calculation of Boundary Layers, NACA, TM No. 959).

69. DuFort, E. C. and Frankel, S. P., "Stability Conditions in Numerical Treatment of Parabolic Differential Equations," Mathematical Tables Aids Computation, Vol. 7, 1953, pp. 135-152.

70. Raetz, G. S., Northrop Aircraft Inc., Hawthorne, California, A Method of Calculating Three-Dimensional Laminar Boundary Layers of Steady Compressible Flows, December 1957, NAI-58-73.

71. Pletcher, R. H., "On a Finite-Difference Solution for the Constant-Property Turbulent Boundary Layer," AIAA Jnl, Vol. 7, No. 2, February 1969, pp. 305-311.

72. Rouleau, W. T. and Osterle, J. F., "Application of Finite-Difference Methods to Boundary Layer Type Flows," J. Aerospace Sci., Vol. 22, No. 4, April 1955, pp. 249-254.

73. Crank, J. and Nicolson, P., "A Practical Method for Numerical Evaluation of Solutions of Partial Differential Equations of the Heat Conduction Type," Proc. Camb. Phil. Soc., Vol. 43, 1947, p. 50.

74. Fussell, D. D. and Hellums, J. D., "The Numerical Solution of Boundary Layer Problems," A. I. Ch. E. Jl., Vol. 11, No. 4, July 1965, pp. 733-739.

75. Fannelop, T. K., "A Method of Solving the Three-Dimensional Laminar Boundary-Layer Equations with Application to a Lifting Re-entry Body," AIAA Jnl. Vol. 6, No. 6, June 1968, pp. 1075-1084.

76. Keller, H. B.,"A New Difference Scheme for Parabolic Problem," in Numerical Solution of Partial Differential Equations, Vol. II, edited by J. Bramble, New York, Academic Press, 1970.

77. Blottner, F. G., "Investigation of Some Finite-Difference Techniques for Solving the Boundary Layer Equations," to be published.

78. Petukhov, I. V., "On a Difference Approximation Scheme for the Numerical Solution of Parabolic Type Equations," Vychisl. Matem i Matem Fiz, Vol. 6, No. 6, 1966, pp. 1019-1028.

79. Blottner, F. G., "Finite-Difference Methods for Solving the Boundary Layer Equations with Second-Order Accuracy," in Proc. of the Second International Conference on Numerical Methods in Fluid Dynamics, Ed. Maurice Holt, Springer-Verlag, Berlin, 1971, pp. 144-150.

80. Davis, R. T. and Flügge-Lotz, Division of Engineering Mechanics, Stanford University, Laminar Compressible Flow Past Axisymmetric Blunt Bodies (Results of a Second-Order Theory), February 1964, Tech. Rep. 143.

81. Shchennikov, V. V., "Calculation of the Laminar Boundary Layer Along the Generating Line of a Sublimating Body of Revolution," J. Computer Math. and Math. Phys., Vol. 5, No. 1, 1965, pp. 139-144.

82. Byrkin, A. P. and Shchennikov, V. V., "A Numerical Method of Calculating a Laminar Boundary Layer," J. Computer Math. and Math. Phys., Vol. 10, No. 1, 1970, pp. 161-171.

83. Dorodnitsyn, A. A., "General Method of Integral Relations and Its Application to Boundary Layer Theory," in Advances in Aeronautical Sciences, Vol. 3, New York, Macmillan Press, 1960.

84. Pallone, A., "Nonsimilar Solutions of the Compressible Laminar Boundary-Layer Equations with Applications to the Upstream-Transpiration Cooling Problem," J. Aerospace Sci., Vol. 28, No. 6, June 1961, pp. 449-457.

85. Bethel, H. E., "Approximate Solution of the Laminar Boundary-Layer Equations with Mass Transfer," AIAA Jnl, Vol. 6, No. 2, February 1968, pp. 220-225.

86. Bossel, H. H., "Boundary-Layer Computation by an N Parameter Integral Method using Exponentials," AIAA Jnl., Vol. 8, No. 10, Oct. 1970, pp. 1841-1845.

87. Kendall, R. M. and Bartlett, E. P., "Nonsimilar Solution of the Multicomponent Laminar Boundary Layer by an Integral Matrix Method," AIAA Jnl, Vol. 6, No. 6, June 1968, pp. 1089-1097.

88. Baker, A. J., "Finite Element Computational Theory for Three-Dimensional Boundary Layer Flow," AIAA No. 72-108, AIAA 10th Aerospace Sciences Meeting, January 17-19, 1972.

89. Oden, J. T. and Wellford, L. C., "Analysis of Flow of Viscous Fluids by the Finite-Element Method," AIAA Jnl., Vol. 10, No. 12, December 1972, pp. 1590-1599.

90. Beckwith, I. E. and Bushnell, D. M., National Aeronautics and Space Administration, Washington, D. C., Detailed Description and Results on a Method for Computing Mean and Fluctuating Quantities in Turbulent Boundary Layers, October 1968, Technical Note D-4815.

91. Blottner, F. G., Johnson, M., and Ellis, M., Sandia Laboratories, Albuquerque, New Mexico, Chemically Reacting Viscous Flow Program for Multi-component Gas Mixtures, December 1971, SC-RR-70-754.

92. Keller, H. B. and Cebeci, T., "Accurate Numerical Methods for Boundary-Layer Flows II: Two-Dimensional Turbulent Flows," AIAA Jnl. Vol. 10, No. 9, September 1972, pp. 1193-1199.

93. Fitzhugh, H. A., "Numerical Studies of the Laminar Boundary Layer for Mach Numbers up to 15," J. Fluid Mech., Vol. 36, Part 2, 1969, pp. 337-366.

94. Werle, M. J. and Senechal, G. D., "A Numerical Study of Separating Supersonic Laminar Boundary Layers," J. of Appl. Mech., Vol. 40, September 1973, pp. 679-684.

95. Bradshaw, P., Ferriss, D. H., and Atwell, N. P., "Calculation of Boundary-Layer Development using the Turbulent Energy Equation," J. Fluid Mech., Vol. 28, Part 3, 1967, pp. 593-616.

96. Nash, J. F., "An Explicit Scheme for the Calculation of Three-Dimensional Turbulent Boundary Layers," J. Basic Engr. Trans. ASME, Series D, Vol. 94, No. 1, March 1972, pp. 131-141.

97. Mellor, G. L., "Incompressible, Turbulent Boundary Layers with Arbitrary Pressure Gradients and Divergent or Convergent Cross Flows," AIAA Jnl., Vol. 5, No. 9, September 1967, pp. 1570-1579.

98. Smith, A. M. O. and Cebeci, T., "Solution of the Boundary-Layer Equations for Incompressible Turbulent Flow," Proc. 1968 Heat Transfer and Fluid Mechanics Institute, edited by A. F. Emery and C. A. Depew, Stanford, California, Stanford University Press, June 1968.

99. Glushko, G. S., "Turbulent Boundary Layer on a Flat Plate in an Incompressible Fluid," Izvestiya Academy of Sciences, USSR: Mechanics No. 4, 1965 pp. 13-23 (translation; NASA TT-F-10,080).

100. Beckwith, I. E. and Bushnell, D. M., "Calculation of Mean and Fluctuating Properties of the Incompressible Turbulent Boundary Layer," Proceedings of the AFOSR-IFP Stanford Conference, Vol. 1, 1968, pp. 275-299.

101. Mellor, G. L. and Herring, H. J., "Two Methods of Calculating Turbulent Boundary Layer Behavior Based on Numerical Solutions of the Equations of Motion I, Mean Velocity Field Method; II. Mean Turbulent Field Method," Proceedings of the AFOSR-IFP Stanford Conference, Vol. 1, 1968, pp. 331-345.

102. Donaldson, C. duP. and Rosenbaum, H., National Aeronautics and Space Administration, Calculation of Turbulent Shear Flows through Closure of the Reynolds Equations by Invariant Modeling, in Compressible Turbulent Boundary Layer, 1969, NASA SP-216, pp. 231-253.

103. Varma, A. K., Beddini, R. A., Sullivan, R. D., and Donaldson, C. DuP., "Application of an Invariant Second-Order Closure Model to Compressible Turbulent Shear Layers," AIAA Paper No. 74-592, June 1974.

104. Blottner, F. G., "Nonuniform Grid Method for Turbulent Boundary Layers," Fourth International Conference on Numerical Methods in Fluid Dynamics, Boulder, Colorado, June 1974.

105. Roberts, G. O., "Computational Meshes for Boundary Layer Problems," Proceedings of the Second International Conference on Numerical Methods in Fluid Dynamics, Edited by Maurice Holt, Berlin, Springer-Verlag, 1971, pp. 171-177.

106. Davis, R. T., Wright-Patterson Air Force Base, Ohio, The Use of Crocco Type Variables in the Solution of Boundary Layer Problems, July 1974, TR 74-0059.

107. Blottner, F. G., "Variable Grid Scheme Applied to Turbulent Boundary Layers," Computer Methods in Applied Mechanics and Engineering, Vol. 4, No. 2, September 1974, pp. 179-194.

108. Denny, V. E. and Landis, R. B., "A New Method for Solving Two-Point Boundary Value Problems using Optimal Node Distribution," Jnl.of Comput. Phys., Vol. 9, 1972, pp. 120-137.

109. Cebeci, T. and Smith, A. M. O., "A Finite-Difference Method for Calculating Compressible Laminar and Turbulent Boundary Layers," J. of Basic Engr. Trans. ASME, Vol. 92, No. 3, September 1970, pp. 523-535.

110. Paskonov, V. M. and Rabin'kina, N. V., "Solution of the Nonstationary Boundary Layer Equations by a Difference Method," Numerical Methods in Gasdynamics, No. 4, Moscow, Moscow University Press, 1965.

111. Dwyer, H. A., "Calculation of Unsteady Leading-Edge Boundary Layers," AIAA Jnl., Vol. 6, No. 12, December 1968, pp. 2447-2448.

112. Hall, M. G., "A Numerical Method for Calculating Unsteady Two-Dimensional Laminar Boundary Layers," Ing. Arch., Vol. 38, 1969, pp. 97-106.

113. Farn, C. L S. and Arpaci, V. S., "On the Numerical Solution of Unsteady, Laminar Boundary Layers," AIAA Jnl. Vol. 4, No. 4, April 1966, pp. 730-732.

114. Oleinik, O. A., "On the Solution of Prandtl Equations by the Method of Finite Differences," Prikl. Mat. Mekh., Vol. 31, No. 1, 1967, pp. 90-100.

115. Katagiri, M., "Unsteady Boundary Layer near the Forward Stagnation Point with Uniform Suction or Injection," J. Phys. Soc. Japan, Vol. 31, No. 3, September 1971, pp. 935-939.

116. Phillips, J. H. and Ackerberg, R. C., "A Numerical Method for Integrating the Unsteady Boundary-Layer Equations when There are Regions of Backflow," J. Fluid Mech., Vol. 58, Part 3, 1973, pp. 561-579.

117. Telionis, D. P., Tsahalis, D. Th., and Werle, M. J., "Numerical Investigation of Unsteady Boundary-Layer Separation," Phys. Fluids, Vol. 16, No. 7, July 1973, pp. 968-973.

118. Krause, E., "Comment on 'Solution of a Three-Dimensional Boundary-Layer Flow with Separation,'" AIAA Jnl. Vol. 7, No. 3, March 1969, pp. 575-576.

119. Bartlett, E. P., Anderson, L. W. and Kendall, R. M., "Time-Dependent Boundary Layers with Application to Gun Barrel Heat Transfer," Proceedings of the 1972 Heat Transfer and Fluid Mechanics Institute, Ed. R. B. Landis and G. J. Hordemann, Stanford, California, Stanford University Press, Stanford, California, 1972.

120. Koob, S. J. and Abbott, D. E., "Investigation of a Method for the General Analysis of Time Dependent Two-Dimensional Laminar Boundary Layers," J. Basic Engr. Trans. ASME, Vol. 90D, No. 4, December 1968.

121. Patel, V. C. and Nash, J. F., "Some Solutions of the Unsteady Two-Dimensional Turbulent Boundary Layer Equations," in Recent Research on Unsteady Boundary Layers, IUTAM Symposium 1971, E. A. Eichelbrenner, Ed., Vol. 1, Laval University Press, 1972, pp. 1106-1164.

122. Cebeci, T. and Keller, H. B., "On the Computation of Unsteady Turbulent Boundary Layers," in Recent Research on Unsteady Boundary Layers, IUTAM Symposium 1971, E. A. Eichelbrenner, Ed., Vol. 1, Laval University Press, 1972, pp. 1072-1105.

123. Dwyer, H. A., "Calculation of Unsteady and Three-Dimensional Boundary Layer Flows," AIAA Jnl. Vol. 11, No. 6, June 1973, pp. 773-774.

124. Tsahalis, D. Th. and Telionis, D. P., "Oscillating Laminar Boundary Layers and Unsteady Separation," AIAA Paper No. 74-100, 12th Aerospace Science Meeting, 1974.

125. Fannelop, T. K., "A Method of Solving the Three-Dimensional Laminar Boundary-Layer Equations with Application to a Lifting Re-entry Body," AIAA Jnl. Vol. 6, No. 6, June 1968, pp. 1075-1084.

126. Howarth, L., "The Boundary Layer in Three-Dimensional Flow - Part II. The Flow Near a Stagnation Point," Phil. Mag., Series 7, Vol. 42, 1951, pp. 1433-1440.

127. Reshotko, E. and Beckwith, I. E., National Aeronautics and Space Administration, Compressible Laminar Boundary Layer over a Yawed Infinite Cylinder with Heat Transfer and Arbitrary Prandtl Number, 1958, NACA Report 1379.

128. Cebeci, T., "Calculation of Three-Dimensional Boundary Layers I. Swept Infinite Cylinders and Small Cross Flow," AIAA Jnl. Vol. 12, No. 6, June 1974, pp. 779-786.

129. Koh, J. C. Y. and Price, J. F., "Nonsimilar Boundary-Layer Heat Transfer of a Rotating Cone in Forced Flow," J. Heat Transfer, May 1967, pp. 139-145.

130. Muraca, R. J., "The Laminar Boundary Layer on Spinning Bodies of Revolution," AIAA Paper No. 70-1377, December 1970.

131. Moore, F. K., National Aeronautics and Space Administration, Laminar Boundary Layer on Cone in Supersonic Flow at Large Angle of Attack, 1953, NACA TR 1132.

132. Wu, P. and Libby, P. A., "Laminar Boundary Layer on a Cone near a Plane of Symmetry," AIAA Jnl., Vol. 11, No. 3, March 1973, pp. 326-333.

133. Seliverstov, S. N., "Calculating the Laminar Boundary Layer on the Dividing Streamline on the Front Surface of a Segmented Body in a Supersonic Gas Flow," Izv. AN SSSR, Mekanika Zhidkosti i Gaza, Vol. 3, No. 4, July-Aug., 1968, pp. 109-114.

134. Wang, K. C., "Three-Dimensional Boundary Layer Near the Plane of Symmetry of a Spheroid at Incidence," J. Fluid Mech., Vol. 43, Part 1, 1970, pp. 187-209.

135. Moore, F. K., National Aeronautics and Space Administration, Three-Dimensional Compressible Laminar Boundary Layer Flow, 1951, NACA TN 2279.

136. Cooke, J. C., Supersonic Laminar Boundary Layers on Cones, Farnborough, England, Royal Aircraft Establishment, 1966, TR 66347.

137. Vvedenskaya, N. D., "Calculation on the Boundary Layer Arising About a Cone Under an Angle of Attack," Zh. vychisl. Mat. mat. Fiz., Vol. 6, No. 2, 1966, pp. 304-312

138. Dwyer, H. A., "Boundary Layer on a Hypersonic Sharp Cone at Small Angle of Attack," AIAA Jnl., Vol. 9, No. 2, February 1971, pp. 277-284.

139. Boericke, R. R., "Laminar Boundary Layer on a Cone at Incidence in Supersonic Flow," AIAA Jnl., Vol. 9, No. 3, March 1971, pp. 462-468.

140. Bashkin, V. A., "Calculation of the Laminar Boundary Layer for Sharp Elliptic Cones in a Supersonic Flow with Zero Angle of Attack," Zh. vychisl. Mat. mat. Fiz., Vol. 10, No. 1, 1970, pp. 255-259.

141. McGowan, J. J. and Davis, R. T., Wright-Patterson Air Force Base, Ohio, Development of a Numerical Method to Solve the Three-Dimensional Compressible Laminar Boundary-Layer Equations with Application to Elliptical Cones at Angle of Attack, December 1970, ARL 70-0341.

142. Raetz, G. S., Northrop Corporation, A Method of Calculating Three-Dimensional Laminar Boundary Layers of Steady Compressible Flows, December 1957, Report No. NAI-58-73.

143. Eichelbrenner, E. A., "Three-Dimensional Boundary Layers," in Annual Review of Fluid Mechanics, Vol. 5, Palo Alto, California, Annual Reviews Inc., Eds. M. Van Dyke, W. G. Vincenti, and J. V. Wehausen, 1973.

144. Moore, F. K., "Three-Dimensional Boundary Layer Theory," in Advances in Applied Mechanics, Vol. 4, New York, Academic Press Inc., Eds. H. L. Dryden and Th. Von Karman, 1956.

145. Wang, K. C., Martin Marietta Laboratories, Baltimore, Maryland, Three-Dimensional Laminar Boundary Layer over Body of Revolution at Incidence, Part VI General Methods and Results of the Case of High Incidence, May 1973, AFOSR-TR-73-1045.

146. Der, J., "A Study of General Three-Dimensional Boundary-Layer Problems by an Exact Numerical Method," AIAA Jnl., Vol. 9, No. 7, July 1971, pp. 1294-1302.

147. Blottner, F. G. and Ellis, M. A., "Finite-Difference Solution of the Incompressible Three-Dimensional Boundary Layer Equations for a Blunt Body," Computers and Fluids, Vol. 1, 1973, pp. 133-158.

148. Shevelev, Yu. D., "Numerical Calculation of the Three-Dimensional Boundary Layer in an Incompressible Fluid," Izv. AN SSSR, Mekhanika Zhidkasti i Gaza, Vol. 1, No. 5, 1966, pp. 112-117.

149. Rizzi, A. W., Klavins, A., and MacCormack, R. W., "A Generalized Hyperbolic Marching Technique for Three-Dimensional Supersonic Flow with Shocks," Fourth International Conference on Numerical Methods in Fluid Dynamics, Boulder, Colorado, June 1974.

150. Fong, M. C., "Similar Solutions for Three-Dimensional Laminar Compressible Boundary Layers," AIAA Jnl., Vol. 2, No. 12, December 1964, pp. 2205-2207.

151. Zemlyanskii, B. A., "Method of Local Similarity for a Three-Dimensional Laminar Boundary Layer with Pressure Gradient," Izv. AN SSSR Mekhanika Zhidkosti i Gaza, Vol. 1, No. 4, 1966, pp. 70-75.

152. Dwyer, H. A. and McCroskey, W. J., "Crossflow and Unsteady Boundary-Layer Effects on Rotating Blades," AIAA Jnl., Vol. 9, No. 8, August 1971, pp. 1498-1505.

153. Fillo, J. A. and Burbank, R., "Calculation of Three-Dimensional Laminar Boundary-Layer Flow," AIAA Jnl., Vol. 10, No. 3, March 1972, pp. 353-355.

154. Cebeci, T., McDonnell Douglas Corporation, Long Beach, California, A General Method for Calculating Three-Dimensional Incompressible Laminar and Turbulent Boundary Layers II Three-Dimensional Flows in Cartesian Coordinates, March 1974, Report No. MDC J6517.

155. Watkins, C. B., "Numerical Solution of the Three-Dimensional Boundary Layer on a Spinning Sharp Body at Angle of Attack," Computers and Fluids, Vol. 1, 1973, pp. 317-329.

156. Vatsa, V. N. and Davis, R. T., National Aeronautics and Space Administration, The Use of Levy-Lees Variables in Three-Dimensional Boundary-Layer Flows, January 1973, NASA-CR-112315.

157. Mayne, A. W., Arnold Air Force Station, Tennessee, Analysis of Laminar Boundary Layers on Right Circular Cones at Angle of Attack, Including Streamline-Swallowing Effects, October 1972, AEDC-TR-72-134.

158. Popinski, Z. and Davis, R. T., National Aeronautics and Space Administration, Three-Dimensional Compressible Laminar Boundary Layers on Sharp and Blunt Circular Cones at Angle of Attack, January 1973, NASA-CR-112316.

159. Warsi, Z. U. A., "A Numerical Method of Solving the Three-Dimensional Boundary Layer Equations with Application to a Rotating Flat Blade," AIAA Paper No. 69-227, February 1969.

160. Dwyer, H. A., "Solution of a Three-Dimensional Boundary-Layer Flow with Separation," AIAA Jnl., Vol. 6, No. 7, July 1968, pp. 1336-1342.

161. Krause, E. and Hirschel, E. H., "Exact Numerical Solutions for Three-Dimensional Boundary Layers," Proceedings of the Second International Conference on Numerical Methods in Fluid Dynamics, Ed. Maurice Holt, Berlin, Springer-Verlag, 1971, pp. 132-137.

162. East, J. L. and Pierce, F. J., "Explicit Numerical Solution of the Three-Dimensional Incompressible Turbulent Boundary-Layer Equations," AIAA Jnl., Vol. 10, No. 9, September 1972, pp. 1216-1223.

163. Dwyer, H. A. and Sanders, B. R., "A Physical Optimum Difference Scheme for Three-Dimensional Boundary Layers," Fourth International Conference on Numerical Methods in Fluid Dynamics, Boulder, Colorado, June 1974.

164. Andreev, G. N. and Shevelev, Yu. D., "On the Three-Dimensional Boundary Layer on a Segmented Body at Supersonic Speeds," Izv. AN SSSR, Mekhanika Zhidkosti i Gaza, Vol. 6, No. 3, May-June 1971, pp. 41-48.

165. Vvedenskaya, N. D., "Three-Dimensional Laminar Boundary Layer on a Blunt Body," Izv. AN SSSR, Mekhanika Zhidkosti i Gaza, Vol. 1, No. 5, 1966, pp. 36-40.

166. Shevelev, Yu. D., "Numerical Study of Three-Dimensional Boundary Layer in a Compressible Gas," Izv. AN SSSR, Mekhanika Zhidkosti i Gaza, Vol. 2, No. 4, 1967, pp. 171-177.

167. Karabelas, A. J. and Hanratty, T. J., "Finite-Difference Solution for Three-Dimensional Boundary Layers with Large Positive and Negative Crossflows," AIAA Jnl., Vol. 9, No. 8, August 1971, pp. 1527-1532.

168. DeJarnette, F. R. and Hamilton, H. H., "Aerodynamic Heating on 3-D Bodies Including the Effects of Entropy-Layer Swallowing," AIAA Paper No. 74-602, June 1974.

169. Krause, E., Hirschel, E. H., and Bothmann, Th., "Numerical Stability of Three-Dimensional Boundary Layer Solutions," Z. angew. Math. Mech., Vol. 48, No. 8, 1968, pp. T205-T208.

170. Hall, M. G., Royal Aircraft Establishment, Farnborough, England, A Numerical Method for Calculating Steady Three-Dimensional Laminar Boundary Layers, June 1967, TR67145.

171. Harris, J. E. and Morris, D. J., "Solution of the Three-Dimensional Compressible, Laminar, and Turbulent Boundary-Layer Equations with Comparisons to Experimental Data," Fourth International Conference on Numerical Methods in Fluid Dynamics, Boulder, Colorado, June 1974.

172. Thomas, L. H., Columbia University, New York, Elliptic Problems in Linear Difference Equations Over a Network, Watson Sci. Comput. Lab. Report, 1949.

173. Isaacson, E. and Keller, H. B., Analaysis of Numerical Methods, New York, John Wiley & Sons, Inc., 1966.

174. von Rosenberg, D. U., Methods for the Numerical Solution of Partial Differential Equations, New York, American Elsevier Publishing Co., Inc., 1969.

175. Varah, J. M., "On the Solution of Block-Tridiagonal Systems Arising from Certain Finite-Difference Equations," Math. of Computn., Vol. 26, No. 120, October 1972.

Difference approximations for time dependent problems.

by

Heinz-Otto Kreiss.

Department of Computer Sciences
Uppsala University
Sturegatan 4B 2tr
S-752-23 Uppsala, Sweden

I. The Cauchy problem for partial differential equations.

I.1. Notations and examples

In this chapter we consider the Cauchy problem for partial differential equations. Let $x = (x_1,\dots,x_s)$ denote a point in the real s dimensional Euclidean space R_s and let t denote the time. Then we consider systems

$$\partial u/\partial t = P(x,t,\partial/\partial x)u \quad , \quad x \in R_s \quad , \quad t \geq t_0 \tag{1.1}$$

for which at time $t = t_0$ initial values

$$u(x,t_0) = f(x) \quad , \quad x \in R_s \tag{1.2}$$

are given. Here

$$u = \begin{pmatrix} u^{(1)} \\ \vdots \\ u^{(n)} \end{pmatrix} , \quad F = \begin{pmatrix} F^{(1)} \\ \vdots \\ F^{(n)} \end{pmatrix} , \quad f = \begin{pmatrix} f^{(1)} \\ \vdots \\ f^{(n)} \end{pmatrix}$$

are vector functions, depending on x and t.

$P(x,t,\partial/\partial x)$ is a general differential operator of order m, i.e.,

$$P(x,t,\partial/\partial x) = \sum_{j=0}^{m} P_j(x,t,\partial/\partial x) \quad , \quad P_j = \sum_{|\nu|=j} A_\nu(x,t)\partial^{|\nu|}/\partial x_1^{\nu_1}\dots\partial x_s^{\nu_s} \tag{1.3}$$

where $A_\nu(x,t)$ are $n \times n$ matrices and ν denotes the multi-index

$$\nu = (\nu_1,\dots,\nu_s) \quad , \quad \nu_j \text{ natural number}, \quad |\nu| = \sum \nu_j \, . \tag{1.4}$$

Now we consider a number of examples.

(1) The most simple initial value problem is

$$\partial u/\partial t = c\partial u/\partial x \quad , \quad u(x,0) = f(x) \, , \tag{1.5}$$

where c is a constant. Its solution is given by

$$u(x,t) = f(x+ct) \ , \tag{1.6}$$

i.e., the solution is constant along the characteristic lines $x+ct = \text{const}$. Another way to obtain the solution of (1.5) is by Fourier transform. Let $f(x) \in L_2(-\infty,\infty)$ then we can represent $f(x)$ in the form

$$f(x) = (2\pi)^{-1/2} \int_{-\infty}^{\infty} e^{i\omega x} \hat{f}(\omega)d\omega \ , \ \hat{f}(\omega) = (2\pi)^{-1/2} \int_{-\infty}^{+\infty} e^{i\omega x} f(x)dx \ . \tag{1.7}$$

Assume that also the solution can be represented by a Fourier integral

$$u(x,t) = (2\pi)^{-1/2} \int_{-\infty}^{+\infty} e^{i\omega x} \hat{u}(\omega,t)d\omega \ . \tag{1.8}$$

Then we get from (1.5) and (1.7) formally

$$0 = \partial u/\partial t - c\partial u/\partial x = (2\pi)^{-1/2} \int_{-\infty}^{+\infty} e^{i\omega x}(\partial \hat{u}/\partial t - i\omega c\hat{u})d\omega \ ,$$

$$0 = u(x,0) - f(x) = (2\pi)^{-1/2} \int_{-\infty}^{+\infty} e^{i\omega x}(\hat{u}(\omega,0) - \hat{f}(\omega))d\omega \ ,$$

i.e.,

$$\partial \hat{u}(\omega,t)/\partial t = i\omega c\hat{u}(\omega,t) \quad , \quad \hat{u}(\omega,0) = \hat{f}(\omega)$$

and therefore

$$\hat{u}(\omega,t) = e^{i\omega ct} \hat{f}(\omega) \ .$$

Thus by (1.8)

$$u(x,t) = (2\pi)^{-1/2} \int_{-\infty}^{+\infty} e^{i\omega(x+ct)} \hat{f}(\omega)d\omega = f(x+ct) \ . \tag{1.9}$$

(2) Another example is the wave equation

$$\partial^2 u/\partial t^2 = \partial^2 u/\partial x^2 \ . \tag{1.10}$$

In this case we have to specify u and $\partial u/\partial t$ as initial conditions for $t = 0$, i.e.,

$$u(x,0) = f(x) \quad , \quad \partial u(x,0)/\partial t = g(x) \ . \tag{1.11}$$

We write (1.10) as a first order system. Let $v(x,t)$ be a function such that

$$\partial u/\partial t = \partial v/\partial x \quad , \quad \partial v/\partial t = \partial u/\partial x \ . \tag{1.12}$$

Differentiating the first equation with respect to t and the second with respect to x and eliminating v, shows that u is a solution of (1.10). u fulfills also the initial conditions (1.11) if we specify $v(x,0)$ in such a way that

$$\partial u/\partial t\big|_{t=0} = \partial v(x,0)/\partial x = g(x) \ .$$

(1.12) can also be written in matrix form

$$\partial w/\partial t = A\partial w/\partial x \quad , \quad A = \begin{pmatrix} 0 & 1 \\ 1 & 0 \end{pmatrix} \quad , \quad w = \begin{pmatrix} u \\ v \end{pmatrix} \ . \tag{1.13}$$

A is a symmetric matrix. Therefore there is an orthogonal matrix O such that

$$O\,A\,O^* = O\,A\,O^{-1} = \begin{pmatrix} \lambda_1 & 0 \\ 0 & \lambda_2 \end{pmatrix} \tag{1.14}$$

where λ_j are the eigenvalues of A. In this case

$$\lambda_1 = +1 \quad , \quad \lambda_2 = -1 \quad , \quad O = \frac{1}{\sqrt{2}} \begin{matrix} 1 & +1 \\ -1 & 1 \end{matrix} \ . \tag{1.15}$$

Introduce therefore new dependent variables by

$$y = \begin{pmatrix} y^{(1)} \\ y^{(2)} \end{pmatrix} = Ow \ .$$

Then

$$(1.16) \qquad \partial y/\partial t = \begin{pmatrix} 1 & 0 \\ 0 & -1 \end{pmatrix} \partial y/\partial x$$

and we get two scalar equations of type (1.5) which can be solved explicitly.

(3) A third example is given by the so-called heat equation.

$$\partial u/\partial t = a\partial^2 u/\partial x^2 \quad , \quad a = \text{const.} > 0 \ ,$$

$$u(x,0) = f(x) \ .$$

Its solution can be easily computed by Fourier transform.

(4) In large scale calculations the underlying partial differential equations are much more complicated. As an example we state the linearized shallow water equations.

$$(1.17) \qquad \frac{\partial}{\partial t} \begin{pmatrix} u \\ v \\ \phi \end{pmatrix} = \begin{pmatrix} U_0 & 0 & \phi_0 \\ 0 & U_0 & 0 \\ 1 & 0 & U_0 \end{pmatrix} \frac{\partial}{\partial x} \begin{pmatrix} u \\ v \\ \phi \end{pmatrix} +$$

$$+ \begin{pmatrix} V_0 & 0 & 0 \\ 0 & V_0 & \phi_0 \\ 0 & 1 & V_0 \end{pmatrix} \frac{\partial}{\partial y} \begin{pmatrix} u \\ v \\ \phi \end{pmatrix} , \quad \phi_0 \neq 0 \ .$$

Here u, v denote velocities in the x, y direction respectively and ϕ represents the potential. U_0, V_0, ϕ_0 are mean values which can be functions of x, t .

Other examples are furnished by the equations of Gas dynamics, Maxwell's equations and the equations governing magneto hydrodynamics.

I.2. Well posed problems

The solutions of problems defined by (1.1), (1.2) are not always well behaved. Consider for example the equation

$$(2.1) \qquad \partial u/\partial t = -\partial^2 u/\partial x^2$$

with initial value

$$(2.2) \qquad u(x,0) = f(x)$$

where the Fourier transform $\hat{f}(\omega)$ of $f(x)$ has compact support, i.e.,

$$(2.3) \qquad f(x) = (2\pi)^{-1/2} \int_{-N}^{N} e^{i\omega x} \hat{f}(\omega) d\omega \ .$$

The solution of this problem is obviously given by

$$u(x,t) = (2\pi)^{-1/2} \int_{-N}^{N} e^{i\omega x + \omega^2 t} \hat{f}(\omega) d\omega \ .$$

Thus by making N large enough we can construct solutions which grow arbitrarily fast exponentially. This is often referred to as exponential explosion. Of course this explosion does not occur if $\hat{f}(\omega)$ decays

sufficiently fast, for example if $|\hat{f}(\omega)| \leq \text{const. } e^{-\omega^3}$. This assumption is in most cases too restrictive because the initial data are often given by measurements and therefore prone to spurious disturbances. The only reasonable assumption one can make is, that there is a constant $p \geq 0$ such that

$$(2.4) \qquad |\hat{f}(\omega)| \leq \text{const. } (|\omega|^p+1)^{-1} ,$$

i.e., that the Fourier transform of the initial values decays polynomial. This can never prevent any exponential explosion.

Consider the differential equation (1.5). Its solution is given by (1.9). Therefore, if $|\hat{f}(\omega)| \leq \text{const. } (|\omega| + 1)^{-p}$ then the same is true for $u(x,t)$, i.e., $|\hat{u}(\omega,t)| \leq \text{const. } (|\omega| + 1)^{-p}$. Thus there is no exponential or polynomial growth of the solution's Fourier transform. In fact we get from Parseval's relation for every fixed t :

$$\int_{-\infty}^{+\infty} |u(x,t)|^2 dx = \int_{-\infty}^{+\infty} |f(x)|^2 dx.$$

An example of polynomial growth is given by the differential equation

$$(2.5) \qquad \frac{\partial}{\partial t}\begin{pmatrix} u \\ v \end{pmatrix} = \begin{pmatrix} 1 & 1 \\ 0 & 1 \end{pmatrix} \frac{\partial}{\partial x}\begin{pmatrix} u \\ v \end{pmatrix} , \quad \begin{pmatrix} u(x,0) \\ v(x,0) \end{pmatrix} = \begin{pmatrix} f^{(1)}(x) \\ f^{(2)}(x) \end{pmatrix} .$$

Its Fourier transform is

$$\frac{d}{dt}\begin{pmatrix} \hat{u} \\ \hat{v} \end{pmatrix} = i\omega\begin{pmatrix} 1 & 1 \\ 0 & 1 \end{pmatrix}\begin{pmatrix} \hat{u} \\ \hat{v} \end{pmatrix} , \quad \begin{pmatrix} \hat{u}(\omega,0) \\ \hat{v}(\omega,0) \end{pmatrix} = \begin{pmatrix} \hat{f}^{(1)}(\omega) \\ \hat{f}^{(2)}(\omega) \end{pmatrix} .$$

Therefore

$$\hat{u}(\omega,t) = e^{i\omega t}\,\hat{f}^{(1)}(\omega) + i\omega t e^{i\omega t}\,\hat{f}^{(2)}(\omega) ,$$

$$\hat{v}(\omega,t) = e^{i\omega t}\,\hat{f}^{(2)}(\omega) ,$$

i.e.,

$$u(x,t) = (2\pi)^{-1/2} \int_{-\infty}^{+\infty} e^{i\omega(x+t)}(\hat{f}^{(1)}(\omega) + i\omega t\hat{f}^{(2)}(\omega))d\omega ,$$

$$v(x,t) = (2\pi)^{-1/2} \int_{-\infty}^{+\infty} e^{i\omega(x+t)}\,\hat{f}^{(2)}(\omega)d\omega .$$

Observing that

$$\int_{-\infty}^{+\infty} |\partial f/\partial x|^2 dx = \int_{-\infty}^{+\infty} \omega^2 |\hat{f}(\omega)|^2 dx$$

we get instead of (2.5)

$$\int_{-\infty}^{+\infty} |u(x,t)|^2 + |v(x,t)|^2 dx \leq \int_{-\infty}^{+\infty} |f^{(1)}(x)|^2 + |f^{(2)}(x)|^2 dx + t \cdot \int_{-\infty}^{+\infty} \left|\frac{\partial f^{(2)}}{\partial x}\right|^2 dx .$$

Thus polynomial growth of the Fourier transform corresponds to the loss of derivatives.

We shall now define what a well posed problem is. Let $L_2(R_s)$ be the space of all quadratically integrable vector functions $u = (u^{(1)},\ldots,u^{(n)})'$ and denote by

$$(2.5) \qquad (u,v) = \sum \int_{R_s} \bar{u}^{(i)} v^{(i)} dx , \quad ||u|| = |(u,u)^{1/2}|$$

the usual scalar product and norm. We define:

Definition 2.1. Consider the Cauchy problem (1.1), (1.2). It is weakly well posed if for every $f \in C_0^r$ (r some number) and every initial time $t = t_0$ there is a unique classical solution $u(x,t)$, (i.e., a solution which belongs to C^m as function of x and C^1 as function of t) with:

$$||u(x,t)|| \leq K\, e^{\alpha(t-t_0)} \sum_{|\alpha|\leq p} ||\partial^{|\alpha|} f/\partial^{\alpha}|| \quad . \tag{2.6}$$

It is strongly well posed if (2.6) holds with $p = 0$. Here K, α, p are constants independent of f and t_0.

I.3. Equations with constant coefficients

In this section we consider systems (3.1)

$$\begin{aligned} &\partial u/\partial t = P(\partial/\partial x)u \\ &u(x,0) = f(x) \end{aligned} \tag{3.1}$$

with constant coefficients. Let $\omega = (\omega_1,\dots,\omega_s)$ denote the (real) dual variables of $x = (x_1,\dots,x_s)$ and denote by

$$f(\omega) = (2\pi)^{-1/2} \int_{-\infty}^{\infty} e^{-i\langle\omega,x\rangle} f(x)dx \quad , \quad \langle\omega,x\rangle = \sum_{i=1}^{s} \omega_i x_i \tag{3.2}$$

the Fourier transform of $f(x)$. We assume that for every $\hat{f}$ there is a constant $R_{\hat{f}}$ such that

$$|\hat{f}(\omega)| = 0 \quad \text{for} \quad |\omega| > R_{\hat{f}} \quad . \tag{3.3}$$

Then it follows that (3.1) has a unique solution belonging to L_2 for every fixed t which is of the form

$$\begin{aligned} u(x,t) &= (2\pi)^{-1/2} \int_{-\infty}^{+\infty} e^{i\langle\omega,x\rangle}\, \hat{u}(\omega,t)d\omega = \\ &= (2\pi)^{-1/2} \int_{|\omega|\leq R_f} e^{i\langle\omega,x\rangle}\, \hat{u}(\omega,t)d\omega \quad . \end{aligned} \tag{3.4}$$

Introducing (3.4) into (3.1) gives us

$$\frac{d\hat{u}(\omega,t)}{dt} = P(i\omega)\hat{u} \quad , \quad \hat{u}(\omega,0) = \hat{f}(\omega) \quad ,$$

where

$$P(i\omega) = \sum_{j=0}^{m} P_j(i\omega) \quad , \quad P_j(i\omega) = \sum_{|\nu|=j} A_\nu (i\omega_1)^{\nu_1} \dots (i\omega_s)^{\nu_s} \quad .$$

Therefore

$$\hat{u}(\omega,t) = e^{P(i\omega)t}\, \hat{f}(\omega)$$

and

$$u(x,t) = (2\pi)^{-s/2} \int_{|\omega|\leq R_f} e^{i\,\omega,x}\; e^{P(i\omega)t}\, \hat{f}(\omega)d\omega \tag{3.5}$$

is the solution of our problem.

We can now prove

Lemma 3.1. The Cauchy problem (3.1) is weakly well posed if and only if there are constants K, α, p

such that

$$|e^{P(i\omega)t}| \leq K|\omega|^p e^{\alpha t} \quad . \tag{3.6}$$

Especially if (3.6) holds with $p = 0$ then the problem is strongly well posed.

Proof: From (3.5) and Parseval's relation we get for every fixed t

$$||u(x,t)||^2 = \int_{|\omega|\leq R_f} |e^{P(i\omega)t}|^2 \, |\hat{f}(\omega)|^2 \, d\omega \quad . \tag{3.7}$$

If (3.6) holds, then (3.7) implies

$$||u(x,t)||^2 \leq K^2 e^{2\alpha t} \int_{-\infty}^{+\infty} |\omega|^{2p} \, |f(\omega)|^2 \, d\omega \leq K^2 e^{2\alpha t} \, ||f||_p^2 \quad .$$

Assume now that there are no constants K, α, p such that (3.6) holds. Then there exist for every triple of constants K, α, p an ω_0, t_0 such that

$$|e^{P(i\omega_0)t_0}| > 2K \, |\omega_0|^p e^{\alpha t_0} \quad .$$

Therefore there is a whole neighborhood of ω_0, such that

$$|e^{P(i\omega)t_0}| > K|\omega|^p e^{\alpha t_0} \quad \text{for} \quad |\omega-\omega_0| < \delta \quad . \tag{3.8}$$

Let us choose $f(x)$ in such a way that

$$\hat{f}(\omega) = 0 \quad \text{for} \quad |\omega-\omega_0| > \delta \quad .$$

Then by (3.7) and (3.8)

$$||u(x,t)||^2 > K^2 e^{2\alpha t} \, ||f||_p^2 \quad .$$

This proves the lemma.

From the last lemma we get

Theorem 3.1. The Cauchy problem (3.1) is weakly well posed if and only if there is a constant α such that for all ω for the eigenvalues λ of $P(i\omega)$ the estimate

$$\text{Real } \lambda \leq \alpha \tag{3.9}$$

holds.

Proof: Let λ be an eigenvalue of $P(i\omega)$. Then

$$|e^{P(i\omega)t}| \geq e^{(\text{Real } \lambda)t} \quad .$$

Therefore (3.9) is a necessary condition.

Assume now (3.9) holds. $e^{P(i\omega)t}$ is the general solution of the system of ordinary differential equations

$$dy/dt = P(i\omega)y \quad .$$

Let $U = U(i\omega)$ be a unitary matrix which transforms $P(i\omega)$ to upper triangular form, i.e.,

$$UPU^* = \Lambda + Q \quad , \quad \Lambda = \begin{pmatrix} \lambda_1 & 0 & & \cdots & 0 \\ 0 & \lambda_2 & 0 & & 0 \\ \cdot & \cdot & \cdot & \cdot & \cdot \\ 0 & \cdot & \cdot & \cdot & \lambda_n \end{pmatrix},$$

$$Q = \begin{pmatrix} 0 & q_{12} & & \cdots & q_{1n} \\ 0 & 0 & q_{23} & \cdots & q_{2n} \\ \cdot & \cdot & \cdot & \cdots & \cdot \\ 0 & \cdot & \cdot & & 0 \end{pmatrix}$$

and introduce new variables

$$v = Uy \quad .$$

v is the solution of

$$dv/dt = (\Lambda+Q)v \quad .$$

Let

$$v = e^{\Lambda t}w \quad ,$$

then w is the solution of

$$dw/dt = Q_1 w \quad , \quad Q_1 = e^{-\Lambda t} Q\, e^{\Lambda t} \quad .$$

Here Q_1 is of the same form as Q. Therefore

$$w(t) = e^{Q_1 t} = \sum_{\nu=0}^{n} Q_1^{\nu} = e^{-\Lambda t} \sum_{\nu=0}^{n} Q^{\nu}\, e^{\Lambda t} \quad ,$$

i.e.

$$y = U^* v = U^* \sum_{\nu=0}^{n} Q^{\nu} t^{\nu} e^{\Lambda t} = e^{P(i\omega)t} \quad . \tag{3.10}$$

The theorem follows from the observation that $|Q| \leq \text{const.} |\omega|^m$, $|e^{\Lambda t}| \leq e^{\alpha t}$.

We thus see that algebraic conditions to decide whether a Cauchy problem is weakly well posed are relatively simple. This is not so for strongly well posed problems. Without proof we shall here state

Theorem 3.2. The Cauchy problem (3.1) is strongly well posed if and only if there are constants K_0, K_1, α and for every ω a nonsingular transformation $\Gamma = \Gamma(\omega)$ with

$$\max\{|\Gamma(\omega)| \, , \, |\Gamma^{-1}(\omega)|\} < K_0 \quad ,$$

$$\Gamma(\omega)P(i\omega)\Gamma^{-1}(\omega) = \begin{pmatrix} \lambda_1 & q_{12} & \cdot & \cdots & q_{1n} \\ 0 & \lambda_2 & q_{23} & \cdots & q_{2n} \\ \cdot & \cdot & \cdot & \cdots & \cdot \\ 0 & \cdot & \cdot & \cdots & \lambda_n \end{pmatrix} \quad ,$$

where

$$\text{Real } \lambda_1 < \text{Real } \lambda_2 < \ldots < \text{Real } \lambda_n < \alpha$$

and

$$|q_{ij}| \leq K_1(|\text{Real } \lambda_i| + 1) \quad .$$

We shall now consider a large number of examples.

(1) Hyperbolic systems. Consider a first order system

$$\partial u/\partial t = \sum A_\nu \, \partial u/\partial x_\nu \quad .$$

It is weakly hyperbolic if the eigenvalues λ of

$$P(i\omega) = i \sum A_\nu \, \omega_\nu \tag{3.11}$$

are purely imaginary. An example is given by the equation (2.6). It is strongly hyperbolic if there is a constant K_1 and a nonsingular transformation $\Gamma = \Gamma(\omega)$ with

$$\max\{|\Gamma(\omega)| \ , \ |\Gamma^{-1}(\omega)|\} \leq K_1 \tag{3.12}$$

such that

$$\Gamma(\omega)P(i\omega)\Gamma^{-1}(\omega) = i \begin{pmatrix} \lambda_1 & 0 & & \dots & 0 \\ & \lambda_2 & 0 & \dots & 0 \\ . & . & . & \dots & . \\ 0 & . & . & \dots & \lambda_n \end{pmatrix} = i\Lambda \quad , \ \lambda_j \text{ real} \ . \tag{3.13}$$

All systems where the matrices A_ν are Hermitian are examples of strongly hyperbolic systems. In that case we can choose the transformation $\Gamma(\omega)$ as a unitary matrix. The wave equation (1.16) is an example. Also the shallow water equations (1.17) are strongly hyperbolic. In this case we can symmetricize the coefficient matrices by introducing new variables

$$\begin{pmatrix} \tilde{u} \\ \tilde{v} \\ \tilde{\phi} \end{pmatrix} = \begin{pmatrix} \phi_0^{-1/2} & 0 & 0 \\ 0 & \phi_0^{-1/2} & 0 \\ 0 & 0 & 1 \end{pmatrix} \begin{pmatrix} u \\ v \\ \phi \end{pmatrix}$$

and get

$$\frac{\partial}{\partial t} \begin{pmatrix} \tilde{u} \\ \tilde{v} \\ \phi \end{pmatrix} = \begin{pmatrix} U_0 & 0 & \phi_0^{1/2} \\ 0 & U_0 & 0 \\ \phi_0^{1/2} & 0 & U_0 \end{pmatrix} \frac{\partial}{\partial x} \begin{pmatrix} \tilde{u} \\ \tilde{v} \\ \phi \end{pmatrix} +$$

$$+ \begin{pmatrix} V_0 & 0 & 0 \\ 0 & V_0 & \phi_0^{1/2} \\ 0 & \phi_0^{1/2} & V_0 \end{pmatrix} \frac{\partial}{\partial y} \begin{pmatrix} \tilde{u} \\ \tilde{v} \\ \phi \end{pmatrix} \quad .$$

The Cauchy problem for weakly hyperbolic systems is weakly well posed. This follows from Theorem 3.1. For strongly hyperbolic systems the Cauchy problem is strongly well posed. This follows from Theorem 3.2, but also directly from

$$|e^{P(i\omega)t}| = |\Gamma^{-1}\Gamma e^{P(i\omega)t}\Gamma^{-1}\Gamma| \leq K_1^2 \, |e^{i\Lambda t}| = K_1^2$$

and Lemma 3.1.

The simplest parabolic differential equation is the heat equation

$$\partial u/\partial t = \partial^2 u/\partial x^2 \quad .$$

The Cauchy problem is strongly well posed because

$$P(i\omega) = -\omega^2 \quad , \quad \text{i.e.,} \quad |e^{P(i\omega)t}| \leq e^{-\omega^2 t} \leq 1 \quad .$$

Generally we define

Definition 3.1. A system (3.1) is called parabolic if its order is even, i.e., $m = 2q$ and the eigenvalues κ of the highest order term $P_m(i\omega)$ fulfill an inequality

$$\text{Real } \kappa \leq -\delta|\omega|^m \quad , \quad \delta = \text{const.} > 0 \quad . \tag{3.14}$$

We want to prove

Theorem 3.3. For parabolic equations the Cauchy problem is strongly well posed.

Proof: For $|\omega| \neq 0$ we can write $P(i\omega)$ in the form

$$P(i\omega) = P_m(i\omega)(I + \sum_{j=0}^{m-1} P_m^{-1}(i\omega)P_j(i\omega))$$

where by (3.14)

$$\lim_{|\omega|\to\infty} P_m^{-1}(i\omega)P_j(i\omega) = 0 \quad .$$

Therefore there is a constant α such that for the eigenvalues λ of $P(i\omega)$ the inequality

$$\text{Real } \lambda \leq -\frac{1}{2}\delta|\omega|^m + \alpha \tag{3.15}$$

holds. Therefore the representation (3.10) gives us

$$|e^{P(i\omega)t}| \leq \text{const.}(|\omega|^m \cdot t)^n \cdot e^{-\frac{1}{2}\delta|\omega|^m t} \cdot e^{\alpha t} \leq$$

$$\leq \text{const.} \left(\frac{2n}{\delta}\right)^n e^{-n} e^{\alpha t} \leq \text{const.}\ e^{\alpha t} \quad .$$

A very useful sufficient criteria to determine whether a Cauchy problem is strictly well posed is

Lemma 3.2. Assume that

$$P(i\omega) + P^*(i\omega) \leq \alpha I \tag{3.16}$$

then

$$|e^{P(i\omega)t}| \leq e^{\alpha t}$$

and therefore the Cauchy problem is strongly well posed.

Proof: $e^{P(i\omega)t}$ is the general solution of

$$dy/dt = P(i\omega)y \quad .$$

Therefore

$$\frac{d}{dt}|y|^2 = y^*(P(i\omega) + P^*(i\omega))y \leq \alpha|y|^2$$

and the lemma follows immediately.

In many applications the equations are mixed hyperbolic-parabolic. A typical example is

$$\partial u/\partial t = A\ \partial u/\partial x + B\ \partial u/\partial y + C(\partial^2 u/\partial x^2 + \partial^2 u/\partial y^2)$$

where A, B, C are symmetric matrices with $C \geq 0$. The Cauchy problem is strongly well posed because

$$P(i\omega) + P^*(i\omega) \leq 0 \quad .$$

Another type of equations appearing in applications are the Schrödinger equations. The simplest example is

$$\partial u/\partial t = i\, \partial^2 u/\partial x^2 \quad .$$

The Cauchy problem is strongly well posed because

$$P(i\omega) = -i\omega^2 \quad , \quad \text{i.e.,} \quad |e^{P(i\omega)t}| \leq 1 \quad .$$

Another equation is given by

$$\frac{\partial u}{\partial t} = A \frac{\partial^2 u}{\partial x^2} + B \frac{\partial u}{\partial x} + C\, u \quad .$$

Here

$$A = -A^* \quad , \quad B = B^* \quad .$$

Again the problem is strongly well posed because

$$P(i\omega) + P^*(i\omega) = C + C^* \quad .$$

I.4. The Cauchy problem for equations with variable coefficients I .

Consider the system (1.1)

(4.1) $$\partial u/\partial t = P(x,t,\partial/\partial x)u$$

with variable coefficients. Connected with (1.1) are the systems with constant coefficients

(4.2) $$\partial w/\partial t = P(x_0,t_0,\partial/\partial x)u$$

which we get from (4.1) by freezing the coefficients at a point $x = x_0$, $t = t_0$. In the last section we have learned to decide whether the Cauchy problem is well posed for equations with constant coefficients. Therefore it is natural to ask the following question: Assume that the Cauchy problem is well posed for all systems (4.2) with constant coefficients. Is it true that then also the Cauchy problem for (4.1) is well posed?

Unfortunately general existence theorems using the principle of freezing the coefficients are only known for strongly hyperbolic and parabolic systems which are defined by

Definition 4.1. The system (4.1) is parabolic (strongly hyperbolic) if all the systems (4.2) are uniformaly parabolic (strongly hyperbolic), i.e., the inequality (3.14), ((3.12)) holds with a universal constant $\delta > 0$ (K_1) .

We have

Theorem 4.3. Assume that the system (4.1) is parabolic and that its coefficients are Lipschitz continuous. Then the Cauchy problem is well posed.

Theorem 4.4. Assume that the system (4.1) is strongly hyperbolic and that the coefficients are sufficiently smooth. Then for every x_0, t_0 there is a Hermitian matrix $H = H(i\omega,x_0,t_0)$ such that (4.10) and (4.11) holds. The Cauchy problem is well posed if one can choose $H(i\omega,x_0,t_0)$ as a sufficiently smooth function of x_0, t_0 and ω .

There are two classes of equations for which the conditions of Theorem 4.4 hold.

(1) Symmetric hyperbolic systems.

$$\partial u/\partial t = \sum A_\nu(x,t)\, \partial u/\partial x_\nu$$

where $A_\nu(x,t) = A_\nu^*(x,t)$ are symmetric matrices. In this case

$$P(i\omega,x_0,t_0) = i \sum A_\nu(x_0,t_0)\omega_\nu = -P^*(i\omega,x_0,t_0) \quad ,$$

and we can choose $H \equiv I$.

(2) Strictly hyperbolic systems. They are defined in the following way.

Definition 4.2. A first order system

$$\partial u/\partial t = \sum A_\nu(x,t)\, \partial u/\partial x_\nu$$

is strictly hyperbolic if the eigenvalues of

$$-i\, P(i\omega,x_0,t_0) = \sum A_\nu(x_0,t_0)\omega_\nu \quad ,$$

are all real and distinct for all values of x_0, t_0 and ω with $|\omega| = 1$.

We collect the last statements in

Theorem 4.5. The Cauchy problem is strongly well posed for first order symmetric systems and for strictly hyperbolic systems.

I.5. The Cauchy problem for equations with variable coefficients II.

In the last section we have seen that for parabolic and hyperbolic systems one can decide whether the Cauchy problem is well posed or not by "freezing the coefficients". For equations of other types this procedure is not possible. Instead one can use the so called Energymethod. We start with

Lemma 5.1. Let u, v be vector functions of $x = (x_1,\dots,x_s)$ and assume that $u(x),v(x) \in S^1(L_2)$ i.e., u, v and its first derivatives belong to $L_2(R_s)$. Let $A(x)$ $C^1(R_s)$ be a matrix then

$$(5.1) \qquad (u,A(x)\, \partial v/\partial x_i) = -(\partial u/\partial x_i, A(x)v) - (u,\, \partial A/\partial x_i\, v) \quad .$$

If A is symmetric then

$$(5.2) \qquad 2\,\mathrm{Real}(u,\, A(x)\, \partial u/\partial x_i) = -(u,\, \partial A/\partial x\, u)$$

Proof: Let u, v belong to C_0^∞ . Then partial integration gives us

$$\int_{-\infty}^{+\infty} u^* A(x)\, \partial v/\partial x_i \, dx_i = -\int_{-\infty}^{+\infty} \frac{\partial}{\partial x_i} (Au)^* \cdot v \, dx_i =$$

$$\int_{-\infty}^{+\infty} \partial u^*/\partial x_i \, A\, v \, dx_i + \int_{-\infty}^{+\infty} u^*\, \partial A/\partial x_i \, v \, dx_i \quad .$$

Therefore (5.1) holds for all functions u, $v \in C_0^\infty$. Now C_0^∞ is dense in $S^1(L_2)$ and therefore (5.1) holds also for all functions in $S^1(L_2)$. Let $u \equiv v$ then (5.2) follows immediately from (5.1) observing that $(u,v) = (\overline{v,u})$.

Consider now the scalar Schrödinger equation

$$(5.3) \qquad \partial u/\partial t = i\, \partial/\partial x(p\, \partial/\partial x\, u) + b\, \partial u/\partial x + c\, u = Pu$$

where p, b and c are real functions of x, t belonging to $C^1(R_s)$. Let $u \in S^2(L_2)$ be a solution

of (5.3). By Lemma (5.1) we have

$$\frac{1}{2}\frac{\partial}{\partial t}(u,u) = \frac{1}{2}((\partial u/\partial t,\ u) + (u,\ \partial u/\partial t)) =$$

$$\text{Real}(u,\ \partial u/\partial t) = \text{Real}\ i(u,\ \partial/\partial x(p\ \partial u/\partial x)) +$$

$$\text{Real}(u,\ b\ \partial u/\partial x) + \text{Real}(u,\ c\ u) =$$

$$(u,\ (c - \frac{1}{2}\partial b/\partial x)u) \leq \alpha(u,u)$$

where

$$\alpha = \max_{x,t}\ (c - \frac{1}{2}\partial b/\partial x) \quad .$$

Therefore

$$(5.4) \qquad ||u(x,t)|| \leq e^{\alpha t}\ ||u(x,0)|| \quad ,$$

i.e., an estimate of type (2.6) with $p = 0$ holds.

This result can be generalized considerably. We have

Theorem 5.1. Consider a system of differential equations

$$(5.5) \qquad \partial u/\partial t = \sum_{\nu=1}^{s} \left(\frac{\partial}{\partial x_\nu}\left(A_\nu \frac{\partial u}{\partial x_\nu}\right) + \frac{1}{2}\left(\frac{\partial}{\partial x_\nu}(B_\nu u) + B_\nu \frac{\partial u}{\partial x_\nu}\right)\right) + C\,u \quad .$$

Assume that either

$$(1) \qquad A_\nu + A_\nu^* \geq 0 \quad , \quad B_\nu = B_\nu^*$$

or

$$(2) \qquad A_\nu + A_\nu^* > \delta > 0 \quad .$$

Then an estimate of type (5.4) holds. In the first case $\alpha = \frac{1}{2}\max_{x,t}(C + C^*)$. In the second case

$$\alpha = \frac{1}{2}\max_{x,t}(C + C^*) + (4\delta)^{-1}\left(\max_{x,t,\nu}|B_\nu - B_\nu^*|\right)^2 \quad .$$

Proof: In the same way as for the example we get

$$\frac{\partial}{\partial t}||u(x,t)||^2 = 2\ \text{Real}\left(u,\ \frac{\partial u}{\partial t}\right) =$$

$$\text{Real}\left\{\sum_{\nu=1}^{s}\left(2\left(u,\ \frac{\partial}{\partial x_\nu}\left(A_\nu \frac{\partial u}{\partial x_\nu}\right)\right) + \left(u,\ \frac{\partial}{\partial x_\nu}(B_\nu u)\right) + \left(u,\ B_\nu \frac{\partial u}{\partial x_\nu}\right)\right) + 2(u,Cu)\right\}$$

$$= \sum_{\nu=1}^{s} -\left(\left(\frac{\partial u}{\partial x_\nu},(A_\nu + A_\nu^*)\frac{\partial u}{\partial x_\nu}\right) + \left(u,\ (B_\nu - B_\nu^*)\frac{\partial u}{\partial x_\nu}\right)\right) + (u,\ C + C^*u) \quad .$$

In the first case we get therefore

$$\frac{\partial}{\partial t}||u(x,t)||^2 \leq (u,\ (C + C^*)u) \leq 2\alpha||u(x,t)||^2$$

and the estimate follows immediately.

In the second case we observe that

$$-\left(\frac{\partial u}{\partial x_\nu}\,,\,(A_\nu + A_\nu^*)\frac{\partial u}{\partial x_\nu}\right) \le -\delta||\partial u/\partial x_\nu||^2$$

and

$$\left|\left(u,\,(B - B_\nu^*)\frac{\partial u}{\partial x_\nu}\right)\right| \le \max_{x,t}|B_\nu - B_\nu^*|\,||u||\cdot||\partial u/\partial x|| \le$$

$$\le (4\delta)^{-1}\left(\max_{x,t}|B_\nu - B_\nu^*|\right)^2||u||^2 + \delta||\partial u/\partial x_\nu||^2 \quad .$$

Therefore

$$\frac{\partial}{\partial t}||u||^2 \le \frac{1}{2}(u\,,\,(C + C^*)u) + \beta||u||^2$$

where

$$\beta = (4\delta)^{-1}\left(\max_{x,t,\nu}|B_\nu - B_\nu^*|\right)^2 .$$

This proves the theorem.

For systems of type (5.5) one can show:

Theorem 5.2. Assume that the conditions of Theorem 5.1 hold. Assume furthermore that either all $A_\nu \equiv 0$ or that the operator $P_2 u = \sum \frac{\partial}{\partial x_\nu} A_\nu \frac{\partial u}{\partial x_\nu}$ is elliptic, i.e., there is a constant $\delta > 0$ such that for all x, t, ω the eigenvalues κ of

$$\sum A_\nu(x,t)\omega_\nu^2$$

fulfill the condition

$$|\kappa| \ge \delta|\omega|^2 \quad .$$

Then the Cauchy problem is strongly well posed provided the coefficients A_ν, B_ν, C belong to C^1.

I.6. The Cauchyproblem for nonlinear equations.

Not much is known for nonlinear equations

(6.1) $\qquad \partial u/\partial t = P(x,t,u,\partial/\partial x)u \quad .$

The only general result is the following:
Assume that $u(x,t) = U(x,t) + \tilde{u}(x,t)$ where $U(x,t)$ represents a smooth known mean flow and $\tilde{u}(x,t)$ a disturbance. Linearizing (6.1) with respect to this mean flow gives us a linear system

$$\partial\tilde{u}/\partial t = P_1(x,t,U\,\partial/\partial x)\tilde{u} + F(U,x,t) .$$

Then the following theorem holds.

Theorem 6.1. Assume that U is sufficiently smooth and $F(U,x,t)$ sufficiently small. If $P_1(x,t,U,\partial/\partial x)$ fulfills the conditions of theorems 4.3 or 4.4 then 6.1 has in a given time interval $0 \le t \le T$ a smooth solution.

Though the result of this theorem is quite weak it shows anyway the importance of the linear theory.

II. Difference approximation for the Cauchyproblem.

II.1. Some simple examples.

Consider the differential equation

(1.1) $\partial u/\partial t = \partial u/\partial x$

with initial values

(1.2) $u(x,0) = e^{2\pi i\omega x}$.

Its solution is given by

(1.3) $u(x,t) = e^{2\pi i\omega(x+t)}$,

i.e. the solution is a wave which travels with speed one. We approximate (1.1) by a number of difference methods. For that reason we introduce a timestep $\Delta t > 0$ and a meshwidth $\Delta x = N^{-1}$, N natural number. Let (x_ν,t_ν), $x_\nu = \nu\Delta x$, $\nu = 0, \pm 1, \pm 2,\ldots$; $t = \mu\Delta t$, $\mu = 0,1,2,\ldots$; denote the gridpoints and define gridfunctions $v_\nu(t)$ by

(1.4) $v_\nu(t) = u(x_\nu,t), \qquad t = \mu\Delta t$.

Furthermore, the fundamental difference operators I, E, E^{-1}, D_o, D_+, D_-, D_+D_- are defined by

(1.5) $I\, v_\nu(t) = v_\nu(t)$, identity operator

(1.6) $E\, v_\nu(t) = v_{\nu+1}(t)$, $E^{-1}v_\nu(t) = v_{\nu t}(t)$ translation operator

(1.7) $2\Delta x\, D_o\, v_\nu(t) = v_{\nu+1}(t) - v_{\nu-1}(t)$ centered difference operator

(1.8) $\Delta x\, D_+\, v_\nu(t) = v_{\nu+1}(t) - v_\nu(t)$ forward difference operator

(1.9) $\Delta x\, D_-\, v_\nu(t) = v_\nu(t) - v_{\nu-1}(t)$ backward difference operator

(1.10) $(\Delta x)^2\, D_+D_-\, v_\nu(t) = \Delta x D_+(v_\nu(t)-v_{\nu-1}(t)) =$

$= v_{\nu+1}(t) - 2v_\nu(t) + v_{\nu-1}(t)$ second order centered difference operator.

Now we approximate (1.1) by one of the following formulas

(1.11) $v_\nu(t+\Delta t) = v_\nu(t) + \Delta t\, D_o\, v_\nu(t)$,

(1.12) $v_\nu(t+\Delta t) = v_\nu(t) + \Delta t\, D_o\, v_\nu(t+\Delta t)$,

(1.13) $v_\nu(t+\Delta t) = v_\nu(t-\Delta t) + 2\Delta t\, D_o\, v_\nu(t)$,

(1.14) $v_\nu(t+\Delta t) = v_\nu(t) + \Delta t\, D_o\, v_\nu(t) + \frac{\Delta t^2}{2}\, D_+D_-\, v_\nu(t)$,

(1.15) $(I - \frac{1}{2}\Delta t\, D_o)v_\nu(t+\Delta t) = (I + \frac{1}{2}\Delta t\, D_o)v_\nu(t)$.

Remark: The construction of all methods except (1.14) is obvious. (1.14) is obtained in the following way: For the solution of (1.1) we have

$$u(x,t+\Delta t) = u(x,t) + \Delta t u_t + \frac{1}{2}(\Delta t)^2 u_{tt} + \mathcal{O}((\Delta t)^3)$$

$$= u(x,t) + \Delta t u_x + \frac{1}{2}(\Delta t)^2 u_{xx} + \mathcal{O}((\Delta t)^3) =$$

$$u(x,t) + \Delta t\, D_o u(x,t) + \frac{1}{2}(\Delta t)^2 D_+ D_- u(x,t) = \mathcal{O}((\Delta t)^3 + \Delta t(\Delta x)^2) .$$

All these difference approximations can be written in the form

$$(1.16) \qquad (I - Q_1)v_\nu(t+\Delta t) = Q_o v_\nu(t) + Q_1 v_\nu(t-\Delta t) .$$

Here Q_j are operators composed of D_o, D_+, D_-. Practically all used difference methods are of this form. The truncation error is defined in the following way.

Definition 1.1. Let $u(x,t)$ by the solution of the differential equation. Then

$$(1.17) \qquad R_\nu(t) = (I - Q_{+1})u(x_\nu,t+\Delta t) - Q_o u(x_\nu,t) - Q_{-1}u(x_\nu,t-\Delta t)$$

denotes the truncation error. If

$$(1.18) \qquad |R_\nu(t)| \le M\,\Delta t((\Delta x)^r + (\Delta t)^s) ,$$

where the constant M may depend on the derivatives of u, then the method is called of order (r,s).

There is never any trouble to determine the order of a difference method. One needs only to expand the solution into a Taylorseries. For example:

$$u(x_\nu,t+\Delta t) - u(x_\nu,t) - \Delta t\, D_o u(x_\nu,t) = \Delta t(u_t - u_x) +$$

$$(\frac{\Delta t}{2})^2 u_{tt} + \frac{\Delta t(\Delta x)^2}{6} u_{xxx} + \ldots$$

Thus the method is of order (1,2). The same is true for the second method while all the others are of order (2,2).

As initial values for the above approximations we choose

$$(1.19) \qquad v_\nu(0) = e^{2\pi i\omega x_\nu} .$$

Then $v_\nu(t)$ is completely determined except the solution of (1.14). In that case we have also to specify $v_\nu(\Delta t)$. For example

$$v_\nu(\Delta t) = u(x_\nu,0) + \Delta t\, u_t(x_\nu,0) = (1+2\pi i\omega\Delta t)e^{2\pi i\omega x_\nu} .$$

The equations (1.11) - (1.15) are all equations with constant coefficients. Therefore we can solve them explicitely. The solutions are of the form

$$(1.20) \qquad v_\nu(t) = \hat{v}(t)e^{2\pi i\omega x} .$$

Here $\hat{v}(t)$ is the solution of the ordinary difference equations:

$$(1.11a) \qquad \hat{v}(t+\Delta t) = (1 + \lambda i \sin\xi)\hat{v}(t),$$

$$(1.12a) \qquad \hat{v}(t+\Delta t) = (1 + \lambda i \sin\xi)^{-1}\hat{v}(t),$$

$$(1.13a) \qquad \hat{v}(t+\Delta t) = \hat{v}(t-\Delta t) + 2\lambda i \sin\xi\, \hat{v}(t),$$

$$(1.14a) \qquad \hat{v}(t+\Delta t) = (1 + \lambda i \sin\xi - 2\sin^2\tfrac{\xi}{2})\hat{v}(t),$$

(1.15a) $$\hat{v}(t+\Delta t) = \left(1 + \tfrac{1}{2} i\lambda \sin\xi\right)/\left(1 - \tfrac{1}{2} i\lambda \sin\xi\right)\hat{v}(t),$$

with $\lambda = \Delta t/\Delta x$ and $\xi = 2\pi\omega\Delta x$. The initial values are now

(1.21) $$\hat{v}(0) = 1,$$

and in the case of (1.13a) also

(1.22) $$\hat{v}(\Delta t) = 1 + 2\pi i\omega\Delta x \quad .$$

The solution of (1.11a) is

$$\hat{v}(t) = (1 + \lambda i \sin\xi)^{t/\Delta t}\hat{v}(0) \quad .$$

For every fixed ω we have

$$\lim_{\Delta t, \Delta x \to 0} (1 + \lambda i \sin\xi)^{t/\Delta t} = e^{2\pi i\omega t} \quad .$$

Therefore the solution of the difference approximation converges to the solution of the differential equation. However, in actuell computations rounding errors always produce so called "2Δx-waves". In this case $\xi = \frac{\pi}{2}$. If we choose $\Delta t/\Delta x = \frac{1}{2}$ then

$$|\hat{v}(t)|^2 = |(1 + \lambda i \sin\xi)^{t/\Delta t}|^2 = (1 + \tfrac{1}{4})^{t/\Delta t} \; |\hat{v}(0)|^2 \; .$$

Thus

$t/\Delta t$	1	10	100	500
$\lvert v^2(t)\rvert^2/\lvert\hat{v}(0)\rvert^2$	1	9.3	$4.9\cdot10^9$	$2.6\cdot10^{48}$

and the computation is soon useless. If this happens then the method is called unstable. One can show that the method (1.11) is for fixed relations $\Delta t/\Delta x = \lambda > 0$ always unstable. For the method to be useful we must have

(1.23) $$|\hat{v}(t)| = |\hat{v}(t,\omega)| \leq K|\hat{v}(0,\omega)|$$

for all frequencies ω. Here K does not depend on ω. It is easy to see that all the other methods are stable if we add in the case of (1.13), (1.14) the restriction $\Delta t/\Delta x \leq 1$.

The methods (1.12), (1.15) are called unconditioned stable because they are stable for all $\lambda = \Delta t/\Delta x$. The other two methods are called conditional stable.

Besides stability and truncation error there are two other important concepts namely dissipation and dispersion, which we shall discuss now. Consider the difference approximation (1.12) with initial values (1.19). Its solution is given by

$$v_\nu(t) = (1 - \lambda i \sin\xi)^{-t/\Delta t} e^{2\pi i\omega x} \quad .$$

For sufficiently small ξ we have

$$1 - \lambda i \sin\xi = e^{-i\lambda\xi + \frac{1}{2}\lambda^2\xi^2 + \mathcal{O}(\xi^3)} \quad .$$

Therefore $\xi = 2\pi\omega\Delta x$ gives us

$$(1 - \lambda i \sin\xi)^{-t/\Delta t} = e^{2\pi i\omega t - (2\pi\omega)^2\lambda^{-1}\Delta x t + \mathcal{O}(\omega^3(\Delta x)^2 t)} \quad .$$

This shows that the amplitude of the numerical solution decays. The higher the frequency the faster is the decay. This is a purely numerical effect because the corresponding solution of the differential equation does not decay. Methods which have this property are called dissipative. If the amplitudes

decay like

$$e^{-\delta(2\pi\omega)^r(\Delta x)^{r-1}t} \quad , \qquad \delta = \text{const.} > 0$$

the method is said to be dissipative of order r. The method (1.12) is dissipative of order 2 while (1.14) is dissipative of order 4. (The higher the order the slower the decay).

Not all methods are dissipative. For example (1.13), (1.15) are nondissipative. We consider (1.15). In this case

$$v_\nu(t) = \left(\frac{1 - \frac{\lambda i}{2}\sin\xi}{1 + \frac{\lambda}{2} i \sin\xi}\right)^{t/\Delta t} e^{2\pi i\omega x} \quad .$$

and it is obvious that

$$\left|\frac{1 - \frac{\lambda i}{2}\sin\xi}{1 + \frac{\lambda}{2} i \sin\xi}\right| = 1$$

However, for sufficiently small ξ

$$\frac{1 + \frac{\lambda i}{2}\sin\xi}{1 - \frac{\lambda}{2} i \sin\xi} = e^{i\xi - \frac{1}{12} i\xi^3 + (\xi^5)}$$

Therefore

$$v_\nu(t) = e^{2\pi i\omega(x+dt)} \quad , \qquad d = 1 - \frac{1}{12}\lambda^{-2}(2\pi\omega\Delta x)^2 \quad ,$$

which means that the phasespeed depends on the frequency, i.e. there is dispersion. This again is a purely numerical effect because there is no dispersion for the solution of (1.1). This phase error can destroy the accuracy of sharp signals. It is then often better to make the approximation dissipative such that the waves with wrong phase speed will be damped at the same time. This can be done by changing (1.15) into

$$(I - \tfrac{1}{2}\Delta t\, D_o + \sigma_1 \Delta t(\Delta x)^3 D_+^2 D_-^2) v_\nu(t+\Delta t) = (I + \tfrac{1}{2}\Delta t\, D_o - \sigma_1 \Delta t(\Delta x)^3 D_+^2 D_-^2) v_\nu(t) \ .$$

The simplest parabolic differential equation is given by

(1.24) $$\partial u/\partial t = \partial^2 u/\partial x^2 \ .$$

If we in (1.11) - (1.15) replace D_o by D_+D_- and D_+D_- by $D_+^2D_-^2$ then we get difference approximations for (1.24). The first and the fourth method are conditional stable the second and fifth method are unconditional stable while the third method is unstable. However, we can stabilize the third method (Du Fort-Frankel) if we replace it by:

$$v_\nu(t+\Delta t) = v_\nu(t-\Delta t) + \frac{\Delta t}{\Delta x^2}(v_{\nu+1}(t) - v_\nu(t+\Delta t) - v_\nu(t-\Delta t) + v_{\nu-1}(t)) \ .$$

The above methods are the prototypes of methods commonly used in practical applications (see [1]). One uses one of the in (1.11) - (1.15) described techniques to replace the time derivatives and then replaces the space derivatives by centered differences.

The methods are then referred to as: First order explicit (1.11), Completely implicit (1.12), Leap-frog (1.13), Lax-Wendroff (1.14) and Crank-Nicolson (1.15).

II.2. Stability and convergence.

For systems (1.16) with constant coefficients the stability can be decided in the same way. One introduces the "ansatz" (1.20) into (1.16) and obtains a system of ordinary difference equation

(2.1) $$(I-\hat{Q}_1)\hat{v}(t+\Delta t) = \hat{Q}_0\hat{v}(t) + Q_{-1}\hat{v}(t-\Delta t),\ \hat{v}(t) = \hat{v}(t,\omega)$$

which can be solved explicitely. If (1.23) holds then the method is stable.

For systems with variable coefficients

(2.2) $$(I-Q_1(x,t))v_\nu(t-\Delta t) = Q_0(x,t)v_\nu(t) + Q_{-1}(x,t)v_\nu(t-\Delta t)$$

this simple test is not directly applicable. However, in the same way as for the differential equation one freezes the coefficients in (2.2) and considers all systems

(2.3) $$(I-Q_1(x_0,t_0))v_\nu(t+\Delta t) = Q_0(x_0,t_0)v_\nu(t) + Q_{-1}(x_0,t_0)v_\nu(t-\Delta t)$$

with constant coefficients, in the hope that if all systems (2.3) are stable then the same is true for the original system (2.2). Threre is a large body of theory for this (see [1]). As an example we state:

Theorem 2.1. Consider a strictly hyperbolic system of partial differential equations and approximate it by (2.2). If all systems (2.3) are dissipative then (2.2) is stable.

Theorem 2.2. Consider a parabolic system of partial differential equations and approximate it by (2.2). If all systems (2.3) are dissipative then (2.2) is stable.

Stability garantees convergence. The following theorem holds. (see [1].)

Theorem 1.1. Assume that the method is stable and that an estimate of the truncation error is given by (1.18). Then

(2.4) $$||u(x,t) - v_\nu(t)||^2 \le K^2M^2t^2 \cdot ((\Delta r)^r + (\Delta t)^3)$$

Here $||\omega_\nu||^2 = \sum_\nu |\omega_\nu|^2\ \Delta x$ denotes the discret L_2-norm.

For nonlinear equations there are two situations. 1) The solution of the differential equation is smooth. In this case we have [3].

Theorem 2.3. Consider a difference approximation to a nonlinear system of partial differential equations and assume that the solution $u(x,t)$ of the differential equations is smooth. Linearize the difference equations around $u(x,t)$ and assume that the resulting linear system is stable. Then the solution of the difference approximation converges to the solution of the differential equation and an estimate of type (2.4) holds.

2) For the other situation, namely that the solution of the differential equation is not smooth, practically no theoretical results are available. However, experience tells that if the solution of the differential equations is smooth except for shocks and contact discontinuities then there are difference approximations whose solutions converge. In this case the approximations have to be dissipative and have to be written in conservation form.

II.3. On the choice of a difference scheme.

In this chapter we want to discuss different methods of integrating the scalar equation

(3.1) $$\partial u/\partial t = -c\partial u/\partial x,\ u(x,0) = e^{2\pi iwx},$$

which has the solution

$$u(x,t) = e^{2\pi iw(x-ct)}.$$

We ignore any errors due to discretization in time, i.e., we consider the differential-difference equation

$$\frac{\partial}{\partial t} v(x,t) = - cD_o(h)v(x,t) \tag{3.2}$$

which has local truncation error $\mathcal{O}(h^2)$.

If $v(x,0) = e^{i2\pi wx}$ then (10.2) has the solution

$$v(x,t) = e^{i2\pi w(x - c_1(w)t)} \tag{3.3}$$

where

$$c_1(w) = c \frac{\sin 2\pi wh}{2\pi wh} \quad . \tag{3.4}$$

The phase error, e_1, is

$$e_1(w) = 2\pi wt(c - c_1(w)) \ . \tag{3.5}$$

A fourth order approximation is

$$\frac{\partial}{\partial t} v(x,t) = - c(\frac{4}{3} D_o(h) - \frac{1}{3} D_o(2h))v(x,t) \ . \tag{3.6}$$

If, as before, $v(x,0) = e^{i2\pi wx}$, then (3.6) has the solution

$$v(x,t) = e^{i2\pi w(x - c_2(w)t)} \tag{3.7}$$

where

$$c_2(w) = c(\frac{8 \sin 2\pi wh - \sin 4\pi wh}{12\pi wh}) \ . \tag{3.8}$$

The phase error, e_2, is

$$e_2(w) = 2\pi wt(c - c_2(w)) \ . \tag{3.9}$$

We now look for conditions such that the solutions (3.3) and (3.7) satisfy

$$e_1(w) < e \ , \tag{3.10}$$

$$e_2(w) < e \ , \tag{3.11}$$

for $0 < e_i < \frac{1}{2}$ and $0 < t < \frac{j}{wc}$. j denotes the number of periods we want to compute in time. It is easily seen from (3.4), (3.5), (3.8), and (3.9) that e_1 and e_2 are increasing functions of t. Therefore, (3.10) and (3.11) are satisfied for $0 < t < \frac{j}{wc}$ if we choose $N = (wh)^{-1}$ such that

$$e_1(w,j) = 2\pi j(1 - \frac{\sin (2\pi/N)}{2\pi/N}) = e \tag{3.12}$$

and

$$e_2(w,j) = 2\pi j(1 - \frac{8 \sin (2\pi/N) - \sin (4\pi/N)}{12\pi/N}) = e \ . \tag{3.13}$$

N denotes the number of points per wave length.

We develop the left hand sides of (3.12) and (3.13) in power series in $(2\pi/N)$ and retain only the terms of lowest order. Then we have

$$e_1(j,N_1) \sim \frac{(2\pi)^3}{6} jN_1^{-2} \tag{3.14}$$

and

$$e_2(j,N_2) \sim \frac{(2\pi)^5}{30} jN_2^{-4} \quad . \tag{3.15}$$

Consider N_1 and N_2 as functions of j. Let e be the maximum phase error allowed. Utilizing (3.14) and (3.15) we have

$$N_1(j) \sim 2\pi(2\pi/6e)^{1/2} j^{1/2} \tag{3.16}$$

and

$$N_2(j) \sim 2\pi(2\pi/30e)^{1/4} j^{1/4} \quad . \tag{3.17}$$

A similar computation for the sixth order scheme

$$v_t = -c(\tfrac{3}{2} D_o(h) - \tfrac{3}{5} D_o(2h) + \tfrac{1}{10} D_o(3h))v(t) \tag{3.18}$$

yields

$$N_2(j) \sim 2\pi(72\pi/7!e)^{1/6} j^{1/6} \quad . \tag{3.19}$$

If $e = 0.1$ then

$$N_1(j) \sim 20j^{1/2} \ ,$$

$$N_2(j) \sim 7j^{1/4} \ ,$$

$$N_3(j) \sim 5j^{1/6} \ ,$$

and if $e = 0.1$ then

$$N_1(j) \sim 64j^{1/2} \ ,$$

$$N_2(j) \sim 13j^{1/4} \ ,$$

$$N_3(j) \sim 8j^{1/6} \ .$$

Observe that the operation count of the sixth order method is approximately 3/2 times that of the fourth order method. The fourth order method has approximately twice the operation count of the second order method. The table above clearly illustrates the superiority of the fourth and sixth order schemes over the second order scheme. The superiority is much more pronounced for smaller errors. However, considering the additional effort the sixth order method requires over the fourth order method the table above illustrates that little or nothing is gained by using the sixth order scheme, as long as we allow an error of 1% and the integrations are not over extremely long time intervals, which is natural for many practical calculations. The superiority of the higher order methods is even greater when the computations are extended over long time intervals since N_1 grows like $j^{1/2}$, N_2 like $j^{1/4}$, and N_3 like $j^{1/6}$. Thus, for long integrations the sixth order method is more economical but the saving is small.

We now consider even higher order approximations to the differential operator $\partial/\partial x$. Let us now approximate the problem (3.1) by

$$\frac{\partial v}{\partial t} = -cD^{[2m]}(h)v, \quad v(x,0) = e^{i2\pi wx}$$

where

$$D^{[2m]}(h) = \sum_{\nu=1}^{m} \lambda_\nu D_o(\nu k), \quad \lambda_\nu = \frac{-2(-1)^\nu (m!)^2}{(m+\nu)!(m-\nu)!} \quad .$$

When $m = 1, 2, 3$ we have the second, fourth, and sixth order schemes discussed earlier. As before we let $N_{2m} = (wh)^{-1}$ denote the number of points per wavelength and $j = cwt$ the number of periods to be computed. In this case it can be shown, Kreiss and Oliger [3], that $N_{2m}(j) \to 2$ as $2m \to \infty$. Thus we must always have at least 2 points per wavelength.

Observe that the amount of work the above $2m$ th order method requires is approximately m times the work of the second order scheme. In light of (3.18) it is doubtful that difference methods of order greater than six have any practical advantage for practical calculations.

There is another method for increasing the order of accuracy, namely Richardson extrapolation. The basis for Richardson extrapolation is that the solution of (3.2) can be expanded in a series

$$v(x,t) = v(x,t,h) = u(x,t) + h^2 w_1(x,t) + h^4 w_2(x,t) + h^6 w_3(x,t) + \dots \tag{3.26}$$

where the $w_j(x,t)$ are the solutions of certain inhomogenous equations:

$$\partial w_j/\partial t - c\partial w_j/\partial x_j + r_j(x),\ w_j(x,0) = 0 .$$

Let us determine the w_j. Substituting (3.26) into (3.2) yields

$$\begin{aligned} &\partial u/\partial t + h^2 \partial w_1/\partial t + h^4 \partial w_2/\partial t + \dots \\ &= - c(D_o u + h^2 D_o w_1 + h^4 w_2 + \dots) . \end{aligned} \tag{3.27}$$

$$D_o u = \partial u/\partial x + \frac{h^2}{3!}\,\partial^3 u/\partial x^3 + \frac{h^4}{5!}\,\partial^5 u/\partial x^5 + \dots$$

and the corresponding expansions hold for the $w_j(x,t)$. Introducing these expressions into (3.27) gives us, after collecting terms in powers of h,

$$\begin{aligned} \frac{\partial w_1}{\partial t} &= - c\,\frac{\partial w_1}{\partial x} - \frac{c}{3!}\,\partial^3 u/\partial x^3, \\ \frac{\partial w_2}{\partial t} &= - c\,\frac{\partial w_2}{\partial x} - \frac{c}{5!}\,\partial^5 u/\partial x^5 - \frac{c}{3!}\,\partial^3 w_1/\partial x^3, \\ \frac{\partial w_3}{\partial t} &= - c\,\frac{\partial w_3}{\partial x} - \frac{c}{7!}\,\partial^7 u/\partial x^7 - \frac{c}{5!}\,\partial^5 w_1/\partial x^5 - \frac{c}{3!}\,\partial^3 w_2/\partial x^3 \\ &\ \ \vdots \end{aligned}$$

$u = e^{2\pi i\omega(x - ct)}$ and therefore w_1 is the solution of

$$\partial w_1/\partial t = - c\,\frac{\partial w_1}{\partial x} - \frac{c(2\pi i\omega)^3}{3!}\,e^{2\pi i\omega(x - ct)} ,$$

$$w_1(x,0) = 0,$$

i.e.,

$$w_1(x,t) = - \frac{c(2\pi i\omega)^3}{3!}\,t \cdot e^{2\pi i\omega(x - ct)} .$$

Correspondingly we get

$$w_2(x,t) = \frac{c}{5!}\,(2\pi i\omega)^5 \cdot t \cdot e^{2\pi i\omega(x - ct)} + \frac{(2\pi i\omega)^6}{3! \cdot 3! \cdot 2}\,c^2\,t^2\,e^{2\pi i\omega(x - ct)}$$

$$w_3(x,t) = \left(- \frac{c}{7!}\,(2\pi i\omega)^7\,t + \frac{c^2(2\pi i\omega)^8}{3! \cdot 5!}\,t^2 - \frac{c^3(2\pi i\omega)^9}{3! \cdot 3! \cdot 3! \cdot 3!}\,t^3\right) e^{2\pi i\omega(x - ct)}$$

$$\ \ \vdots$$

Let us compute $v(x,t) = v(x,t,h)$ for a specific h_0 and then also for $2h_0$. We get

$$v(x,t,2h_0) = u(x,t) + 4h_0^2 w_1(x,t) + 16h_0^4 w_2(x,t) + \dots$$

and therefore,

$$u(x,t) = \frac{1}{3}\left(4v(x,t,h_0) - v(x,t,2h_0)\right) + 4h_0^4 w_2(x,t) + \ldots .$$

Thus, if we neglect higher order terms, we have after j periods in time

$$\left|u(x,t) - \frac{1}{3}\left(4v(x,t,h_0) - v(x,t,2h_0)\right)\right| \approx 4h^4 |w_2(x,t)| \approx 4\left(\frac{2\pi}{4}\right)^4 \cdot \frac{(2\pi)^2 \cdot j^2}{48} ,$$

where N is defined as before. Corresponding to equation (3.17) we have

$$N = 2\pi \cdot (2\pi)^{1/2} \cdot (1/12e)^{1/4} \cdot j^{1/2} = \begin{cases} 15j^{1/2} & \text{for } e = 0.1 \\ 26.8\, j^{1/2} & \text{for } e = 0.01 . \end{cases}$$

Thus the improvement over the original leap-frog method (see equation (3.16)) is not so impressive for the 10% error limit but is substantial for the 1% error limit. In any case, the fourth order method (3.18) is better.

One can of course also compute $v(x,t,h)$ for $h = 3h_0$. Then we can also eliminate the h^4 term in (3.26) and obtain

$$N = \begin{cases} 12.9j^{1/2} & \text{for a 10\% error} \\ 19.0j^{1/2} & \text{for a 1\% error} \end{cases}$$

Thus not much is gained. The fourth order method (3.18) is again better.

References:

1. Richtmyer, R.D. and Morton, K.W., Difference methods for initial value problems. Interscience publisher 1967.

2. Strang, G., Accurate partial difference methods II, nonlinear problems, Numerische Mathematik, vol 6, p. 37.

3. Kreiss, H.O. and Oliger, J., Comparison of accurate methods for the integration of hyperbolic equations, Tellus, Vol. 24, p. 199.

III. Initial boundary value problems for hyperbolic partial differential equations.

III.1. Differential equations in one space dimension.

The simples hyperbolic differential equation is given by

(1.1) $\partial u/\partial t = c\, \partial u/\partial x,$

where c is a constant. Its general solution is

$$u(x,t) = F(x+ct),$$

i.e., it is constant along the "characteristic lines" $x + ct = \text{const.}$ (see fig. 1.). Therefore, if we want to determine

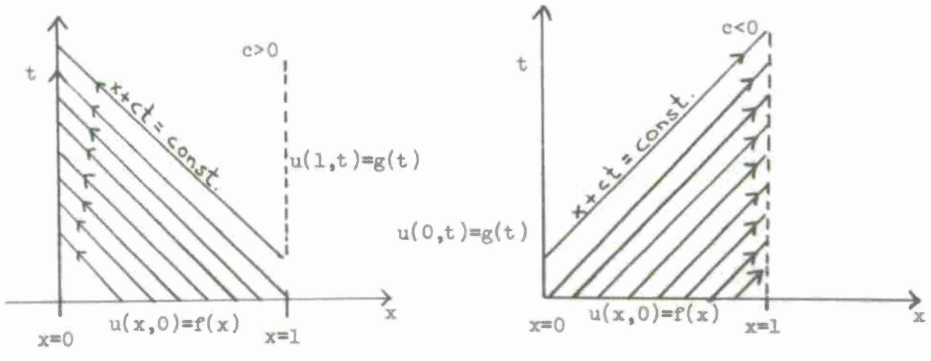

fig. 1.

the solution of (1.1) in the region $0 \le x \le 1$, $t \ge 0$ we have to describe initial conditions

(1.2) $u(x,0) = f(x)$,

for $t = 0$ and boundary conditions

(1.3) $u(1,t) = g(t)$ if $c > 0$ or $u(0,t) = g$ if $c < 0$,

for $x = 1,0$ respectively.

There is no difficulty to generalize the above results to systems

(1.4) $\partial u/\partial t = A\, \partial u/\partial x$

Here $u(x,t) = (u^{(1)}(x,t),\ldots,u^{(n)}(x,t))'$ denotes a vector function and A a constant $n\times n$ matrix. Hyperbolicity implies that A can be transformed to real diagonal form, i.e., there is a nonsingular transformation S such that

$$(1.5) \qquad S\,A\,S^{-1} = \begin{pmatrix} A^{I} & 0 \\ 0 & A^{II} \end{pmatrix} = \tilde{A}$$

where

$$A^{I} = \begin{pmatrix} a_1 & 0 & \ldots & 0 \\ 0 & a_2 & \ldots & 0 \\ \ldots & \ldots & \ldots & \ldots \\ 0 & \ldots & 0 & a_r \end{pmatrix} < 0, \quad A^{II} = \begin{pmatrix} a_{r+1} & 0 & \ldots & 0 \\ 0 & a_{r+2} & \ldots & 0 \\ \ldots & \ldots & \ldots & \ldots \\ 0 & \ldots & 0 & a_n \end{pmatrix} > 0$$

are definite diagonal matrices. We can thus introduce new variables

(1.6) $\quad v = Su$

and get

(1.7) $\quad \partial v/\partial t = \tilde{A}\, \partial v/\partial x$.

The last equation can also be written in partitioned form

(1.8) $\quad \partial v^{I}/\partial t = A^{I}\, \partial v^{I}/\partial x, \quad \partial v^{II}/\partial t = A^{II} \partial v^{II}/\partial x,$

where $v^{I} = (v^{(1)},\ldots,v^{(r)})'$, $v^{II} = (v^{(r+1)},\ldots,v^{(n)})'$. (1.5) represents n scalar equations. Therefore we can write down its general solution:

(1.9) $\quad v^{(j)}(x,t) = v^{(j)}(x+a_j t), \quad j = 1,2,\ldots,n,$

which are constant along the characteristic lines $x + a_j t = \text{const.}$. The solution is uniquely determined in the domain $0 \le x \le 1$, $t \ge 0$ and can be computed explicitely if we specify initial conditions

(1.10) $\quad v(x,0) = f(x), \quad 0 \le x \le 1,$

and boundary conditions

(1.11) $\quad v^{II}(0,t) = R_0 v^{II}(0,t) + g_0(t), \; v^{II}(1,t) = R_1 v^{II}(1,t) + g_1(t)$.

Here R_0, R_1 are rectangular matrices and g_0, g_1 are given vector functions. If we consider wave propagation, then the boundary conditions describe how the waves are reflected at the boundary.

Nothing essentially is changed if $A = A(x,t)$ and $R_j = R_j(t)$ are functions of x, t. Now the characteristics are not straight lines but the solutions of the ordinary differential equations

$$dx/dt = a_j(x,t) .$$

More general systems

(1.12) $\quad \partial v/\partial t = \tilde{A}(x,t)\, \partial v/\partial x + B(x,t)v + F(x,t)$,

can be solved by the iteration

(1.13) $\quad \partial v^{[n+1]}/\partial t = \tilde{A}(x,t)\partial v^{[n+1]}/\partial x + F^{[n]}$

where

$$F^{[n]} = B(x,t)v^{[n]} + F \quad .$$

Furthermore, it is no restriction to assume that $\tilde{A}$ has diagonal form. If not, we can, by a change of dependent variables, achieve the form (1.10).

We can therefore develop a rather complete theory for initial boundary value problems by using characteristics. This has of course been known for a long time. The only trouble is, that this theory cannot be easily generalized to problems in more than one space dimension. For difference approximations it is already inadequate in one space dimension.

III.2. The energymethod.

The main tool for proving the existence of solutions in more than one space dimension consists of "a priori estimates". Once these estimates have been established the existence and uniqueness of solutions follow by standard functional analytic arguments. The estimate are of the following type.

Consider a system of partial differential equations

(2.1) $\partial u/\partial t = P(x,t, \partial/\partial x)u$

in a domain Ω with initial conditions

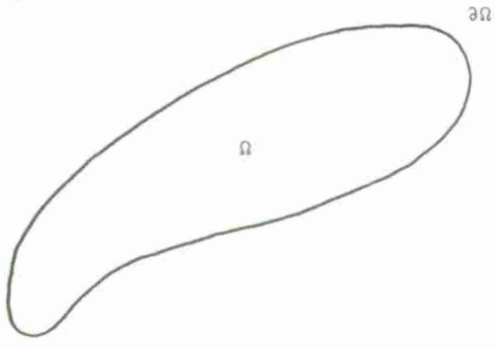

(2.2) $u(x,t_1) = f(x)$

at some time $t = t_1$, and boundary conditions

(2.3) $R(x,t)u = 0$

on $\partial\Omega$. The problem is called weakly well posed if

$$(2.4) \qquad ||u(x,t_2)||_\Omega \leq Ke^{\alpha(t_2-t_1)}||u(x,t_2)||_{\Omega,p}$$

Here $||\cdot||_\Omega$ denotes the usual L_2-norm over Ω and $||\cdot||_{\Omega,p}$ the L_2-norm which also contains all space derivatives up to order p. If $p = 0$ then we call the problem strongly well posed.

There is a large class of problems for which the estimate (2.4) is immediate. This is the class of problems for which P is semibounded, i.e., for every fixed t and all sufficiently smooth w which fulfill the boundary conditions we have

$$(2.5) \qquad (w,Pw) + (Pw,w)_\Omega \leq 2\alpha||w||_\Omega^2 \ .$$

Here α is some constant, independent of w. (2.5) implies for all sufficiently smooth solutions:

$$\frac{\partial}{\partial t}||u||_\Omega^2 = (\partial u,\partial t,u)_\Omega + (u.\ \partial u/\partial t)_\Omega = (Pu,u)_\Omega +$$

$$+ (u,Pu)_\Omega \leq 2\alpha||u||_\Omega^2 \ .$$

Therefore

$$||u(x,t_2)||_\Omega \leq e^{\alpha(t_2-t_1)}||u(x,t_2)||_\Omega \ .$$

For symmetric hyperbolic systems this theory has been developed by K.O. Friedrichs [3] . As an example consider a first order system

$$(2.6) \qquad \partial u/\partial t = A\partial u/\partial x_1 + \sum_{j=2}^{m} B_j \partial u/\partial x_j = P(\partial/\partial x)u$$

with constant coefficients for $t \geq 0$ and $x \in \Omega$. Here Ω denotes the halfspace $0 \leq x_1 < \infty$, $-\infty < x_j < \infty$, $j=2,\ldots,m$. Furthermore A has the diagonalform (1.5) and the B_j are symmetric matrices.

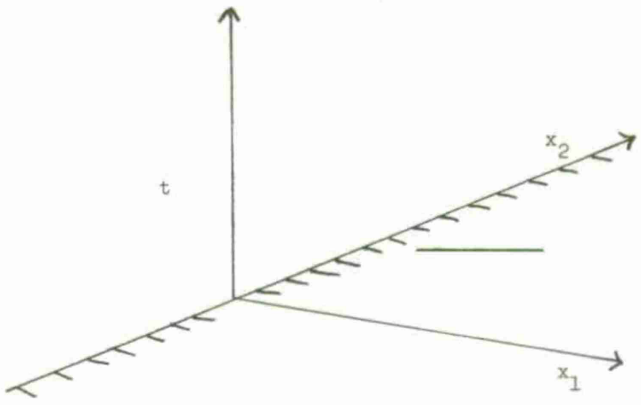

fig. 2.

For $t = 0$ initial values

(2.7) $\quad u(x,0) = f(x), \quad ||f||_\Omega < \infty$,

and for $x_1 = 0$ boundary conditions

(2.8) $\quad u^I(0,x_-,t) = R_0\, u^{II}(0,x_-,t), \; x_- = (x_2,\dots,x_m)$

are given.

Partial integration gives for all sufficiently smooth $w \in L_2(\Omega)$, which fulfill the boundary conditions

$$(w,Pw)_\Omega + (Pw,w)_\Omega = -\int_{\partial\Omega} w^* Aw/_{x_1=0}\, dx_- =$$

$$= -\int_{\partial\Omega} (w^{II})^*(A^{II} + R_0^* A^I R_0) w^{II}/_{x_1=0}\, dx_- \,.$$

Therefore the operator P is semibounded if R_0 is such that

$$A^{II} + R_0^* A^I R_0 \geq 0$$

This is for example the case if $|R_0|$ is sufficiently small. The disadvantage of the energy method is that is a trick. When it works it is the most simple method to derive existence theorems. But it does not give necessary and sufficient conditions. We shall now discuss another technique based on the Laplace transform which gives necessary and sufficient conditions.

III.3. Laplace transform.

We consider again the problem (2.6) - (2.8) and assume now that the system is either symmetric or strictly hyperbolic, i.e., the matrices A and B_j are symmetric or the eigenvalues of the symbol

$$P(i\omega) = i(A\omega_1 + \sum_{j=2}^{m} \omega_j B_j), \quad \omega_\nu \text{ real}, \quad \sum|\omega_\nu|^2 \neq 0$$

are all distinct and purely imaginary. Furthermore the matrix A has the form (1.5) which is obviously no restriction.

In one space dimension the initial boundary value problem is always well posed. This is not true in higher dimension. Already S. Agmon [2] has observed

Lemma 3.1. Assume that the problem (2.6) - (2.8) has a solution of the form

$$w(x,t) = e^{st+i<\omega_- x_->}\phi(x),\ <\omega_-,x_-> = \sum_{j=2}^{m} \omega_j x_j,\quad \omega_j \text{ real}$$

where

$$||\phi(x_1)||^2 = \int_0^\infty |\phi|^2\, dx_1 < \infty \quad .$$

Then the problem is ill posed.

Proof: If $w(x,t)$ is a solution then the same is true for

$$w_\tau(x,t) = e^{\tau(st+i<\omega_-,x_->)}\ \phi(\tau x_1)$$

for all real numbers $\tau > 0$. Thus there are solutions which grow arbitrarily fast with time.

We shall now derive algebraic conditions such that there are solutions of the above form. Introducing (3.1) into (2.1) gives us

Lemma 3.2. There is a solution of type (3.1) if and only if the eigenvalue problem

$$(3.1)\qquad s\phi = Ad\phi/dx_1 + i\,B(\omega_-)\phi\ ,\ B(\omega_-) = \sum B_j\omega_j$$

$$||\phi|| < \infty\ ,\qquad \phi^I(0) = R_0\,\phi^{II}(0)$$

has an eigenvalue with Real $s > 0$.

(3.1) is a system of ordinary differential equations which can also be written in the form

$$(3.2)\qquad d\phi/dx_1 = M\phi\ ,\quad M = A^{-1}(s-i\,B(\omega_-))\ .$$

For M we have

Lemma 3.3. For real $s > 0$ the matrix M has no eigenvalues κ with Real $\kappa = 0$. The number of eigenvalues with real $\kappa < 0$ is equal to r the number of boundary conditions.

Therefore the general solutions of (3.1) belonging to L_2 can be written as

$$(3.3)\qquad \sum_{j=1}^{r} \lambda_j\ \phi_j(x)\ .$$

Introducing (3.4) into the boundary conditions gives us a system of linear equations

$$C(s)\lambda = 0\quad ,\quad \lambda = (\lambda_1,\ldots,\lambda_r)'\ .$$

Thus we can express our results also in the following form:

Lemma 3.4. The problem (2.6) - (2.8) is not well posed if Det $|C(s)| = 0$ for some s with real $s > 0$. The main result of this section is (see [7] , [14] , [13]).

Theorem 3.1. Assume that Det $|C(s)| \neq 0$ for Real ≥ 0 then the problem is strongly well posed.

There is still the boundary case that Det $|C(s)| = 0$ for some $s = i\xi$, ξ real. As R. Hersch [5] has shown these are weakly well posed problems. The main trouble is that the generalization of these boundary cases to variable coefficients is very difficult.

III.4. Problems with variable coefficients in general domains.

Now we consider systems (2.6) - (2.8) with variable coefficients in a general domain $\Omega \times (0 \leq t \leq T)$

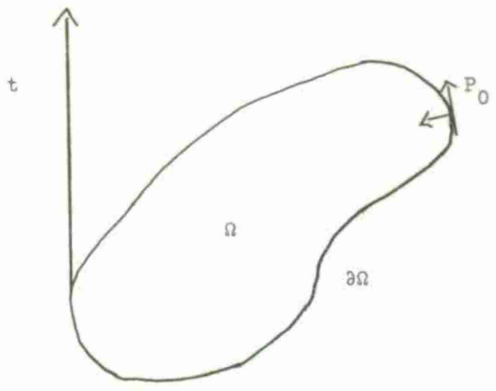

Here we assume that the coefficients and the boundary $\partial\Omega$ are sufficiently smooth. Connected with this problem there is a set of halfplan problems which we get in the following way: Let $P_0 = (x_0,t_0) \in \partial\Omega \times (0 \le t \le T)$ be a boundary point and let $\tilde{x} = S(x)$, $\tilde{t} = t - t_0$ with $S(x_0) = 0$ be a smooth transformation which locally transforms the boundary into the halfplan $\tilde{x}_1 = 0$. Apply this transformation to the differential equations and the boundary conditions, freeze the coefficients at $\tilde{x} = \tilde{t} = 0$ and consider the halfplan problem with constant coefficients. Then we have

Theorem 4.1. Assume that for all these halfplan problems the conditions of section 2 hold, i.e., that all the operators connected with the halfplan problems are semibounded. Then the original problem is strongly well posed. (see [3].)

Theorem 4.2. If the system (2.6) is strictly hyperbolic and if for all the halfplan problems with frozen coefficients the determinant condition of theorem 3.1 is fulfilled then the original problem is strongly well posed. (see [7], [14], [13].)

Remarks. 1) It is not known whether the determinant condition garantees wellposedness for symmetric systems which are not strictly hyperbolic. This is a rather disturbing gap in the theory.

2) Quite a lot of progress has been made for the boundary case that $\text{Det } |C(s)| = 0$ for some $s = i\xi$, ξ real. The key is to consider not only the halfplan problem for $\partial u/\partial t = Pu$ but also all perturbed problems $\partial u/\partial t = Pu + Bu$ where B is a constant matrix.

3) It is assumed that A is nonsingular. However, progress has been made also for the singular case. (see [12].)

4) If the boundary is not smooth then new serious problems arise. See for example [10], [11].

III.5. Difference approximations in one space dimension.

We start with an example which explains most of our difficulties. Consider the differential equation

(5.1) $\qquad \partial u/\partial t = \partial u/\partial x$

in the quarter plane $x \ge 0$, $t \ge 0$ with initial values

(5.2) $\qquad u(x,0) = f(x)$.

From section 1 we know that no boundary conditions need to be specified for $x = 0$, $t \ge 0$. We want to solve the above problem using the leap-frog scheme. For that reason we introduce a time step $\Delta t > 0$ and a mesh with $\Delta x > 0$ and divide the x-axis into intervals of length Δx. Using the notation

$$v_\nu(t) = v(x_\nu,t), \quad x_\nu = \nu\Delta x, \quad t = t_\mu = \mu\Delta t ,$$

we approximate (5.1), (5.2) by

$$v_\nu(t+\Delta t) = v_\nu(t-\Delta t) + 2\Delta t\, D_0\, v_\nu(t), \quad \nu = 1,2,... \tag{5.3}$$

with initial values

$$v_\nu(0) = f(x_\nu), \quad v_\nu(\Delta t) = f(x_\nu) + \Delta t\ f(x_\nu)/\partial x \ . \tag{5.4}$$

Here

$$D_0 v_\nu = (v_{\nu+1} - v_{\nu-1})/2\Delta x$$

denotes the usual centered difference operator. We assume that (5.3) is stable for the Cauchy-probelm, i.e., $0 < \Delta t/\Delta x \leq 1$.

It is obvious that the solution of (5.3), (5.4) is not yet uniquely determined. We must give an additional equation for v_0. For example

$$v_0 = 0 \ . \tag{5.5}$$

This relation is obviously not consistent. In general it will destroy the convergence. Let $f(x) \equiv 1$. Then $u(x,t) \equiv 0$ and

$$v_\nu(t) = 1 + (-1)^\nu\, y_\nu(t) \ ,$$

where $y_\nu(t)$ is the solution of

$$\begin{aligned} &y_\nu(t+\Delta t) = y_\nu(t-\Delta t) - 2\Delta t\, D_0\, y_\nu(t), \quad \nu = 1,2,... \\ &y_\nu(0) = y_\nu(\Delta t) = 0 \ , \end{aligned} \tag{5.6}$$

with boundary conditions

$$y_0(t) = -1 \ . \tag{5.7}$$

(5.6) and (5.7) is an approximation to the problem

$$\partial w/\partial t = -\partial w/\partial x \ ,$$

$$w(x,0) = 0, \quad w(0,t) = -1 \ ,$$

i.e.

$$w(x,t) = \begin{cases} 0 & \text{for } t < x \\ -1 & \text{for } t \geq x \ . \end{cases}$$

Therefore

$$v_\nu(t) \sim \begin{cases} 1 & \text{for } t < x. \\ 1 - (-1)^\nu & \text{for } t \geq x. \end{cases}$$

This behaviour is typical for all nondissipative centered schemes. Therefore one needs to be very careful when overspecifying boundary conditions. The oscillation decays if the approximation is dissipative. However, near the boundary the error is as bad and, for systems, it can be propergated into the interior via the ingoing characteristics.

Now we replace (5.5) by an extrapolation rule

$$v_0(t) - 2v_1(t) + v_2(t) = 0. \tag{5.8}$$

which is the same as using for $\nu = 1$ the one-sided difference formula

$$(5.9) \qquad v_1(t+\Delta t) = v_1(t-\Delta t) + \frac{2\Delta t}{\Delta x}\,(v_2(t) - v_1(t)) \quad .$$

The approximation is only useful if it is stable. If we choose

$$v_\nu(0) = \begin{cases} 1 & \text{for} \quad \nu = 0 \\ 0 & \text{for} \quad \nu > 0 \end{cases}, \quad v_\nu(\Delta t) \equiv 0 \quad \text{for all } \nu$$

as initial values then an easy calculation shows that

$$||v(t)||_{\Delta x} = \text{const.}\ (t/\Delta t), \quad ||v||_{\Delta x} = \sum |v|^2 \ \Delta x \ .$$

This growth rate is the worst possible and one might consider the approximation to be useful. However, if we consider (5.1) in a finite interval $0 \le x \le 1$ and add the boundary condition

$$(5.10) \qquad u(1,t) = v_N(t) = 0 \qquad N\Delta x = 1$$

for both the differential equation and the difference approximation, then there are solutions which grow like

$$(5.11) \qquad ||v(t)||_{\Delta x} = \text{const.}\ (t/\Delta t)^t \ ,$$

which is not tolerable. This behviour can be explained as follows: At the boundary $x = 0$ a wave is created which grows like $t/\Delta t$. This wave is reflected at the boundary $x = 1$ and is increased by another factor $t/\Delta t$ when it hits the boundary $x = 0$ again, and so on.

All these difficulties can be avoided by using, instead of (5.9), the onesided approximation

$$v_1(t+\Delta t) = v_1(t) + \frac{\Delta t}{\Delta x}\,(v_2(t) - v_1(t))$$

or

$$v_1(t+\Delta t) = v_1(t-\Delta t) + \frac{\Delta t}{\Delta x}\,(v_2(t) - \tfrac{1}{2}(v_1(t+\Delta t) + v_1(t-\Delta t)))$$

One can also keep (5.8) if one replaces the leap-frog scheme by the Lax-Wendroff approximation or any other dissipative approximation.

Let us discuss the general theory. (For details see [4], [7], [8]). We consider general difference approximations

$$(5.12) \qquad v_{\nu+1}(t+\Delta t) = Q\, v_\nu(t)$$

with boundary conditions

$$(5.13) \qquad Bv_0 = 0$$

such that the solution is uniquely determined by the initial values

$$v_\nu(0) = f_\nu \quad .$$

The approximation is useful only if it is

1) consistent, i.e. it converges formally to the continuous problem

2) stable (weakly or strongly) which is the difference analog of wellposedness.

There is never any problem to derive consistent approximations. It is the stability which causes the problem. Corresponding to the continuous problem there are two methods to decide whether a given method is stable: Laplace transform and energy method.

The theory based on Laplace transform is analog to the theory for the continuous case. The stability

is determined by the properties of the eigenvalue problem

$$(5.14)\qquad (z - Q)\phi_\nu = 0,\quad B\ \phi_0 = 0,\quad ||\phi||_{\Delta x}^2 = \sum|\phi_\nu|^2\ \Delta x < \infty\ .$$

Corresponding to lemma 3.2 we have under reasonable assumptions for Q.

Lemma 5.1. Assume that (5.14) has an eigenvalue $z = z_0$ with $|z_0| > 1$. Then the approximation is not stable.

This condition can also be expressed as a determined condition

$$\text{Det}\ |C(z_0)| = 0 \quad \text{for some}\quad z = z_0 \quad \text{with}\quad |z_0| > 1\ .$$

Then, corresponding to theorem 3.1, we have

Theorem 5.1. The approximation is strongly stable if $\text{Det}\ |C(z)| \neq 0$ for $|z| \geq 1$.

Now we turn to the energy-method. Consider again the differential equation (5.1), (5.2). The problem is well posed because there is an energy equality

$$(5.15)\qquad (u,\ \partial u/\partial x) + (\partial u/\partial x,\ u) = -\ |u(0)|^2\ .$$

Therefore we want to construct approximations to $\partial/\partial x$ which have the corresponding property.

We define a discrete norm

$$(5.16)\qquad (u,v)_{\Delta x} = \tilde{u}^* A \tilde{v}\ \Delta x + \sum_{\nu=r}^{\infty} u_\nu^*\, v_\nu\ \Delta x.$$

Here $\tilde{u} = (u_0,\ldots,u_{r-1})'$, $\tilde{v} = (v_0,\ldots,v_{r-1})'$ denote the first r components of u,v and $A = A^*$ is a positive definite $r\times r$-matrix. In [9] we have shown that one can construct accurate approximations Q for which (5.16) hold. The main trouble is that the norm and the approximation near the boundary are very complicated. This makes its generalisation to approximations in more than one space dimension on general domains difficult. Furthermore, it is not known how to include dissipation in the construction. However, it should be pointed out that this construction also works in more than one space dimension provided the net follows the boundary.

III.6. Difference approximations in more than one space dimension.

Nothing essentially new needs to be added to derive the theory of difference approximations for halfplanes because Fourier transforming the tangential variabels x_- gives us a set of one dimensional problems. The situation becomes much more complicated if we consider general domains with smooth boundaries. Observe, that this is not the case for the differential equations because we can always introduce a local coordinate system, thus reducing the problem to a set of halfplane problems. This is not possible for difference approximations. Once we have picked the net everything is fixed. D. Schäeffer [15] has tried to handle this situation and has developed a beautiful theory.

However, its practical importance is somewhat doubtful. Let us consider a very simple example. We want to solve the differential equation

$$(6.1)\qquad \partial u/\partial t = -\partial u/\partial x$$

in the two dimensional domains $2y - x \leq 0$. The initial values are

$$(6.2)\qquad u(x,y,0) = f(x,y)\quad \text{for}\quad 2y - x \leq 0,\ t = 0,$$

and the boundary conditions are given by

$$(6.3)\qquad u(x,y,t) = g(x,y,t),\quad \text{for}\ \ 2y - x = 0,\ \ t \geq 0\ .$$

We introduce gridpoints by $x_j = j\Delta x$, $y_i = i\Delta y$, $\Delta x = \Delta y$.

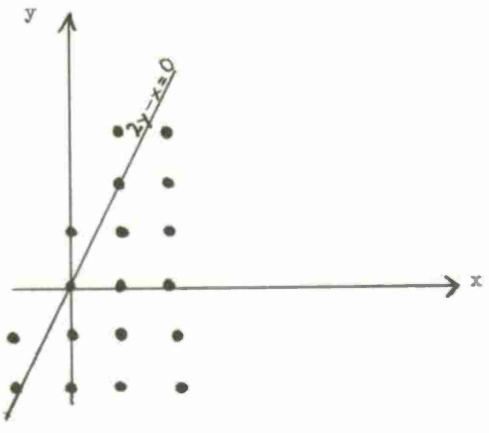

fig. 3.

Thus, there is a gridpoint on the boundary only on every second row. Now we approximate (6.1) by the Leapfrog scheme and the boundary conditions by

$$v_{i,j} = g_{i,j} \quad \text{if} \quad 2j=i \; ; \quad v_{i,j} + v_{i+1,j} = 2g_{i+\frac{1}{2},j}, \quad \text{if} \quad 2j=i+1.$$

Here $v_{i,j} = v(i\Delta x), j\Delta y, t)$. Therefore we get two different solutions on two different meshes. As long as the solution of the differential equation is smooth the solutions of the difference equation on these different meshes fit together. However, if for example $f \equiv 0$ and $g \equiv 1$ then the solution of the differential equation is a discontinuous wave propagating into the interior. Now the solutions of the difference approximation on the different nets do not fit together.

We get osciallations in the tangential direction of the wave. There are two possible methods for remedying the situation. 1) Add dissipation to smooth out the tangential oscillations. 2) Introduce curved meshes which follow the boundary. The second procedure is much more accurate and should be prefered if possible. A lot of progress has been made in this direction. See for example [1].

References:

1. Amsden, A.A. and Hirt, C.W., A simple scheme for generating general curvilinear grids. Journal of Computational physics, Vol. II, Nr. 3. 1973.

2. Agmon, S., Problème mixte pour les équations hyperboliques d'ordre supérieur, Colloque CNRS, Paris (1962), p. 13 - 18.

3. Friedrichs, K.O., Symmetric hyperbolic linear differential equations, Comm. Pure and Appl. Math. Vol. 7, (1954), pp. 345 - 392.

4. Gustafsson, B., Kreiss H.O. and Sundström, A., Stability theory for difference approximations of mixed initial boundary value problems II, Math. Comp. vol. 26, 1972.

5. Hersh, R., Mixed problems in several variables, J. Math. Mech 12 (1963), pp. 317 - 334.

6. Kreiss, H.-O., Initial boundary value problems for hyperbolic systems, Comm. Pure. Appl. Math., vol 23, 1970, 277 - 298.

7. Kreiss, H.-O., Stability theory for difference approximations of mixed initial boundary value problems I, Math. Comp. vol. 22, 1968.

8. Kreiss, H.-O., Difference approximations for initial boundary value problems. Proc. Roy. Soc. Lond. A 323, 1971.

9. Kreiss, H.-O. and Scherer, G., Difference and finite element methods for initial boundary value problems; to appear.

10. Osher, S., Initial boundary value problems for hyperbolic systems in regions with corners I, A.M.S. Trans. (to appear).

11. Osher, S., Initial boundary value problems for hyperbolic systems in regions with corners II, Report, Department of Comp. Sciences, Uppsala University, Sweden, 1973.

12. Osher, S., to appear.

13. Rauch, J., L_2 is a continuable initial condition for Kreiss' mixed problems. Comm. Pure Appl. Math. vol 25 (1972), pp. 265 - 285.

14. Sakamoto, R., Mixed problem for hyperbolic equations I and II., J. Math., Kyoto Univ., vol. 10, 1970, pp. 349 - 473 and 403 - 417.

15. Schäeffer, D.G., An application of von Neumann algebras to finite difference equations. Ann. of Math. (2) 95 (1972), pp. 117 - 129.

STABILITY AND ACCURACY OF NUMERICAL APPROXIMATIONS TO TIME DEPENDENT FLOWS

by
K.W. Morton
Professor of Applied Mathematics
Department of Mathematics
University of Reading
Whiteknights, Reading RG6 2AX, England

ABSTRACT

The basic Lax-Richtmyer theory of the stability and convergence of linear difference schemes is by now well established and widely known. We discuss here some of the more demanding requirements met in practical fluid flow calculations, including the control of non-linear instabilities, dissipation and dispersion; the modelling of conservation properties and the implementation of boundary conditions are also considered. The use of the modified equation approach is studied as an alternative to the Lax-Richtmyer theory. Finally, an error analysis for finite element methods is given showing the high accuracy that may sometimes be achieved with the correct treatment of non-linear terms.

NOTATION

Each notation is defined in the text where it first occurs but for convenience the more frequently used symbols are gathered here.

Δx, Δt, mesh lengths in x, t; $\lambda = \Delta t/\Delta x$

U_j^n, the value of U at $x = j\Delta x$, $t = n\Delta t$

$\delta U_j = U_{j+\frac12} - U_{j-\frac12}$ $\quad \mu U_j \equiv \overline{U}_j = \frac12(U_{j+\frac12} + U_{j-\frac12})$

$\Delta_o U_j = \frac12(U_{j+1} - U_{j-1})$ $\quad \Delta_o \equiv \mu\delta$

$\langle \underline{u}, \underline{v}\rangle = \int \underline{u}.\underline{v}\, dV$ or $\sum_{(j)} \Delta V\, \underline{u}_j.\underline{v}_j$, vector or scalar, any dimensionality

$||\underline{u}||^2 = \langle \underline{u}, \underline{u}\rangle$

k, wave number of fourier mode

$\hat{u}$, $\hat{P}$, fourier transforms of variable u, operator P; $(\widehat{Pu}) = \hat{P}\hat{u}$

κ, an eigenvalue of the amplification matrix of a difference scheme

$S = \sin k\Delta x$, $C = \cos k\Delta x$, $s = \sin \frac12 k\Delta x$, $c = \cos \frac12 k\Delta x$

1. LAX-RICHTMYER STABILITY THEORY

The equations of fluid flow for the vector of unknowns $\underline{w}(\underline{r}, t)$ may be written in the general form

$$\underline{w}_t + \underline{P}(\underline{w}) = 0, \qquad \underline{w}(\underline{r}, 0) \text{ given}, \tag{1}$$

where the subscript t denotes partial differentiation and $\underline{P}$ is a non-linear differential operator in the spatial variables $\underline{r}$. A general two-level finite difference scheme may be written similarly as

$$\underline{W}^{n+1} + \Delta t \underline{P}_1(\underline{W}^{n+1}) = \underline{W}^n - \Delta t \underline{P}_o(\underline{W}^n), \qquad \underline{W}^o \text{ given}, \tag{2}$$

where $\underline{W}^n$ is to approximate $\underline{w}$ at $t = n\Delta t$ and $\underline{P}_o$, $\underline{P}_1$ are difference operators whose sum is to approximate $\underline{P}$. It is well-known that for $\underline{W}^n$ to converge to $\underline{w}$ at $n\Delta t$ as the t and $\underline{r}$ meshes are refined it is necessary not only that $\underline{P}_1 + \underline{P}_o$ be consistent with $\underline{P}$ but also that the difference scheme (2) be stable.

For linear problems, the relationship between these three concepts is made precise by the Lax Equivalence Theorem (see Lax and Richtmyer [1], Richtmyer and Morton [2]) which states succinctly

consistency + stability <=> convergence.

Here consistency is defined in terms of the truncation error, T.E., obtained from applying the difference scheme to the solution of the differential problem; with proper normalisation,

$$\text{T.E.} = \frac{\underline{w}^{n+1} - \underline{w}^n}{\Delta t} + \underline{P}_1(\underline{w}^{n+1}) + \underline{P}_o(\underline{w}^n). \tag{3}$$

The scheme (2) is said to be consistent with the equation (1) if T.E. $\to 0$ under the mesh

refinement. For a linear scheme, which we signify by removing the brackets from the argument of $\underline{P}$, stability is defined as the existence of a constant K, for which

$$||\underline{W}^n|| = ||[(I + \Delta t P_1)^{-1}(I - \Delta t P_o)]^n \underline{W}^o|| \leq K||\underline{W}^o||, \qquad n\Delta t \leq 1, \quad (4)$$

the relation to hold uniformly under the mesh refinement: the norm for our purposes may be taken as the root-mean-square norm.

In effect the theory focuses all the attention on the difference scheme and the establishment of stability. It had reached a high state of development by about 1964. Kreiss [3] had established necessary and sufficient criteria for deciding the stability of any constant coefficient scheme by means of fourier analysis: this completed the analysis begun by von Neumann which led to the necessary stability condition associated with his name. Moreover Kreiss [4] had shown for hyperbolic systems of equations how the addition of a small amount of dissipation could maintain stability in the presence of coefficients varying smoothly with $\underline{r}$. This in turn opened the way for applying Strang's [5] demonstration of convergence for smooth solutions of non-linear hyperbolic systems if the corresponding linearised difference scheme is stable.

However, this rather complete theory was already beginning to show its limitations as more refined criteria were applied to the selection of methods, and the requirements of high accuracy in complex situations led to more sophisticated difference schemes.

2. PRACTICAL LIMITATIONS OF THE L-R THEORY

Even in quite simple situations the dependence of the stability definition on what happens only as $\Delta t \to 0$, is confusing and misleading. For example, the following situation arises if the simultaneous convection and diffusion in the equation

$$u_t + a u_x = b u_{xx} \quad (5)$$

is approximated by the scheme

$$\frac{U^{n+1} - U^n}{\Delta t} + a\,\frac{\Delta_o U^n}{\Delta x} = b\,\frac{\delta^2 U^n}{(\Delta x)^2}\,, \quad (6)$$

where $\Delta_o U_j = \tfrac{1}{2}(U_{j+1} - U_{j-1})$, $\delta^2 U_j = U_{j+1} - 2U_j + U_{j-1}$ and j labels the mesh-points. The amplification factor, giving the growth per time step of the fourier mode e^{ikx}, is

$$\kappa(k, \Delta x, \Delta t) = 1 - \frac{a\Delta t}{\Delta x}\, i \sin k\Delta x - \frac{4b\Delta t}{(\Delta x)^2} \sin^2 \tfrac{1}{2} k\Delta x\,. \quad (7)$$

Thus stability requires that $b\Delta t \leq \tfrac{1}{2}(\Delta x)^2$ and, if $b > 0$, this ensures that

$$|\kappa|^2 \leq 1 + \left(\frac{a\Delta t}{\Delta x}\right)^2 \leq 1 + \left(\frac{a^2}{2b}\right)\Delta t \quad (8)$$

which is sufficient for L-R stability. However, for even modest values of a^2/b this growth rate is quite unacceptable in practice. As a result the more stringent definition of "practical" stability [2] or "strict" stability [6] is often used:

$$||\underline{W}^n|| \leq e^{\alpha t}\, ||\underline{W}^o||\,, \quad (9)$$

where α is the smallest constant for which $||\underline{w}(t)|| \leq e^{\alpha t}\, ||\underline{w}(0)||$ applies to the differential equation. In the present example $\alpha = 0$, and the condition for strict stability becomes

$$\left(\frac{a\Delta t}{\Delta x}\right)^2 \leq \frac{2b\Delta t}{(\Delta x)^2} \leq 1 \quad (10)$$

which properly indicates the limited value of the scheme.

More seriously, terms which are $O(\Delta t)$ occur throughout the development of the L-R stability theory for variable coefficient and non-linear problems and are properly neglected. Thus for the simple non-linear advective equation

$$u_t + u u_x = 0 \quad (11)$$

no distinction is made in this theory between the two schemes

$$\frac{U^{n+1} - U^{n-1}}{2\Delta t} + U^n\,\frac{\Delta_o U^n}{\Delta x} = 0 \quad (12a)$$

and

$$\frac{U^{n+1} - U^{n-1}}{2\Delta t} + \frac{1}{3\Delta x}\left[U^n\, \Delta_o U^n + \Delta_o (U^n)^2\right] = 0\,. \quad (12b)$$

The former, however, exhibits the non-linear instability first demonstrated by Philips [7], while the latter largely eliminates this through its energy conservation property - see Arakawa [8] and Morton [9]. If $U\Delta t/\Delta x < 1$, the growth rate of the linearised equations in both cases is given, apart from terms which are $O(\Delta t)$, by the familiar quadratic for the leap-frog method $\kappa^2 - 1 + 2i\lambda US\kappa = 0$, where $\lambda = \Delta t/\Delta x$ and $S = \sin k\Delta x$. Moreover, when the $O(\Delta t)$ terms are included the two equations are only modified to

$$\kappa_a^2 - 1 + \lambda(2iUS + \Delta_o U)\kappa_a = 0 \tag{13a}$$

$$\kappa_b^2 - 1 + \lambda(2i\bar{U}S + \frac{2C+1}{3}\Delta_o U)\kappa_b = 0 , \tag{13b}$$

where $\bar{U}_j = \frac{1}{3}(U_{j-1} + U_j + U_{j+1})$ and $C = \cos k\Delta x$. These are sufficient to demonstrate the well-known leap-frog jitter: when $\Delta_o U > 0$, corresponding to a rarefaction wave, the spurious root $\kappa \sim -(1 - \lambda^2U^2S^2)^{\frac{1}{2}} - i\lambda US$ grows, while the principal root grows only when $\Delta_o U < 0$. This is an example of weak or relative instability, familiar in ordinary differential equations but more complicated here because of the space dependence. But the point to note here is that equations (13a) and (13b) do not distinguish in any important way between the two methods. To achieve proper understanding of this situation it is best to go to a non-linear analysis [10]. However, in more complicated situations this may not be feasible. Then it is encouraging to find that, if we abandon the approach of studying the stability of the difference scheme quite separately from the accuracy with which it approximates the differential equation, then the clear improvement of (12b) over (12a) can be seen. We shall do this below in our consideration of the "modified equation" approach.

The difficulty of the analysis necessary to apply the Lax-Richtmyer theory rigorously is the third and final limitation that we raise against it. As an example, we consider the "donor-cell" scheme for the Eulerian equations of fluid flow as studied by Hirt [11], omitting the artificial viscosity terms:

$$\rho^{n+1} = \rho^n - \frac{\Delta t}{\Delta x}\delta[\langle\rho^n\rangle\bar{u}^n] , \tag{14}$$

$$(\rho u)^{n+1} = (\rho u)^n - \frac{\Delta t}{\Delta x}\delta[\langle(\rho u)^n\rangle\bar{u}^n + \bar{p}^n] , \tag{15}$$

$$(\tfrac{1}{2}\rho u^2 + p/\gamma\text{-}1)^{n+1} = (\tfrac{1}{2}\rho u^2 + p/\gamma\text{-}1)^n - \frac{\Delta t}{\Delta x}\delta[\langle(\tfrac{1}{2}\rho u^2 + p/\gamma\text{-}1)^n\rangle\bar{u}^n + \bar{p}^n\bar{u}^n] , \tag{16}$$

where ρ, u, p are density, velocity and pressure, δ is the central difference operator $\delta w_j = w_{j+\frac{1}{2}} - w_{j-\frac{1}{2}}$, $\bar{w}_{j+\frac{1}{2}} = \frac{1}{2}(w_j + w_{j+1})$ and the donor-cell differencing is defined by

$$\langle w\rangle_{j+\frac{1}{2}} = \begin{cases} w_j & \text{if } \bar{u}_{j+\frac{1}{2}} \geq 0 \\ w_{j+1} & \text{if } \bar{u}_{j+\frac{1}{2}} < 0 . \end{cases} \tag{17}$$

The dependent variables we take to be ρ, $m = \rho u$ and p, with corresponding perturbations to $\rho + \Delta\rho$, $m + \Delta m$ and $p + \Delta p$. The linearised equations for the perturbations are then obtained in the usual way: we consider only the case where $\bar{u} \geq 0$ everywhere and look at the terms arising from the space differencing in the first equation. Note that $\bar{u}_{j+\frac{1}{2}} = \frac{1}{2}[(m_{j+1}/\rho_{j+1}) + (m_j/\rho_j)]$ so that we obtain after a little manipulation,

$$\tfrac{1}{2}\{\frac{\rho_j}{\rho_{j+1}}(\Delta m)_{j+1} + (1 - \frac{\rho_{j-1}}{\rho_j})(\Delta m)_j - (\Delta m)_{j-1}$$
$$- u_{j+1}\frac{\rho_j}{\rho_{j+1}}(\Delta\rho)_{j+1} + (u_{j+1} + u_j\frac{\rho_{j-1}}{\rho_j})(\Delta\rho)_j - u_j(\Delta\rho)_{j-1}\} .$$

This is already fairly unmanageable unless we abandon terms which are $O(\Delta x)$, and because of the stability condition also $O(\Delta t)$, even though they were seen to be very useful in the previous simple example. We then get for equation (14)

$$(\Delta\rho)^{n+1} = (\Delta\rho)^n - \frac{\Delta t}{\Delta x}[\Delta_o(\Delta m)^n - \tfrac{1}{2}u^n\delta^2(\Delta\rho)^n] . \tag{18}$$

Carrying out a local fourier analysis on just this equation shows the stabilising effect of the last term and one might deduce that without it the system of equations would be unconditionally unstable. However, Hirt claimed that if the first term were evaluated at the new time, giving $\Delta_o m^{n+1}$ in (14) and $\Delta_o(\Delta m)^{n+1}$ in (18), the system would be stable according to a fourier analysis. Presumably, this was on the basis of a treatment of this equation in isolation from the other two and replacing $(\Delta m)^{n+1}$ by $u(\Delta\rho)^{n+1}$. Then, of course, the amplification factor satisfies

$$|\kappa|^2 = 1/(1 + (uS\Delta t/\Delta x)^2) \leq 1 . \tag{19}$$

But the coupling between the equations is important in the stability analysis and the correct result is not so easily obtained. If all the equations are expanded as in (18), the resulting determinantal equation for κ when the donor-cell differencing of (18) is used, becomes very complicated; so we restrict our attention here to the special case in which $\Delta p = c_s^2 \Delta\rho$, when only two equations have to be dealt with. The equation for κ then becomes, with $\lambda = \Delta t/\Delta x$,

$$\det \begin{vmatrix} 1 - 2\lambda u s^2 - \kappa & -i\lambda S \\ i\lambda(u^2 - c_s^2)S & 1 - 2\lambda u s^2 - 2i\lambda u S - \kappa \end{vmatrix} = 0 . \qquad (20)$$

This yields $\kappa = 1 - 2\lambda u s^2 - i\lambda S(u \pm c_s)$ and hence the stability condition

$$|\kappa|^2 = 1 - 4\lambda s^2\{u - \lambda[u^2 s^2 + (u \pm c_s)^2 c^2]\} \leq 1 \quad \text{if} \quad (u + c_s)^2\lambda \leq u . \qquad (21)$$

When the central difference $\delta_o(\Delta m)^n$ is used instead in equation (18), the top left term in (20) becomes $1 - \kappa$ and the equation for κ becomes

$$(\kappa - 1)^2 + 2(\kappa - 1)\lambda u(s^2 + iS) + \lambda^2 S^2(c_s^2 - u^2) = 0 . \qquad (22)$$

On the other hand when $\delta_o(\Delta m)^{n+1}$ is used, the top right term is multiplied by κ and we obtain

$$(\kappa - 1)^2 + 2(\kappa - 1)\left[\lambda u(s^2 + iS) + \tfrac{1}{2}\lambda^2 S^2(c_s^2 - u^2)\right] + \lambda^2 S^2(c_s^2 - u^2) = 0 . \qquad (23)$$

The analysis of the stability conditions arising from these two equations is typical of the practical difficulties of applying fourier analysis to systems of equations. One can, however, see immediately that the condition

$$c_s^2 \geq u^2 \qquad (24)$$

is necessary to the stability of both equations: for otherwise the sum of the arguments of the two roots for $\kappa - 1$ is π or 3π, while for stability the argument of each must lie in the open interval $(\pi/2, 3\pi/2)$. A complete analysis shows (22) to be stable if $2c_s(u + c_s)\lambda \leq u \leq c_s$ and (24) if $0 < 4u\lambda \leq 2(u + c_s)\lambda \leq 1$ or $\lambda c_s \leq 2$ if $u = 0$.

3. DISSIPATION, DISPERSION AND CONSERVATION

Once the gross stability of the difference scheme has been assured, many other properties need to be considered, all to do with the relationship of the scheme to the differential equation: as we have seen even the consideration of strict stability requires this comparison to be made. The one possible exception to this statement is the property of dissipation. This was first defined in terms of the growth factor of a single fourier mode, a scheme being termed dissipative if all the eigenvalues of the locally evaluated amplification matrix satisfy

$$|\kappa(x, k, \Delta x, \Delta t)| \leq 1 - \sigma(k\Delta x)^{2s} , \qquad -\pi \leq k\Delta x \leq \pi , \qquad (25)$$

for some constant $\sigma > 0$ and some positive integer s. Such a requirement was used by Kreiss [4] in his development of the stability theory of variable coefficient hyperbolic systems, the dissipation being small enough not to affect the truncation error of the schemes but sufficient to control the instabilities generated by the variable coefficients. However, even earlier John [12] used the same requirement on κ in demonstrating the stability of variable coefficient parabolic equations where, for small $k\Delta x$, the property arises immediately from the consistency of any difference scheme with a parabolic operator.

Subsequently, many authors [13] [14] [15] [16] carried out quantitative comparisons of the dissipation of various schemes as applied to simple model situations. Typically the advective equation, $u_t + au_x = 0$, is used and the damping compared for a range of mesh ratios $a\Delta t/\Delta x$ and for all modes spanning a reasonable number of mesh intervals, e.g. $2\pi/k\Delta x \geq 4$. At the same time the dispersion of the scheme may be studied by comparing $\arg \kappa$ with the phase change $ka\Delta t = k\Delta x(a\Delta t/\Delta x)$ produced by the differential equation in one time step. Notice that these errors may be regarded as arising more or less directly from the fourier transform of the truncation error defined in (3). For, in that notation, but for a scalar variable, $\kappa = (1 - \Delta t\hat{P}_o)/(1 + \Delta t\hat{P}_1)$ and substituting $u = e^{ikat}e^{ikx}$ we have

$$e^{-ika\Delta t} - \kappa = (1 + \Delta t\hat{P}_1)^{-1}.\Delta t.(\widehat{T.E.}) . \qquad (26)$$

These studies clearly show, for example, the severe dissipation associated with the upwind differencing scheme, the dominant phase lag error in the Lax-Wendroff scheme and the attractive properties of the leap-frog scheme. They have stimulated the development of more accurate one dimensional schemes of third and fourth order which are becoming increasingly important in practical fluid flow calculations. Apart from Fromm [15], however, much less study has been

given to these phenomena in several dimensions and a good deal more probably remains to be learned this way in that case.

Though they provide important guide lines in the choice of methods, not all of the results of these studies of dissipation and dispersion can be immediately transferred to more realistic situations. Moreover, the presence of non-linear terms requires a much greater choice of difference scheme to be made; for example, in equation (11) should one replace uu_x by the difference $U\Delta_o U$ as in (12a) or combine this in some way with $\frac{1}{2}\Delta_o U^2$ as in (12b)? Also, in a system of equations one has to make the choice of dependent variables and the mesh that each of them should be regarded as centred at. However, the use of fourier modes is still helpful in analysing the errors involved and, in particular, the phenomenon of aliasing, i.e. the tendency of a finite grid representation to confuse the modes created by non-linear interactions.

Suppose that over a grid of $2J + 1$ equally spaced points, mesh functions u and v are expanded as

$$u_j = \sum_{(k)} \hat{u}_k e^{ikj\Delta x} , \qquad v_j = \sum_{(k)} \hat{v}_k e^{ikj\Delta x} , \tag{27}$$

where the sums run over $k\Delta x = 0, \pm\pi/J, \pm 2\pi/J, \ldots, \pm(J-1)\pi/J, \pm\pi$. Now if u and v were considered as continuous functions of the continuous variable $x = j\Delta x$ and substituted into $(uv)_x$, we get

$$(uv)_x = \sum_{(\ell)} \Big[i \sum_{k+k'=\ell} \ell \hat{u}_k \hat{v}_{k'} \Big] e^{i\ell x} , \tag{28}$$

where $\ell\Delta x$ may now span $(-2\pi, 2\pi)$. The higher frequencies are unrepresentable on the mesh and when a mesh approximation to vu_x is calculated they appear, shifted by 2π, in the original frequency range; this is aliasing. Thus we get the following if we substitute the mesh functions into $(u\Delta_o v + v\Delta_o u)/\Delta x$

$$\frac{u_j \Delta_o v_j + v_j \Delta_o u_j}{\Delta x} = \sum_{(\ell)} \Big[i \sum_{\substack{k+k'=\ell \\ k+k'=\ell\pm 2\pi/\Delta x}} (\Delta x)^{-1} (\sin k\Delta x + \sin k'\Delta x) \hat{u}_k \hat{v}_{k'} \Big] e^{i\ell j\Delta x} \tag{29}$$

By comparing the coefficients of $\hat{u}_k \hat{v}_{k'}$ in the two expansions, one may obtain very detailed information on the errors arising from the aliasing and the finite difference operators. This has been done for a number of approximations to the shallow water equations in two dimensions by Grammeltvedt [17].

Apart from its handling of fourier modes, the other broad area in which a difference scheme is compared with its differential system concerns its conservation properties. The equations of fluid flow are basically conservation equations for mass, momentum and energy. If they are written in this conservation form, $\underline{w}_t + \underline{\nabla}.\underline{f}(\underline{w}) = 0$, before derivatives are replaced by divided differences then when a sum is taken over all the mesh points the differences cancel except at the boundaries and the conservation properties are correctly modelled by the mesh sums of the variables. This often gives improved accuracy, especially in situations like shocked flows where the integral conservation laws are very important, and there is some indication that conservation of the lower velocity moments is most important: thus one should always aim to conserve mass, while the total energy may not be an appropriate variable to work with.

More generally, one may attempt to model any conservation property of the differential system involving functions of the dependent variables [9]. Most commonly these are quadratic functions representing energy or vorticity squared as in the well-known schemes of Arakawa [8]. While fourier analysis is essentially a means of analysing a scheme once it has been proposed, these conservation arguments are key elements in motivating the design of new schemes.

A general technique for carrying out this process consists of first writing out the details of the manipulation of the differential equation leading to the establishment of the conservation property. Then difference replacements are made for all the differential operators in such a way that the identities used are carried over into their discrete counterparts. The essential operation is usually integration-by-parts or use of Gauss' Theorem and the difference operators are therefore chosen to satisfy summation-by-parts formulae. Consider the simple advection equation (11). Premultiplication by u and integration with respect to x leads to

$$\frac{d}{dt}||u||^2 = -\langle u, uu_x \rangle = \langle \tfrac{1}{2}(u^2)_x, u \rangle .$$

Hence the correct combination of the equivalent forms uu_x and $\frac{1}{2}(u^2)_x$ leads to

$$\frac{d}{dt}||u||^2 = -\frac{1}{3}\langle u, uu_x + (u^2)_x \rangle = 0 , \tag{30}$$

and the adoption of the energy conserving scheme (12b) for this equation. Useful basic difference operators in these manipulations are the central difference δ and average μ: δ has adjoint $-\delta$ and μ is self-adjoint with respect to an inner product $\langle u, v \rangle$ in which each argument is on a mesh staggered half a step with respect to the other. In one dimension this usually means that μ and δ appear in the combination $\mu\delta = \Delta_o$ as in (12b) so that only one mesh is involved. But in two dimensions it is often a great advantage to replace $\partial/\partial x$ by $\mu_y\delta_x$ and $\partial/\partial y$ by $\mu_x\delta_y$ and use one mesh consisting of the centres of the squares formed by

the other - see Morton [18].

Grammeltvedt's [17] paper is largely devoted to a study of the advantages of these conservation properties. Broadly, he finds that the quadratically conserving or energy conserving schemes are more stable but increased stability is to some extent paid for by worse phase errors. See also Roache [19] for further references to studies of these and other phenomena. It is worth noting that Torrance et al [20] found that conservation was a more important property than the order of accuracy of the truncation error.

4. THE MODIFIED EQUATION APPROACH

We have shown in the previous two sections the need to study truncation error and accuracy in conjunction with stability. The tendency to separate the two aspects arose essentially from the Lax-Richtmyer theory of stability and convergence and an alternative approach, based on the "modified equation", has recently attracted increased attention. The technique is usually attributed to Hirt [11] but similar ideas have been widely used (see, e.g. Ref. [2] pp. 331-2). It has been put on a more methodical basis by Warming and Hyett [21], who considered linear equations and compared the approach to the L-R theory in a number of model problems.

More generally, let us write the (non-linear) differential and difference equations for u and U respectively as

$$L(u) = 0 , \qquad L_\Delta(U) = 0 . \tag{31}$$

Then the L-R theory defines the truncation error $T_\Delta(u)$ by substitution of u into the difference scheme, evaluates it by Taylor expansion and considers

$$L_\Delta(u) - L_\Delta(U) = T_\Delta(u) \tag{32}$$

as an equation for $u - U$: the homogeneous equation is used to study stability and the inhomogeneous equation to study accuracy and convergence. The alternative approach is to extend U to be a function with an infinite Taylor series expansion and to find a modified differential equation which it satisfies, by substitution of this expansion into the difference scheme. Corresponding to (32), we obtain

$$L(u) - L(U) = T(U) \tag{33}$$

as the main object of study. Note that before any manipulations are made to simplify $T_\Delta(u)$ and $T(U)$ they are formally identical expressions

$$T_\Delta(u) \equiv L_\Delta(u) - L(u) , \qquad T(U) \equiv L_\Delta(U) - L(U) . \tag{34}$$

However, in the L-R theory the equation $L(u) = 0$ must be used to simplify $T_\Delta(u)$, while in the modified equation approach the equation $L_\Delta(U) = 0$, or equivalently $L(U) + T(U) = 0$, must be used to obtain an equation of the form required.

The immediate advantage of using (33) is that one is working with differential rather than difference operators: this is convenient with linear equations but the advantage becomes progressively greater as one considers first linear perturbations of a non-linear equation and then the full non-linear equation. Consider the linear equation $u_t + Pu = 0$. This leads to a well-posed initial-value problem if P is semi-bounded, that is, $\langle u, Pu\rangle \geq -\alpha||u||^2$ for some $\alpha > 0$, for then $||u||^2$ can only grow like $e^{\alpha t}$. Hence when the stability of the difference scheme is considered with the equation $U_t + PU + T(U) = 0$, establishment of $\langle T(U), U\rangle \geq -\beta||U||^2$ will yield stability. Moreover, some of this approach can be extended to non-linear equations: if $\langle P(u) - P(U), u - U\rangle \geq -\alpha||u - U||^2$, P is called monotone and leads to a well-posed problem. As an example, let us return to the advective equation (11). With $\varepsilon = u - U$ we have

$$\frac{d}{dt}||\varepsilon||^2 + \tfrac{1}{2}\langle u - U, (u^2)_x - (U^2)_x\rangle = \langle \varepsilon, T(U)\rangle ,$$

i.e.

$$\frac{d}{dt}||\varepsilon||^2 + \tfrac{1}{2}\langle \varepsilon^2, (u + U)_x\rangle = \langle \varepsilon, T(U)\rangle \tag{35}$$

after two integrations by parts. The inner product on the left is positive definite when $(u + U)_x > 0$ everywhere so that the operator P is monotone then, expressing the fact that the advection equation (11) is well-posed for rarefaction waves. For the non-linear stability of a difference scheme one needs to study the monotonicity of $T(U)$ and, for convergence, the inner product $\langle u - U, T(U)\rangle$: for scheme (12a) the coefficient of $(\Delta x)^2/6$ in $T(U)$ is $-UU_{xxx}$ while for (12b) it is $-(UU_{xxx} + 2U_x U_{xx})$; thus the fact that the inner product of U with the second expression is obviously zero, while not that with the first, is encouraging though the details of the implication have yet to be established.

However, greatest use of the modified equations has so far been made to study dissipation and dispersion properties and to obtain "heuristic" stability criteria. For linear equations,

Warming and Hyett advocate the systematic replacement of all time differentials in the expression for $T(U)$. Thus for $u_t + Pu = 0$, a difference scheme will give $U_t + PU + T(U) = 0$ and repeated substitution of this and its derivatives to eliminate all time derivatives in $T(U)$ yields the form

$$U_t + PU = QU \ , \tag{36}$$

where both P and Q are space differential operators: Q will be an infinite power series in Δt, Δx and, for instance, for the Lax-Wendroff scheme in one dimension applied to the model problem $u_t + au_x = 0$

$$QU \equiv -\frac{a}{6}\left[(\Delta x)^2 - a^2(\Delta t)^2\right]u_{xxx} - \frac{a^2}{8}\Delta t\left[(\Delta x)^2 - a^2(\Delta t)^2\right]u_{xxxx} + \ldots \ . \tag{37}$$

From the leading even order derivative one obtains the heuristic stability condition $|a|\Delta t \leq \Delta x$ by requiring that this term should not give negative dissipation, i.e. lead to ill-posedness of the solution. Similarly, the leading odd order derivative gives some measure of the dispersion in the scheme. Note that the leading few terms in Q are the same as if $U_t + PU = 0$ were used to carry out the substitution for the time differentials: thus these will be the same as in a conventional approach but beyond a number of terms, determined by the order of accuracy of the scheme, differences will occur.

Hirt [11] in the same way obtains the left inequality in the condition (10) needed to obviate the weak instability in the mixed advection and diffusion equation (5) approximated by (6). However, in general, complete stability conditions cannot be obtained by looking at the leading term in QU, and the whole series must be considered. Warming and Hyett overcome this to some extent by appealing to the form of the fourier transform $\hat{Q}$ of Q regarded as a function of $s = \sin^2 \tfrac{1}{2}k\Delta x$. But then, as they point out, this amounts to considering the amplification factor of the L-R theory and their analysis could be just as readily applied to that.

It would seem that with this approach one should not try to follow the analysis of the L-R theory but instead exploit the differential equation theory at one's disposal. Thus in considering problem (5), (6) Hirt did not immediately eliminate the time differentials: his leading terms in $T(U)$ then gave him a hyperbolic equation with a wave speed of $(2b/\Delta t)^{\frac{1}{2}}$ and use of the Courant-Friedrichs-Lewy condition on that yielded the second part of the inequality in (10). In the same paper he studied the terms in $T(U)$ up to fourth order for the difference scheme (14)-(16) and various replacements for (14): the instabilities found in numerical experiments were then attributed to various differences in these terms between the schemes. Similarly, Lerat and Peyret [22] have studied a general class of predictor-corrector methods for the gas dynamic equations which generalise the two-step Lax-Wendroff scheme. They obtained the leading terms in $T(U)$ and then compared their dissipative and dispersive effects along the characteristics of the original equations. In this way they were able to make specific choices of 'best' schemes for particular problems, the validity of which was confirmed by numerical experiment.

5. BOUNDARY CONDITIONS

In the foregoing we have ignored all effects of boundaries in order to keep the arguments as simple as possible. But in practice the best treatment of boundary conditions is one of the more difficult judgements to make and a poor choice can lead to inaccuracies and instabilities. The difficulties start with the differential equations where the proper boundary conditions are still not always known: recent advances here have been made by H.O. Kreiss who will be speaking on this topic, and the associated results for difference schemes, in this lecture series. The problem is compounded in the difference schemes where quite often extra boundary conditions are needed because the schemes are of higher order than the differential equation, e.g. in the use of the Lax-Wendroff or leap-frog methods for a first order hyperbolic equation.

Understanding of the resulting effects is again most completely achieved by a modal analysis like the fourier analysis used in the interior. Godunov and Ryabenkii [23] first gave necessary stability conditions for one-dimensional problems by considering modes of the form $u_j^n \sim \kappa^n \mu^j$, where $|\mu| < 1$ and j counts mesh points away from the boundary. Kreiss [24] has greatly refined the approach giving only mildly stricter conditions which are sufficient for stability and recently has achieved the major step of extending the theory to plane boundaries in multi-dimensional problems. However, as might be expected, the analysis is in general even more awesome than that for the interior although some important simple cases have now been studied in detail [25]. Moreover, in practical problems curved and angled boundaries provide much of the interest as well as raising many more problems regarding how they should be approximated. Thus one looks to carefully controlled numerical experiments for information on the stability and accuracy of boundary approximations. Abbet [26] has studied the behaviour of some twenty-five schemes as applied to supersonic steady flows and Chu and Sereny [27] have conducted similar experiments in one-dimensional time-dependent flows. (See Roache [19] for further references.) The conclusion is overwhelming, though not of course unexpected, that due account should be taken of the characteristics of the differential system and the combinations of dependent variables carried along them. Full use of the characteristics entails calculating all those carrying information to or from the boundary and using interpolation on the mesh to approximate

their effect. To do this explicitly can be a lengthy procedure which is why simpler methods are called for; however, it seems from Abbet's results that the performance of a method is heavily dependent on how closely it is related to this basic procedure. Apart from this, both papers find that simple extrapolation performs reasonably well in most cases and much better than formally more accurate extrapolation methods. It is also noteworthy then that a new method which Abbet proposes and which is both accurate and fast combines an explicit extrapolating predictor step with a simple wave corrector step.

Chu and Sereny attempt to correlate their results by reference to a simple analytical test similar to those of dispersion and dissipation discussed earlier for the interior schemes. Slightly modified and applied to the wave equation

$$\begin{aligned} u_t + v_x &= 0 \qquad r = u + v = \text{const.} \quad \text{on} \quad t - x = \text{const.} \\ v_t + u_x &= 0 \qquad s = u - v = \text{const.} \quad \text{on} \quad t + x = \text{const.} \end{aligned} \tag{38}$$

it consists of reflecting the plane wave $s = -\exp[ik(t + x)]$ at the boundary $x = 0$, where the condition $u = 0$ is imposed. Assuming that up to $t = 0$, the correct reflected wave $r = \exp[ik(t - x)]$ has been produced, we calculate r_o^1, the reflected wave at $x = 0$, $t = \Delta t$ produced by the scheme under test and compare it with $e^{ik\Delta t}$. For three typical simple schemes for imposing a boundary condition on v when the Lax-Wendroff method is used in the interior, one has the following results,

Scheme	r_o^1
Exact	$e^{ik\Delta t}$
Characteristic method	$1 - \lambda + \lambda e^{ik\Delta x}$
One-sided first order: $\dfrac{v_o^{n+1} - v_o^n}{\Delta t} + \dfrac{u_1^n - u_o^n}{\Delta x} = 0$	$1 + i\lambda S$
First order extrapolation: $v_o = v_1$	$C + i\lambda S[\lambda + (1 - \lambda)C]$

This shows clearly the origin of the overshooting experienced with the one-sided scheme and the attractions of the extrapolation procedure - while never amplified, for $\lambda = 1$ it is exact, like the characteristic method.

Besides the use of characteristics, analytical guide lines on the choice of boundary conditions are obtained by consideration of conservation properties. When the equations are differenced in conservation form using a "control volume" or "donor-cell" technique, the layout of variables on the mesh and the imposition of boundary conditions becomes strongly motivated - see Roache [19] for many examples. As a simple case, suppose that $\partial f(u)/\partial x$ in a conservation law is being approximated: if a one-sided difference $(f_{j+1} - f_j)/\Delta x$ is used the boundary terms will be f_J, f_o and physical boundary conditions should be imposed at mesh points; but if the central difference $\Delta_o f_j$ is used boundary terms will be $(f_J + f_{J-1})/2$, $(f_o + f_1)/2$ and the conditions imposed at the mid-points. Further guidance, particularly for non-physical boundary conditions, comes when conservation of quadratic quantities is attempted: the summation-by-parts manipulations entailed in establishing conservation lead to specific boundary terms whose behaviour must be controlled by imposition of appropriate boundary conditions.

6. ERROR ANALYSIS IN EVOLUTIONARY FINITE ELEMENT PROBLEMS

Finite element methods are becoming increasingly popular for fluid flow problems [28]. Their behaviour in steady state situations is now well understood but, for evolutionary problems, optimal procedures and their analysis are only beginning to be developed. We conclude then with an analysis of the errors induced by approximating the non-linear term $u\partial v/\partial x$ in various ways, as developed by Cullen [29, 30] for integration of the shallow water equations.

Suppose the solution u of $u_t = Lu$, $u(t = 0) = u^o$ is to be approximated by U from a space S^h, spanned by the basis functions $\phi_j(x)$, i.e.

$$U^n(x) = \sum_{(j)} U_j^n \phi_j(x), \qquad n = 0, 1, 2, \ldots \tag{39}$$

approximates $u(x, n\Delta t)$. Introduce the projection operator P from the solution space into S^h:

$$(Pu)(x) = \sum_{(j)} u_j \phi_j(x) \qquad \langle Pu, \phi_k \rangle = \langle u, \phi_k \rangle, \forall\, k\ . \tag{40}$$

Then the generation of U can be considered in three parts: first the initial data is approximated in S^h by $U^o = Pu^o$; then the spacial operator L is approximated by an operator $\tilde{L} : S^h \to S^h$; and thirdly the time integration is approximated by an appropriate quadrature

formula. Standard practice is to take $\tilde{L} = PL$, so that if the leap-frog method is used we obtain

$$(2\Delta t)^{-1}(U^{n+1} - U^{n-1}) = PLU^n, \qquad U^0 = Pu^0 ; \tag{41}$$

i.e.
$$(2\Delta t)^{-1}M(\underline{U}^{n+1} - \underline{U}^{n-1}) = K\underline{U}^n , \qquad M\underline{U}^0 = \{<u^0, \phi_j>\} , \tag{42}$$

where we denote by $\underline{U}$ the vector $\{U_j\}$ and M and K are the mass and stiffness matrices $M_{ij} = <\phi_i, \phi_j>$, $K_{ij} = <\phi_i, L\phi_j>$.

The errors committed in the approximation can be distinguished in a corresponding manner. The last, a simple quadrature error, will be set aside for this discussion. Then, using an Euler method integration with a sufficiently small time step, the true solution at time $n\Delta t$ is given by $u(n\Delta t) = (I + \Delta t\, L)^n u^0$, while the approximation is given by

$$U^n = (I + \Delta t\tilde{L})^n Pu^0 .$$

Writing A for $I + \Delta tL$ and B for $I + \Delta t\tilde{L}$, the difference can be resolved as

$$(A^n - B^nP)u^0 = \{(A^n - PA^n) + (PA - BP)A^{n-1} + B(PA - BP)A^{n-2} + \ldots$$
$$\ldots B^{n-2}(PA - BP)A + B^{n-1}(PA - BP)\}u^0 .$$

That is,

$$u(n\Delta t) - U^n = (I - P)u(n\Delta t) + \Delta t \sum_{s=0}^{n-1} (I + \Delta t\tilde{L})^{n-s-1}(PL - \tilde{L}P)u(s\Delta t) . \tag{43}$$

Thus the error is made up of a final projection error and an accumulated evolutionary error. The former is estimated by straightforward approximation theory - if S^h contains all polynomials of degree up to $(\mu - 1)$, then in general the error will be $O(h^\mu)$. The latter is the key object of our analysis and can be helpfully visualised as the difference between the two routes in the diagram:

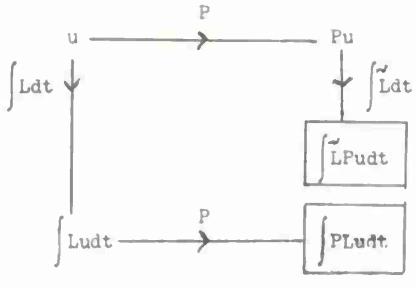

If L is an operator of order m, the usual error estimate for $(PL - \tilde{L}P)u$ will be $O(h^{\mu-m})$. But for some choices of S^h and $\tilde{L}$ it can be as small as $O(h^{2\mu})$ - see Thomée [31], Wendroff [32] and Cullen [30].

Suppose $L \equiv \partial/\partial x$ and a uniform mesh is used with spline functions of order μ as basis functions (that is, piecewise polynomials of degree $\mu - 1$ with continuous derivatives up to order $\mu - 2$). Then Thomée showed that the nodal parameters U_j^n are related by what can be regarded as a finite difference formula and that its truncation error was $O(h^{2\mu})$. Cullen identified this as the error $(PL - PLP)u$ and thus was able to obtain the same result for a wider class of differential equations, including non-linear ones.

Special interest attaches to the case of linear splines $(\mu = 2)$. Because of the uniform mesh, fourier analysis may be used so we take $u = \hat{u}e^{ikx}$. Then we have in (40) $\phi_j(x) = \phi(x/h - j)$ and

$$\phi(x) = \begin{cases} 1 + x, & -1 \le x \le 0 \\ 1 - x, & 0 \le x \le 1 \end{cases} . \tag{44}$$

Now $$<\phi_j, e^{ikx}> = \int \phi(x/h - j)e^{ikx}dx = he^{ij\xi}\hat{\phi}(\xi), \quad \text{where } \xi = kh.$$

Hence, using the familiar mass matrix for linear elements, the nodal parameters u_j satisfy

$$\frac{h}{6}(u_{j-1} + 4u_j + u_{j+1}) = \hat{hue}^{ij\xi}\hat{\phi}(\xi) \ , \tag{45}$$

giving $u_j = \hat{u}\alpha(\xi)\exp(ij\xi)$, where $\alpha(\xi) = 3\hat{\phi}(\xi)/(2 + \cos\xi)$. A simple computation gives $\hat{\phi}(\xi) = (2\xi^{-1}\sin\tfrac{1}{2}\xi)^2$ so that

$$u_j/\hat{ue}^{ij\xi} = \alpha(\xi) = \frac{6(1 - \cos\xi)}{\xi^2(2 + \cos\xi)} \sim 1 + \frac{\xi^2}{12} \quad \text{as} \quad \xi \to 0 \ . \tag{46}$$

When $L \equiv \partial/\partial x$, $Lu = iku$ so we have immediately

$$PLu = ik\hat{u}\alpha(\xi) \sum_{(j)} e^{ij\xi}\phi_j(x) \ . \tag{47}$$

The familiar Galerkin equations for $v = PL(Pu)$ give

$$\frac{h}{6}(v_{j-1} + 4v_j + v_{j+1}) = \frac{u_{j+1} - u_{j-1}}{2} \tag{48}$$

whence $v_j = ik\beta(\xi)u_j$ and

$$\beta(\xi) = \frac{3\sin\xi}{\xi(2 + \cos\xi)} \sim 1 - \frac{\xi^4}{180} \quad \text{as} \quad \xi \to 0 \ . \tag{49}$$

Thus we have

$$PLPu = ik\hat{u}\alpha(\xi)\beta(\xi) \sum_{(j)} e^{ij\xi}\phi_j(x) \tag{50}$$

and comparison with (47) shows the error to be $O(\xi^4) = O(h^4)$. Notice how the $O(h^2)$ error arising from the projection, and expressed by the difference of $\alpha(\xi)$ from unity, is eliminated as a common factor: the crucial error, expressed by the difference of $\beta(\xi)$ from unity, could have been calculated simply from the finite difference equation (48).

Now consider the problem when $Lu = u\partial u/\partial x$. The usual Galerkin approach essentially approximates the equation $v = u\partial u/\partial x$ for the time derivative in one step by substituting $u = \sum u_j\phi_j$ into both parts of the product. In experiments on the shallow water equations with linear elements, Cullen found the accuracy most disappointing. The trouble is that the derivative of the linear approximation is piecewise constant and not even in the space S^h, let alone being the best approximation in S^h. The solution was to solve the equation in two parts,

$$v = \frac{\partial u}{\partial x} \ , \qquad w = uv \tag{51}$$

using Galerkin at each stage separately. Thus $L \equiv L_2L_1$ where L_1 represents calculation of the derivative and L_2 the product with u. This is replaced by $\tilde{L} \equiv \tilde{L}_2(PL_1)$, so we have

$$PLu - \tilde{L}Pu = [PL_2(L_1u) - \tilde{L}_2P(L_1u)] + [\tilde{L}_2(PL_1u) - \tilde{L}_2(PL_1Pu)] \ , \tag{52}$$

the non-linearity of the operator L_2L_1 preventing common factors from being separated out. It is clear, however, that carrying out the product operation to 4th order will give an overall 4th order evolutionary error.

An analysis of three ways of constructing approximations to $u\partial v/\partial x$ using linear elements and with $u = \hat{u}\exp(i\xi x/h)$, $v = \hat{v}\exp(i\eta x/h)$ yields the following results: as with (47) we have

$$P\left(u\frac{\partial v}{\partial x}\right) = \hat{u}\hat{v}(i\eta/h)\alpha(\xi + \eta) \sum_j e^{ij(\xi+\eta)}\phi_j(x) \ . \tag{53}$$

(i) Single stage Galerkin results in an extra factor

$$\gamma_1(\xi,\eta) = \frac{\alpha(\xi)\alpha(\eta)\left[\frac{2}{3}\sin\eta + \frac{1}{3}\sin(\xi+\eta) - \frac{1}{3}\sin\xi\right]}{2\eta[1 - \cos(\xi+\eta)]/(\xi+\eta)^2}$$

$$\text{i.e.} \quad \gamma_1(\xi,\eta) \sim 1 + (2\xi^3\eta - 7\xi^2\eta^2 - 8\xi\eta^3 - 4\eta^4)/720, \tag{54}$$

which reduces to $1 - 17\xi^4/720$ when $\xi = \eta$.

(ii) Two stage Galerkin has an extra factor

$$\gamma_2(\xi,\eta) = \alpha(\xi)\alpha(\eta)\beta(\eta)\frac{\left[\frac{1}{2} + \frac{1}{6}(\cos\xi + \cos\eta + \cos(\xi+\eta))\right]}{2[1 - \cos(\xi+\eta)]/(\xi+\eta)^2}$$

$$\text{i.e.} \quad \gamma_2(\xi,\eta) \sim 1 + (2\xi^3\eta + 3\xi^2\eta^2 + 2\xi\eta^3 - 4\eta^4)/720, \tag{55}$$

reducing to $1 - 3\xi^4/720$ when $\xi = \eta$.

(iii) Galerkin followed by nodal point multiplication has the corresponding factor

$$\frac{a(\xi)a(\eta)}{a(\xi+\eta)} \quad 1 - \frac{\xi\eta}{6} . \tag{56}$$

The last is very easy to implement but is only 2nd order accurate and very poor in practice. Both of the others are 4th order and although the coefficients in (54) and (55) do not seem very different, presumably the factor of nearly six improvement in the two-stage process when $\xi = \eta$ is the basis of its superior performance in practice when used on $\underline{u}.\nabla\underline{u}$.

REFERENCES

1. Lax, P.D. and R.D. Richtmyer. "Survey of the stability of finite difference equations." Comm. Pure Appl. Math. 9, 1956, p.267.

2. Richtmyer, R.D. and K.W. Morton. Difference methods for initial-value problems. New York, Interscience, 1967.

3. Kreiss, H.O. "Über die Stabilitätsdefinition für Differenzen gleichungen die partielle Differentialgleichungen approximieren." Nordisk Tidske. Informations-behandling 2, 1962, p.153.

4. Kreiss, H.O. "On difference approximations of the dissipative type for hyperbolic differential equations." Comm. Pure Appl. Math. 17, 1964, p.335.

5. Strang, W.G. "Accurate partial difference methods II: non-linear problems." Numer. Math. 6, 1964, p.37.

6. Kreiss, H.O. and J. Oliger. "Methods for the approximate solution of time dependent problems." GARP Publications Series No. 10, 1973.

7. Philips, N.A. "An example of non-linear computational instability." The Atmosphere and the Sea in Motion. Bert Bolin, ed., Rockefeller Institute Press, New York, 1959, p.501.

8. Arakawa, A. "Computational design of long-term numerical integration of the equations of fluid motion: I. Two-dimensional incompressible flow." J. Comp. Phys. 1, 1966, p.119.

9. Morton, K.W. "The design of difference schemes for evolutionary problems." Numerical Solution of Field Problems in Continuum Physics, SIAM-AMS Proc. 2, Amer. Math. Soc., 1970, p.1.

10. Kreiss, H.O. and J. Oliger. "Comparison of accurate methods for the integration of hyperbolic equations." Tellus 24, 1972, p.199.

11. Hirt, C.W. "Heuristic stability theory for finite-difference equations." J. Comp. Phys. 2, 1968, p.339.

12. John, F. "On the integration of parabolic equations by difference methods." Comm. Pure Appl. Math. 5, 1952, p.155.

13. Roberts, K.V. and N.O. Weiss. "Convective difference schemes." Math. Comp. 20, 1966, p.272.

14. Fromm, J.E. "A method for reducing dispersion in convective difference schemes." J. Comp. Phys. 3, 1968, p.176.

15. Fromm, J.E. "Practical investigation of convective difference approximations of reduced dispersion." Phys. Fluids Suppl. II, Amer. Inst. Phys., New York, 1969, p.3.

16. Morton, K.W. "Stability and convergence in fluid flow problems." Proc. Roy. Soc. A323, 1971, p.237.

17. Grammeltvedt, A. "A survey of finite difference schemes for the primitive equations of a barotropic fluid." Mon. Wea. Rev. 97, 1969, p.384.

18. Morton, K.W. "The design of difference schemes for studying physical instabilities." Proc. Conf. on Numerical Solutions of Differential Equations, J.L. Morris, ed., Springer-Verlag, Berlin, 1973, p. .

19. Roache, J. Computational Fluid Dynamics, Albuquerque, New Mexico, Hermosa Publishing Co., 1972

20. Torrance, K., R. Davis, K. Eike, P. Gill, D. Gutman, A. Hsui, S. Lyons and H. Zien. "Cavity flows driven by buoyancy and shear." J. Fluid Mech. 51, Pt. 2, 1972, p.221.

21. Warming, R.F. and B.J. Hyett. "The modified equation approach to the stability and accuracy analysis of finite-difference methods." J. Comp. Phys. 14, 1974, p.159.

22. Lerat, A. and R. Peyret. "The problem of spurious oscillations in the numerical solution of the equations of gas dynamics." To appear in Proc. 4th Intl. Conf. on Numerical Methods in Fluid Dynamics, 1974.

23. Godunov, S.K. and V.S. Ryabenkii. Introduction to the theory of difference schemes. Interscience, New York, 1964.

24. Kreiss, H.O. "Stability theory for difference approximations of mixed initial boundary-value problems I." Math. Comp. 22, 1968, p.703.

25. Gustafson, B., H.O. Kreiss and A. Sundstrom. "Stability theory of difference approximations for mixed initial boundary-value problems II." Math. Comp. 26, 1972, p.649.

26. Abbet, M. "Boundary conditions and computational procedures for inviscid supersonic steady flow field calculations." Aero Therm Report 71-41, 1971.

27. Chu, C.K. and A. Sereny. "Boundary conditions in finite difference fluid dynamic codes." J. Comp. Phys. 15, 1974, p.555.

28. Oden, J.T., O.C. Zienkiewicz, R.H. Gallagher and C. Taylor, eds. Finite Element Methods in Flow Problems, Univ. of Alabama, Huntsville Press, 1974.

29. Cullen, M.J.P. "A finite element method for a non-linear initial-value problem." J. Inst. Maths. Applics. 13, 1974, p.233.

30. Cullen, M.J.P. "Convergence estimates for the finite element method in evolutionary problems." Submitted to Numer. Math.

31. Thomée, V. "Spline Galerkin methods for initial-value problems with constant coefficients." Lecture Notes in Mathematics No. 363, Springer-Verlag, Berlin, 1973, p.164.

32. Wendroff, B. "Spline Galerkin methods for initial-value problems with variable coefficients." Ibid. p.189.

ACKNOWLEDGEMENT

These lectures were written while the author was Visiting Professor at Columbia University, New York. He is grateful to the Department of Mechanical Engineering for their hospitality and particularly to Professor C.K. Chu for numerous discussions on the subject of the lectures.

NUMERICAL SOLUTION OF THE NAVIER-STOKES EQUATIONS FOR COMPRESSIBLE FLUIDS

Roger PEYRET

CNRS, Institut de Mécanique théorique et appliquée, Université PARIS VI
Collaborateur extérieur de l'ONERA

Henri VIVIAND

Office National d'Etudes et de Recherches Aérospatiales (ONERA)
92320 CHATILLON - France

Summary

Numerical methods for the solution of the Navier-Stokes equations for compressible fluids are discussed. A short review of the Navier-Stokes equations and of their qualitative mathematical properties, and a discussion of their interest in aerodynamics problems are first presented. Then the following aspects of numerical methods are considered : limitation of the domain of calculation and boundary conditions on the outer boundary; various approaches in finite-difference methods and properties of some representative schemes; treatment of the boundary condition at a solid wall; treatment of shock waves and general considerations on accuracy and computation times.

1. Introduction

The considerable development of numerical methods in aerodynamics in the past twenty years has mostly concerned boundary layer problems and inviscid flow problems, that is to say the two fundamental approximations of fluid mechanics for the description of large Reynolds number flows. As numerical methods became currently used for these two classes of flows, and as problems of increasing complexity were considered, a greater attention was given to the shortcomings of these approximations. The numerical solution of the full Navier-Stokes equations is now taken into consideration as a means of predicting flow fields for problems of practical interest, although it is obviously too costly at this time to be accepted as an engineer's tool.

Besides early fundamental work on Burgers equation, one-dimensional flows and low Reynolds number flows, the first applications of numerical methods to the Navier-Stokes equations for compressible flows seem to have been motivated by atmospheric reentry problems, i.e. essentially the blunt body problem and the base flow problem, which involve low density, moderate Reynolds number flows. Progress in numerical analysis and in computer performances allowed the computation of flows at increasing Reynolds numbers, and the most recent studies are concerned with such difficult problems as shock-boundary layer interaction in the turbulent regime.

The purpose of this paper is to discuss the problems arising in the numerical solution of the Navier-Stokes equations for compressible fluids and to present some of the numerical schemes used. We shall consider only finite-difference methods based on the unsteady equations of motion, which, at this time, are the most currently used. It is also for this class of methods that the difference between the compressible and the incompressible cases is the most marked because of the different nature of the continuity equation in the two cases.

After a short review of the Navier-Stokes equations and of their qualitative mathematical properties in section 2, the interest of these equations for aerodynamics is discussed in section 3. The problem of the definition of the computation domain is considered in section 4. Various representative finite-difference schemes are presented in section 5, and the problems of the numerical treatments of boundary conditions at a wall and of shock waves are considered in sections 6 and 7 respectively. Some questions relating to accuracy and computer time are discussed in section 8, and a list of works grouped according to different types of problems is given in section 9.

2. The Navier-Stokes equations

The general motion of a non reacting fluid with respect to a Galilean frame of reference is governed by the following partial differential equations which express the fundamental principles of classical mechanics and thermodynamics for mass conservation (eq. 2.1), momentum change (eq. 2.2) and energy change (eq. 2.3) in a continuous medium :

$$\frac{\partial \rho}{\partial t} + \operatorname{div}(\rho \vec{V}) = 0 \tag{2.1}$$

$$\frac{\partial}{\partial t}(\rho \vec{V}) + \operatorname{div}(\rho \vec{V}\vec{V} - \underline{\underline{\sigma}}) = \vec{f_e} \tag{2.2}$$

$$\frac{\partial}{\partial t}(\rho E) + \operatorname{div}(\rho E \vec{V} - \underline{\underline{\sigma}}\,\vec{V} + \vec{q}) = \vec{f_e}\cdot\vec{V} . \tag{2.3}$$

In these equations, t is the time, ρ the density, $\vec{V}$ the fluid velocity, and E the total specific energy : $E = e + \vec{V}^2/2$ where e is the specific internal energy; $\underline{\underline{\sigma}}$ is the stress tensor, $\vec{q}$ is the heat flux vector, and $\vec{f_e}$ is the external force per unit volume.

Equations (2.1) to (2.3) are said to correspond to the Eulerian description of the fluid motion : flow properties are defined as functions of time and of space coordinates in the frame of reference. An alternative description is provided by the Lagrangian formulation in which one considers properties of fluid particles followed in their motion : flow properties are defined as functions of time and of parameters used to identify fluid particles (usually the coordinates of the particle at some initial time). The Lagrangian formulation can be useful for particular problems, especially those involving interfaces; however it is not so widely used as the Eulerian formulation and it will not be considered here.

To close the system of equations (2.1) to (2.3), one must add constitutive relationships for the stress tensor $\underline{\underline{\sigma}}$ and for the heat flux vector $\vec{q}$. Usual fluids, such as air and water, in ordinary conditions follow Fourier's heat conduction law for $\vec{q}$ and Newton's law (or Navier-Stokes' law) for $\underline{\underline{\sigma}}$:

$$\vec{q} = -k\,\operatorname{grad} T \tag{2.4}$$

$$\begin{cases} \underline{\underline{\sigma}} = -p\,\underline{\underline{I}} + \underline{\underline{\tau}} & (\underline{\underline{I}} = \text{unit tensor}) \\ \underline{\underline{\tau}} = \lambda \operatorname{div}\vec{V}\,\underline{\underline{I}} + \mu\,\operatorname{def}\vec{V} & (\operatorname{def}\vec{V} = \operatorname{grad}\vec{V} + (\operatorname{grad}\vec{V})^T) \end{cases} \tag{2.5}$$

where T is the absolute temperature and p is the pressure; k is the thermal conductivity coefficient, and λ and μ are the two coefficients of viscosity.

Fluids which follow Fourier's law and Newton's law are said to be Newtonian; the Navier-Stokes* equations are the general equations of motion for Newtonian fluids, i.e. equations (2.1) to (2.5). These equations must be complemented by thermodynamic relations connecting the thermodynamic variables, ρ, e, T and p. In the case of a simple fluid, the thermodynamic state of a fluid particle can be defined by the two variables ρ and e, and all the thermodynamic properties of the fluid (assuming local thermodynamic equilibrium) can be deduced from a single fundamental relation such as :

$$S = S(\rho, e)$$

where S is the specific entropy. In particular the pressure p and the temperature T can be calculated in terms of ρ and e :

(2.6) $$p = p(e,\rho) \quad , \quad T = T(e,\rho).$$

A particular, but important, case is that of a perfect gas with constant specific heats, for which (2.6) is :

(2.7) $$p = (\gamma - 1)\rho e \quad , \quad e = C_v T$$

where $\gamma = \frac{C_p}{C_v}$ and C_p, C_v are the specific heats.

The viscosity and thermal conductivity coefficients depend on the local thermodynamic state; in usual conditions they depend only on the temperature :

(2.8) $$k = k(T) \quad , \quad \lambda = \lambda(T) \quad , \quad \mu = \mu(T).$$

It can be shown from the second law of thermodynamics that λ and μ must verify the following conditions :

(2.9) $$3\lambda + 2\mu \geq 0 \quad ; \quad \mu \geq 0.$$

In the absence of internal relaxation phenomena which would involve departure from local thermodynamic equilibrium, Stokes' relation is considered to hold :

(2.10) $$3\lambda + 2\mu = 0.$$

The system of equations (2.1) to (2.10) is then closed, in the sense that there are as many equations as unknowns. The basic unknowns, in terms of which all other dependent variables can be expressed, are ρ, $\rho\vec{V}$ (or $\vec{V}$), and ρE (or E, or e). Note that this system is in the normal form with respect to time, i.e. the time derivatives of the basic unknowns are explicitly given in terms of their spatial derivatives. Another feature of equations (2.1) to (2.3) is their divergence, or conservative, form which results directly from the application of the fundamental conservation laws to a finite fluid system.

The unsteady compressible N.S. equations are of hybrid parabolic-hyperbolic type, while in the steady state they are of elliptic-hyperbolic type. To let the nature of these equations show up, we develop the space derivatives of highest order (i.e. second order). The momentum equation, neglecting external forces, can be written :

(2.11) $$\rho \frac{D\vec{V}}{Dt} + \operatorname{grad} p = \lambda'(T)\operatorname{div}\vec{V}\operatorname{grad}T + \mu'(T)\operatorname{grad}T \operatorname{def}\vec{V} + \mathcal{L}\vec{V}$$

where $\mathcal{L}$ is a second-order differential operator :

$$\mathcal{L}\vec{V} = \mu\Delta\vec{V} + (\lambda+\mu)\operatorname{grad}(\operatorname{div}\vec{V})$$

and where $D/Dt = \partial/\partial t + \vec{V}.\operatorname{grad}$ is the material derivative. It is easily verified that the operator $\mathcal{L}$ is elliptic except if $\lambda + 2\mu = 0$ but from conditions (2.9), $\lambda + 2\mu$ must be positive. Equation (2.11) for the unknown $\vec{V}$ is parabolic with respect to time. Similarly, the energy equation expressed in terms of T instead of E, assuming a perfect gas with constant specific heats, becomes :

(2.12) $$\rho C_v \frac{DT}{Dt} + p\operatorname{div}\vec{V} = \Phi + k(T)(\operatorname{grad}T)^2 + k\Delta T$$

and it is parabolic with respect to time. Φ is the dissipation function :

(2.13) $$\Phi = \underline{\underline{\tau}}.\operatorname{grad}\vec{V} = \lambda(\operatorname{div}\vec{V})^2 + \frac{1}{2}\mu \operatorname{def}\vec{V}.\operatorname{def}\vec{V}.$$

Note also that the left-hand side of (2.12) is equal to $\rho T \frac{DS}{Dt}$ where S is the specific entropy.

Expressions (2.11) and (2.12) of the momentum and energy equations show that these equations are quasi-linear, i.e. they are linear with respect to the second order derivatives of $\vec{V}$ and T respectively.

The continuity equation (2.1) can be written :

(2.14) $$\frac{D}{Dt}\ln\rho + \operatorname{div}\vec{V} = 0.$$

Considered as a first order equation for the unknown ρ, its characteristic base curves are the trajectories of fluid particles.

Problems to be solved in practice are either mixed initial and boundary-value problems or time-independent boundary-value problems, and there does not seem to exist rigourous mathematical results concerning the boundary conditions to impose in order to insure existence and unicity of the solution. One should resort to physical intuition and take into account the mathematical nature of the equations; the latter indicates that on any boundary one should be given one scalar condition for each scalar momentum equation and one condition for the energy equation; the simplest conditions are $\vec{V}$ and T given. An additional condition for ρ should be given only if the fluid enters the computational domain through the boundary.

The usual physical conditions on a solid impermeable wall for viscous fluids are that the relative velocity of the fluid with respect to the wall be zero and that the fluid and the wall be at the same temperature. In general one considers either that the wall temperature T_w is given or that the heat flux at the wall, q_w, is given; the boundary conditions are then :

(2.15) $$\vec{V}_t = \vec{V} - \vec{V}_w = 0$$

where $\vec{V}_w$ is the velocity of a given material point of the wall, and

(2.16) $$\begin{cases} T = T_w \\ \text{or} \\ -k\frac{\partial T}{\partial n} = q_w \quad (= 0 \text{ for an adiabatic wall}). \end{cases}$$

The above conditions must be modified in the so-called slip-flow regime when slight rarefaction effects come into play through the boundary conditions at the wall without invalidating the N.S. equations in the flow field; there exists then a tangential slip velocity and a temperature jump at the wall, given by the kinetic theory of gases :

(2.17) $$\begin{cases} V_t = C_1 \ell \frac{\partial V_t}{\partial n} + C_2 a\ell \frac{1}{T}\frac{\partial T}{\partial t} \\ T - T_w = C_3 \frac{\ell}{P_r}\frac{\partial T}{\partial n} \quad (P_r = \frac{\mu C_p}{k} = \text{Prandtl number}) \end{cases}$$

where $\partial/\partial n$ and $\partial/\partial t$ are respectively the normal and tangential derivatives at the wall, ℓ is the molecular mean free path, a the sound speed; C_1, C_2 and C_3 are dimensionless constants which depend on the laws of interaction of the molecules with the wall. Concerning the connection between the kinetic theory of gases and gas dynamics, one can consult, for example, ref. [1] and [2].

To close these general considerations, and for reference purposes, we consider the expressions of the N.S. equations a) in dimensionless vectorial form, and b) in dimensionless form in a cartesian coordinate system for two-dimensional flows. We neglect external forces and we assume a perfect gas with constant specific heats.

a) The only characteristic quantities which need be used to define dimensionless variables are :
a length L, a velocity V^*, a density ρ^*, values μ^* and k^* of the coefficients of viscosity and thermal conductivity. From these, other reference quantities are derived : L/V^* for the time t, $\rho^* V^{*2}$ for the pressure, and V^{*2} for the total energy E and for the internal energy e.

---

* Hereafter we shall abbreviate «Navier-Stokes» by the initials N.S.

Using the same notations as previously for the dimensionless variables, the equations (2.1) to (2.3) remain unchanged in dimensionless form. The constitutive relationships (2.4) and (2.5) become

$$(2.18)\quad \begin{cases} \vec{q} = -\dfrac{\gamma}{R_e P_r}\, k\, \mathrm{grad}\, e \\ \underline{\tau} = -p\, \underline{I} + \dfrac{1}{R_e}\, \underline{\tau} \\ \underline{\tau} = \lambda\, \mathrm{div}\, \vec{V}\, \underline{I} + \mu\, \mathrm{def}\, \vec{V} \end{cases}$$

where $R_e = \dfrac{V^* L \rho^*}{\mu^*}$ is a characteristic Reynolds number

and $P_r = \dfrac{\mu^* C_p}{k^*}$ is a characteristic Prandtl number.

If a characteristic temperature T^* is used to define a dimensionless temperature T, the laws of state (2.7) become :

$$(2.19)\quad \begin{cases} p = (\gamma - 1)\, \rho e & \text{(unchanged)} \\ e = \dfrac{1}{\gamma(\gamma-1) M^{*2}}\, T \end{cases}$$

where $M^* = \sqrt{\dfrac{V^*}{\gamma R T^*}}$ is a characteristic Mach number.

If we choose $T^* = V^{*2}/C_v$, we get simply $e = T$. Other parameters will enter the problem through the boundary conditions (e.g. ratio of wall temperature to free-stream temperature) and also through the laws used for $\mu(T)$ and $k(T)$.

b) The N.S. equations for two-dimensional flow can be written in a cartesian coordinate system (coordinates x, y, velocity components u, v) in the following form :

$$(2.20)\quad \frac{\partial W}{\partial t} + \frac{\partial F}{\partial x} + \frac{\partial G}{\partial y} = \frac{1}{R_e}\left(\frac{\partial F_1}{\partial x} + \frac{\partial G_1}{\partial y} \right)$$

where W, F, G, F_1 and G_1 are 4-component vectors : the first components correspond to the continuity equation (2.1); the second and third components correspond to the projections of the momentum equation (2.2) on the x and y axis respectively; and the fourth components yield the energy equation (2.3).

$$(2.21)\quad W = \begin{vmatrix} \rho \\ \rho u \\ \rho v \\ \rho E \end{vmatrix},\quad F = \begin{vmatrix} \rho u \\ \rho u^2 + p \\ \rho u v \\ (\rho E + p) u \end{vmatrix},\quad G = \begin{vmatrix} \rho v \\ \rho u v \\ \rho v^2 + p \\ (\rho E + p) v \end{vmatrix}$$

$$(2.22)\quad F_1 = \begin{vmatrix} 0 \\ \tau_{xx} \\ \tau_{xy} \\ \dfrac{\gamma}{P_r} k \dfrac{\partial e}{\partial x} + u\tau_{xx} + v\tau_{xy} \end{vmatrix},\quad G_1 = \begin{vmatrix} 0 \\ \tau_{xy} \\ \tau_{yy} \\ \dfrac{\gamma}{P_r} k \dfrac{\partial e}{\partial y} + u\tau_{xy} + v\tau_{yy} \end{vmatrix}$$

with

$$\tau_{xx} = (\lambda + 2\mu) \frac{\partial u}{\partial x} + \lambda \frac{\partial v}{\partial y}$$

$$\tau_{xy} = \mu \left(\frac{\partial u}{\partial y} + \frac{\partial v}{\partial x} \right)$$

$$\tau_{yy} = (\lambda + 2\mu) \frac{\partial v}{\partial y} + \lambda \frac{\partial u}{\partial x}.$$

With Stokes' assumption $3\lambda + 2\mu = 0$ we have :

$$\tau_{xx} = \frac{2}{3}\mu \left(2 \frac{\partial u}{\partial x} - \frac{\partial v}{\partial y} \right)$$

$$\tau_{yy} = \frac{2}{3}\mu \left(2 \frac{\partial v}{\partial y} - \frac{\partial u}{\partial x} \right).$$

3. Interest of the Navier-Stokes equations

To briefly discuss the practical interest of the N.S. equations in aerodynamics, it is convenient to distinguish between two broad classes of flow fields according to the order of magnitude of a characteristic Reynolds number.

If the Reynolds number is large, the flow field is made up of regions which, to a great extent, can be described either by Euler's equations for inviscid flow, or by Prandtl's equations for boundary-layer flow. However the N.S. equations remain usually needed for the description of the flow in local zones where the above approcimations fail; the existence of such zones is the rule rather than the exception in the flow fields encountered in practice. These N.S. regions, although they may be of small extent, usually have an important influence over the complete flow, and they are an essential feature of the flow field for the determination of a unique solution. Figure 1 shows some classical examples of N.S. regions imbedded in large Reynolds number flows.

Large Reynolds number flows are likely to be turbulent, and this is indeed the most usual case in aeronautical applications. The N.S. equations remain valid for turbulent flows, but the numerical prediction of such flows with existing methods and computers cannot be based on the computation of the turbulent fluctuations from the exact un-

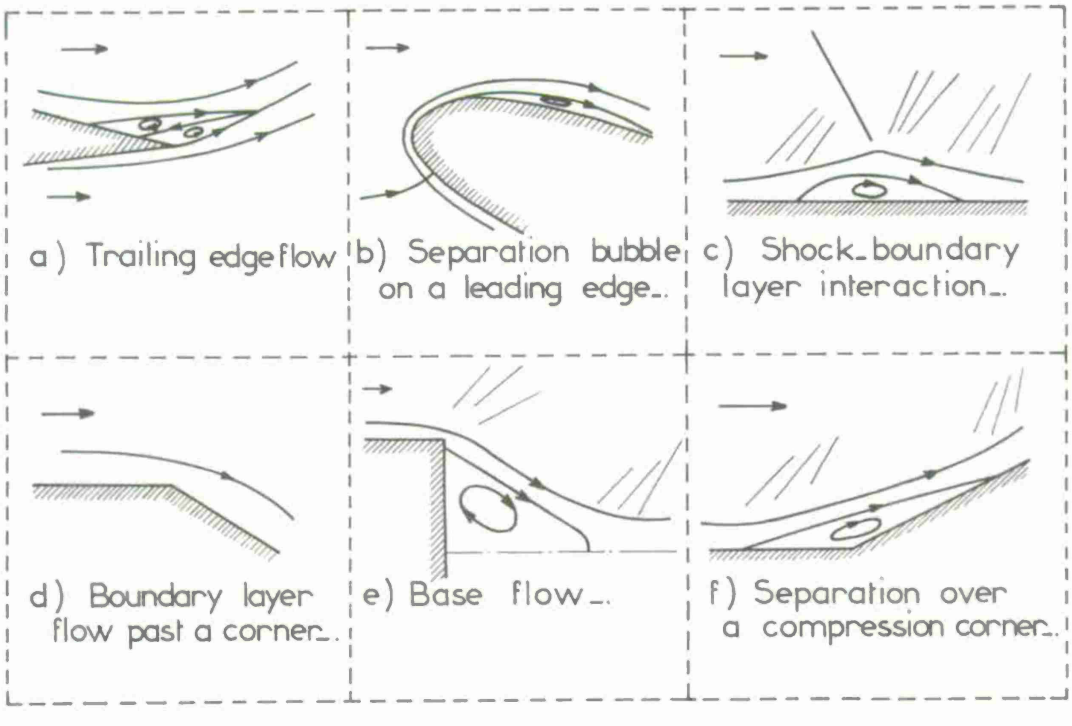

Fig. 1 – Navier-Stokes regions in large Reynolds number flows.

steady N.S. equations, because these fluctuations involve very small time and space scales. As is well known, one must consider the time-averaged (or ensemble-averaged) N.S. equations for the determination of the mean motion, complemented by additional relations or differential equations for the various correlation terms in order to close the system of the averaged equations. This set of additional equations, which constitutes a turbulence model, is necessarily largly empirical. Thus although the N.S. equations present the same importance for turbulent flows as for laminar flows for a correct description of flow phenomena in local zones, their practical interest is linked to the validity of the turbulence model which is used. The particular aspects of the numerical calculation of turbulent flows will not be considered in this paper.

On the other hand, if the Reynolds number is low enough, as for example in flows about small obstacles or in the first phase of atmospheric reentry, then viscous effects are nowhere negligible and the entire flow field must be described by the N.S. equations.

An intermediate situation is that of a flow in which it is possible to identify regions where dissipative effects are negligible, i.e. quasi-inviscid regions, but in which the other viscous regions cannot be described by the boundary-layer approximation, because they are very thick and they interact strongly with the inviscid flow regions. In that case the N.S. equations are needed only in these viscous regions, but the interaction with the inviscid flow should be properly taken into account in the numerical method. Such a situation, which occurs at moderate Reynolds number, is illustrated on figure 2 in the case of supersonic flows about a blunt body and about a slender body; the viscous regions are indicated by shaded areas. When the Reynolds number decreases the viscous regions extend until they occupy the entire flow field, merging with the bow shock wave. At still lower Reynolds numbers, the shock-thickness cannot be considered negligible on a macroscopic scale, and one reaches conditions which stand at the limit of validity of the N.S. equations.

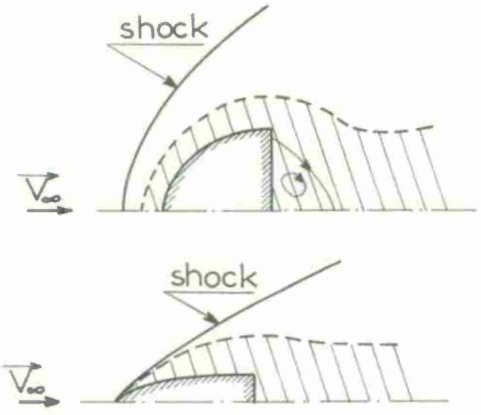

Fig. 2 – Moderate Reynolds number flows.

4. The computation domain

Finite-difference methods operate over a finite number of calculation points, so that the computation domain must always be a bounded domain. How to define this domain is the first question which arises in the setting-up of a numerical method, the second question being that of the conditions to be imposed on the boundaries.

Part of the boundary is given by the physics of the problem (wall, axis of symmetry .....), but-excluding cavity type flows- it is always necessary to define an out er non physical boundary in a more or less arbitrary fashion.

a) Consider first the case of a N.S. region imbedded in a large Reynolds number flow. By definition this region is bounded, and the only requirement is that it should extend over sufficient distances so as to overlap the adjacent inviscid flow region or boundary layer flow region; of course some preliminary knowledge of the problem to be solved is necessary in that case for the definition of the N.S. region. Figure 3 shows two examples of N.S. regions which might be used in a shock-boundary layer interaction (fig. 3 a) and in a base flow problem (fig. 3 b). The outer boundary ABCD separates the N.S. region from the inviscid flow region (1) and from the boundary layer flow regions (2) and (3). The conditions to be applied on this outer boundary should express the matching between the solution of the N.S. equations in the N.S. region and the solutions of the approximate equations used in the adjacent regions. Of course the solutions in region (1), (2) and (3) depend on other boundary conditions to be imposed on the outer boundaries of these regions. In general the matching conditions on the boundary ABCD can be satisfied only through an iterative procedure. However, in some cases, the calculation of the solution in the N.S. region is uncoupled from the solutions in the external regions. This is the case in the two examples of figure 3 if the inviscid flow in region (1) is supersonic and is made of simple wave flows along A'BC (fig. 3 a) or along BC (fig. 3 b).

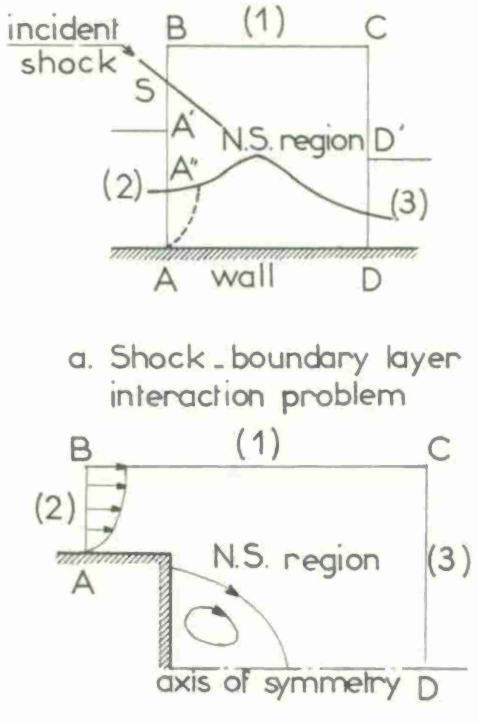

Fig. 3 – Computational domains for Navier-Stokes regions.

Thus, in the shock-boundary layer problem (fig. 3 a) considered in [3] and [4], the flow quantities are held fixed along AB and BC : a boundary layer profile is given on AA" and uniform flows along A"S, SB and BC, compatible with the incident given shock. Along DC, the flow quantities are equated to the values computed at the next previous column of points; this is an approximate way of expressing the condition that the flow downstream of DC does not influence the flow in the N.S. region since the N.S. solution merges in an inviscid supersonic flow along D'C and in a boundary layer flow along DD'.

For the base flow problem (fig. 3 b) computed in [5], the boundary conditions along ABCD are the following ones : a boundary layer profile is imposed on AB, an extrapolation of the flow quantities is used on DC; finally, the flow in (1) along BC is assumed to be inviscid and to be represented by a simple wave so that the flow quantities on BC are obtained by continuations along characteristic lines from points inside the N.S. region.

b) Consider now the case when the entire flow field is computed by means of the N.S. equations and when steady uniform flow conditions are imposed at infinity. Different techniques can be used. First, it is possible to use a coordinate transformation which maps the entire physical plane (assuming two-dimensional flow) into a finite domain in the transformed plane where the computation will be carried out; images of the points at infinity in the physical plane form a portion of the boundary (which can be called the outer boundary) of the computation

domain. An example of such a method is the classical conformal mapping of the exterior of a profile into the interior of a circle, the computation plane being the (r , θ) plane where r , θ are polar coordinates in the plane of the circle (fig. 4).

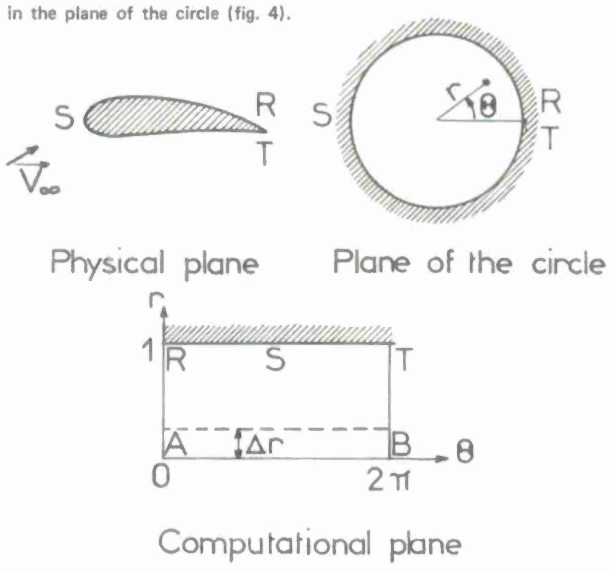

Fig. 4 — Conformal mapping of a profile into a circle.

The image of infinity is the center of the circle, so that the outer boundary in the computational domain is the segment AB ($r = 0$, $0 \leq \theta \leq \pi$); flow quantities are given on this outer boundary. Note that the first mesh between $r = 0$ and $r = \Delta r$ corresponds to an infinite mesh in the physical plane; differencing accross this first mesh will not cause problems in general if the dependent variables are bounded at infinity.

This method works as long as the flow quantities on the first line $r = \Delta r$ are close enough to the uniform flow conditions, so that it is not very much different from a second technique in which an outer boundary is chosen at a large but finite distance and the uniform flow conditions at infinity are imposed on this boundary.

A third technique, illustrated on figure 5 (flow around a finite body delimited by two arcs of parabolas [6]), consists in choosing an outer boundary at a finite distance and in dividing this boundary into two parts* : on the upstream part BAD (through which the fluid enters the domain of calculation) one imposes the uniform flow conditions at infinity; on the downstream part BCD (through which the fluid leaves the domain of calculation) condition of a more empirical nature are imposed, e.g. extrapolation.

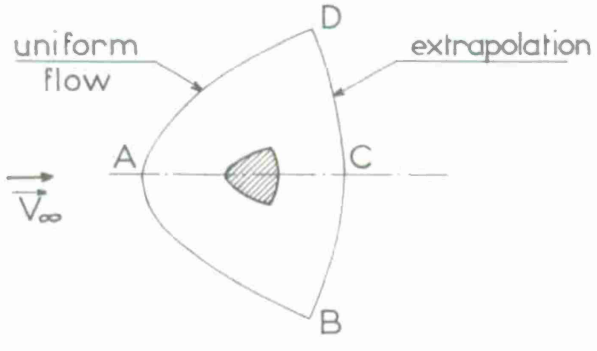

Fig. 5 — Artificial limitation of the computational domain.

The physical justification of this technique is that the downstream part of the boundary is too close to the body for the flow to reach again the same conditions as at upstream infinity, but far enough for its upstream influence to be small.

A fourth technique is similar to the one discussed for the case of a finite N.S. region : the outer boundary is chosen at a finite but large enough distance so that the flow outside this boundary can be calculated by means of a small perturbation analysis; this outer solution depends on unknown constants (the first constants to appear in this analysis are related to aerodynamic force and moment) which must be determined by matching with the flow field calculated inside the boundary. This technique is the most rigourous from a mathematical point of view but, probably because of its complexity, it does not seem to have been used for the compressible N.S. equations.

It was implicitly assumed in the preceding discussion that the flow perturbations were felt far away in all directions; this is not the case for a body in a supersonic flow, the flow field remaining unperturbed upstream of a bow shock wave. The computation domain can then be limited either by a boundary located at a short distance upstream of the bow shock or by the bow shock itself, depending on whether the shock is treated as a sharp but continuous transition zone (shock-capturing method) or as a true discontinuity (shock-fitting method). If the upstream boundary is taken upstream of the shock uniform flow conditions are used as boundary conditions. If the shock itself is used as upstream boundary, the determination of the shock position and of the flow quantities behind the shock require more elaborate methods.

5. Finite-difference methods

5.1. Generalities : various approaches

Apart from a few integral methods [7], [8], all other methods used for solving the compressible N.S. equations are finite-difference methods. Some of them, for example [9] [10] [11], consider the steady two-dimensional equations associated with the vorticity-stream function formulation. The discussion here will be limited to unsteady or « pseudo-unsteady » methods for the solution of the N.S. equations written in terms of the primary dependent variables as described in section 2.

When the flow to be computed is unsteady, the numerical scheme must obviously be consistent with the exact unsteady equations, and it must be accurate enough in time as well as in space (second order in general).

On the other hand, various approaches can be considered for the computation of steady flows :

a) In the first approach the unsteady N.S. equations (2.20) are solved by a finite difference scheme consistent (with or without condition) with these unsteady equations. The steady solution is obtained in the limit $t \to \infty$. The initial condition can be arbitrary. In the case when the initial condition is physically realistic and if the boundary conditions are treated in a consistent way with respect to the unsteady problem, the transient solution has a physical meaning and the physical interpretation of the problem may allow an easier control of the results during the transient stage. If the initial condition is physically unrealistic and/or the boundary conditions compatible with the steady problem only, the transient solution has no physical meaning. In this case the use of the unsteady equations appears as a device to build an iterative procedure for the solution of the steady equations :

$$\frac{\partial F}{\partial x} + \frac{\partial G}{\partial y} = \frac{1}{R_e}\left(\frac{\partial F_1}{\partial x} + \frac{\partial G_1}{\partial y}\right) \tag{5.1}$$

and the time step Δt can be interpreted as a convergence parameter.

b) If we do not require the transient solution to have a physical meaning, it is not necessary that the scheme used be consistent with the unsteady equations. The only requirement for the scheme is to give a steady solution when $t \to \infty$ which must be an approximation to the solution of the steady equation (5.1); hence the scheme must become consistent with (5.1) when convergence is reached. This pseudo-unsteady approach was suggested by Crocco [12].

The eventual advantages to be looked for in constructing a non consistent scheme are : (i) a stability criterion which allows a larger time step than with a consistent scheme, (ii) a faster convergence to the steady state.

c) Going a step further in the pseudo-unsteady nature of the method we can try to obtain a faster convergence and/or a larger time step by modifying the unsteady equations themselves, i.e. by replacing

* We must assume that a streamline cuts the boundary only in two points.

the vector W by another vector W^* and by solving the pseudo-unsteady system :

$$\frac{\partial W^*}{\partial t} + \frac{\partial F}{\partial x} + \frac{\partial G}{\partial y} = \frac{1}{R_e}\left(\frac{\partial F_1}{\partial x} + \frac{\partial G_1}{\partial y}\right). \tag{5.2}$$

For the solution of (5.2) it is possible to use again a non consistent scheme.

Such an approach was used in [6] for the computation of a flow field with a base flow region. With the exact W, i.e. $W=(\rho,\rho u,\rho v,\rho E)^T$ the scheme used [see eq. (5.22)] leads to a stability criterion of the type : $\Delta t \approx R_e \rho \Delta x^2$. In the base region, the density ρ becomes very small; as a consequence the maximum allowable time step Δt is so small that the computation becomes impracticable. By simply choosing $W^* = (\rho, u, v, T)^T$ the associated stability criterion is independent of ρ and the above difficulty is avoided.

The determination of a non physical W^* in view of obtaining a fast convergence of the solution of (5.2) is much more difficult, and it has not yet been carried out except in special cases : for example, the idea was used in [13] for a one-dimensional incompressible boundary layer flow.

In the next section, we present some representative finite difference schemes which have been effectively applied for computation of viscous compressible flows. Some of them are consistent with the unsteady equations, and others not. For simplicity, the schemes are presented with model scalar equation :

$$\frac{\partial u}{\partial t} + \frac{\partial}{\partial x} f(u) = \varepsilon \frac{\partial^2 u}{\partial x^2} \quad , \quad \varepsilon > 0 . \tag{5.3}$$

The following notation is used :

$$A(u) = \frac{d}{du} f(u) \tag{5.4}$$

$$\begin{cases} x_i = i\,\Delta x,\ t_n = n\,\Delta t, & i \text{ and } n \text{ are integers},\ \Delta x>0,\ \Delta t>0 \\ u_i^n = u(x_i, t_n)\ ,\ f_i^n = f(u_i^n)\ ,\ \tilde{f}_i^n = f(\tilde{u}_i^n) \end{cases} \tag{5.5}$$

$$\sigma = \frac{\Delta t}{\Delta x} \quad , \quad \nu = \varepsilon \frac{\Delta t}{\Delta x^2} . \tag{5.6}$$

5.2. Schemes consistent with the unsteady equations

5.2.1. One-step explicit method (Victoria-Widhopf [14])

This is a leap-frog Du Fort Frankel scheme :

$$u_i^{n+1} = u_i^{n-1} - \sigma\left(f_{i+1}^n - f_{i-1}^n\right) + 2\nu\left[u_{i+1}^n - \left(u_i^{n+1} + u_i^{n-1}\right) + u_{i-1}^n\right]. \tag{5.7}$$

The principal part of the truncation error is $\varepsilon\sigma^2(\partial^2 u/\partial t^2)$ therefore the consistency is obtained if $\varepsilon\sigma^2 = o(1)$ when $\Delta t, \Delta x \to 0$. At steady state the accuracy is $O(\Delta x^2)$. A linear stability analysis, assuming $A = df/du = \text{const.}$, yields the Courant-Friedrichs-Lewy (CFL) condition :

$$|A|\,\sigma \leq 1 . \tag{5.8}$$

The curve (1) of figure 6 shows the domain of stability in the plane $(|A|\,\Delta x/\varepsilon\ ,\ \varepsilon\Delta t/\Delta x^2)$.

This scheme possesses the interesting property to have a stability criterion independent of the viscosity ε ; however if $\varepsilon = 0$, the resulting (leap-frog) scheme is nonlinearly unstable, as it is well known [15]. Note that the theoretical consistency of the scheme during the transient stage implies the use of a much smaller time step than the one allowed by (5.8).

5.2.2. One-step implicit method (Briley-MacDonald [16])

This method is based on an implicit discretization of the equation (5.3) associated with a technique of linearization of the nonlinear term $\partial f/\partial x$. The discretization in time is

$$\frac{u_i^{n+1} - u_i^n}{\Delta t} + \left(\frac{\partial f}{\partial x}\right)_i^{n+1} = \varepsilon\left(\frac{\partial^2 u}{\partial x^2}\right)_i^{n+1} . \tag{5.9}$$

The term $(\partial f/\partial x)_i^{n+1}$ is expanded as :

$$\left(\frac{\partial f}{\partial x}\right)_i^{n+1} = \left(\frac{\partial f}{\partial x}\right)_i^n + \Delta t\left[\frac{\partial}{\partial t}\left(\frac{\partial f}{\partial x}\right)\right]_i^n + O(\Delta t^2) \tag{5.10}$$

now

$$\frac{\partial}{\partial t}\left(\frac{\partial f}{\partial x}\right) = \frac{\partial}{\partial x}\left(\frac{\partial f}{\partial t}\right) = \frac{\partial}{\partial x}\left(\frac{df}{du}\frac{\partial u}{\partial t}\right) = \frac{\partial}{\partial x}\left(A\frac{\partial u}{\partial t}\right). \tag{5.11}$$

Finally, by bringing (5.11) and (5.10) into (5.9) and approximating the derivatives we get the scheme :

$$u_i^{n+1} - u_i^n + \frac{\sigma}{2}\left(f_{i+1}^n - f_{i-1}^n\right) + \frac{\sigma}{2}\left[A_{i+1}^n\left(u_{i+1}^{n+1} - u_{i+1}^n\right) - A_{i-1}^n\left(u_{i-1}^{n+1} - u_{i-1}^n\right)\right] - \nu\left(u_{i+1}^{n+1} - 2u_i^{n+1} + u_{i-1}^{n+1}\right) = 0 \tag{5.12}$$

which is a linear finite difference equation of the general form :

$$a_i^n u_{i-1}^{n+1} + b_i^n u_i^{n+1} + c_i^n u_{i+1}^{n+1} = d_i^n . \tag{5.13}$$

This equation corresponds to a tridiagonal matrix which can be easily inverted by the technique of factorization (Gaussian elimination).

The scheme (5.12) is first order accurate in time and second order in space (second order at steady state). For the calculation of unsteady flows the accuracy in time can be increased up to second order by using a Crank-Nicholson discretization in (5.9) :

$$\frac{u_i^{n+1} - u_i^n}{\Delta t} + \frac{1}{2}\left[\left(\frac{\partial f}{\partial x}\right)_i^{n+1} + \left(\frac{\partial f}{\partial x}\right)_i^n\right] = \frac{\varepsilon}{2}\left[\left(\frac{\partial^2 u}{\partial x^2}\right)_i^{n+1} + \left(\frac{\partial^2 u}{\partial x^2}\right)_i^n\right]. \tag{5.14}$$

Because of its implicit character the scheme (5.12) is linearly stable without condition; however the application of the technique of factorization to the solution of (5.13) may impose some limitation on the coefficients of (5.13) (diagonally dominant matrix).

In [16] the method is extended to multi-dimensional N.S. equations by using an alternating direction implicit technique (Douglas-Gunn [17]). For three-dimensional flows the problem reduces to the solution of a 3 X 3 block-tridiagonal system and of two simple tridiagonal systems. The solution of these systems requires about one third to one half of the total computer time per time step; but the computation can be done with a very large time step Δt (in some cases, up to 1250 times the Δt given by the C.F.L. condition).

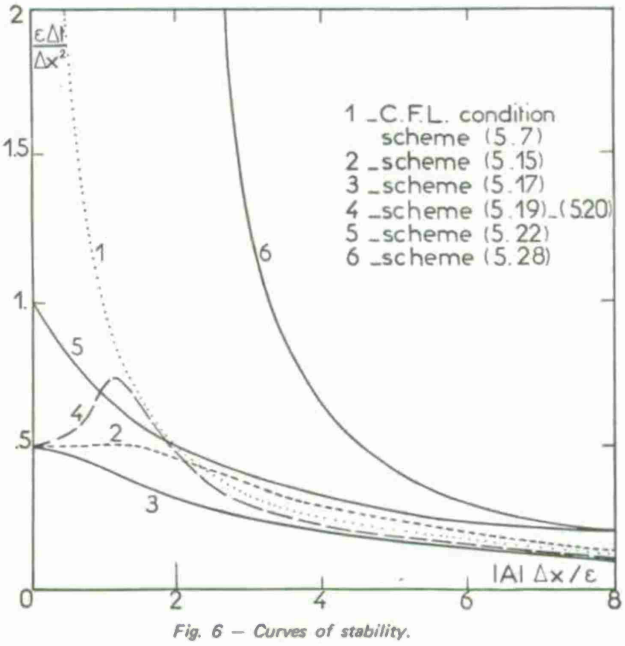

Fig. 6 — Curves of stability.

5.2.3. Two-step explicit methods

a) Brailovskaya [18].

The two-step explicit scheme proposed by Brailovskaya is the following one :

$$\text{(5.15 a)}\quad \tilde{u}_i^{n+1} = u_i^n - \frac{\sigma}{2}\left(f_{i+1}^n - f_{i-1}^n\right) + \nu\left(u_{i+1}^n - 2u_i^n + u_{i-1}^n\right)$$

$$\text{(5.15 b)}\quad u_i^{n+1} = u_i^n - \frac{\sigma}{2}\left(\tilde{f}_{i+1}^{n+1} - \tilde{f}_{i-1}^{n+1}\right) + \nu\left(u_{i+1}^n - 2u_i^n + u_{i-1}^n\right).$$

The accuracy is $O(\Delta t + \Delta x^2)$ during the transient state, $O(\Delta x^2)$ in the steady state. The stability criterion given in [18] is :

$$\text{(5.16)}\quad \Delta t \leq \mathrm{Min}\left\{\frac{\Delta x^2}{4\varepsilon}\,,\ \frac{\Delta x}{|A|}\right\}.$$

The study of the amplification factor for the scheme (5.15) with A = const. is very complicated, and it can only be shown that (5.16) is a sufficient condition. In fact, by doing a numerical study of the amplification factor, we found (5.16) to be too restrictive : the curve (2) of fig. 6 shows the domain of stability obtained numerically. Note that $\Delta t \approx \Delta x^2$ when $\varepsilon \approx 1$, so that the accuracy is of second order even during the transient state.

b) Thommen [19]

Some of the methods used for solving the equations of motion of viscous fluids are direct extensions of methods primarily devised for inviscid flows. So, the two-step Lax-Wendroff-Richtmyer scheme [15] has been extended to the N.S. equations by Thommen [19] in the following manner :

$$\text{(5.17 a)}\quad \tilde{u}_{i+\frac{1}{2}}^{n+\frac{1}{2}} = \frac{1}{2}\left(u_{i+1}^n + u_i^n\right) \mp \frac{\sigma}{2}\left(f_{i+1}^n - f_i^n\right) + \frac{\nu}{4}\left[\left(u_{i+2}^n - 2u_{i+1}^n + u_i^n\right) + \left(u_{i+1}^n - 2u_i^n + u_{i-1}^n\right)\right]$$

$$\text{(5.17 b)}\quad u_i^{n+1} = u_i^n - \sigma\left(\tilde{f}_{i+\frac{1}{2}}^{n+\frac{1}{2}} - \tilde{f}_{i-\frac{1}{2}}^{n+\frac{1}{2}}\right) + \nu\left(u_{i+1}^n - 2u_i^n + u_{i-1}^n\right).$$

The accuracy is $O(\varepsilon\Delta t + \Delta x^2)$ during the transient state, $O(\Delta x^2)$ at steady state and the exact linear stability criterion (curve (3) of fig. 6) is

$$\text{(5.18)}\quad A^2\sigma^2 + 2\nu \leq 1.$$

From (5.18) we deduce that the effective accuracy with respect to time, $O(\varepsilon\Delta t)$, is higher than first order : if $\varepsilon \approx 1$ then $\Delta t \approx \Delta x^2$ and if $\varepsilon \ll 1$, then $\varepsilon\Delta t \ll \Delta t$

c) MacCormack [20].

In one-dimension, there are two variants of MacCormack scheme :

1) The forward-backward scheme :

$$\text{(5.19 a)}\quad \tilde{u}_i^{n+1} = u_i^n - \sigma\left(f_{i+1}^n - f_i^n\right) + \nu\left(u_{i+1}^n - 2u_i^n + u_{i-1}^n\right)$$

$$\text{(5.19 b)}\quad u_i^{n+1} = \frac{1}{2}\left(u_i^n + \tilde{u}_i^{n+1}\right) - \frac{\sigma}{2}\left(\tilde{f}_i^{n+1} - \tilde{f}_{i-1}^{n+1}\right) + \frac{\nu}{2}\left(\tilde{u}_{i+1}^{n+1} - 2\tilde{u}_i^{n+1} + \tilde{u}_{i-1}^{n+1}\right)$$

2) The backward-forward scheme :

$$\text{(5.20 a)}\quad \tilde{u}_i^{n+1} = u_i^n - \sigma\left(f_i^n - f_{i-1}^n\right) + \nu\left(u_{i+1}^n - 2u_i^n + u_{i-1}^n\right)$$

$$\text{(5.20 b)}\quad u_i^{n+1} = \frac{1}{2}\left(u_i^n + \tilde{u}_i^{n+1}\right) - \frac{\sigma}{2}\left(\tilde{f}_{i+1}^{n+1} - \tilde{f}_i^{n+1}\right) + \frac{\nu}{2}\left(\tilde{u}_{i+1}^{n+1} - 2\tilde{u}_i^{n+1} + \tilde{u}_{i-1}^{n+1}\right)$$

The truncation errors for the two variants are of same order $O(\Delta t^2 + \Delta x^2)$, but their expressions are different. In the inviscid case ($\varepsilon = 0$), with $f = u^2/2$, a study [21] of the truncation errors has shown why (5.19) can give shock profiles without oscillation when the shock propagates toward the right ($x > 0$) whereas (5.20) has the same property in the reverse case.

An approximate stability condition has been given in [22] :

$$\text{(5.21)}\quad \begin{cases} A^2\sigma^2 - 4\nu^2 + 2\nu \geq 0 & \text{if } A^2\sigma^2 - 3\nu^2 < 0 \\ A^2\sigma^2 - 4\nu^2 + 2\nu \leq 1 & \text{if } A^2\sigma^2 - 3\nu^2 > 0 \end{cases}$$

It is not valid near $A^2\sigma^2 - 3\nu^2 = 0$, i.e. near $|A|\Delta x/\varepsilon = \sqrt{3}$. The curve 4 of fig. 6 shows the exact domain of stability determined by a numerical study of the amplification factor.

5.3. Schemes non consistent with the unsteady equations

As already explained it may be interesting to consider schemes which are not consistent with the unsteady equations. In that case, the scheme must satisfy two conditions : (i) to give a solution which tends toward a steady state, (ii) to be consistent, in the steady state, with the steady equations. Such a pseudo-unsteady approach can be interpreted as a way to build an iterative procedure for solving the finite difference equations approximating the steady partial differential equations.

5.3.1. One-step scheme (Peyret – Viviand [23])

The following scheme is suggested by the Gauss-Seidel technique :

$$\text{(5.22)}\quad u_i^{n+1} = u_i^n - \frac{\sigma}{2}\left(f_{i+1}^n - f_{i-1}^{n+1}\right) + \nu\left(u_{i+1}^n - 2u_i^n + u_{i-1}^{n+1}\right).$$

It is clear that (5.22) is consistent with the steady equation associated with (5.3) if a steady state ($u_i^{n+1} = u_i^n$) is obtained. In order to have informations about the existence of a steady solution, we shall consider (i) the stability of (5.22) and (ii) the partial differential equation with which (5.22) is consistent.

If $A = df/du = \text{const.}$, we obtain the stability condition :

$$\text{(5.23)}\quad -\frac{A}{2}\sigma + \nu \leq 1.$$

Taylor expansions in (5.22) show that the scheme (5.22) is consistent with the following equation of evolution :

$$\text{(5.24)}\quad \frac{\partial u}{\partial t} + K\left(\frac{\partial f}{\partial x} - \varepsilon\frac{\partial^2 u}{\partial x^2}\right) = 0$$

with

$$\text{(5.25)}\quad K = \frac{1}{1 - \left(\nu + \frac{A}{2}\sigma\right)}$$

(where A may be a function of u). The equation (5.24) is parabolic in the direction $t > 0$ if $K > 0$. This is a necessary condition for the solution of (5.24) to tend toward a steady limit when $t \to \infty$. The condition $K > 0$, i.e. $\frac{A}{2}\sigma + \nu < 1$, and condition (5.23) give the necessary condition of convergence :

$$\text{(5.26)}\quad \frac{|A|}{2}\sigma + \nu < 1.$$

The domain of convergence determined by (5.26) is limited by curve (5) on fig. 6.

In the case A = const., the scheme (5.22) is nothing else than the application of the successive relaxation method to the solution of

$$\text{(5.27)}\quad \frac{A}{2\Delta x}\left(u_{i+1} - u_{i-1}\right) - \frac{\varepsilon}{\Delta x^2}\left(u_{i+1} - 2u_i + u_{i-1}\right) = 0$$

with $\omega = 2\varepsilon\Delta t/\Delta x^2$ as the relaxation parameter :

$$\tilde{u}_i^{n+1} = -\frac{A\Delta x}{4\varepsilon}\left(u_{i+1}^n - u_{i-1}^{n+1}\right) + \frac{1}{2}\left(u_{i+1}^n + u_{i-1}^{n+1}\right)$$

$$u_i^{n+1} = \omega\,\tilde{u}_i^{n+1} + (1-\omega)\,u_i^n.$$

By application of theorems on the convergence of this method [24] for the solution of (5.27) with Dirichlet boundary conditions, it is possible to show that condition (5.26) is sufficient to insure the convergence of the iterative procedure if $A > 0$; if $A < 0$, it can be shown that conditions (5.26) and $|A|/\Delta x < 2\varepsilon$ are sufficient for convergence. The connection between relaxation methods and equations of evolution has been discussed for instance in [45].

Assuming (5.26) to be satisfied, we have the following results :

(i) if $A > 0$, then $K > 1$

(ii) if $A < 0$ and $|A|\,\Delta x < 2\varepsilon$, then $K > 1$

(iii) if $A < 0$ and $|A|\,\Delta x > 2\varepsilon$, then $1/2 < K < 1$.

If $A < 0$, it would be necessary to consider u_{i+1} instead of u_{i-1} at iteration $n+1$ in order to have $K > 1$ without other condition than (5.26). When $K > 1$, the convergence toward the steady solution is faster than the convergence given by a consistent scheme (for the same Δt). Finally, we note that the criterion (5.26) is less restrictive than the criterion of the fully explicit scheme (by a factor of 2 if $A = 0$).

5.3.2. Two-step scheme (Allen-Cheng [5])

The method of Cheng-Allen is a modification of Brailovskaya scheme (5.15), based on a non-consistent discretization (with respect to time) of the dissipative term $\partial^2 u/\partial x^2$ already used by Crocco [12]. This two-step scheme is :

(5.28 a) $$\tilde{u}_i^{n+1} = u_i^n - \frac{\sigma}{2}\left(f_{i+1}^n - f_{i-1}^n\right) + \nu\left(u_{i+1}^n - 2\tilde{u}_i^{n+1} + u_{i-1}^n\right)$$

(5.28 b) $$u_i^{n+1} = u_i^n - \frac{\sigma}{2}\left(\tilde{f}_{i+1}^{n+1} - \tilde{f}_{i-1}^{n+1}\right) + \nu\left(\tilde{u}_{i+1}^{n+1} - 2u_i^{n+1} + \tilde{u}_{i-1}^{n+1}\right).$$

The non-consistency of this approximation leads to a sufficient stability condition independent of the viscosity coefficient ε (the C.F.L. condition) :

(5.29) $$|A|\,\sigma \leq 1.$$

A numerical study of the amplification factor corresponding to (5.28) with A = const. shows that this condition is too restrictive. The curve limiting the domain of stability (curve (6) on fig. 6) is asymptotic to $|A|\,\Delta x/\varepsilon = 2$, and the scheme is linearly stable without limitation on Δt if $|A|\,\Delta x/\varepsilon < 2$.

As for the previous non-consistent scheme (5.22), we consider the partial differential equation which is effectively discretized by (5.28); it is an equation of the form (5.24) with K given by :

(5.30) $$K = \frac{1+4\nu}{(1+2\nu)^2}.$$

From (5.30) we deduce :

(i) $K > 0$, so that the equation (5.24) is parabolic in the right direction $t > 0$, which is a necessary condition for convergence towards a steady limit when $t \to \infty$.

(ii) $K < 1$, hence the convergence is slower than the one given by a consistent scheme, but this relative slowness is balanced by the good stability property which allows large time steps. The rapidity of convergence of the iterative procedure corresponding to (5.28) can be characterized by the parameter $K\Delta t$ which is inversely proportional to the number of time steps required to reach a given state. From (5.30), $K\Delta t$ is an increasing function of Δt, so that it is advantageous to use values of Δt as large as possible (despite the fact that K decreases when Δt increases). If $|A|\,\Delta x/\varepsilon < 2$, there is no limitation on Δt from stability (of course Δt must remain a small quantity for eq. (5,24) to be meaningful), and the larger ν the faster the convergence is; for $\nu \gg 1$, one gets $K \sim \nu^{-1}$ and $K\Delta t \sim \Delta x^2/\varepsilon$: the rapidity of convergence is comparable to that given by an explicit consistent scheme for which $K = 1$ and $\Delta t \sim \Delta x^2/\varepsilon$ (because of the stability condition). If $|A|\,\Delta x/\varepsilon \gg 2$, stability imposes $\nu \ll 1$, hence $K \to 1$, and $\Delta t \sim \Delta x$; again the rapidity of convergence is comparable to that of a consistent discretization with the C.F.L. condition.

Numerical applications of the schemes (5.19), (5.22) and (5.28) for the linearized form of eq. (5.3), with $A = 1$, $\varepsilon = 0{,}1$, have been presented in [39]. The results are in agreement with the previous discussion of the convergence based on the equation (5.24) effectively discretized by the scheme.

6. Boundary conditions at a wall

The problem of the treatment of boundary conditions on an impermeable wall in viscous compressible flow reduces to that of the calculation of the pressure (or of the density). Indeed the velocity and the temperature at the wall are easily determined : in the continuum flow regime, the relative velocity is zero (eq. 2.15) and in general either the temperature or the heat flux are given (eq. 2.16); in the slip flow regime, the velocity and the temperature are related to their gradients (eq. 2.17); discretization of these boundary conditions allows the determination of velocity and temperature at the wall from the values of these quantities at neighbouring points.

The wall pressure or density cannot be obtained from boundary conditions, and it must be deduced from the N.S. equations themselves. Examination of the two-dimensional N.S. equations written in a coordinate system (ξ, η) such that $\eta = 0$ represents the wall, but else arbitrary, reveals that knowledge of the pressure at the wall is eventually required only in order to determine the value of the pressure gradient $\partial p/\partial \eta$ in the momentum equations written on the line $\eta = \Delta\eta$ next to the wall (fig. 7), for instance :

(6.1) $$\left(\frac{\partial p}{\partial \eta}\right)_1 = \frac{p_2 - p_0}{2\Delta\eta}.$$

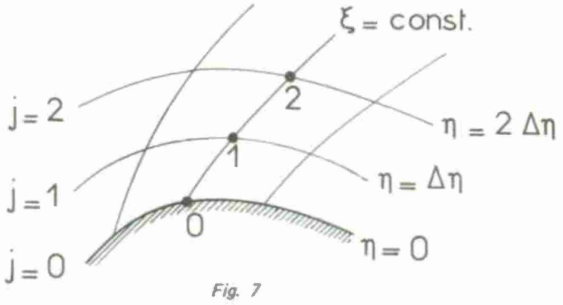

Fig. 7

In this case it is necessary to compute p_0. Other possibilities are either to define $(\partial p/\partial \eta)_1$ without using the value p_0, or to find a method which does not necessitate the knowledge of the gradient $(\partial p/\partial \eta)_1$. We present now these different approaches, and, in order to simplify the presentation, we consider two-dimensional flow in cartesian coordinates (x, y) so that the wall is $y = 0$. At the wall the velocity is zero : $u_0 = v_0 = 0$. All the flow quantities are determined at same mesh points.

a) A first technique consists in calculating the density at the wall ρ_0 from the continuity equation :

(6.2) $$\frac{\partial \rho}{\partial t} + \frac{\partial}{\partial y}(\rho v) = 0 \quad \text{at} \quad y = 0.$$

This technique is of delicate use and may lead to divergence of the results for $t \to \infty$. In particular, in the case of separated flows (see [5], [6], [25]), negative values of density may be obtained. However, a special discretization of (6.2) based on leap-frog scheme (5.7) has been used with good results for blunt body problems (steady [14] or unsteady [26]). This discretization is :

(6.3) $$\rho_0^{n+1} = \rho_0^{n-1} - \frac{\Delta t}{\Delta y}\left[(\rho v)_1^n - (\rho v)_1^n\right].$$

The quantity $(\rho v)_1^n$ (see fig. 8) is determined by a second order extrapolation in space and time of the form :

(6.4) $$(\rho v)_1^n = 2(\rho v)_0^{n-1} - (\rho v)_1^{n-2} = -(\rho v)_1^{n-2}.$$

This method amounts to use the following first order approximation for $\partial(\rho v)/\partial y$ in (6.2) :

(6.5) $$\left[\frac{\partial}{\partial y}(\rho v)\right]_0^{n-1} = \frac{1}{\Delta y}\left\{\frac{1}{2}\left[(\rho v)_1^n + (\rho v)_1^{n-2}\right] - (\rho v)_0^{n-1}\right\}$$

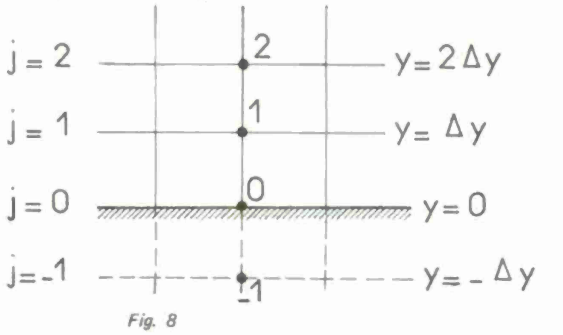

Fig. 8

b) A completely different approach is to approximate $(\partial p/\partial y)_1$ with a formula which does not involve the pressure at the wall. For instance, noncentered difference formulae can be used; with first order accuracy :

$$(6.6) \qquad \left(\frac{\partial p}{\partial y}\right)_1 = \frac{1}{\Delta y}\,(p_2 - p_1)$$

and with second order accuracy :

$$(6.7) \qquad \left(\frac{\partial p}{\partial y}\right)_1 = \frac{1}{2\Delta y}\,(-p_3 + 4p_2 - 3p_1)\,.$$

A more involved variant makes use of the value of $(\partial p/\partial y)_0$ which is obtained from the momentum equation at the wall $y = 0$. More precisely, interpolation between the points $y = 0$ and $y = 3\Delta y/2$ gives the second order accurate formula :

$$(6.8) \qquad \left(\frac{\partial p}{\partial y}\right)_1 = \frac{1}{3}\left(\frac{\partial p}{\partial y}\right)_0 + \frac{2}{3}\left(\frac{\partial p}{\partial y}\right)_{3/2} = \frac{1}{3}\left(\frac{\partial p}{\partial y}\right)_0 + \frac{2}{3}\,\frac{p_2 - p_1}{\Delta y}$$

where $(\partial p/\partial y)_0$ has to be calculated with second order accuracy from the transversal momentum equation at the wall

$$(6.9) \qquad \left(\frac{\partial p}{\partial y}\right)_0 = \left\{ \frac{\mu}{3}\left(\frac{\partial^2 u}{\partial x\,\partial y} + 4\,\frac{\partial^2 v}{\partial y^2}\right) + \mu'(T)\left(\frac{4}{3}\,\frac{\partial v}{\partial y}\,\frac{\partial T}{\partial y} + \frac{\partial u}{\partial y}\,\frac{\partial T}{\partial x}\right)\right\}_0$$

The discretization of the right-hand side of (6.9) requires the use of noncentered differences in the y-direction but presents no difficulty.

In a high Reynolds number boundary layer type flow, $(\partial p/\partial y)_0$ will be very small, and could be considered as equal to zero. For this reason some authors have simply used $p_0 = p_1$.

[Note : in the general coordinate system (ξ , η) of fig. 7, $\partial p/\partial \eta$ and $\partial p/\partial \xi$ will occur in both scalar momentum equations; the expression of the gradient ($\partial p/\partial \eta$)$_0$ is then obtained from a combination of these two scalar equations].

If the value of p_0 is wanted, it can easily be deduced from $(\partial p/\partial y)_0$, for instance using :

$$(6.10) \qquad p_0 = \frac{1}{3}\left[4p_1 - p_2 - 2\Delta y\left(\frac{\partial p}{\partial y}\right)_0\right].$$

An analogous technique has been used in [27] in association with a two-step explicit method in which the predictor is computed at mid-points as in (5.17).

c) When only the steady state solution is of interest, it is not necessary that boundary conditions be consistent with the unsteady problem. Moreover in the cartesian system of fig. 8 (or any orthogonal system associated to the body, $\vec{V}$ being projected along the coordinate lines), the value of $(\partial p/\partial y)_1$ occurs only in the transversal momentum equation at point 1 which determines the velocity component v_1 . These remarks explain a procedure [23] in which v_1^{n+1} is calculated not from the corresponding momentum equation, but from the steady condition :

$$(6.11) \qquad \left(\frac{\partial v}{\partial y}\right)_0 = 0$$

which is a consequence of the steady continuity equation written at point 0 (see eq. 6.2). A noncentered approximation of (6.11) yields :

$$(6.12) \qquad v_1^{n+1} = \frac{1}{4}\left(3v_0^{n+1} + v_2^{n+1}\right) = \frac{1}{4}\,v_2^{n+1}\,.$$

When the steady state is reached a centered discretization of the transversal momentum equation at point 1 gives the value of p_0 .

d) In references [5], [28], [29] the wall is not a mesh line but is located at mid-distance between two mesh lines (fig. 9).

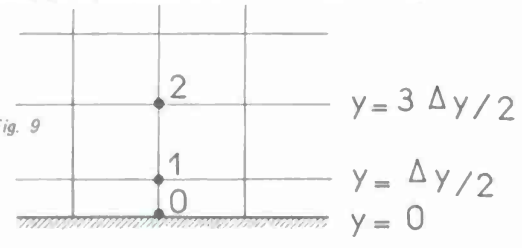

Fig. 9

The technique successfully used in [5], [28] for a wall at specified temperature, consists in the determination of ρ_0^{n+1} by a linear extrapolation :

$$(6.13) \qquad \rho_0^{n+1} = \frac{3}{2}\,\rho_1^{n+1} - \frac{1}{2}\,\rho_2^{n+1}\,.$$

However, which such a mesh, it is necessary to use appropriate differences when values at point 1 are computed. In the particular case of the base flow (fig. 3 b), it has been found [5] [28] very important to approximate the derivatives $(\partial \varphi/\partial y)_1$ where

$$\varphi = \rho v\,,\ \rho v^2,\ \rho u v\,,\ \rho E v$$

by second order accurate differences :

$$(6.14) \qquad \left(\frac{\partial \varphi}{\partial y}\right)_1 = \frac{1}{3\Delta y}\left(\varphi_2 + 3\varphi_1 - 4\varphi_0\right).$$

A first order approximation such as

$$(6.15) \qquad \left(\frac{\partial \varphi}{\partial y}\right)_1 = \frac{1}{\Delta y}\left[\frac{1}{2}\left(\varphi_2 + \varphi_1\right) - \varphi_0\right]$$

gives an under-estimation of ρ_1 and $(\rho v)_1$ which leads to the appearance of negative densities.

7. The treatment of shocks and shock-layers

The numerical treatment of shocks in viscous flows leads to different problems depending on the importance of dissipative effects.

In supersonic low Reynolds number flows, shock waves cannot exist as lines of discontinuities, but they appear as regions of strong compression which we call here shock-layers. The gradients of flow properties in such layers are high, but they are not of an order of magnitude greater than in the rest of the flow, so that their structure can be correctly represented over several mesh points without special mesh refinement. All the schemes presented in section 5 will be able to calculate the flow in shock-layers.

At large Reynolds numbers, the thickness of a shock becomes quite small compared to the scale of flow gradients outside the shock, and it is no longer possible to consider a sufficiently refined mesh to describe the shock structure; but this is not necessary if the Reynolds number is large enough because the shock structure has no influence on the flow field, only the jumps of flow properties across the shock being of interest. In this case the flow is practically inviscid in the vicinity of the shock and the jump relations are the usual Rankine-Hugoniot relations. Of course the N.S. equations are then not really needed to calculate the shock, but in many cases it may be more convenient to solve the N.S. equations in the whole flow field when the inviscid flow region is of small extent (e.g. in the cases of fig. 2). The treatment of shock waves in this case leads to the same problems as for strictly inviscid flows.

The case of intermediate values of the Reynolds number (for instance in the blunt body problem) is more delicate because it is difficult to known whether or not the inner shock structure should be calculated as a part of the flow; furthermore the validity of the N.S. equations to describe the structure of thin strong shocks is in doubt. If the shock structure, as given by the N.S. equations, is calculated, the mesh must be very fine in the shock and this leads to computational difficulties; if one considers the shock as a discontinuity, the question of the determination of correct jump conditions arises. A theory has been established [40] to take into account the dissipative effects in the jump relations; this theory is based on a small perturbation analysis valid for large Reynolds numbers, and it yields corrections to be brought to the Rankine-Hugoniot relations; however this analysis rests upon the use of the N.S. equations to describe the shock structure. In [112] the supersonic flow around a blunt body has been calculated using simplified N.S. equations associated with approximate viscous jump relations.

To the best of our knowledge, the numerical solutions of the complete N.S. equations published at this time have involved only either low Reynolds number shock-layers spread over several mesh points, or quasi-inviscid shock waves treated by the methods used for inviscid flows and which we briefly review below.

Two types of methods can be considered for computation of shock waves in inviscid gas dynamics : the 'shock-capturing' methods, and the 'shock-fitting' methods. Each of them presents its own advantages and defects.

The shock-capturing methods are based on an appropriate discretization of the equations in divergence form [30], [31], and the shock points are computed as ordinary points. The major advantage is that no special treatment is required for the shock; on the other hand the shock is no longer a discontinuity but it has a fictitious structure spread over a few mesh points. Moreover, spurious oscillations often appear near the shock.

Concerning the schemes described in section 5, it can be noted that the finite difference schemes (5.17) and (5.19) or (5.20) reduce, for $\mathcal{C} = 0$, to schemes very often used for computation of shock waves in inviscid flows by shock-capturing methods. The schemes (5.15) and (5.28) have been used for the computation (based on the N.S. equations) of the shock wave in the hypersonic viscous flow over a flat plate respectively in [32] and [33]. At the limit $\mathcal{C} = 0$, the scheme (5.7) reduces to the leap-frog scheme which is known to be unable to compute shock waves. The same negative conclusion applies to the inviscid limit of (5.22). Finally, we do not know at this time whether the implicit method (5.12) is able or not to compute shock waves, although it has been proved that some implicit schemes [34] permit such a calculation.

Shock-fitting methods are based on a special treatment of the shock which preserves the discontinuous character of the flow. It is then necessary to introduce an additional dependent variable related to the shock position. The shock speed as well as the jumps of flow quantities are determined by means of the Rankine-Hugoniot conditions associated with an additional relation. This supplementary condition is deduced from the equations of motion : for instance, it is a compatibility relation along a characteristic line [35], [36] or it is the value of the pressure behind the shock given directly by the finite difference scheme [37].

Shock-fitting methods present the advantages that there is no smearing of the shock wave nor spurious oscillations in its neighbourhood. However, instabilities may appear in the shock front and convergence toward a stationary state may be difficult to obtain if the transient state if far from being realistic.

In viscous flows, shock-fitting methods have been applied to the blunt body problem using, as in the inviscid case, a coordinate transformation such that the bow shock becomes a fixed boundary in the transformed computation plane. A more general approach, which is presently studied for inviscid flows [38], is a floating shock-fitting technique for imbedded shocks : the shock is not associated with a mesh line, but is left free to move through a fixed mesh.

8. Problems relating to accuracy and computer time

In this section we would like to discuss from a practical point of view some aspects of computational fluid mechanics, related to the problems of accuracy and computer time. These problems are not specific to the numerical solution of the N.S. equations, but they do have an increased importance in this case because the N.S. equations are of interest in general for the calculation of flows with a complicated structure, at least in the case of large Reynolds numbers.

The computation of viscous compressible flows is expensive in terms of computer storage and computer time for several reasons : (i) the number and the algebraic complexity of the equations, (ii) the convergence toward a steady limit of the solution of the unsteady N.S. equations is the slower the larger the Reynolds number is, (iii) the complexity of the solution, especially for large Reynolds number flows. Thin boundary layer type regions require a very fine mesh for their correct description; the problem of constructing such a mesh is made much more difficult in the case of separated viscous layers since the location of these layers may not be known in advance, even approximately. Similar difficulties arise in moderate Reynolds number flows with shock waves if one wants to take into account the structure of the shocks.

To keep the computing time within reasonable bounds it is important first to minimize the number of mesh points, and this usually requires that the mesh system be taken non uniform in the physical plane. This can be achieved by imposing a variable mesh spacing in a given coordinate system, or by means of a coordinate transformation, or by a combination of both techniques. The coordinate transformation is generally also chosen so as to make the boundaries of the computation domain (in particular solid walls) coïncide with lines of the mesh system; this considerably simplifies the treatment of boundary conditions.

A coordinate system being chosen, and the mesh size being imposed by accuracy requirements, various techniques exist to reduce the computing time as much as possible for a given numerical scheme. With an explicit scheme subjected to a stability condition, the local maximum time step depends strongly on the local mesh size in the physical space; if the physical mesh varies in an important way throughout the computational domain, the time step will be determined by the smallest mesh and will be very small. It is then practically indispensable to divide the domain in several regions in each of which a different time step is used so as to reduce the total number of operations necessary to advance the solution in time in the entire field. This technique necessitates a matching of the solutions at the interface of two regions with different time steps; for the transient solution to have a physical meaning, the matching must be made with values obtained at the same time in the two regions; if no interest is attached to the transient stage, the matching can be made with values obtained at different times, but it is difficult to take advantage of this freedom to determine what would be the optimum procedure. Going further in this direction, the local value of the time step can be used at each mesh point [41]; this very simple device eliminates the matching, but one cannot be sure that it will not make the calculation diverge.

Another procedure which is often used to reduce the computing time consists in carrying out successive calculations with mesh refinement (local or general) from one calculation to the next one; thus the calculation with the finest mesh, which is the most time consuming, starts with initial values which are already a good approximation to the exact solution.

Still considering the case of explicit schemes, it can be advantageous to use a splitting method [42] when the mesh spacing in the physical space is much smaller in one direction than in the other direction (as is the case for a thin viscous layer); in such a method, based on the discretization of multi-dimensional equations by means of a series of one-dimensional finite difference operators, the very small time step associated with the smaller mesh dimension has to be used only for the corresponding one-dimensional operators, whereas a much larger time step can be used for the one-dimensional operators in the other direction.

Time-step limitation is the main drawback of explicit methods; nevertheless these methods have been much used because of their simplicity and of the fact that the number of numerical operations at each step is kept to a minimum. Another approach which is attracting more attention now is the use of implicit schemes which lead to less severe stability conditions or which are unconditionally stable; of course this advantage is counterbalanced by the fact that at each step one must solve large algebraic systems; this numerical task can be much reduced by using fractional step methods : splitting methods [81], or alternating directions methods [16], [66], [67].

No clear-cut conclusion can be drawn at this time regarding the best type of methods (implicit or explicit). The answer might be found in the use of different schemes in different regions of the flow field : for instance an implicit one-step method in a strongly viscous flow region with a very fine mesh, and an explicit two-step method in a region with small viscous effects (eventually with shock waves) where a coarse mesh is sufficient.

9. Bibliography

To conclude this lecture, we give a list of references relating to

numerical calculations of viscous compressible flows based on the Navier-Stokes equations, and grouped according to the type of problem treated.

A. General studies

[29], [39], [46] to [52], [113].

B. One-dimensional flows

[12], [19], [49], [51], [53] to [66].

C. Two-dimensional flows

a. Internal flows

laminar : [11], [18], [67] to [75].

turbulent : [9], [10], [76].

b. Flat plate

[19], [22], [32], [33], [42], [60], [61], [75], [77] to [81].

c. Shock - boundary layer interaction

laminar : [42], [60] to [62], [111].

turbulent : [3], [4], [44].

d. Expansion and compression corners

[82]; [32], [44], [80].

e. Blunt body problems

Shock layer flows or shock-capturing methods : [7], [8], [14], [19], [23], [26], [41], [83] to [89].

Shock-fitting methods : [37], [90] to [93].

f. Base flows and steps

[5], [28], [29], [79], [94] to [101].

g. Complete flows around finite bodies

laminar : [6], [27], [57], [79], [84], [85], [102] to [107].

turbulent : [43].

D. Three-dimensional flows

duct flow : [16], [108].

blunt body (shock-fitting) : [109].

E. Various problems

[20], [66], [72] to [75], [110].

RÉFÉRENCES

1. GUIRAUD, J.P. — *Gas dynamics from the point of view of kinetic theory* in Applied Mechanics, Proceed. 13th Intern. Congr. Theoret. Appl. Mech., Moscow, Aug. 1972, p. 104-123 - Springer Verlag 1973.

2. KOGAN, M.N. — *Molecular gas dynamics.* Annual Review of fluid Mechanics, vol. 5, p. 383-404. Annual Review Inc. 1973.

3. BALDWIN, B.S. and MacCORMACK, R.W. — *Numerical solution of the interaction of a strong shock wave with a hypersonic turbulent boundary layer.* AIAA paper No. 74.558, June 1974.

4. BALDWIN, B.S., and MacCORMACK, R.W. — *Interaction of strong shock wave with turbulent boundary layer.* 4th Intern. Conf. Numerical Methods in Fluid Dynamics, Boulder, Colorado, June 1974. To be published in Lecture Notes in Physics, Springer Verlag.

5. ALLEN, J.S. and CHENG, S.I. — *Numerical solutions of the compressible Navier-Stokes equations for the laminar near wake.* Phys. of Fluids, vol. 19, No. 1, 1970, p. 37-52.

6. PEYRET, R. et VIVIAND, H. — *Calcul de l'écoulement d'un fluide visqueux compressible autour d'un obstacle de forme parabolique.* Lecture Notes in Physics, vol. 19, p. 222-229, Springer Verlag 1973.

7. MOLODTSOV, V.K. — *The numerical calculation of the supersonic circulation of a current of viscous perfect gas round a sphere.* USSR Comput. Math. and Math. Phys., vol. 9, No. 5, 1969, p. 320-329 (translation of Zh. vych. Mat. mat. Fiz., vol. 9, No. 5, 1969, p. 1211-1217.

8. MOLODTSOV, V.K., and TOLSTYKH, A.N. — *Calculation of supersonic viscous flow around a blunt body* (In russian). Proceed. 1st Intern. Conf. Numerical Methods in Fluid Dynamics, Novosslbirsk 1969, vol. 1, p. 37-54.

9. GOSMAN, A.D., PUN, W.M., RUNCHAL, A.K., SPALDING, D.B., and WOLFSHTEIN, M. — *Heat and mass transfer in recirculating flow.* Academic Press 1969.

10. ANASOULIS, R.F., MacDONALD, H., and BUGGEIN, R.C. — *Development of a combustor flow analysis, Part I : Theoretical studies.* United Aircraft Research Lab. Techn. Report AFAPL-TR-73-98, Part I, Jan. 1974.

11. ADAMS, J.C., Jr. — *Numerical calculation of hypersonic laminar cavity flows.* AIAA paper No. 74.707 - ASME 74.HT.27, 1974.

12. CROCCO, L. — *A suggestion for the numerical solution of the steady Navier-Stokes equations.* AIAA Journ., vol. 3, No. 10, 1965, p. 1824-1832.

13. PEYRET, R. — *Sur la résolution numérique d'un problème de couche limite.* La Recherche Aérospatiale, n° 1971-3, p. 133-138.

14. VICTORIA, K.J. and WIDHOPF, G.F. — *Numerical solution of the unsteady Navier-Stokes equations in curvilinear coordinates : the hypersonic blunt body merged layer problem.* Lecture Notes in Physics, vol. 19, p. 254-267, Springer Verlag 1973.

15. RICHTMYER, R.D. and MORTON, K.W. — *Difference methods for initial value problems.* Interscience Publ. 1967.

16. BRILEY, W.R. and MacDONALD, H. — *An implicit numerical method for the multidimensional compressible Navier-Stokes equations.* United Aircraft Research Lab. Report M911363-6, Nov. 1973.

17. DOUGLAS, J. and GUNN, J.E. — *A general formulation of alternating direction methods.* Numerisch Math., vol. 6: 1964, p. 428-453.

18. BRAILOVSKAYA, I. Yu. — *A difference scheme for numerical solution of the two-dimensional, nonstationary Navier-Stokes equations for a compressible gas.* Soviet Physics - Doklady, vol. 10, No. 2, 1965, p. 107-110 (Translation of D.A.N. SSSR, vol. 160, No. 5, 1965, p. 1042-1045).

19. THOMMEN, H.U. — *Numerical integration of the Navier-Stokes equations.* Z.A.M.P., vol. 17, No. 3, 1966, p. 369-384.

20. MacCORMACK, R.W. — *The effect of viscosity in hypervelocity impact cratering.* AIAA paper No. 69-354, May 1969.

21. LERAT, A. and PEYRET, R. — *Non centered schemes and shock propagation problems.* Computers and Fluids, vol. 2, 1974, p. 35-52.

22. TANNEHILL, J.C., MOHLING, R.A., and RAKICH, J.V. — *Numerical computation of the hypersonic rarefied flow near the sharp leading edge of a flat plate.* AIAA Paper No. 73.200, 1973.

23. PEYRET, R. et VIVIAND, H. — *Calcul numérique de l'écoulement supersonique d'un fluide visqueux sur un obstacle parabolique.* La Recherche Aérospatiale, n° 1972-3, p. 123-131.

24. VARGA, R.S. — *Matrix iterative analysis.* Prentice Hall, 1962.

25. ROACHE, P.S. — *Computational fluid dynamics.* Hermosa Publ. Albuquerque 1972.

26. WIDHOPF, G.F., and VICTORIA, K.J. — *Numerical solution of the unsteady Navier-Stokes equations for the oscillatory flow over a concave body.* 4th Intern. Conf. Numerical Methods in Fluid Dynamics, Boulder, Co. June 24-28, 1974. To be published in Lecture Notes in Physics.

27. PALUMBO, D.J. and RUBIN, E.L. — *Solution of the two-dimensional, unsteady compressible Navier-Stokes equations using a second-order accurate numerical scheme.* J. Comput. Phys., vol. 9, n° 3, 1972, p. 466-495.

28. ALLEN, J.S. Jr. – *Numerical solutions of the compressible Navier-Stokes equations for the laminar near wake in supersonic flow.* Ph. D. Dissertation, Princeton Univ., 1968.

29. ROACHE, P.J. and MUELLER, T.J. – *Numerical solutions of laminar separated flows.* AIAA Journ., vol. 8, No. 3, 1970, p. 530-538.

30. LAX, P.D. – *Weak solutions of nonlinear hyperbolic equations and their numerical computation.* Comm. Pure Appl. Math., vol. 7, 1954, p. 159-193.

31. LAX, P.D., and WENDROFF, B. – *Systems of conservation laws.* Comm. Pure Appl. Math., vol. 13, 1960, p. 217-237.

32. CARTER, J.E. – *Numerical solution of the supersonic laminar flow over a two-dimensional compression corner.* Lecture Notes in Physics, vol. 19, p. 69-78, Springer Verlag 1973.

33. CHENG, S.I., and CHEN, J.H. – *Finite difference treatment of strong shock over a sharp leading edge with Navier-Stokes equations.* Lecture Notes in Physics, vol. 19, p. 92-99, Springer Verlag 1973.

34. MASSON, B.S. – *An implicit finite difference method for eulerian fluid dynamics.* J. Comput. Phys., vol. 12, No. 1, 1973, p. 88-102.

35. MORETTI, G. and ABBETT, M. – *A time-dependent computational method for blunt body flows.* AIAA Journ., vol. 4, 1966, p. 2136-2141.

36. MORETTI, G., and PANDOLFI, M. – *Entropy layers.* Computers and Fluids, vol. 1, 1973, p. 19-35.

37. HOLST, T.L., and TANNEHILL, J.C. – *Numerical computation of two-dimensional viscous blunt body flows with an impinging shock.* Engineering Res. Inst., Iowa State Univ., Final Report - Part II, ISU-ERI, AMES - 74057, Feb. 1974.

38. MORETTI, G. – *Floating shock fitting technique for imbedded shock in unsteady multidimensional flows.* Proceed. 1974 Heat Transfer and Fluid Mech. Institute, Stanford Univ. Press, 1974, p. 184-201.

39. PEYRET, R. et VIVIAND, H. – *Résolution numérique des équations de Navier-Stokes pour les fluides compressibles.* Lecture Notes in Computer Sciences, vol. 11, p. 160-184, Springer Verlag 1974.

40. GERMAIN, P. – *Shock waves, jump relations, and structure* In Advances in Applied Mechanics, vol. 12, p. 131-194, ed. by C.S. Yih, Academic Press 1972.

41. LI, C.P. – *Hypersonic non equilibrium flow past a sphere at low Reynolds numbers.* AIAA Paper No. 74-173, 1974.

42. MacCORMACK, R.W. – *Numerical solution of the interaction of a shock wave with a laminar boundary layer.* Lecture Notes in Physics, vol. 8, p. 151-163, Springer Verlag 1971.

43. DEIWERT, G.S. – *Numerical simulation of high Reynolds number transonic flows.* AIAA Paper No. 74-603, 1974; see also : 4th Intern. Conf. Numerical Methods in Fluid Dynamics, Boulder, Colorado, June 1974, to be published in Lecture Notes in Physics, Springer Verlag.

44. WILCOX, D.C. – *Numerical study of separated turbulent flows.* AIAA Paper No. 75-584, 1974.

45. GARABEDIAN, P.R. – *Estimation of the relaxation factor for small mesh size.* Math. Tables, Aids Comput., vol. 10, 1956, p. 183-185.

46. CHENG, S.I. – *Numerical integration of Navier-Stokes equations.* AIAA Journ. vol. 8, No. 12, 1970, p. 2115-2122.

47. CHENG, S.I. – *A critical review of the numerical solution of Navier-Stokes equations.* Lecture Notes, Progress in Numerical Fluid Dynamics, von Karman Institute, Rhode-St Genèse, Belgium, Jan. 1974.

48. WIRZ, H.J., and SMOLDEREN, J.J. – *Numerical integration of Navier-Stokes equations.* AGARD Lecture Series No. 64 on Advances in Numerical Fluid Dynamics, 1973.

49. ISHIGURO, T. – *An evaluation of several difference schemes for compressible Navier-Stokes equations* (in japanese). NAL-TR-310, Nation. Aerosp. Lab., Chofu, Tokyo, 1973.

50. BRAILOVSKAYA, I. Yu., KUSKOVA, T.V., PAVLOV, B.M., and CHUDOV, I.A. – *The application of difference methods to the calculation of viscous liquid and gas flows.* Heat Transfer - Soviet Res., vol. 5, No. 5, 1973, p. 119-123.

51. TAYLOR, T.D. – *An evaluation of cell type finite difference methods for solving viscous flow problems.* Computers and Fluids, vol. 1, No. 1, p. 3-18, 1973.

52. TAYLOR, T.D. – *Numerical methods for predicting subsonic, transonic and supersonic flow.* AGARDograph No. 187, Jan. 1974.

53. FILLER, L., and LUDLOFF, H.F. – *Stability analysis and integration of the viscous equations of motion.* Math. of Comput. vol. 15, 1961, p. 261-274.

54. KURZROCK, J.W., and MATES, R.E. – *Exact numerical solutions of the time dependent compressible Navier-Stokes equations.* AIAA Paper No. 66-30, 1966.

55. POLEZHAEV, V.I. – *Numerical solution of the system of one dimensional unsteedy Navier-Stokes equations for a compressible gas.* Fluid Dynamics, vol. 1, No. 6, 1966, p. 21-27 (transl. of Izv. A.N. SSSR., Mekh. Zhid. i Gaza, vol. 1, No. 6, 1966, p. 33-44).

56. SCALA, S.M., and GORDON, P. – *Reflection of a shock wave at a surface.* Phys. of Fluids, vol. 9, No. 6, 1966, p. 1158-1166.

57. SCALA, S.M., and GORDON, P. – *Solution of the Navier-Stokes equations for viscous supersonic flows adjacent to isothermal and adiabatic surfaces.* Proceed. 1969 Symp. on Viscous Interaction phenomena in supersonic and hypersonic flow, p. 319-391, Univ. of Dayton Press, Ohio, 1970.

58. RUBIN, E.L., and BURSTEIN, S.Z. – *Difference methods for the inviscid and viscous equations of a compressible gas.* J. Comput. Phys., vol. 2, No. 2, 1967, p. 178-196.

59. RUBIN, E.L., and KHOSLA, P.M. – *A time-dependent method for the solution of one-dimensional radiating flow.* ZAMP, vol. 21, No. 6, 1970, p. 962-977.

60. SKOGLUND, V.J., COLE, J.K., and STAIANO, E.F. – *Development and verification of two-dimensional numerical technique for viscous compressible flows with shock waves.* Report SC-CR-67-2679, Sandia Lab., Albuquerque, N.M. Aug. 1967.

61. SKOGLUND, V.J., COLE, J.K., and STAIANO, E.F. – *Numerical techniques for viscous compressible flows with shock waves.* Proceed. 1968 Heat transfer and fluid Mech. Inst., p. 151-173, Stanford Univ. Press 1968.

62. SKOGLUND, V.J., and GAY, B.D. – *Improved numerical techniques and solution of a separated interaction of an oblique shock wave and a laminar boundary layer.* Final Report ME-41(69) S-068, Univ. of New Mexico, Bureau of Eng. Res., June 1968.

63. MORETTI, G., and SALAS, M.D. – *Numerical analysis of viscous one-dimensional flows.* J. Comput. Phys. vol. 5, No. 3, 1970, p. 487-506.

64. SALAS, M.D. – *On the reflection of a shock wave from a wall.* PIBAL Report No. 70-23, Polytechnic Inst. of Brooklyn, May 1970.

65. BENISON, G.I., and RUBIN, E.L. – *A time-dependent analysis for quasi-one-dimensional, viscous, heat conducting, compressible Laval nozzle flows.* J. Eng. Math., vol. 5, No. 1, 1971, p. 39-49.

66. BAUM, E., and NDEFO, E. – *A temporal ADI computational technique.* Proceed. AIAA Comput. Fluid Dynamics Conf. Palm Springs, Calif., July 1973, p. 133-140.

67. POLEZHAEV, V.I. – *Numerical solution of the system of two-dimensional unsteady Navier-Stokes equations for a compressible gas in a closed region.* Fluid Dynamics, vol. 2, No. 2, 1967, p. 70-74 (transl. of Izv. A.N. SSSR., Mekh. Zhid. i Gaza, vol. 2, No. 2, 1967, p. 103-111).

68. AL'BER, S.I., BEKNEVA, E.V., KOGAN, V.R., PETRAZHITSKII, G.B., and STANKEVICH, N.M. – *Numerical solution of the two-dimensional unsteady Navier-Stokes equations for viscous heat-conducting compressible gas flow in a closed annular region.* Fluid Dynamics, vol. 3, No. 3, 1968, p. 95-99 (transl. of Izv. A.N. SSSR. Mekh. Zhid. i Gaza, vol. 3, No. 3, 1968, p. 140-146).

69. CHIU, P.B. – *A proposed technique for discretization of boundary conditions in time-dependent, viscous, compressible flows.* Ph. D. Dissertation, Purdue Univ., 1972.

70. ISHIGURO, T. – *Calculations of flow around a semi-infinite flat plate in a shock tube.* AIAA Journ. vol. 12, No. 3, 1974, p. 376-378.

71. BYRKIN, A.P., and SHCHENNIKOV, V.V. – *The calculation of viscous gas flows in plane channels.* U.S.S.R. Comput. Math. and Math. Phys. vol. 13, No. 3, 1973, p. 244-254 (transl. of Zh. vychisl. Mat. mat. Fiz., vol. 13, No. 3, 1973, p. 728-736).

72. RIVARD, W.C., FARMER, O.A., BUTLER, T.D., and O'ROURKE, P.J. – *A method for increased accuracy in eulerian fluid dynamics calculations.* Informal Report LA-5426-MS, Los Alamos Scientific Lab., Oct. 1973.

73. RIVARD, W.C., BUTLER, T.D., and FARMER, O.A. – *The transient dynamics of chemically reactive gaseous mixtures with turbulence.* 4th Intern. Conf. Numerical Methods in Fluid Dynamics, Boulder, Colorado, June 1974. To be published in Lecture Notes in Physics, Springer Verlag.

74. BUTLER, T.D. – *Recent advances in computational fluid dynamics.* Lecture Notes in Computer Science, vol. 11, p. 1-21, Springer Verlag 1974.

75. TRULIO, J.G., WALITT, L., and NILES, W.J. – *Numerical calculations of viscous compressible fluid flow over a flat plate and step geometry.* NASA, CR-1466, Feb. 1970.

76. KIRKPATRICK, J.R. and WALKER, W.F. – *Numerical method for describing turbulent compressible subsonic separated jet flows.* J. Comput. Phys., vol. 10, No. 2, 1972, p. 185-201.

77. TANNEHILL, J.C., MOHLING, R.A., and RAKICH, J.V. – *Numerical computation of hypersonic viscous flow over a sharp leading edge.* AIAA Journ. vol. 12, No. 2, 1974, p. 129-130.

78. BUTLER, T.D. – *Numerical solutions of hypersonic sharp-leading edge flows.* Phys. of Fluids, vol. 10, No. 6, 1967, p. 1205-1215.

79. GOODRICH, W.D., LAMB, J.P., and BERTIN, J.J. – *On the numerical solution of two-dimensional, laminar compressible flows with imbedded shock waves.* ASME Paper No. 72-FE-7, 1972.

80. CARTER, J.E. – *Numerical solutions of the Navier-Stokes equations for the supersonic laminar flow over a two-dimensional compression corner.* NASA TR R.385, July 1972.

81. BEREZIN, Yu. A., KOVEKIA, V.M., and YANENKO, N.N. – *An implicit scheme for the calculation of the flow of a viscous heat-conducting gas* (in russian). Numer. Meth. in Continuum Mech., A.N. SSSR Siberian Comput. Center, Novossibirsk, vol. 3, No. 4, 1972, p. 3-18.

82. BRAILOVSKAYA, I. Yu. – *Calculation of viscous compressible gas flow past a corner.* Fluid Dynamics, vol. 2, No. 3, 1967, p. 49-55 (transl. of Izv. A.N.SSSR. Mekh. Zhid. i Gaza, vol. 2, No. 3, 1967, p. 82-92).

83. MAGNUS, R.J. and GALLAHER, W.H. – *Rarefied hypersonic flow over the forward part of a blunted cone.* AGARD-CP-60-70 Numerical Methods in Viscous Flows, 1970, p. 30-33.

84. PAVLOV, B.M. – *Calculation of supersonic flow past blunt bodies using the complete Navier-Stokes equations.* Fluid Dynamics, vol. 3, No. 3, 1968, p. 88-90 (transl. of Izv. A.N. SSSR., Mekh. Zhid. i Gaza, vol. 3, No. 3, 1968, p. 128-133).

85. PAVLOV, B.M. – *Solution of the complete Navier-Stokes equations for the flow around blunt bodies* (in russian). Proceed. 1st Intern. Conf. Numerical Methods in Fluid Dynamics, Novossibirsk 1969, vol. 1, p. 55-66.

86. TOLSTYKH, A.I. – *A method for the numerical solution of the Navier-Stokes equations for a compressible gas in a large domain of Reynolds number* (In russian) D.A.N. SSSR, vol. 210, No. 1, 1973, p. 48-51.

87. LI, C.P. – *Shock layer structures in rarefied gas flow.* 8th Intern. Symp. on Rarefied Gas Dyn., Stanford Univ., July 1972, Book of Abstracts, vol. I, p. 208-213.

88. LI, C.P. – *Numerical solution of viscous reacting blunt body flows of a multicomponent mixture.* AIAA Paper No. 73-202, 1973.

89. WIDHOPF, G.F., and VICTORIA, K.J. – *On the solution of the unsteady Navier-Stokes equations including multicomponent finite rate chemistry.* Computers and Fluids, vol. 1, No. 2, p. 159-184, 1973.

90. MORETTI, G., and SALAS, M.D. – *The blunt body problem for a viscous rarefied gas flow.* AIAA Paper No. 69-139, 1969.

91. MORETTI, G., and SALAS, M.D. – *Numerical analysis of the viscous supersonic blunt body problem. Part 1.* PIBAL Report No. 70-48 Polytechnic Inst. of Brooklyn, Nov. 1970.

92. SMITH, K.W., and SKOGLUND, V.J. – *Numerical techniques and solutions for axisymmetrical viscous compressible flows.* Report No. OAS-TR-72-4, Off. Assistant for Study Support, Kirtland Air force Base, N.M., May 1972. See also, SMITH, K.W., Ph. D. Dissertation, Univ. of New Mexico, 1972.

93. GOLOVACHEV, Yu. P., KUZ'MIN, A.M., and POPOV, F.D. – *Calculation of the supersonic flow past blunt bodies using the complete and simplified Navier-Stokes equations.* U.S.S.R. Comput. Math. and Math. Phys., vol. 13, No. 4, 1973, p. 241-249 (transl. of Zh. Vychisl. Mat. mat. Fiz. vol. 13, No. 4, 1973, p. 1021-1028).

94. ROACHE, P.J. – *Numerical solution of compressible and incompressible laminar separated flows.* Ph. D. Dissertation, Univ. of Notre Dame, 1968.

95. ROACHE, P.J., and MUELLER, T.J. – *Numerical solutions of compressible and incompressible separated flows.* AIAA Paper No. 68-741, 1968.

96. MYSHENKOV, V.I. – *Study of the formation of separated flow downstream of a plate by numerical solution of the Navier-Stokes equations.* Proceed. 1st Intern. Conf. Numerical Methods in Fluid Dynamics, Novossibirsk 1969, vol. 1, p. 67-82.

97. MYSHENKOV, V.I. – *Subsonic and transonic viscous gas flow in the wake of a two-dimensional body.* Fluid Dynamics, vol. 5, No. 2, 1970, p. 236-241 (transl. of Izv. A.N. SSSR. Mekh. Zhid. i Gaza, vol. 5, No. 2, 1970, p. 73-79).

98. VICTORIA, K.J., and STEIGER, M.H. — *Exact solutions of the 2-D laminar near wake of a slender body in supersonic flow at high Reynolds number.* Report No. APP-0059 (S9990)-5, Aerospace Co., San Bernardino, Calif., October 1970.

99. BRAILOVSKAYA, I. Yu. — *Flow in the near wake.* Soviet Physics - Doklady, vol. 16, No. 3, 1971, p. 197-199 (transl. of D.A.N. SSSR, vol. 197, No. 3, 1971, p. 542-544).

100. ROSS, B.B., and CHENG, S.I. — *A numerical solution of the planar supersonic near-wake with its error analysis.* Lecture Notes in Phys. vol. 8, p. 164-169, Springer Verlag 1971.

101. ROSS, B.B., and CHENG, S.I. — *The application of finite difference methods to the supersonic near wake.* AIAA Paper No. 72-115, 1972.

102. SCALA, S.M., and GORDON, P. — *Solution of the time-dependent Navier-Stokes equations for the flow of dissociating gas over a circular cylinder.* Report R67SD56, Space Sci. Lab., Missile and Space Div. General Electric, May 1967.

103. SCALA, S.M., and GORDON, P. — *Solution of the time-dependent Navier-Stokes equations for the flow around a circular cylinder.* AIAA Journ., vol. 6, No. 5, 1968, p. 815-822.

104. TRULIO, J.G., WALITT, L., and LIU, C.Y. — *Numerical calculations of separated flows.* Proceed. 1969 Symp. on Viscous interaction phenomena in supersonic and hypersonic flow. p. 393-425, Univ. of Dayton, Ohio, 1970.

105. KITCHENS, C.W. Jr. — *Numerical experiments to integrate the Navier-Stokes equations.* BRL Report No. 1580, Ballistic Research Lab., April 1972.

106. KITCHENS, C.W. Jr. — *Numerical experiments with the compressible Navier-Stokes equations.* Lecture Notes in Phys., vol. 18, p. 120-129, Springer Verlag 1973.

107. MYSHENKOV, V.I. — *Numerical solution of the Navier-Stokes equations for flow of gas around a rectangle.* Fluid Dynamics, No. 4, 1972, p. 544-550 (transl. of Izv. A.N. SSSR, Mekh. Zhid. i Gaza, No. 4, 1972, p. 10-17).

108. BRILEY, W.R., and MacDONALD, H. — *Solution of the three-dimensional compressible Navier-Stokes equations by an implicit technique.* 4th Intern. Conf. Numerical Methods in Fluid Dynamics, Boulder, Colorado, June 1974, to be published in Lecture Notes in Physics, Springer Verlag.

109. LI, C.P. — *A numerical study of laminar flow separation on blunt flared cones at angle of attack.* AIAA Paper No. 74-585, 1974.

110. HARLOW, F.H., and AMSDEN, A.A. — *A numerical fluid dynamics calculation method for all flow speeds.* J. Comput. Phys., vol. 3, No. 2, 1971, p. 197-213.

111. HANIN, M., WOLFSHTEIN, M., and LANDAU, U.E. — *Numerical solution of Navier-Stokes equations for interaction of shock wave with laminar boundary layer.* ICAS Paper No. 74-17, Aug. 1974.

112. TOLSTYKH, A.I. — *Numerical computation of the supersonic flow of a viscous gas round a blunt body.* USSR Comput. Math. Math. Phys., vol. 6, No. 1, 1966, p. 160-170 (transl. of Zh. vȳchisl. Mat. mat. Fiz, vol. 6, No. 1, 1966, p. 113-120).

113. KRAUSE, E. — *Numerical solution of the Navier-Stokes equations.* Lecture Notes, International Center of Mechanical Sciences Udine, Italy, Oct. 1974.

APPLICATIONS OF FINITE ELEMENT METHODS IN FLUID DYNAMICS

by

C.Bellevaux
LIMSI (CNRS) and ENSTA, Paris

and

M.Maillé
Université Pierre et Marie Curie and ENSTA, Paris

INTRODUCTION

This paper is divided into two parts, the first devoted to a general presentation of the finite element method, and the second to some applications in fluid dynamics.

In the first part, we consider a simple example, the resolution of which will allow us to show the successive steps common to all finite element methods and thus demonstrate the problems of functional analysis and the numerical techniques to be used. We then generalize this example using elements of functional analysis necessary for a rigorous formulation.

In the second part we outline briefly the well-known method of singularities, because of its application to potential flows. We then treat separately the linear and non-linear case of Navier-Stokes equations for viscous flows.

1. THE FINITE ELEMENT METHOD

1.1 Example

1.1.1 Strong Form

The formulation of physical problems leads in most cases to a system of the type:

$$\begin{aligned} &\frac{\partial u}{\partial t} + Au = f \quad \text{in} \quad \Omega \times [0,T] \\ &Bu = 0 \quad \text{on} \quad \partial\Omega \; ; \quad u = u_0 \quad \text{for} \quad t = 0 \, . \end{aligned} \tag{1}$$

Where Ω is a bounded domain of R^n and $\partial\Omega$ its boundary. In general u is a vector–valued function and for problems in fluid dynamics A is a non-linear operator with partial derivatives up to the second order and B is an operator of the first order which does not "cover" A. This system with appropriate regularity conditions is called the strong form of the problem and its solution is said to be strong. Numerical methods using Equations (1) directly can be built up with finite differences. We shall leave aside these techniques and introduce other methods based on finite elements which require other formulations (weak or variational). We introduce this using as an example the classical Neumann problem.

Neumann problem: strong form

Let $u(x,y)$ with continuous derivatives up to the second order verify:

$$\begin{aligned} &\frac{\partial^2 u}{\partial x^2} + \frac{\partial^2 u}{\partial y^2} = -f(x,y) \quad \text{in} \quad \Omega \\ &\frac{\partial u}{\partial n} = -g(x,y) \quad \text{on} \quad \partial\Omega \, . \end{aligned} \tag{2}$$

Where n is the unit normal vector oriented outward on $\partial\Omega$.

For the existence and uniqueness of the solution of problem (2) it is necessary to add a following condition on the data f and g :

$$\iint_\Omega f\,dx\,dy + \int_{\partial\Omega} g\,ds = 0 . \tag{3}$$

By means of an additional regularity hypothesis on $\partial\Omega$, f, g, which we do not discuss, we can demonstrate the existence of a solution and its uniqueness provided that we identify any two solutions differing only by a constant. To obtain a unique solution we add the supplementary condition on u

$$\iint_\Omega u(x,y)\,dx\,dy = 0 . \tag{4}$$

The equation and boundary condition (2) define the strong form of the Neumann problem. Equality (3) is a condition of compatibility and (4) is a condition of uniqueness.

1.1.2 Weak Form

For a steady problem the Equation (1) becomes:

$$Au = f$$

and is replaced by the formal identity:

$$\langle Au,v\rangle = \langle f,v\rangle \quad \text{for any} \quad v \tag{5}$$

where

$$\langle w,v\rangle = \iint_\Omega wv\,dx\,dy$$

is the scalar product in $L^2(\Omega)$*. To obtain a weak solution u it is necessary to determine the functional space U to which solution u belongs and the functional space V to which the test function v belongs (note that the spaces U and V are not necessarily identical).

The boundary condition $Bu = 0$ on $\partial\Omega$ can either be included in the definition of U or in the equality (5).

In the first case the solution u belongs to a space U of functions w verifying $Bw = 0$.

In the second case equation (5) is modified to obtain a new equality:

$$a(u,v) = \langle f,v\rangle .$$

For homogenous elliptic problems we can prove the existence and uniqueness of the weak solution u (the Lax-Milgram Theorem).

The question of whether the weak and strong forms are equivalent is exceedingly complex, and we shall not discuss it further.

Neumann problem: weak form

Let v(x,y) be defined in Ω with sufficient smoothness. Multiplying (1) by v and integrating on (Ω) gives:

$$\iint_\Omega \left(\frac{\partial^2 u}{\partial x^2} + \frac{\partial^2 u}{\partial y^2}\right) v\,dx\,dy = -\iint_\Omega fv\,dx\,dy .$$

Using Green's formula and taking into consideration the boundary condition $\partial u/\partial n = -g$ we obtain:

$$\iint_\Omega \left(\frac{\partial u}{\partial x}\frac{\partial v}{\partial x} + \frac{\partial u}{\partial y}\frac{\partial v}{\partial y}\right) dx\,dy = \iint_\Omega fv\,dx\,dy + \int_{\partial\Omega} gv\,ds . \tag{6}$$

Neumann problem: functional considerations

If u is a strong solution of the Neumann problem one can prove that equation (6) is verified. Conversely with additional regularity conditions on the solution u we can proceed backwards and thus prove the equivalence.

---

* $L^2(\Omega)$ is the space of square summable functions on Ω.

If v is a real-valued function on Ω let us define the space $\widetilde{H}_1(\Omega)$ by

$$\widetilde{H}_1(\Omega) = \left\{ v/v , \frac{\partial v}{\partial x} , \frac{\partial v}{\partial y} \in L^2(\Omega) , \quad \iint_\Omega v \, dx \, dy = 0 \right\}. \tag{7}$$

We shall say that u is a weak solution of the Neumann problem if $u \in \widetilde{H}_1(\Omega)$ and if the following equality is true for any $v \in \widetilde{H}_1(\Omega)$:

$$a(u,v) = (f,v)$$

where

$$a(u,v) = \iint_\Omega \left(\frac{\partial u}{\partial x} \frac{\partial v}{\partial x} + \frac{\partial u}{\partial y} \frac{\partial v}{\partial y} \right) dx \, dy \tag{8}$$

$$(f,v) = \iint_\Omega fv \, dx \, dy + \int_{\partial\Omega} gv \, ds . \tag{9}$$

Existence and uniqueness of the weak solution

With the compatibility condition previously stated we can prove the existence and uniqueness of u but this demonstration is too technical for this paper.

1.1.3 Variational Form

When the functional spaces U and V are identical the equality of the weak form: $a(u,v) = (f,v)$ for any $v \in U$ is sometimes equivalent to the minimization of a functional $L(u)$. This is called a variational form of the differential problem and can be stated as follows:

Find $u \in U$ so that $L(u)$ is minimized.

Case of positive definite bilinear forms

In this case:

$$a(v,v) > 0 \quad \text{if} \quad v \neq 0 . \tag{10}$$

We can choose

$$L(v) = a(v-u, v-u) - a(u,u) . \tag{11}$$

From equation (10) we can say that $L(v)$ is minimized if $a(v-u, v-u) = 0$. In other words if $v = u$.

$L(v)$ seems to depend of the unknown solution u but in fact

$$L(v) = a(v,v) - 2a(u,v)$$

is the same as $$L(v) = a(v,v) - 2(f,v) .$$

Variational form of the Neumann problem

In this case $a(u,v)$ defined in (8) verifies (10).

So we can state: $$L(v) = \iint_\Omega \left(\left(\frac{\partial v}{\partial x} \right)^2 + \left(\frac{\partial v}{\partial y} \right)^2 \right) dx \, dy - 2 \iint_\Omega fv \, dx \, dy - 2 \int_{\partial\Omega} gv \, ds .$$

1.1.4 Approximated Solution by Finite Elements

Introduction

The purpose of the finite elements method is to provide an approximated solution of a differential problem starting from its variational form.

A formulation by finite elements requires three stages:

(i) representation of the domain Ω ;

(ii) choice of the functional space U_h approximating U and in which the approximated solution u_h is to belong;

(iii) minimization of L (or of a functional L_h approximating L) on the space U_h .

The choice of a finite dimensional space for U_h leads to a finite system of equations.

In the linear case the solution of this system can be made either by classical techniques of elimination or iteration, or by approximate methods of elimination which take into consideration the structure of the matrix.

Representation of the domain

The boundary $\partial\Omega$ of the region Ω is approximated by a polygonal line $\partial\Omega_h$.

In most cases we subdivide into triangles the region Ω_h bounded by $\partial\Omega_h$.

Let S be the set of vertices of the triangles T_j. The elements belonging to S are indexed by two systems of numbering:

(a) A global system where the vertices are indexed from 1 to n_s (number of vertices in S);

(b) A local system of two indexes (i,j) where the vertices are indexed in connexion with the triangle which they belong.

The index j varies here from 1 to 3 and the index i from 1 to n_t (number of triangles).

The matrix of permutation R allowing the mapping of the global system into the local one is called the matrix of reduction.

This matrix R is rectangular with $3n_t$ rows and n_s columns.

Let $s \in S$. This vertex has an index k in the global system, and indexes i, j in the local system. If f is a function defined on S its value is noted either by f_k or by $f_{i,j}$ and to change from one notation to the other, we use the relation:

$$\{f_{i,j}\} = R\{f_k\} . \tag{12}$$

As an example, let the domain D_h be formed by the two triangles 1 and 2. In the global system the numbering of the vertices goes from 1 to 4 and in the local system we have (Fig.1):

$$(1,1), (1,2), (1,3), (2,1), (2,2), (2,3)$$

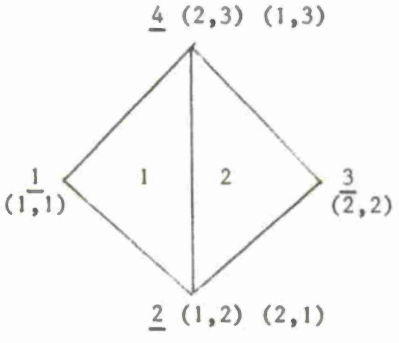

Figure 1

To change from the global system to the local system we use the equality:

$$\begin{bmatrix} f_{1,1} \\ f_{1,2} \\ f_{1,3} \\ f_{2,1} \\ f_{2,2} \\ f_{2,3} \end{bmatrix} = \begin{bmatrix} 1 & 0 & 0 & 0 \\ 0 & 1 & 0 & 0 \\ 0 & 0 & 0 & 1 \\ 0 & 1 & 0 & 0 \\ 0 & 0 & 1 & 0 \\ 0 & 0 & 0 & 1 \end{bmatrix} \begin{bmatrix} f_1 \\ f_2 \\ f_3 \\ f_4 \end{bmatrix} .$$

Choice of the space U_h

The functions f will be obtained by local interpolation from a set of discrete values f_k or f_{ij} given on S.

$$f(x,y) = \sum_{i=1}^{n_t} N_i(x,y,f_{i1},f_{i2},f_{i3}) . \tag{13}$$

Notice that f is defined separately on each triangle T_i.

The choice of the functions N_i is conditioned by the problem to be solved, and by the desired accuracy.

For second order problems to be solved with poor accuracy we can choose functions N_i of the following type:

$$N_i(x,y,f_{i1},f_{i2},f_{i3}) = 0 \quad \text{if} \quad (x,y) \notin T_i$$

$$N_i(x,y,f_{i1},f_{i2},f_{i3}) = \sum_{j=1}^{3} N_{ij}(x,y) f_{ij} \quad \text{if} \quad (x,y) \in T_i \,. \tag{14}$$

The functions N_{ij} are linear:

$$N_{ij}(x,y) = a_{ij} + b_{ij}x + c_{ij}y \,.$$

The coefficients a_{ij}, b_{ij}, c_{ij} are chosen in order that N_{ij} equal 1 at the vertex s_{ij} and equal 0 at the other two vertices of the triangle T_i.

We now introduce barycentric coordinates.

If the cartesian coordinates of M are x, y, and if the cartesian coordinates of the vertex s_{ij} are x_{ij}, y_{ij} then the barycentric coordinates $\lambda_1, \lambda_2, \lambda_3$ of M are determined by the following system of linear equations.

$$\left.\begin{aligned} \lambda_1 x_{i1} + \lambda_2 x_{i2} + \lambda_3 x_{i3} &= x \\ \lambda_1 y_{i1} + \lambda_2 y_{i2} + \lambda_3 y_{i3} &= y \\ \lambda_1 \quad + \lambda_2 \quad + \lambda_3 \quad &= 1 \,. \end{aligned}\right\} \tag{15}$$

If M is the vertex s_{ij} then $\lambda_j = 1$ and $\lambda_k = 0$ $(k \neq j)$. Hence we can write:

$$N_{ij} = \lambda_j$$

or

$$N_{ij} = \frac{\begin{vmatrix} x & x_{i1} & x_{ik} \\ y & y_{i1} & y_{ik} \\ 1 & 1 & 1 \end{vmatrix}}{\begin{vmatrix} x_{ij} & x_{i1} & x_{ik} \\ y_{ij} & y_{i1} & y_{ik} \\ 1 & 1 & 1 \end{vmatrix}}$$

where $(j,1,k)$ is a permutation of $(1,2,3)$.

For the Neumann problem previously stated the space U_h is the discrete subspace defined by the uniqueness condition: $\iint_{\Omega_h} u_h \, dx \, dy = 0$.

Discrete variational formulation

We know that the weak solution u minimizes the functional:

$$L(v) = \iint_{\Omega} \left\{ \left(\frac{\partial v}{\partial x}\right)^2 + \left(\frac{\partial v}{\partial y}\right)^2 - 2fv \right\} dx \, dy - 2 \int_{\partial\Omega} gv \, ds \,.$$

We use the Ritz method to approximate u in U_h. Then the discrete problem is:

Find $u_h \in U_h$ minimizing the functional

$$L_h(v_h) = \iint_{\Omega_h} \left\{ \left(\frac{\partial v_h}{\partial x}\right)^2 + \left(\frac{\partial v_h}{\partial y}\right)^2 - 2fv_h \right\} dx \, dy - 2 \int_{\partial\Omega_h} gv_h \, ds \,.$$

L is often called an energy.

The forms of the discrete and continuous problems are the same and thus we have good reason to think that u_h will be a good approximation to u provided that the space U_h is close enough to the space U.

Let:

$$u_h(x,y) = \sum_{i=1}^{n_t} N_i(x,y,u_{i1},u_{i2},u_{i3}) . \tag{16}$$

The functions N_i are given by the relations (14); the quantities u_{ij} represent the n_s values of the function u at the vertices of the triangle in the local system of numbering. In this way we can define the function u_h on Ω_h.

The interpolation functions N_i vanish on the outside of triangle T_i and their first derivatives are well defined functions but are discontinuous at the boundary of triangle T_i. Then we can obtain the value of the total energy $L_h(u_h)$ by summing up the energy in each triangle:

$$L_h(u_h) = \sum_{i=1}^{n_t} L_i(u_h) . \tag{17}$$

Where:

$$L_i(u_h) = \iint_{T_i} \left\{ \left(\frac{\partial N_i}{\partial x}\right)^2 + \left(\frac{\partial N_i}{\partial y}\right)^2 - 2fN_i \right\} dx\,dy - 2\int_{\partial\Omega_h} gN_i\,ds . \tag{18}$$

If $L_h(u_h)$ is minimum we have:

$$\frac{\partial L_h}{\partial u_k} = 0 \qquad 1 \leq k \leq n_s .$$

And:

$$\left\{\frac{\partial L_h}{\partial u_k}\right\} = R^t \left\{\frac{\partial L_i}{\partial u_{ij}}\right\} . \tag{19}$$

Where R^t is the transpose of the reduction matrix defined by (12).

From the relations (12) we obtain the following expression for $L_i(u_h)$:

$$L_i(u_h) = \iint_{T_i} \left\{ \left(\sum_{k=1}^{3} \frac{\partial N_{ik}}{\partial x} u_{ik}\right)^2 + \left(\sum_{k=1}^{3} \frac{\partial N_{ik}}{\partial y} u_{ik}\right)^2 - 2\sum_{k=1}^{3} N_{ik}u_{ik}f \right\} dx\,dy - 2\int_{\partial\Omega_h} \sum_{k=1}^{3} N_{ik}u_{ik}g\,ds .$$

Then:

$$\frac{\partial L_i}{\partial u_{ij}} = 2\iint_{T_i} \left\{ \left(\sum_{k=1}^{3} \frac{\partial N_{ik}}{\partial x}\frac{\partial N_{ij}}{\partial x} + \frac{\partial N_{ik}}{\partial y}\frac{\partial N_{ij}}{\partial y} \right) u_{ik} - N_{ij}f \right\} dx\,dy - 2\int_{\partial\Omega_h} N_{ij}g\,ds .$$

This relation can be written:

$$\frac{\partial L_i}{\partial u_{ij}} = \sum_{k=1}^{3} \alpha_{ijk}u_{ik} - \beta_{ij} .$$

Where:

$$\alpha_{ijk} = 2\iint_{T_i} \left(\frac{\partial N_{ik}}{\partial x}\frac{\partial N_{ij}}{\partial x} + \frac{\partial N_{ik}}{\partial y}\frac{\partial N_{ij}}{\partial y} \right) dx\,dy$$

$$\beta_{ij} = 2\iint_{T_i} N_{ij}f\,dx\,dy + 2\int_{\partial\Omega_h} gN_{ij}\,ds .$$

Or in matrix notation:

$$\left\{\frac{\partial L_i}{\partial u_{ij}}\right\} = A\{u_{ik}\} - \{\beta_{ij}\} . \tag{20}$$

Where A is a $3n_t \times 3n_t$ matrix.

Using the above Equation (20), Equation (19) can be written:

$$R^tAR\{u_j\} - R^t\{\beta_{ij}\} = 0 . \tag{21}$$

So we obtain a linear system of order n_s .

1.2 General Presentation of the Finite Element Method

We now describe the finite element method applied to differential problems. Assuming that the continuous problem to be solved is in its variational form:

Find u so that $\quad L(u) = \underset{v \in V}{\text{Min}}\ L(v)$

where L is a quadratic functional containing derivatives of orders up to m,

V is a functional space on (Ω),

(Ω) is a bounded domain of R^n.

In all cases we have as before the same three stages (see 1.1):

(i) Choice of Ω_h and of the finite elements;

(ii) Choice of the discrete space U_h ;

(iii) Assemblage and solution of the equations obtained.

1.2.1 Choice of the Discrete Space U_h

The fundamental idea of the finite element method for solving functional equations is to use *piecewise polynomial* approximations of the unknown functions u_h so as to obtain a finite system of equations.

Thus, the first step consists in the "choice of the pieces". If the functions are defined on a domain Ω we subdivide it into subregions named *finite elements* of simple shapes and possibly of various sizes.

The second step is to choose in every element Ω_i the finite set of parameters q_{ij} $(j = 1, n_i)$ which describe the function, and the *shape functions* N_{ij} associated with these parameters:

$$u_h\big|_{\Omega_i} = \sum_{j=1}^{n_i} q_{ij} N_{ij} .$$

In most cases the parameters q_{ij} defining the interpolate u_h are associated with *nodal values* of the function u_h on points z_j located inside Ω_i or on its boundary:

$$q_{ij} = D_j(u_h(z_j))$$

where D_j is a derivative operator,

$z_j \in \Omega_i$ a *node*.

Note that it is possible to have *multiple nodes* where, for example, $z_{j_1} = z_{j_2}$ but $D_{j_1} \neq D_{j_2}$.

The third step of the definition of the interpolate is to relate values of the parameters of adjacent elements so as to ensure continuity of the function u_h and moreover of its derivatives of order up to m (conforming elements). The simplest way is to take as parameters some values of the function or its derivatives on the boundary of the element. In this way some local values are shared by several elements so that we must distinguish between the local set of parameters defining $u_h|\Omega_i$ and the global set of parameters defining u_h on Ω. We describe later (1.2.5) some classical types of elements and the associated interpolation procedures.

Thus we have defined a discrete space U_h .

1.2.2 Assemblage

After having defined the finite elements we must establish the equations. We proceed element by element in an arbitrary (but convenient) order to compute the energy $L_h(v_h)$. Note that it is possible to compute this functional element by element if the elements are *conforming*, i.e., if the derivatives of order $(m-1)$ are continuous on the inter-elements boundaries.

In the local system of coordinates with local parameters the quadratic part of the energy L_i of the element i can be defined by a symetric matrix k_i often called the *stiffness matrix*, so that if we denote by q_i the parameters vector $q_i = (q_{ij})\ j = 1, \ldots, n_i$

$$L_i = q_i^t k_i q_i + \ldots .$$

In other words, we have a quadratic functional of the local variables q_{ij} .

In the same way we can compute the linear part of the functional L_i

$$-2(f,v) = -2f_i^t q_i .$$

Before computing the total energy L_h we note that to obtain the final system of equations we have only to compute the coefficients of a global matrix K. To obtain K we must change the local names of the parameters into global ones and to transform the formula which gives the local energy in the local system of coordinates into a formula using the global one. We explain this with notations in matrix format.

Let Q be the array of global parameters. For each element we can define a rectangular incidence matrix P_i so that:

$$\bar{q}_i = P_i Q .$$

Then $\bar{q}_i$ is the subarray of Q related to element i. We can define the transformation matrices r_i and R_i so that:

$$q_i = r_i \bar{q}_i = r_i P_i Q = R_i Q .$$

In R_i we take into account the two different systems of coordinates. Then we need only add local energies in a proper way to obtain the global energy and the global matrix K :

$$L = \sum_i L_i = \sum_i q_i^t k_i q_i - 2 \sum_i f_i^t q_i$$

or

$$L = \sum_i (Q^t R_i^t k_i R_i Q - 2 f_i^t R_i Q) .$$

The matrix $K = \sum_i R_i^t k_i R_i$ is called the *global stiffness* matrix, and the vector $F^t = \sum_i f_i^t R_i$ the *generalized force*. We obtain the quadratic functional:

$$L(Q) = Q^t K Q - 2 F^t Q .$$

Obviously the minimum Q of this functional is the solution of the linear system:

$$KQ = F .$$

1.2.3 Finite Elements and Galerkine Method

Up to now we have used the Ritz method to solve variational problems. However many problems cannot be formulated in a variational way but only in a weak way.

Let the continuous problem P be:

$$(P) \quad \left\| \begin{array}{l} \text{Find } u \in U \text{ so that} \\ \qquad a(u,v) = (f,v) \quad \text{for any} \quad v \in V \\ \\ \text{where } U \text{ and } V \text{ are functional spaces,} \\ \qquad a(u,v) \text{ a bilinear form bounded on } U \times V , \\ \qquad (f,v) \text{ a linear form on } V . \end{array} \right.$$

Let $U_h \subset U$ and $V_h \subset V$ be two discrete spaces of the same dimension $N(h)$ where h is a positive parameter representing the accuracy of the discretization. When $h \to 0$ then $N(h) \to \infty$. In the Galerkine method we solve the sequence of discrete problems P_h :

$$(P_h) \quad \left\| \begin{array}{l} \text{Find } u_h \in U_h \text{ so that} \\ \qquad a_h(u_h,v_h) = (f,v_h) \quad \text{for any} \quad v_h \in V_h \end{array} \right.$$

where U_h and V_h are the vector spaces formed by linear combinations of the $N(h)$ basis functions $(\Phi_i,\ j = 1, .., N(h))$, $(\Psi_i,\ i = 1, .., N(h))$.

If $u_h = \sum_{i=1}^{N(h)} u_i \phi_i$ is the discrete solution we must have for all $v_h = \sum_{j=1}^{N(h)} v_j \psi_j$ the equality:

$$\sum_{ij} u_i v_j a_h(\phi_i, \psi_j) = \sum_j v_j (f, \psi_j)$$

which leads to the following linear system of order $N(h)$:

$$\sum_{i=1}^{N(h)} u_i a_h(\phi_i, \psi_j) = (f, \psi_j) .$$

Generally we choose $U_h = V_h$. However the so-called *collocation method* ($\psi_j = \delta_{zj}$) has the advantage of simplifying the calculation of the coefficients $a(\phi_i, \psi_j)$, but requires smoother functions ψ_j .

We now study the case where the spaces U_h and V_h are defined by using finite elements.

We could of course associate to each nodal value k a global basic function ϕ_k the restriction of which to each element e_i is the local basic function N_{ik} corresponding to this nodal value. This brings us back to the previous formulation, but it is no longer a matter of finite elements.

To avoid this we proceed as follows, operating element by element as before. Let a_i be the restriction on the element e_i of the bilinear functional a , let $q_{ik} k = 1, .., n_i$ be the associated nodal values and let N_{ik} be the associated basic functions.

On e_i we cannot write that:

$$\sum_{k,j=1}^{n_i} q_{ik} q'_{ij} a_{hi}(\phi_{ik}, \phi_{ij}) = \sum_j q'_{ij}(f, \phi_{ij})$$

for any q'_{ij} , $j = 1, .., n_i$ since this equality is verified only for the basic global functions.

Therefore on each element e_i and for each test function ϕ_{ij} we introduce the correcting terms Φ_{ij} so that the following equalities are verified:

$$\sum_{k=1}^{n_i} q_{ik} a_{hi}(\phi_{ik}, \phi_{ij}) + \Phi_{ij} = (f, \phi_{ij}) .$$

The auxiliary unknowns Φ_{ij} will be eliminated immediately (though they have a physical interpretation that we explain later). These auxiliary unknowns Φ_{ij} and the nodal values (Q_i, $i = 1, .. N(h)$) are determinated by the equalities:

$$\sum_{m=1}^{N(h)} Q_m a_h(\phi_m, \phi_n) = (f, \phi_n)$$

for $n = 1, ..., N(h)$. As before we obtain this system by summing the equations corresponding to the same global node, without taking into consideration the auxiliary unknowns. So we write that the sum of the associated auxiliary unknowns is zero. It is clear that in this way we obtain the same equations as in the Ritz method where we minimize the functional:

$$a(u,v) - 2(f,u) = L(u) .$$

Interpretation of the auxiliary unknowns

The following physical interpretation of the auxiliary unknowns as surface forces can be explained more easily on the continuous problem:

Find $u \in U$ such that

$$a(u,v) = (f,v) \quad \text{for any} \quad v \in V .$$

Let $\Omega' \subset \Omega$.

Note that $a'(u,v)$ and $(f,v)'$ are the restrictions to Ω' of the previous a and (f,v) . Generally the following equality is not true:

$$a'(u,v) = (f,v)' \quad \text{for any} \quad v \in V$$

this is because of the influence of the elements in $\Omega - \Omega'$ on the element Ω' .

So we state:

$$a'(u,v) - (f,v)' = ((\Phi,v))$$

where $((\Phi,v))$ is an unknown linear form on V. Note that if the supp* $(v) \subset \Omega'$ or if the supp $(v) \subset \Omega - \Omega'$

---

* Supp $(v) = \{x | x \in \Omega, v(x) \neq 0\}$.

then $((\Phi,v)) = 0$. Hence $((\Phi,v))$ is a surface integral on $\partial\Omega'$. This integral takes into account all the influence of $\Omega - \Omega'$ on the element Ω'. This is a mathematical explanation for the surface forces which apply when we cut up a part of a body mentally.

Analytically the auxiliary unknowns are the Lagrange multipliers which are necessary to minimize $L(v)$ on all the elements, because they take into account the constraints of equality of the nodal values shared by several elements.

Example: Let $a(u,v)$ be (see 1.1):

$$a(u,v) = \sum_{i=1}^{2} \int_{\Omega} \frac{\partial u}{\partial x_i} \frac{\partial v}{\partial x_i} \, dx$$

$$(f,v) = \int_{\Omega} fv \, dx \, .$$

Using Green's formula we obtain:

$$a'(u,v) - (f,v)' = \int_{\partial\Omega'} \frac{\partial u}{\partial n} v \, ds = ((\Phi,v))$$

where ds is the surface element on $\partial\Omega'$.

In this case Φ is the normal derivative of u on $\partial\Omega'$. If u is a potential, then $\partial u/\partial n$ is called the normal strain.

1.2.4 Simultaneous Assembly and Elimination

In some problems where there are many unknowns and thus it is difficult to write explicitly the matrix K. In fact the size of the matrix K can often exceed the core memory of the computer. In this case we can use the so called *frontal method.*

We start from the reciprocal of the incidence matrix R which gives the relation:

set of global unknowns → set of local unknowns .

As before we proceed element by element. If we make a suitable choice in the numbering of global unknowns, it is possible to carry out elimination of a row as soon as every element associated with this row has been accounted for. In other words the global unknown associated with this row is written in terms of the other unknowns. This is stored and we can then eliminate the corresponding row and column of K. We pursue such a procedure until total elimination.

Note that in all cases we first eliminate the unknowns corresponding to internal nodes, which are related only to nodes of the same element (*static condensation*). In this respect the frontal method is just a generalization of the static condensation.

1.2.5 Usual Finite Elements

Many finite elements have been studied. The finite element method has given a new impulse to the old mathematical theory of multivariate interpolation. We first study the one-dimensional case, which will outline the problem but is of no practical interest. However, with regular meshes in multi-dimensional space we can deduce by tensor product some useful formulae.

One-dimensional elements: in this case we have only one shape for the element. Every element can be mapped by translation and scaling on $[0,1]$. If the polynomial to be found is of degree k it is necessary to have $(k+1)$ nodal values. In this way we preserve all polynomials of degree k. When we choose the nodal values and the nodes we must put sufficient nodal values in 0 and 1 to ensure continuity of the derivatives and to reduce the dimension of V_h. We show below some elements corresponding to $k = 1, 2, 3$. As usual we denote by C^p the class of real valued functions with continuous derivatives of order up to p.

$k = 1$. The nodes are 0 and 1 and the nodal values are the two values u_0 and u_1 of the function u at these nodes. After assemblage the function u_h obtained is of class C^0. The shape functions N_j are:

$$N_1(x) = 1 - x \quad \text{(node 0)} \qquad N_2(x) = x \quad \text{(node 1)}.$$

$k = 2$. We add one node at the center of the elements.

$k = 3$. We can proceed in two different ways:

(i) add one more internal node: a method seldom used.

(ii) keep only nodes 0 and 1 but give to each node the two nodal values u and u′. Thus each nodal value is shared by two elements and we have fewer degrees of freedom. Moreover the function u obtained is of class C^1. This is the so-called Hermite interpolation. The shape functions N_j are:

$$N_1(x) = (x-1)^2(2x+1) \quad \text{(for the nodal value } u_0\text{)}$$
$$N_2(x) = x(x-1)^2 \quad \text{(for the nodal value } u'_0\text{)}$$
$$N_3(x) = x^2(3-2x) \quad \text{(for the nodal value } u_1\text{)}$$
$$N_4(x) = (x-1)x^2 \quad \text{(for the nodal value } u'_1\text{)} \quad \text{(see Figure 2).}$$

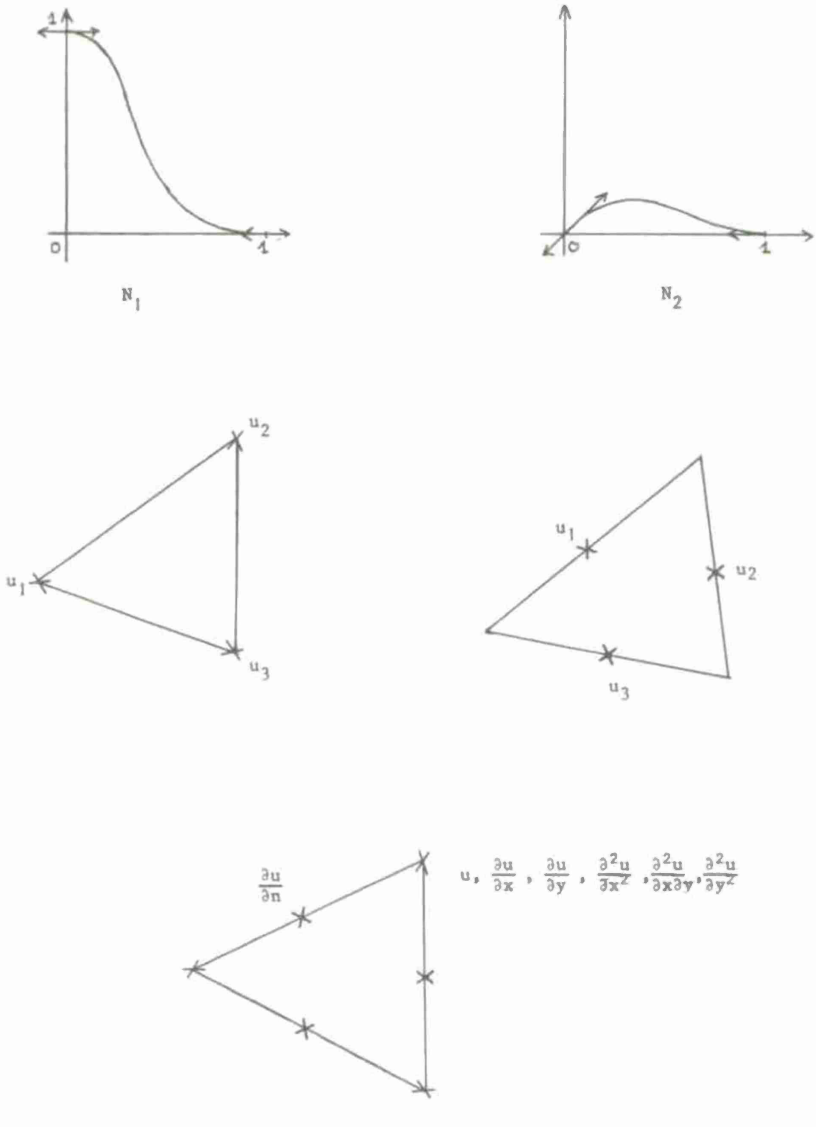

Fig.2 Basic functions of Hermite interpolation and some typical elements

Two-dimensional elements: the two fundamental shapes are triangles and rectangles.

Triangles: As before we classify the finite elements by the degree k of the interpolation polynomials.

$k = 1$. With nodes at the vertices of the triangle this is the best known case of the finite elements (since Courant 1943). We obtain a function of class C^0. Another solution (whose interest is purely academic) is to take as nodes the midpoints of the edges. The function obtained is no longer continuous and the number of unknowns is multiplied by three. However one can use these supplementary degrees of freedom to impose constraints.

In fact let $\vec{U} = (u,v)$ be a vector valued function to be interpolated so that $\operatorname{div} \vec{U} = 0$. On the triangle T we have:

$$\vec{U}|_T = \sum_{i=1}^{3} \vec{U}_i N_i(x,y)$$

where:

$$N_i(x,y) = 1 - 2\lambda_i \quad (\lambda_1,\lambda_2,\lambda_3 \text{ are as usual barycentric coordinates in T}) .$$

so

$$N_1(x,y) = \frac{y_2x_3 - x_2y_3 + xy_3 - yx_3 + yx_2 - xy_2}{y_2x_3 - x_2y_3 + x_1y_3 - y_1x_3 + y_1x_2 - x_1y_2} = \frac{P(x,y)}{Q}$$

hence

$$\operatorname{div} \vec{U} = \frac{\partial u}{\partial x} + \frac{\partial v}{\partial y} = \sum_{i=1}^{3} u_i \frac{\partial N_i}{\partial x} + v_i \frac{\partial N_i}{\partial y}$$

$\partial N_1/\partial x = (y_3 - y_2)/Q$ is a known constant, and so is $\partial N_1/\partial y$, $\partial N_2/\partial x$, ... Thus we obtain one homogeneous linear equation in each triangle:

$$\sum_{i=1}^{3} \alpha_i u_i + \beta_i v_i = 0 .$$

k = 2. We need 6 nodal values so we choose the midpoints of the edges and the vertices. We obtain an interpolation of class C^0.

k = 3. We can again choose additional nodes on the edges but we prefer to ensure more continuity by choosing as nodal values u, $\partial u/\partial x$, $\partial u/\partial y$ at the vertices. The remaining nodal value is taken at the centroid of the triangle. We ensure in this way continuity of the first derivatives at every vertex.

k = 4. In order to obtain conforming elements to solve fourth-order problems it is necessary to have continuity of the first derivatives on every edge. This is done in a straightforward way by using at every vertex the nodal values

$$u , \frac{\partial u}{\partial x} , \frac{\partial u}{\partial y} , \frac{\partial^2 u}{\partial x^2} , \frac{\partial^2 u}{\partial y^2} , \frac{\partial^2 u}{\partial x \partial y}$$

and at the midpoint of every edge the normal derivative $\partial u/\partial n$.

Rectangles: The interpolation functions $N(x,y)$ are obtained in this case by "tensor product" of the corresponding one-dimensional functions:

$$N_{i,j}(x,y) = N_i(x)\, N_j(y) .$$

Thus we obtain bilinear, bicubic elements.

1.2.6 Rates of Convergence

To study the convergence of the finite element method we start from the following basic property of the approximated solution u_h.

$$a(u - u_h, u - u_h) = \operatorname*{Min}_{v_h \in U_h} [a(u - v_h, u - v_h)] .$$

Proof

The weak solution u verifies:

$$L(u) = \operatorname*{Min}_{v \in U} [a(v - u, v - u) - a(u,u)] .$$

The discrete solution u_h verifies:

$$L(u_h) = \operatorname*{Min}_{v_h \in U_h} [a(u - v_h, u - v_h) - a(u,u) .$$

So we have: $$a(u - u_h, u - u_h) - a(u,u) \leqslant a(u - v_h, u - v_h) - a(u,u) .$$

For all $v_h \in U_h$. This proves the assertion.

In other words u_h(resp. u) is the best approximation of u in U_h(resp. U) with the norm $\|w\|^2 = a(w,w)$. This is the so-called energy norm.

To study the convergence we proceed in three steps:

(a) Examine how we can approach in various norms any function u by a finite element approximation U_h.

(b) Apply the previous results to estimate the error in the energy norm.

(c) Estimate the error in other norms.

(a) *First step*

The norms to be used are the so-called Sobolev norms or H^m norms:

$$\|u\|_m^2 = \int_\Omega \sum_{|\alpha| \leq m} |D^\alpha u|^2 dx .$$

Here α is a multi-index $\alpha = (\alpha_1, ..., \alpha_n)$ with $|\alpha| = \alpha_1 + ... + \alpha_n$, $dx = dx_1, ..., dx_n$ is the volume element of $\Omega \subset R^n$.

Note that: $\|u\|_0^2 = \int_\Omega |u|^2 dx$ is the well-known L^2-norm.

It is difficult to find in each norm the best approximation u_h of u. So we consider only the less good but more tractable approximation u_I obtained by *interpolation* of u:

$$u_I(x)|_{\Omega_i} = \sum_{j=1}^{n_i} D_j u(z_j) N_{i,j}(x) .$$

The goal is to obtain an upper estimate of $\|u - u_I\|_m$. It is clear that it is sufficient to consider the effect on each element Ω_i.

The standard procedure is to use one of the Taylor expansions of u : $u = p + R$ where p is a polynomial "near" u and R is the remainder. Thus, it is important to know the maximal degree of the polynomials p which are preserved by the interpolation process.

Suppose that D_j, z_j, $N_{i,j}$ are chosen so that for all polynomials of degree less than k we have:

$$p = p_I \quad \text{on} \quad \Omega_i .$$

To obtain an upper estimate of $\|u - u_I\|_m$ it is sufficient to obtain an upper estimate of the residual remainder $\|R_I - R\|_m$. It is clear that this estimate will depend on the diameter h of Ω_i and the variations of the $(k+1)$th-derivatives of u. It is a classical routine to obtain the estimate:

$$\|u - u_I\|_0 \leq C h^{k+1} \left(\sum_{|\alpha| = k+1} \int_{\Omega_i} |D^\alpha u|^2 dx \right)^{1/2} .$$

We seek an estimate of the derivatives of $u - u_I$; it is easy to see that, provided the basic functions $N_{i,j}$ have sufficient derivatives, we lose one order of the power of h for each order of derivative. So

$$\|u - u_I\|_s \leq C h^{k+1-s} \left(\sum_{\alpha = k+1} \int_{\Omega_i} |D^\alpha u|^2 dx \right)^{1/2}$$

(C are various constants).

In other words if the interpolation process preserves the polynomials of degree k the rate of convergence of the s-derivative is of order $k + 1 - s$.

(b) *Second step*

To prove the existence and the uniqueness of the solution u of the continuous problem we must assume for a $2m$ order elliptic problem the following inequalities:

$$\underline{C} \|u\|_m^2 \leq a(u,u) \leq \bar{C} \|u\|_m^2 .$$

We have, u_h being the best approximation:

$$a(u - u_h, u - u_h) \leq a(u - u_I, u - u_I) \leq \bar{C} \|u - u_I\|_m^2 .$$

From the first step we obtain:

$$a(u-u_h,\, u-u_h) \leqslant Ch^{2(k+1)-2m} \sum_{|\alpha|=k+1} \int_\Omega |D^\alpha u|^2 \, dx \, .$$

Using the coercivity of a we have:

$$\|u-u_h\|_m \leqslant Ch^{k+1-m} \left(\sum_{\alpha=k+1} \int_\Omega |D^\alpha u|^2 \, dx \right)^{1/2} .$$

So we can say that *if* $k + l > m$ the f.e.m. converges with a rate of convergence $k + l - m$ in the energy norm.

The condition $k + l > m$ is called the constant strain condition.

(c) *Third step*

At this point we know only the rate of convergence of the m-th derivatives. We can expect to have for the values of u a rate of convergence of order $k + l - m + m = k + l$ as in the interpolation. This is not quite true because u_h is the best approximation of u only in the energy norm and it is possible to obtain in another norm a rate of convergenee less good than those obtained by interpolation. Precisely, we have the following result (see Strang[43]).

If the order of the derivatives of $u - u_h$ is greater than $2m - k - l$ we have:

$$\|u-u_h\|_s \leqslant Ch^{k+1-s}|u|_{k+1} \quad \text{for} \quad s \geqslant 2m-k-l \, .$$

This is the expected rate of convergence.

But if the order of the derivatives $u - u_h$ is less than $2m - k - l$ we cannot obtain better than $2(k + l - m)$ for any order of derivative s :

$$\|u-u_h\| \leqslant Ch^{2(k+1-m)}|u|_{k+1} \quad \text{for} \quad s \leqslant 2m-k-l \, .$$

Here:

$$|u|_{k+1} = \left(\sum_{|\alpha|=k+1} \int_\Omega |D^\alpha u|^2 \, dx \right)^{1/2} .$$

The following conclusions can now be drawn:

(a) to improve convergence it is necessary to use finite elements of higher degree,

(b) to ensure convergence it is necessary to use finite element of such degree that $k + l > m$.

For example in the case of fourth order problems ($m = 2$) it is necessary to preserve polynomials of degree 2. The obtained rates of convergence are:

$$\|u-u_h\|_2 \leqslant Ch|u|_3$$

$$\|u-u_h\|_1 \leqslant Ch^2|u|_3$$

$$\|u-u_h\|_0 \leqslant Ch^2|u|_3 \, .$$

Note that for values of u we cannot obtain a better rate of convergence than for the values of derivatives.

1.2.7 Choice of the Quadrature Formulae

For elements of high degree or for curved elements it is not possible to compute precisely the coefficients of the stiffness matrix; it is necessary to use some quadrature formulae to compute these numbers. This procedure will induce errors and the problem is to choose quadrature formulae so as to obtain the expected accuracy in the solution.

First we introduce some definitions concerning quadrature formulae.

To compute

$$I = \int_D f(x) \, dx$$

where D is a given domain of R^n (generally a simple one), dx the differential element $dx_1 .. dx_n$ and f any function, we use nodes $\xi_1, \xi_2, ..., \xi_m$ belonging or not to D, and compute the weighted sum:

$$\tilde{I} = \sum_{i=1}^{m} w_i f(\xi_i) .$$

The accuracy of the formula is estimated by the maximal degree q of the polynomials for which $I = \tilde{I}$. The number of nodes ξ_i increases with the degree q. For $n = 1$, if the nodes $\xi_1, ..., \xi_m$ are given, we can choose the weights $w_1, ..., w_m$ to maximize the accuracy q, or for a given q to minimize some measure of the residual error.

For $n > 1$ the same problems are not yet completely solved. The formulae used in these cases are product formulae derived from the unidimensional case.

The key result is if the piecewise polynomials used on every finite element are of degree $k - 1$ and if the quadrature formulae is exact up to a degree q the error in the minimization of a quadratic functional in which appear derivatives up to order m, is of order $2(q - k + m + 2)$.

Thus, to converge we must precisely integrate the derivatives of order m of the shape functions. Note that it is not necessary for convergence precisely to integrate the square of the m-th derivatives, but obviously this involves a loss of accuracy. Each increase in the order of the formulae used gives an additional power on the rate of convergence. Note also that we need to obtain a positive definite stiffness matrix after numerical integration. This condition is often more difficult to verify.

1.2.8 Curved elements

Until now the elements have been triangles or rectangles. In order to obtain greater accuracy in the approximation of the domain and of the boundary conditions we introduce elements with curved boundaries. We shall again use the example (1.1) to explain how to obtain curved elements by changing the space-coordinates x,y into new ones α, β.

The goal is to formulate the problem in a new domain R that is simpler than the previous one. For this it is necessary to have a bijection $x(\alpha, \beta), y(\alpha, \beta)$ between Ω and R.

We choose as R a rectangle $[0,1] \times [0,\beta_0]$ and subdivide $\partial\Omega$ into the four curves $\Gamma_1, \Gamma_2, \Gamma_3, \Gamma_4$, corresponding to the four sides of the rectangle.

Given the following parametric representation of the curve Γ_i:

$$x = f_i(s) , y = g_i(s) \qquad 0 \leq s \leq S_i$$

We impose the following boundary conditions on the bijection:

$$x(\alpha,0) = f_1(S_1\alpha) , \quad y(\alpha,0) = g_1(S_1\alpha) \quad 0 \leq \alpha \leq 1$$

$$x(1,\beta) = f_2\left(S_2 \frac{\beta}{\beta_0}\right), \quad y(1,\beta) = g_2\left(S_2 \frac{\beta}{\beta_0}\right) \quad 0 \leq \beta \leq \beta_0$$

$$x(\alpha,1) = f_3(S_3\alpha) , \quad y(\alpha,1) = g_3(S_3\alpha) \quad 0 \leq \alpha \leq 1$$

$$x(0,\beta) = f_4\left(S_4 \frac{\beta}{\beta_0}\right), \quad y(0,\beta) = g_4\left(S_4 \frac{\beta}{\beta_0}\right) \quad 0 \leq \beta \leq \beta_0 .$$

At this stage it is not necessary to state the bijection precisely. It is enough to be sure that it exists and is sufficiently smooth.

We subdivide R into elements with linear sides.

For example, we choose a step h and β_0 so that:

$$h = \frac{1}{N} , \quad \beta_0 = \frac{K}{N} .$$

We subdivide R into triangles the sides of which lie on the lines:

$$\begin{aligned} \alpha &= nh \qquad 0 \leqslant n \leqslant N \\ \beta &= kh \qquad 0 \leqslant k \leqslant K \\ \alpha + \beta &= l \qquad 0 \leqslant l \leqslant \mathrm{Max}(N,K) \end{aligned}$$

$\beta_0 = Kh$

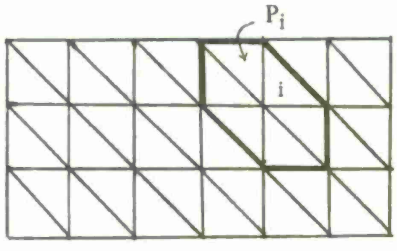

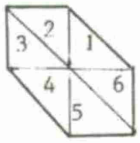

$Nh = 1$

At the vertex i we call P_i the interior of the polygon which is the union of the triangles $T_{i1}, T_{i2}, T_{i3}, T_{i4}, T_{i5}, T_{i6}$ with the common vertex i. Subsequently we omit the index i when the omission will not cause confusion. We use on P_i the interpolation functions $\eta_i(\alpha,\beta)$ verifying:

$$\eta_i(\alpha,\beta) = 0 \quad \text{if} \quad (\alpha,\beta) \notin P_i$$

$$\eta_i(\alpha_i,\beta_i) = 1 \quad \text{if} \quad (\alpha_i,\beta_i) \text{ are the coordinates of vertex i .}$$

$$\sum_i \eta_i(\alpha,\beta) = 1 .$$

The restriction of η_i on each triangle T_i is the basic function N_i defined with triangular elements (k = 1).

Here we use Galerkine's method directly. Let:

$$u_h = \sum_j \eta_j(\alpha,\beta) u_j$$

be the approximate solution. Using the weak form of the Neumann problem (1.1.2), we find the equations:

$$\sum_j a_{ij} u_j = f_i$$

where:

$$a_{ij} = \iint_\Omega \left(\frac{\partial \eta_i}{\partial x} \frac{\partial \eta_j}{\partial x} + \frac{\partial \eta_i}{\partial y} \frac{\partial \eta_j}{\partial y} \right) dx\, dy$$

$$f_i = \iint_\Omega f \eta_i \, dx\, dy .$$

Using the variable α, β we obtain the following expressions for a_{ij} and f_i :

$$a_{ij} = \iint_R \left(A \frac{\partial \eta_i}{\partial \alpha} \frac{\partial \eta_j}{\partial \alpha} - B \left(\frac{\partial \eta_i}{\partial \alpha} \frac{\partial \eta_j}{\partial \beta} + \frac{\partial \eta_i}{\partial \beta} \frac{\partial \eta_j}{\partial \alpha} \right) + C \frac{\partial \eta_i}{\partial \beta} \frac{\partial \eta_j}{\partial \beta} \right) d\alpha\, d\beta$$

$$f_i = \iint_R f \eta_i J \, d\alpha\, d\beta$$

where

$$J = \frac{\partial x}{\partial \alpha} \frac{\partial y}{\partial \beta} - \frac{\partial x}{\partial \beta} \frac{\partial y}{\partial \alpha}$$

$$A = \left(\left(\frac{\partial x}{\partial \beta} \right)^2 + \left(\frac{\partial y}{\partial \beta} \right)^2 \right) \Big/ J$$

$$B = \left(\frac{\partial x}{\partial \alpha}\frac{\partial x}{\partial \beta} + \frac{\partial y}{\partial \alpha}\frac{\partial y}{\partial \beta}\right)\Big/ J$$

$$C = \left(\left(\frac{\partial x}{\partial \alpha}\right)^2 + \left(\frac{\partial y}{\partial \alpha}\right)^2\right)\Big/ J .$$

We now explain how to obtain the bijection $x(\alpha,\beta), y(\alpha,\beta)$. The simplest procedure is to give a bijection between the nodes j in R and arbitrary nodes in Ω. By interpolation we can deduce the functions $x(\alpha,\beta), y(\alpha,\beta)$. It is interesting to use further interpolation $x(\alpha,\beta), y(\alpha,\beta)$, the same formula of the finite element method used to compute $u_h(\alpha,\beta)$. In the (x,y) plane we obtain the so-called *isoparametric elements*. When we use as nodal values derivatives of u we take the same nodes but we use the values of x and y only as nodal values. Thus the degree of the polynomials used in the interpolation of x and y is lower than the degree of the polynomials used in the interpolation of u. In this case, we obtain the so-called *sub-parametric elements*.

Another more elaborate technique consists of giving the bijection between the boundaries $\partial\Omega$ and ∂R and making some analytic continuation in Ω. For example we suppose $\alpha(x,y)$ and $\beta(x,y)$ to be harmonic functions, and deduce the equations verified by $x(\alpha,\beta), y(\alpha,\beta)$. Here we have only to solve two Dirichlet problems.

2. APPLICATIONS TO FLUID DYNAMICS

2.1 Introduction

Many methods are available for the solution of fluid dynamics problems, and frequently they use finite difference techniques. When an accurate definition of the domain is required (e.g. calculus of a pressure coefficient along a wing) a finite element technique is generally recommended. Nevertheless another method exists which provides an equivalent precision and is equally simple; this is the so-called "method of singularities". When the fundamental solution is known (as in the case of potential flow) this method leads to the solution of a smaller problem because the boundary conditions alone are approximate. In addition, particular conditions such as conditions on the trailing edge, or at infinity, are easily imposed. From this it follows that, for potential flows, the method of singularities is preferable to the finite element method. On the other hand when the problem is inhomogeneous or when the fundamental solutions are not known straightforwardly the finite element method is to be prefered.

We do not introduce examples about incompressible irrotational flow: numerous cases are treated in References 3, 5, 6, 7. Instead, we limit ourselves to a brief survey of the method of singularities. Then, in connection with the Stokes problem and Navier-Stokes equations, we introduce a discussion of the most significant uses of the finite element method in fluid dynamics problems.

2.2 Method of Singularities

Consider two-dimensional incompressible irrotational flow around an airfoil in a uniform stream U_∞. The perturbation potential for perturbation velocities is an harmonic function independent of time in a reference system relative to the airfoil Ω. On the boundary of the profile the slip condition is written as:

$$\left.\frac{\partial \Phi}{\partial n}\right|_{\partial\Omega} = -\vec{U}_\infty \cdot \vec{n} \qquad (1)$$

where n and $\partial\Phi/\partial n$ represent the outward normal unitary vector and the normal derivative of the function Φ. In order to obtain lift, we need to impose a circulation around the airfoil by the Kutta condition. The boundary $\partial\Omega$ of the body is represented by N straight elements on each of which a constant distribution of singularities is taken as acting. At a point with affix z the complex potential $f(z)$ induced by a density $(\sigma(t) + i\gamma(t))$ of singularities along $\partial\Omega$ is given by:

$$f(z) = \frac{1}{2\pi}\int_{\partial\Omega} \{\sigma(t) + i\gamma(t)\} \log (z - t)\,dt .$$

The unknowns $\sigma(t) + i\gamma(t)$ are determined by the boundary condition (1).

For a linear element $\partial\Omega_j \subset \partial\Omega$, with an origin z_{j-1}, and end z_j, a length $2a$ and an angle of inclination β_j measured from the positive x-axis, we note that $\sigma_j + i\gamma$ is the density of singularities. (It is possible to impose the Kutta condition, with γ constant along $\partial\Omega$.) The associated potential is given by

$$f(z) = \frac{1}{2\pi}\sum_j (\sigma_j + i\gamma) \int_{\partial\Omega_j} \log (z - t)\,dt$$

and the velocity by

$$\Phi_s'(z) - i\Phi_n'(z) = \frac{1}{2\pi}\sum_j (\sigma_j + i\gamma)e^{i(\beta-\beta_j)} \log \frac{(z-z_j)e^{-i\beta_j} + a}{(z-z_j)e^{-i\beta_j} - a}. \qquad (2)$$

The quantities $\Phi_s'(z), \Phi_n'(z)$ represent the derivatives of Φ in the direction β and $\beta + \pi/2$ with respect to the x-axis.

We choose N control points n_j at the midpoint of each segment $\partial\Omega_i$ and because we assume the Kutta condition we choose an extra point η_{N+1} located on the bissector at the trailing edge. By satisfying Equation (1) exactly at the $N+1$ control points we obtain through the relation (2) a system of $N+1$ linear equations for the $N+1$ unknowns: $\{\sigma_1, ..., \sigma_N, \gamma\}$. This system is solved by the normal techniques of elimination or iteration. After having found σ_j and γ we may establish the complete flow pattern, in particular the tangential velocity and the dynamic pressure.

2.3 The Stokes Problem; Solenoidal Element

Consider the motion of an incompressible viscous fluid within the limits of the Stokes approximation. The equations can be written

$$-\mu\Delta u + \frac{\partial p}{\partial x} = f_x$$

$$-\mu\Delta v + \frac{\partial p}{\partial y} = f_y$$

$$\frac{\partial u}{\partial x} + \frac{\partial v}{\partial y} = 0$$

where u, v are the velocity components in the x, y directions,
μ is the kinematic viscosity,
p is the pressure,
f_x, f_y are the components of the external forces.

These equations are to be solved in a domain Ω with the velocities prescribed on the boundary $\partial\Omega$. Note we have no condition for the pressure along the boundary $\partial\Omega$. The above problem has a unique solution.

We give now a simple example of the use of the solenoidal elements in solving the Stokes problem. Often this process is much more complicated, but this simple example serves to illustrate the general principle.

According to a standard procedure the domain Ω is partitioned into triangular subdomains and the unknown velocity and pressure fields are approximated throughout Ω by means of the following equations:

$$u = \sum_i N_i(x,y)u_i$$

$$v = \sum_i N_i(x,y)v_i$$

$$p = \sum_j M_j(x,y)P_j .$$

The nodal values u_i, v_i correspond to the node i while the nodal value p_j is associated with a node j which can be different from the former. Let us denote by

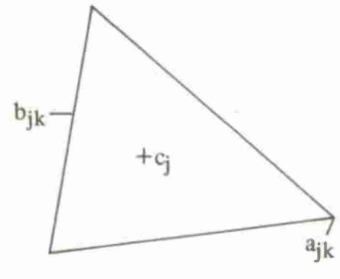

a_{jk} $1 \leq k \leq 3$ the vertices of a triangular subdomain T_j

b_{jk} $1 \leq k \leq 3$ the midpoint of the side opposite to the vertex a_{jk}

c_j the centroid of the triangle T_j

For the velocity components the nodes will be the points b_{jk} and for the pressure components the nodes will be the points c_j .

For a node i coinciding with b_{jk} the shape function $N_i(x,y)$ is given by

$$N_i(x,y)|_{T_j} = 1 - 2\lambda_{jk}$$

where λ_{jk} are the barycentric coordinates of a point of coordinate (x,y) with respect to the vertices a_{jk} of the triangle T_j . The shape functions are linear on each triangle and are equal to one at the node b_{jk} . The nodal value u_i represents the mean velocity along the side opposite to the vertex a_{jk} . We note the expressions for u , v are not continuous throughout the domain; in other words these elements do not conform.

For a node i coinciding with the centroid c_j of the triangle T_j the shape function $M_i(x,y)$ is given by

$$M_i(x,y) = 1 \quad \text{if} \quad (x,y) \in T_j$$

$$M_i(x,y) = 0 \quad \text{if} \quad (x,y) \notin T_j .$$

The momentum equations are stated in a weak form with the test functions N_i

$$\int_\Omega \left(-\mu\Delta u + \frac{\partial p}{\partial x} - f_x\right) N_i(x,y)\,dx\,dy = 0$$

$$\int_\Omega \left(-\mu\Delta v + \frac{\partial p}{\partial y} - f_y\right) N_i(x,y)\,dx\,dy = 0 .$$

The continuity equation is also stated in a weak form with the test functions M_j

$$\int_\Omega \left(\frac{\partial u}{\partial x} + \frac{\partial v}{\partial y}\right) M_j(x,y)\,dx\,dy = 0 .$$

By using one of Green's formulae these equations are reduced to the system of linear equations:

$$\sum_j a_{ij}u_j + \sum_j c_{ij}P_j = e_i \quad (1-a)$$

$$\sum_j a_{ij}v_j + \sum_j d_{ij}P_j = f_i \quad (1-b)$$

$$\sum_i c_{ij}u_i + \sum_i d_{ij}v_j = 0 \quad (1-c)$$

with

$$\left.\begin{aligned}
a_{ij} &= \int_\Omega \left(\frac{\partial N_i}{\partial x}\frac{\partial N_j}{\partial x} + \frac{\partial N_i}{\partial y}\frac{\partial N_j}{\partial y}\right) dx\,dy \\
c_{ij} &= \int_\Omega \frac{\partial N_i}{\partial x} M_j\,dx\,dy \\
d_{ij} &= \int_\Omega \frac{\partial N_i}{\partial y} M_j\,dx\,dy \\
e_i &= \int_\Omega f_x N_i\,dx\,dy + \int_{\partial\Omega} \left(\frac{\partial u}{\partial n} - pl_x\right) N_i\,ds \\
f_i &= \int_\Omega f_y N_i\,dx\,dy + \int_{\partial\Omega} \left(\frac{\partial v}{\partial n} - pl_y\right) N_i\,ds
\end{aligned}\right\} \qquad (2)$$

Here l_x , l_y are direction cosines of the unit outward normal to $\partial\Omega$.

For a node b_{jk} on the boundary $\partial\Omega$ the nodal values u, v are prescribed. The equations $1-a$ and $1-b$ are not stated for this node.

For the pressure, the nodes c_j do not lie on the boundary $\partial\Omega$; so the equation $1-c$ is stated for every node c_j .

If N_u is the number of nodal values for the unknown velocities and if N_p is the number of nodal values for the pressure, then the equations $1-a$, $1-b$ give 2. N_u relations that can be used to calculate the unknown velocities while the equation $1-c$ gives N_p relations we can use to calculate the pressure.

On the other hand note that the surface integrals in Equation (2) vanish from the definition of the basic functions $N_i(x,y)$.

We can explain the Equations (1) as a minimizing problem with constraints. We write

$$A = \begin{bmatrix} (a_{ij}) & (0) \\ (0) & (a_{ij}) \end{bmatrix} \quad \begin{matrix} 1 \leqslant i \leqslant N_u \\ 1 \leqslant j \leqslant N_u \end{matrix}$$

$$C = \begin{bmatrix} c_{ij} \\ d_{ij} \end{bmatrix} \quad \begin{matrix} 1 \leqslant i \leqslant N_u \\ 1 \leqslant j \leqslant N_p \end{matrix}$$

$$X = \begin{bmatrix} u_i \\ v_i \end{bmatrix}, \quad E = \begin{bmatrix} e_i \\ f_i \end{bmatrix} \; 1 \leqslant i \leqslant N_u \; , \quad P = [P_j] \; 1 \leqslant j \leqslant N_p \; .$$

In matrix notation these Equations (1) are equivalent to

$$\left.\begin{aligned} AX + CP &= E \\ C^tX &= 0 \end{aligned}\right\} \tag{3}$$

where C^t is the transpose of the matrix C .

The system (3) results from the minimization of the quantity

$$I(X,P) = \tfrac{1}{2}X^tAX - X^tE + P^tC^tX \; . \tag{4}$$

$$AX = C$$

In other words we must minimize $\frac{1}{2}X^tAX - X^tE$

with the supplementary constraints

$$C^tX = 0 \; .$$

The pressure P appears throughout the Equation (4) as a Lagrange multiplier.

System (3) may be solved by the use of Uzawa's algorithm which can be briefly described as

(a) we choose P^o arbitrarily

(b) we solve the problem

$$AX^{n+1} + CP^n = E$$

(c) we modify the pressure by

$$P^{n+1} = P^n - \epsilon C^tX^{n+1}$$

(ϵ is a small parameter).

We can demonstrate that in the case of Equations (3) this algorithm is convergent.

The elements defined by the relations (3) are not precise. Solenoidal elements may be introduced in order to improve the approximation and to avoid the presence of pressure term in the equations to solve.

The weak form of the Stokes problem is equivalent to:

Find the velocity $\vec{u} \in V$ so that:

$a(\vec{u},\vec{w}) = (\vec{f},\vec{w})$ for all $\vec{w} \in V$ where $\vec{u}, \vec{f}, \vec{w}$ are vectors with components (u,v), (f_x,f_y), (w_x,w_y)

$$a(\vec{u},\vec{v}) = \mu \iint_\Omega \left(\frac{\partial u}{\partial x}\frac{\partial w_x}{\partial x} + \frac{\partial v}{\partial x}\frac{\partial w_y}{\partial x} + \frac{\partial u}{\partial y}\frac{\partial w_x}{\partial y} + \frac{\partial v}{\partial y}\frac{\partial w_y}{\partial y} \right) dx\,dy$$

$$(\vec{f},\vec{w}) = \iint_\Omega (f_x w_x + f_x w_y)\,dx\,dy$$

and V is the space of vector-valued functions v defined by:

$$V = \{\vec{v} | \vec{v} \in (H^1(\Omega))^2, \vec{v}|_\Gamma = 0, \operatorname{div}\vec{v} = 0\} .$$

The condition of incompressibility is carried into the definition of the space to which the solution belongs. The construction of space V_h which approximates V is made by weakening the condition $\operatorname{div}\vec{v} = 0$. This theoretical matter is treated in detail in References 13 and 18.

2.4 Application to the Navier-Stokes Equations

For the resolution of the Navier-Stokes equations:

$$\left.\begin{aligned} \frac{\partial u}{\partial t} + u\frac{\partial u}{\partial x} + v\frac{\partial u}{\partial y} &= -\frac{1}{\rho}\frac{\partial p}{\partial x} + \frac{\nu}{\rho}\left(\frac{\partial^2 u}{\partial x^2} + \frac{\partial^2 u}{\partial y^2}\right) \\ \frac{\partial v}{\partial t} + u\frac{\partial v}{\partial x} + v\frac{\partial v}{\partial y} &= -\frac{1}{\rho}\frac{\partial p}{\partial y} + \frac{\nu}{\rho}\left(\frac{\partial^2 v}{\partial x^2} + \frac{\partial^2 v}{\partial y^2}\right) \end{aligned}\right\} \qquad (1)$$

$$\frac{\partial u}{\partial x} + \frac{\partial v}{\partial y} = 0$$

three finite elements techniques may be used:

(a) the Navier-Stokes equations may be treated directly by Galerkine's method; References 23, 29, 30, 31, 32, 38.

(b) vorticity and stream function may be determined; References 6, 7, 8, 10, 11, 12.

(c) the condition of incompressibility may be introduced in the space solution; in fact this is an extension of the method described in paragraph 2.3; Reference 13.

2.4.1 Method for Solving Using Navier-Stokes Equation Directly

We use triangular elements and continuous shape functions N_j linear on each triangle. Serious difficulties will be encountered in the consideration of the pressure on a wall. A solution, not necessarily the best, consists of using the momentum equations written on the wall in order to obtain the value of the pressure gradient and therefore the value of the pressure on the wall.

We construct an approximate solution of the form:

$$u = \sum_j N_j(x,y)u_j(t)$$

$$v = \sum_j N_j(x,y)v_j(t)$$

$$p = \sum_j N_j(x,y)p_j(t) .$$

By Galerkine's method and from Green's formula, Equations (1) are reduced to the differential system:

$$\sum_j e_{ij}\frac{du_j}{dt} + \sum_j g_{ij}u_j + \sum_j h_{xij}p_j = c_{xi} \qquad (2a)$$

$$\sum_j e_{ij}\frac{dv_j}{dt} + \sum_j g_{ij}v_j + \sum_j h_{yij}p_j = c_{yi} \qquad (2b)$$

$$\sum_j h_{xji} u_j + \sum_j h_{yji} v_j = 0 \qquad (2c)$$

where

$$e_{ij} = \iint_\Omega \rho N_i N_j \, dx \, dy$$

$$g_{ij} = \iint_\Omega \left\{ \rho \sum_k N_i N_k \left(\frac{\partial N_j}{\partial x} u_k + \frac{\partial N_j}{\partial y} v_k \right) + \nu \left(\frac{\partial N_i}{\partial x} \frac{\partial N_j}{\partial x} + \frac{\partial N_i}{\partial y} \frac{\partial N_j}{\partial y} \right) \right\} dx \, dy$$

$$h_{xij} = \iint_\Omega \frac{\partial N_i}{\partial x} N_j \, dx \, dy$$

$$h_{yij} = \iint_\Omega \frac{\partial N_i}{\partial y} N_j \, dx \, dy$$

$$c_{xi} = \int_{\partial\Omega} N_i \left(\frac{\partial u}{\partial n} - p l_x \right) ds$$

$$c_{yi} = \int_{\partial\Omega} N_i \left(\frac{\partial v}{\partial n} - p l_y \right) ds \, .$$

Here l_x, l_y are direction cosines of the outward normal n to (Ω). For elements not contiguous to $(\partial\Omega)$ the terms c_{xi} and c_{yi} are equal to zero.

Three cases of physical boundary conditions are easily introduced:

(a) Nodal values u_i and v_i are prescribed at node i. The Equations (2a) and (2b) are not stated for the node i.

(b) Nodal value p_i is known at node i. The Equation (2c) is not stated but the surface integral involving p must be evaluated in c_{xi} and c_{yi}.

(c) Normal derivatives of u and v are given at node i. The surface integral involving u and v must be evaluated in c_{xi} and c_{yi}.

Many problems may be solved from Equations (2).

(a) *Linearized steady flows* (Oseen approximation) –

In this case the unsteady terms disappear and the quantities g_{ij} do not depend on u_j and v_j. Equations (2) are reduced to a linear system of $3N$ equations for the $3N$ unknowns (u_i, v_i, p_i) and there is reason to believe we can develop a mathod to calculate their solution.

(b) *Steady flows* –

In this case Equations (2) form a non-linear system of equations. For their resolution we can use an iterative scheme, e.g.:

$$\sum_j g_{ij}^n u_j^{n+1} + \sum_j h_{xij} P_j^{n+1} = C_{xi}$$

$$\sum_j g_{ij}^n v_j^{n+1} + \sum_j h_{yij} P_j^{n+1} = C_{yi}$$

$$\sum_j h_{xji} u_j^{n+1} + \sum_j h_{yji} v_j^{n+1} = 0 \, .$$

If a solution exists, schemes of this type or more refined schemes obtained from Newton's method or from its variants, are convergent[20,32].

Unsteady Flows

We write the Equations (2) in the form of a differential system

$$\frac{dy}{dt} = F(y,t) \tag{3}$$

which is integrated by the Runge Kutta method or by the methods available for stiff differential equations with an improved domain of stability. To obtain form (3) we may choose $y = \{u_i, v_i, p_i\}$ or eliminate the pressure and take $y = \{u_i, v_i\}$. In the first case we solve Equations (2a) and (2b) in respect to du_j/dt and dv_j/dt and we differentiate, the resulting equations with respect to t. Then we eliminate the term d^2u_j/dt^2 and d^2v_j/dt^2 using the Equation (2c) differentiated twice in respect to t. In the second case we solve (2a) and (2b) for du_j/dt and dv_j/dt ; with such results, Equation (2c) gives the pressure, and we may use it to eliminate the pressure gradient from Equations (2a) and (2b). These two methods are purely formal and in practice we may encounter difficulties with initial pressure. Nevertheless the initial problem often permits the determination of the initial pressure from the velocity field. Of course, when we integrate Equations (3) we are faced with the usual problems of stability; these problems are overcome in a heuristic way, except in very specific cases when we can estimate the step time Δt (Ref.35).

2.4.2 Method for Solving Using Stream Function and Vorticity

The continuity equation causes the existence of a stream function ψ

$$u = \frac{\partial \psi}{\partial y}, \qquad v = -\frac{\partial \psi}{\partial x}. \tag{1}$$

We define the vorticity ω by

$$\omega = \frac{\partial v}{\partial x} - \frac{\partial u}{\partial y}. \tag{2}$$

Taking into consideration equality (1), the relation (2) gives

$$\Delta \psi = -\omega. \tag{3}$$

The momentum equations are then equivalent to

$$\frac{\partial \omega}{\partial t} + u\frac{\partial \omega}{\partial x} + v\frac{\partial \omega}{\partial y} = \frac{\nu}{\rho}\Delta\omega \tag{4}$$

$$\Delta p = -\rho Q \tag{5}$$

with

$$Q = 2\left(\frac{\partial u}{\partial y}\frac{\partial v}{\partial x} - \frac{\partial u}{\partial x}\frac{\partial v}{\partial y}\right).$$

We solve this problem using the Equations (3), (4), (5); we divide Ω into triangular subdomains and use a weak formulation. The discretization of Equation (3) is then different from that of (4) and (5), and therefore we shall treat each case separately.

Determination of the stream function

In order to solve Equation (4) we need to know the value of the gradient of ψ, rather than the value of ψ itself. We construct the following approximation of ψ :

$$\psi(x,y) = \sum_j \{M_j^1(x,y)\Psi_j + M_j^2(x,y)\psi_{xj} + M_j^3(x,y)\Psi_{yj}. \tag{6}$$

As usual the shape functions M_j^k are equal to zero outside of the subdomain j formed by the union of the triangles T_i, which have the node j as a common vertex. This node j is indexed as the vertex in a triangle T_i. The restriction of the shape functions to the triangle is given by:

$$M_j^1(x,y) = \lambda_1^3 + 3\lambda_1^2\lambda_2 + 3\lambda_1^2\lambda_3 + 2\lambda_1\lambda_2\lambda_3$$

$$M_j^2(x,y) = \lambda_1^2((x_2 - x_1)\lambda_2 + (x_3 - x_1)\lambda_3) - \tfrac{3}{2}x_1\lambda_1\lambda_2\lambda_3$$

$$M_j^3(x,y) = \lambda_1^2((y_2 - y_1)\lambda_2 + (y_3 - y_1)\lambda_3) - \tfrac{3}{2}y_1\lambda_1\lambda_2\lambda_3.$$

In the triangle T_i with vertices $(x_1,y_1), (x_2,y_2), (x_3,y_3)$, $\lambda_1, \lambda_2, \lambda_3$ are the barycentric coordinates of a point of cartesian coordinates (x,y).

We verify that:

$$\left.\begin{array}{lll} M_j^1(x_i,y_i) = \delta_{ij}^{*}\,, & \dfrac{\partial M_j^1}{\partial x}(x_i,y_i) = 0\,, & \dfrac{\partial M_j^1}{\partial y}(x_i,y_i) = 0 \\ M_j^2(x_i,y_i) = 0\,, & \dfrac{\partial M_j^2}{\partial x}(x_i,y_i) = \delta_{ij}\,, & \dfrac{\partial M_j^2}{\partial y}(x_i,y_i) = 0 \\ M_j^2(x_i,y_i) = 0\,, & \dfrac{\partial M_j^3}{\partial x}(x_i,y_i) = 0\,, & \dfrac{\partial M_j^3}{\partial y}(x_i,y_i) = \delta_{ij}\,. \end{array}\right\} \tag{7}$$

With relations (7) we note that:

$$\Psi_j = \psi(x_j,y_j)\,, \quad \Psi_{xj} = \frac{\partial \Psi}{\partial x}(x_j,y_j)\,, \quad \psi_{yj} = \frac{\partial \Psi}{\partial y}(x_j,y_j)\,.$$

The discretization of Equation (3) by the Galerkine method gives three equations at each node i :

$$\sum a_{ij}^k \Psi_j + \sum_j b_{ij}^k \Psi_{xj} + \sum_j c_{ij}^k \Psi_{yj} = d_i^k \qquad k = 1,2,3 \tag{8}$$

with

$$\left.\begin{array}{l} a_{ij}^k = \displaystyle\iint_\Omega \frac{\partial M_j^1}{\partial x}\frac{\partial M_i^k}{\partial x} + \frac{\partial M_j^1}{\partial y}\frac{\partial M_i^k}{\partial y}\,dx\,dy \\ b_{ij}^k = \displaystyle\iint_\Omega \frac{\partial M_j^2}{\partial x}\frac{\partial M_i^k}{\partial x} + \frac{\partial M_j^2}{\partial y}\frac{\partial M_i^k}{\partial y}\,dx\,dy \\ c_{ij}^k = \displaystyle\iint_\Omega \frac{\partial M_j^3}{\partial x}\frac{\partial M_i^k}{\partial x} + \frac{\partial M_j^3}{\partial y}\frac{\partial M_i^k}{\partial y}\,dx\,dy \end{array}\right\} \tag{9}$$

$$d_i^k = \iint_\Omega \omega M_i^k\,dx\,dy\,.$$

When the vorticity ω is known, relations (8) represent a system of linear equations which can be written:

$$AX = B\,. \tag{10}$$

Until now the boundary conditions have not been used; in fact they give a set of supplementary linear equations of the type:

$$CX = D\,. \tag{11}$$

To solve the system of Equations (10) with the constraints (11) we use Lagrange multipliers and we minimize the following functional:

$$I(X) = \tfrac{1}{2}X^tAX - X^tB + \lambda^t(CX - D)\,.$$

Then:

$$\frac{\partial I}{\partial X_i} = 0\,, \quad \frac{\partial I}{\partial \lambda_i} = 0\,. \tag{12}$$

The relations (12) gives us the following system of equations:

$$\begin{bmatrix} A & C^t \\ C & 0 \end{bmatrix}\begin{bmatrix} X \\ \lambda \end{bmatrix} = \begin{bmatrix} B \\ D \end{bmatrix}.$$

Where C^t is the transpose of matrix C.

This system is solved, at least on paper, by eliminating the Lagrange multipliers λ

$$\lambda = (CA^{-1}C^t)^{-1}(CA^{-1}B - D)$$

---

* $\delta_{ij} = 0$ if $i \neq j$, $\delta_{ii} = 1$.

$$X = A^{-1}B - A^{-1}C^{t}(CA^{-1}C^{t})^{-1}(CA^{-1}B - D) . \tag{13}$$

This procedure has the advantage of treating separately the boundary conditions (which can be unsteady) and the operator (which is steady). Matrix A can be either assembled and inverted or factorized.

Calculus of vorticity and pressure

In this case we use the shape functions $N_j(x,y)$ piecewise linear on each triangle as defined in 2.3:

$$\omega = \sum_j N_j(x,y)\omega_j(t)$$

$$P = \sum_j N_j(x,y)P_j(t)$$

$$u = \sum_j N_j(x,y)\Psi_{xj}$$

$$v = \sum_j N_j(x,y)\Psi_{yj}$$

The Equations (4) and (5) give us the relations:

$$\sum_j d_{ij}\frac{d\omega_j}{dt} + \sum_j e_{ij}\omega_j = 0 \tag{14}$$

$$\sum_j f_{ij}P_j = q_i \tag{15}$$

where

$$d_{ij} = \iint_\Omega N_i N_j \, dx\, dy$$

$$e_{ij} = \iint_\Omega N_i\left(\sum_k \Psi_{xk}N_k\frac{\partial N_j}{\partial x} + \sum_k \Psi_{yk}N_k\frac{\partial N_j}{\partial y}\right) + \frac{\nu}{\rho}\left(\frac{\partial N_i}{\partial x}\frac{\partial N_j}{\partial x} + \frac{\partial N_i}{\partial y}\frac{\partial N_j}{\partial y}\right) dx\, dy$$

$$f_{ij} = \iint_\Omega \left(\frac{\partial N_i}{\partial x}\frac{\partial N_j}{\partial x} + \frac{\partial N_i}{\partial y}\frac{\partial N_j}{\partial y}\right) dx\, dy$$

$$q_j = \iint_\Omega qN_i \, dx\, dy .$$

Numerical integration

The numerical integration of these equations can be made by Runge Kutta algorithms. For example from Heun's method we know the velocities and the vorticity at time $t = 0$. From Equation (14) we deduce the value ω_1 of the vorticity at an intermediate time $\Delta t/2$. The solution of Equations (10) yields the velocity field at time $\Delta t/2$. By repeating this operation at time Δt, we obtain a value ω_2 for the vorticity. By classical combination we obtain the final value of ω at time Δt, from which we compute the original value of the velocities. During this procedure the boundary value of ω is readjusted from Equations (3) and (6) as in finite difference methods. Finally the procedure given in 2.4.1 is used to obtain boundary conditions for the pressure, and Equations (15) give the pressure field. The choice of the step of integration Δt is important for the stability of the algorithm and in the present state of knowledge this choice must be heuristic. Thus, finally we obtain an approximation of the unsteady pattern of fluid flow.

CONCLUSION

Generally the finite element method offers a systematic procedure on which to build schemes of high accuracy. Moreover the representation of the boundaries can be performed as accurately as is required.

This method was first used in structural analysis and has proved to be very successful. In fluid dynamics the matter is more complex.

For external potential flows of incompressible fluids the method of singularities (which can be considered as a particular case of the finite element method) works very well. On the other hand, for internal problems or for free surface flows the finite element method is preferable.

For incompressible fluids within the limits of the Navier-Stokes equations certain algorithms have been proposed. However, in most cases the problem of computing the pressure or the vorticity at the wall remains open.

For compressible fluids, successful methods have been developed for the case of subsonic or locally supersonic shock-free inviscid flows. For the case of supersonic flow it is as yet difficult to ensure that discrete problems obtained are relevant.

Finally formulations have been written for the case of compressible Navier-Stokes equations but to our knowledge these have not yet been applied practically.

REFERENCES

1. Ames, W.F. — *Non-Linear Partial Differential Equations in Engineering.* Academic Press, Vol.2, pp.249-256.

2. Argyris, J.H. — *Two- and Three-Dimensional Potential Flow by the Method of Singularities.* Aero. J. R. Aero. Soc. 73, November 1969, pp.959-961.

3. Argyris, J.H. — *The Impact of the Digital Computer on Engineering Sciences.* Aero. J. R. Aero. Soc. 74, January 1970.

4. Argyris, J.H. Mareczek, G. — *Potential Flow Analysis by Finite Element.* Ingr. Arch., 1972, pp.1-25.

5. Argyris, J.H. et al. — *Two- and Three-Dimensional Flow Using Finite Elements.* Aero. J. R. Aero. Soc. 73, November 1969, pp.961-964.

6. Baker, A.J. — *Finite Element Computational Theory for Three-Dimensional Boundary Layer Flow.* AIAA Paper No.72-108.

7. Baker, A.J. — *A Highly Stable Explicit Integration Technique for Computational Continuum Mechanics.* Int. Conf. num. meth. Fluid Dyn., Southampton, September 1973.

8. Baker, A.J. — *Finite Element Solution Algorithm for Viscous Incompressible Fluid Dynamics.* Int. J. Num. Methods Engr. 6.1, May 1973, pp.89-101.

9. Bonnerot, R. Jamet, P. — *Finite Elements for Eulerian Flow.* Service MA, Centre d'Etude de Limeil, BP 27 94190 Villeneuve-St.Georges, France.

10. Bratamov, Th. Ecer, A. — *Finite Element Analysis of Unsteady Incompressible Flow Around an Oscillating Obstacle of Arbitrary Shape.* AIAA Paper 73-91, January 1973.

11. Bratamov, Th. Ecer, A. — *Stability of the Finite Element Method for Analysis of Unsteady Flow Around Oscillating Airfoils.* Int. Conf. num. meth. Fluid Dyn., Southampton, September 1973.

12. Bratamov, Th. Ecer, A. — *Computational Consideration in the Application of the Finite Element Method for Analysis of Unsteady Flow Around Airfoils.* Proc. AIAA Comp. Fluid Dyn. Conf., Palm Springs, July 1973.

13. Crouzeix, M. Raviart, P.A. — *Conforming and Non-Conforming Element Methods for Solving the Stationary Stokes Equations.* Rev. Fr. Informat. Rech. Operat., Vol.7, No.12, December 1973, pp.33-76.

14. De Vries, G. Norrie, D.H. — *The Application of the Finite Element Technique to Potential Flow Problems.* Trans. ASME J. Appl. Mech., December 1971, pp.798-802.

15. De Vries, G. Norrie, D.H. — *Numerical Methods in Fluid Dynamics.* AGARD Lecture Series 48.

16. De Vries, G. Norrie, D.H. — *The Finite Element Method.* Academic Press 1973.

17. Fortin, M. — *Calcul numerique des écoulements des fluides de Bingham.* These, Paris, 1972.

18. Fortin, M. — *Approximation des fonctions à divergence nulle par la méthode des éléments finis.* Proc. Third Int. Conf. Num. Method. Fluid Dyn., Paris, 1972.

19. Fu, C.C. — *A Method for the Numerical Integration of the Equations of Motion Arising from a Finite Element Analysis.* Trans. ASME J. Appl. Mech., September 1970, pp.599-605.

20. Gelder, D. — *Solution of the Compressible Flow Equations.* Int. J. num. meth. Engr 3, 1971, pp.35-43.

21. Grotkop, G. — *Finite Element Analysis of Long Period Water Waves.* Comp. Meth. Appl. Mech. Engr 2, 1973, pp.147-157.

22. Hunt, D.A. — *Discrete Element Structural Theory of Fluids.* AIAA Paper No.70-23, January 1970.

23. Lee, C.H. — *Finite Element Method for Transit Linear Viscous Flow Problems.* Int. Conf. num. meth. Fluid Dyn., Southampton, September 1973.

24. Leon Hard, J.W. — *Finite Element Analysis of Perturbed Compressible Flow.* Int. J. num. Math. Engr 4, 1972, pp.123-132.

25. Luu, T.S. — *Calcul de l'écoulement transonique autour d'un profil.* Bull. ATMA, Session 1972.

26. Luu, T.S. Corniglion, J. — *Ecoulement instationnaire autour d'une grille d'aube.* Bull. ATMA, Session 1972.

27. Morandi-Cecchi, M. — *A Numerical Study of Non-Linear Instability by Means of an Extended Finite Element Method.* Int. Conf. num. meth. Fluid Dyn., Southampton, September 1973.

28. Oden, J.T. Key, J.E. — *On Some Generalizations of the Stiffness Relations for Finite Deformations of Compressible and Incompressible Finite Elements.* Nucl. Engr Design 15, 1971, pp.121-134.

29. Oden, J.T. — *Finite Element Analogue of Navier-Stokes Equations.* J. Eng Mech. Div. 95, 1970.

30. Oden, J.T. Wellford, C. — *Analysis of Flow of Viscous Fluids by the Finite Element Method.* AIAA Journal, Vol.10, No.2, December 1972.

31. Oden, J.T. — *Finite Element of Non-Linear Continua.* McGraw-Hill, 1972.

32. Ortega, J.M. Rheinboldt, W.C. — *Iterative Solution of Non-Linear Equations in Several Variables.* Academic Press, 1970.

33. Skiba, E. et al. — *A Finite Element Solution for a Class of Two-Dimensional Viscous Fluid Dynamics Problems.* Study No.5, Computer Aided Engineering University of Waterloo, 1971.

34. Schmid, G. — *The Harmonic Finite Element Model For Use in Field Problems.* PhD Thesis, University of Washington, 1970.

35. Schmid, G. — *Incompressible Flow in Multiply-Connected Regions.* Int. Conf. num. meth. Fluid Dyn., Southampton, September 1973.

36. Tong, P. — *On the Numerical Problem of the Finite Element Method.* Study No.5, Computer Aided Engineering University of Waterloo, 1971.

37. Wen-Hwa Chu — *A Comparison of Some Finite Element and Finite Difference Methods for a Simple Sloshing Problem.* AIAA Journal, Vols 9–10, September 1971, pp.2094-2096.

38. Taylor, C. Hood, P. — *A Numerical Solution of the Navier-Stokes Equations Using the Finite Element Techniques.* Computer and Fluids, Vol.1, No.1, 1973, pp.73-100.

39. Bellevaux, C. — *Oscillations propres d'un bassin tournant.* These, Paris, Vol.VI, No.A 0-44-07, 1970.

40. Bellevaux, C. — *Oscillations libres d'un bassin en rotation.* Proc. Third Int. Conf. Num. Meth. Fluid Dyn., Paris, 1972.

41. Bellevaux, C. Maria-Sube, R. — *Determination des lignes de jet dans les écoulements rotationnels symétriques.* J. Meca., Vol.11, 1972.

42. Maria-Sube, R. — *Numerical Solution to Free Surface Axisymmetric Rotational Flows.* J. Comp. Phys., Vol.16, 1974.

43. Strang, G. Fix, G.J. — *An Analysis of the Finite Element Method.* Prentice Hall (Englewood Cliffs, N.J., USA), 1973.

The authors gratefully acknowledge the assistance provided by Mr J.H. Trotman of AGARD with the translation of this paper.

Bibliography on Numerical Methods for 2D and 3D Viscous Flows

N74-25807
Computer Program for Calculating Laminar, Transitional and Turbulent Boundary Layers for a Compressible Axisymmetric Flow
James A. Albers and John L. Gregg, Apr. 1974, 174 p, refs
National Aeronautics and Space Administration, Lewis Research Center, Cleveland, Ohio
NASA-TN-D-7521; E-7819

N74-22920
A Survey of Computational Methods for 2D and 3D Transonic Flows with Shocks
H. Yoshihara
In: AGARD, Advan. in Numerical Fluid Dyn., Feb. 1973, 35 p, refs
AGARD-LS-64

N74-22919
Survey of Computational Methods for Three-Dimensional Supersonic Inviscid Flows with Shocks
R.W. MacCormack and R.F. Warming
In: AGARD, Advan. in Numerical Fluid Dyn., Feb. 1973, 20 p, refs
AGARD-LS-64

N74-22918
Numerical Treatment of Boundary-Layer Problems
Egon Krause
In: AGARD, Advan. in Numerical Fluid Dyn., Feb. 1973, 21 p, refs
AGARD-LS-64

N74-22917
Numerical Integration of Navier-Stokes Equations
H.J. Wirz and J.J. Smolderen
In: AGARD, Advan. in Numerical Fluid Dyn., Feb. 1973, 13 p, refs
AGARD-LS-64

N74-22914
Advances in Numerical Fluid Dynamics
Feb. 1973, 146 p, refs
Advisory Group for Aerospace Research and Development, Paris (France)
AGARD-LS-64

N74-21923
A Finite-Element Formulation for Subsonic Flows around Complex Configurations
Luigi Morino, Dec. 1973, 79 p, refs
Boston Univ., Mass., Dept. of Aerospace Engineering
NASA-CR-138142; TR-73-05

N74-19640
Input Description for Jameson's Three-Dimensional Transonic Airfoil Analysis Program
Perry A. Newman and Ruby M. Davis, 7. Feb., 1974, 27 p, refs
National Aeronautics and Space Administration, Langley Research Center, Langley Station, Va.
NASA-TM-X-71919

N74-17982
Asymptotic and Numerical Approaches of Sonic Flows
D. Euvrard, F. Grosjean and G. Tournemine, 1973, 60 p, refs. Presented at the EUROMECH, 40. Colloq. Transonic Aerodyn., Saltsjoebaden, Sweden, 10-13 Sep. 1973
Ecole Nationale Superieure de Techniques Avancees, Paris (France)

N74-17044
An Implicit Numerical Method for the Multidimensional Compressible Navier-Stokes Equations
W. Roger Briley and Henry McDonald, Nov. 1973, 56 p, refs
United Aircraft Corp., East Hartford, Conn. Research Labs.
AD-770224; UARL-M911363-6

N74-15988
Transonic Flow Calculations in Two and Three Dimensions, Interim Report
P.K. Khosla and S.G. Rubin, Jun. 1973, 32 p, refs
Polytechnic Inst. of Brooklyn, Farmingdale, N.Y., Dept. of Aerospace Engineering and Applied Mechanics
AD-769301;, PIBAL-73-13; AFOSR-73-1976TR

N74-13992
Calculation of the Boundary-Layer Flow in the Windward Symmetry Plane of a Spherically Blunted Axisymmetric Body at Angle of Attack, Including Stream Line-Swallowing Effects, Final Report, Sep. 1971 - Dec. 1972
Arloe W. Mayne, Jr., Oct. 1973, 57 p, refs
ARO, Inc., Arnold Air Force Station, Tenn.
AD-768340; ARO-VKF-TR-73-102; AEDC-TR-73-166

N74-13975
Numerical Prediction of Three-Dimensional Flows
S.V. Patankar and D.B. Spalding, Jun. 1972, 29 p, refs
Imperial Coll. of Science and Technology, London (England), Dept. of Mechanical Engineering
EF/TN/A/46

N73-33226
Solution of the Time-Dependent Navier-Stokes Equation with a Periodic Boundary Condition
Louis W. Ehrlich, Jul. 1973, 30 p, refs
Applied Physics Lab., Johns Hopkins Univ., Silver Spring, Md.
AD-764582; APL-TG-1219

N73-32176
A Proposed Technique for Discretization of Boundary Conditions in Time-Dependent, Viscous, Compressible Flows, Ph.D. Thesis
Palmer Bang-Ming Chiu, 1972, 183 p
Purdue Univ., Lafayette, Ind.
Univ. Microfilms Order No. 73-15785

N73-29156
The Numerical Calculation of Three-Dimensional Boundary Layers, Ph.D. Thesis
Richard Allen Burbank, 1972, 149 p
Massachusetts Univ., Amherst
Univ. Microfilms Order No. 73-5530

N73-29152
An Implicit Numerical Solution for the Laminar and Turbulent Flow of an Incompressible Fluid along the Axis of a 90 Degree Corner, Ph.D. Thesis
David Tillman Klinksiek, 1973, 147 p
Virginia Polytechnic Inst. and State Univ., Blacksburg
Univ. Microfilms Order No. 73-5874

N73-28148
Reacting and Nonreacting Analysis of Supersonic Viscous Flow, Ph.D. Thesis
Robert Cavalleri, 1972, 178 p
New York Univ., N.Y.
Univ. Microfilms Order No. 73-9068

N73-26302
Solving Three Dimensional Potential Flow Problems by Means of an Inverse Formulation and Finite Differences
Allen L. David and Roland W. Jeppson, Mar. 1973, 51 p, refs
Utah State Univ., Logan
AD-760347; PRWG-96-2

N73-24325
Numerical Solution of the Three Dimensional Boundary Layer on a Spinning Sharp Body at Angle of Attack
C.B. Watkins, Jr., 1973, 33 p, refs. Presented at Symp. on Appl. of Computers to Fluid Dyn. Anal. and Design, Farmingdale, N.Y., 3. Jan. 1973
Howard Univ., Washington, D.C.
SC-CR-72-3182; Conf-730101-1

N73-23399
Fluid Mechanics and Finite Elements
David F. Dyer, 29. Dec. 1972, 18 p, refs
Office of Naval Research, London (England)
AD-757266; ONRL-R-21-72

N73-23389
A Study of Implicit Finite Difference Techniques for Compressible Viscous Flow, Final Report
Bruce S. Masson, Jan. 1973, 34 p, refs
Ultrasystems, Inc., Irvine, Calif.
AD-756242; SN-262/FR

N73-22218
Analysis of Laminar Boundary Layers on Right Circular Cones at Angle of Attack, Including Streamline-Swallowing Effects, Ph.D. Thesis
Arloe Wesley Mayne, Jr., 1972, 107 p
Tennessee Univ., Knoxville
Univ. Microfilms Order No. 72-27486

N73-21290
Viscous Flow over a Cone at Moderate Incidence. 2: Supersonic Boundary Layer
T.C. Lin and S.G. Rubin, Sep. 1972, 102 p, refs
Polytechnic Inst. of Brooklyn, Farmingdale, N.Y., Dept. of Aerospace Engineering and Applied Mechanics
AD-755862; PIBAL-72-27; AFOSR-73-0219TR

N73-21285
Theoretical Investigation of a Viscous Compressible Flow in a Curved Nozzle
R.A. Duerr, Sep. 1972, 9 p, refs
Kernforschungszentrum, Karlsruhe (West Germany), Inst. für Kernverfahrenstechnik
KFK-1630

N73-21277
The Use of Levy-Lees Variables in Three-Dimensional Boundary-Layer Flows, Final Report
Veer Narain Vatsa and R.T. Davis, Jan. 1973, 73 p, refs
Cincinnati Univ., Ohio, Dept. of Aerospace Engineering
NASA-CR-112315

N73-19277
A Finite Difference Method for Predicting Supersonic Turbulent Boundary Layer Flows with Tangential Slot Injection, Ph.D. Thesis
Earnest Wade Miner, 1972, 124 p
Virginia Polytechnik Inst. and State Univ., Blacksburg
Univ. Microfilms Order No. 72-24454

N73-16241
Numerical Solution of a Viscous Compressible Swirling Flow through a Delaval Nozzle, Ph.D. Thesis
Robert Dohn Kissinger, 1971, 311 p
Purdue Univ., Lafayette, Ind.
Univ. Microfilms Order No. 72-7979

N73-14282
On the Numerical Treatment of Viscous Flow Problems
G. Marshall, Mar. 1972, 35 p, refs
Technische Hogeschool, Delft (Netherlands), Mathematisch Inst.
NA-7

N73-11293
The Mathematical Formulation of Viscous-Inviscid Interaction Problems in Supersonic Flow
Gabriel Miller, Jun. 1972, 30 p, refs
New York Univ., N.Y., Dept. of Aeronautics and Astronautics
AD-746891; NYU-AA-72-11

N73-10341
An Implicit Fourth Order Difference Method for Viscous Flows
D.S. Watanaba and J.R. Flood, Jun. 1972, 21 p, refs
Illinois Univ., Urbana, Coordinated Science Lab.
AD-746389; R-572; UILU-ENG-72-2233

N73-10314
Shock Waves and Drag in the Numerical Calculation of Isentropic Transonic Flow
Joseph L. Steger and Barrett S. Baldwin, Oct. 1972, 46 p, refs
National Aeronautics and Space Administration, Ames Research Center, Moffett Field, Calif.
NASA-TN-D-6997; A-4519

N72-33284
Studies to Develop and Investigate an Inverse Formulation for Numerically Solving Three-Dimensional Free Surface Potential Fluid Flows
Roland W. Jeppson, Mar. 1972, 43 p, refs
Utah State Univ., Logan
AD-744701; PRWG-96-1

N72-28291
On the Movements of a Viscous, Compressible, Heat-Conducting Fluid in a Spherical Layer
N.M. Astafyeva, I. Yu Brailovskaya and I.M. Yavorskaya
NASA, Aug. 1972, 23 p, refs
Transl. into English of "O Dvizheniyakh Vyazkoy Szhimay Teploprovodnoy Zhidkosti v Sfericheskom Sloye", Rept. Pr-96, Acad. Sci. USSR, Moscow, 1972, 28 p
NASA-TT-F-14373

N72-27311
Numerical Solutions of the Navier-Stokes Equations for the Supersonic Laminar Flow over a Two-Dimensional Compression Corner
James E. Carter, Jul. 1972, 81 p, refs
National Aeronautics and Space Administration, Langley Research Center, Langley Station, Va.
NASA-TR-R-385; L-8306

N72-27299
Numerical Solution of the Navier-Stokes Equations at High Reynolds Numbers and the Problem of Discretization of Convective Derivatives
Jacob E. Fromm
In: AGARD, Numerical Methods in Fluid Dyn., May 1972, 47 p, ref
AGARD-LS-48

N72-27298
Numerical Solution of Steady State Navier-Stokes Equations
M. Fortin
In: AGARD, Numerical Methods in Fluid Dyn., May 1972, 8 p, refs
AGARD-LS-48

N72-27297
The Approximation of Navier-Stokes Equations for Viscous Incompressible Fluids (Sur l'Approximation des Equations de Navier-Stokes des Fluides Visqueux Incompressibles)
M. Fortin and R. Teman
In: AGARD, Numerical Methods in Fluid Dyn., May 1972, 7p, refs
AGARD-LS-48

N72-27296
Approximation of Navier-Stokes Equations
R. Teman
In: AGARD, Numerical Methods in Fluid Dyn., May 1972, 6 p, refs
AGARD-LS-48

N72-27293
Numerical Methods in Fluid Dynamics
J.J. Smolderen, ed., May 1972, 328 p, refs
Advisory Group for Aerospace Research and Development, Paris (France)
AGARD-LS-48

N72-23616
Numerical Methods in Solving Steady-State Equations of Gas Dynamics
O.M. Belotserkovskiy
In: Numerical Methods for Solving Probl. of Mech. of Continuous Media, May 1972, p 97-195, refs
NASA-TT-F-667

N72-23612
Difference Methods in Solving Problems of Gas Dynamics
V.V. Rusanov
In: Numerical Methods for Solving Probl. of Mech. of Continuous Media, May 1972, p 5-34, refs
NASA-TT-F-667

N72-20308
Calculation of Unsteady Compressible Flows Insolving Shocks
S.V. Patankar, Dec. 1971, 18 p, refs
Imperial Coll. of Sciences and Technology, London (England), Dept. of Mechanical Engineering
UF/TN/A/4

N72-20285
A Calculation Method for Three Dimensional Incompressible Turbulent Boundary Layers
P. Wesseling and J.P.F. Lindhout
In: AGARD, Turbulent Shear Flows, Jan. 1972, 13 p, refs
AGARD-CP-93

N72-16228
Remarks about Variational Principles for Unsteady and Steady Three and Two Dimensional Gas Flows
K.G. Guderley and O.P. Bhutani, Aug. 1971, 59 p, refs
Aerospace Research Labs., Wright-Patterson AFB, Ohio
AD-731801; ARL-71-0136

N72-15296
A Numerical Solution for Flow between Rotating and Stationary Finite Disks
Donald H. McCoy, Jun. 1971, 52 p
Ballistic Research Labs., Aberdeen Proving Ground, Md.
AD-731217; BRL-1541

N72-12242
An Implicit Numerical Solution of the Turbulent Three Dimensional Incompressible Boundary Layer Equations, Interim Technical Report
F.J. Pierce and W.F. Klinksiek, Jul. 1971, 129 p, refs
Virginia Polytechnic Inst., Blacksburg, Coll. of Engineering
AD-728126; VPI-E-71-14; AROD-6858-6-E; ITR-3

N72-12215
A Numerical Method for Computing Three Dimensional Viscous Supersonic Flow Fields about Slender Bodies
Leonard Walitt and John G. Trulio, Nov. 1971, 103 p, refs
Applied Theory, Inc., Los Angeles, Calif.
NASA-CR-1963

N71-36678
Flow in the Near Wake (Techeniye v blizhnem slede)
I. Yu Brailovskaya, Oct. 1971, 7 p, refs
Transl. into English from Dokl. Akad. Nauk SSSR (Moscow), v. 197, 21. Mar. 1971, p 542-544
NASA-TT-F-13993

N71-23584
Numerical Solutions on the Navier-Stokes Equations for Incompressible Uniform Flow past a Parabola: A Study of Finite Grid Size Effect
William C. Boswell, Jr. and Michael J. Werle, Feb. 1971, 48 p, refs
Virginia Polytechnic Inst., Blacksburg, Dept. of Engineering Mechanics
AD-718362; VPI-E-71-5

N71-18426
A Study of Compressible Turbulent Boundary Layers Using the Method of Invariant Modeling
John E. Yates, Coleman duP. Donaldson and Barry D. Gilligan, Jan. 1971, 16 p, refs
Aeronautical Research Associates of Princeton, Inc., N.J.
NASA-CR-116781; ARAP-71-4

N71-18401
Contribution to the Study of Sonic Flows past an Obstacle
D. Euvrard, Feb. 1971, 17 p, refs
Transl. into English from Proceedings of the 8th Symp. on Advanced Probl. and Methods in Fluid Dyn. (Tarda), 18.-25. Sep. 1967, p 369-377
NASA-TT-F-13472

N71-12673
The Numerical Solution of Partial Differential Equations Governing Convection
Harvard Lomax, Paul Kutler and F.B. Fuller, Oct. 1970, 54 p, refs
Advisory Group for Aerospace Research and Development, Paris (France)
AGARDograph-146

N71-11533
A Time-Dependent Method for Calculating Supersonic Blunt-Body Flow Fields with Sharp Corners and Embedded Shock Waves
Richard W. Barnwell, Nov. 1970, 67 p, refs
National Aeronautics and Space Administration, Langley Research Center, Langley Station, Va.
NASA-TN-D-6031; L-7284

N70-41733
Flow over Airfoils in the Transonic Regime. Volume 2: Computer Programs, Final Report, 15. Nov. 1968 - 12. Dec. 1969
Richard J. Magnus and William H. Gallaher, 1. Mar. 1970, 362 p, refs
General Dynamics/Convair, San Diego, Calif.
AD-709378; AFFDL-TR-70-16-Vol-2

N70-41166
Computation of Three-Dimensional Supersonic Flows with Shock Waves
I.O. Bohachevsky, 6. Aug. 1970, 31 p, refs
Bellcomm, Inc., Wahington, D.C.
NASA-CR-113884; TM-70-1011-7

N70-38683
Solution of the Three-Dimensional Time-Dependent Navier-Stokes Equations by the Difference Method (Die Lösung der dreidimensionalen instationären Navier-Stokes-Gleichungen mit dem Differenzverfahren)
Willi Schoenauer, Apr. 1970, 135 p, refs
Deutsche Forschungs- und Versuchsanstalt für Luft- und Raumfahrt
DLR-FB-70-15

N70-38028
Finite-Difference Approximations of the Vorticity of Laminar Flows at Solid Surfaces
Hans J. Lugt and Yermiyahu Rimon, Apr. 1970, 35 p, refs
Naval Ship Research and Development Center, Washington, D.C.
AD-706328; Rept-3306

N70-24228
Numerical Integration of the Navier-Stokes Equations in Two Dimensions
S.C.R. Dennis and Gau-Zau Ghang, Jul. 1969, 95 p, refs
Wisconsin Univ., Madison, Mathematics Research Center
AD-699001; MRC-TSR-859

N70-23742
The Stability of Boundary Conditions in the Numerical Solution of the Time-Dependent Navier-Stokes Equations
P.J. Taylor, 1970, 47 p, refs
Southampton Univ. (England), Dept. of Mathematics
ARC-CP-1066; ARC-30406

N70-21376
A New Method for Analysis of Transonic Flow
Theodore Katsanis
In: Anal. Methods in Aircraft Aerodyn., 1970, p 597-621, refs
NASA-SP-228

N70-17369
Difference Method for the Navier-Stokes Equation
Hajime Miyoshi, 1969, 25 p, refs
National Aerospace Lab., Tokyo (Japan)
NAL-TR-174

A74-34320
The Calculation of Subsonic and Transonic Turbulent Boundary Layers on an Infinite Yawed Airfoil
J.C. Adams, Jr.
American Institute of Aeronautics and Astronautics, Fluid and Plasma Dynamics Conference, 7th, Palo Alto, Calif., June 17-19, 1974, 19 p, 43 refs
Paper 74-557

A74-31384
A Numerical Method for Solving the Navier-Stokes Equations (Ob odnom chislennom metode resheniia uravnenii Nav'e-Stoksa)
V.A. Gushchin and V.V. Shchennikov
Zhurnal Vychislitel'noi Matematiki i Matematicheskoi Fiziki, vol. 14, Mar.-Apr. 1974, p 512-520, 8 refs

A74-25312
Three-Dimensional Calculation of Compressible Fluids by the Finite Difference Method (Calcul Tridimensionnel de Fluides Compressibles par la Methode des Éléments finis)
J. Periaux
Association Aéronautique et Astronautique de France, Colloque d'Aérodynamique Appliquée, 10th, Université de Lille I, Lille, France, Nov. 7-9, 1973, Paper, 85 p, 14 refs

A74-24316
Numerical Solution of the Navier-Stokes Equations for Compressible Fluids(Résolution numérique des Équations de Navier-Stokes pour les Fluides Compressibles)
R. Peyret and H. Viviand
Institut de Recherche d'Informatique et d'Automatique, Colloque International sur les Méthodes de Calcul Scientifique et Technique, Paris, France, Dec. 17-21, 1973, 27 p, 56 refs
ONERA-TP-1319

A74-24001
Partial Implicitization
R.A. Graves, Jr.
Journal of Computational Physics, vol. 13, Nov. 1973, p 439-444, 8 refs

A74-23620
A Grid Method of Solving Problems of Viscous Incompressible Fluid Dynamics (Setochnyi metod resheniia zadach dinamiki viazkoi neszhimaemoi zhidkosti)
V. Ia. Rivkind
In: Boundary Value Problems of Mathematical Physics, 8, Leningrad, Izdatel'stvo Nauka, 1973, p 173-186, 16 refs

A74-23619
Certain Convergent Difference Schemes for the Navier-Stokes Equations (O nekotorykh skhodiashchikhsia raznostnykh skhemakh dlia uravnenii Nav'e-Stoksa)
A.P. Oskolkov
In: Boundary Value Problems of Mathematical Physics, 8, Leningrad, Izdatel'stvo Nauka, 1973, p 164-172, 5 refs

A74-23614
Boundary Value Problems of Mathematical Physics. 8 (Kraevye zadachi matematicheskoi fiziki. 8)
Matematicheskii Institut imeni V.A. Steklova, Trudy, Volume 125, 1973, 232 p

A74-23207
Calculations of Flow around a Semi-Infinite Flat Plate in a Shock Tube
T. Ishiguro
AIAA Journal, vol. 12, Mar. 1974, p 376-378, 5 refs

A74-22377
Numerical Method for Predicting Three-Dimensional Steady Flow in Ducts
W.R. Briley
Journal of Computational Physics, vol. 14, Jan. 1974, p 8-28, 15 refs

A74-22373
An Implicit Fourth Order Difference Method for Viscous Flows
J.R. Flood
Mathematics of Computation, vol. 28, Jan. 1974, p 27-32, 6 refs

A74-21098
Numerical Simulation of Viscous Incompressible Flows
S.A. Orszag and M. Israeli
In: Annual Review of Fluid Mechanics, Volume 6, Palo Alto, Calif., Annual Reviews, Inc., 1974, p 281-318, 163 refs

A74-18877
Three Dimensional Supersonic Flow Field Analysis of the B-1 Airplane by a Finite Difference Technique and Comparison with Experimental Data
L. D'Attorre, M.A. Bilyk and R.J. Sergeant
American Institute of Aeronautics and Astronautics, Aerospace Sciences Meeting, 12th, Washington, D.C., Jan. 30 - Feb. 1, 1974, 23 p, 10 refs
Paper 74-189

A74-18838
Analysis of Three-Dimensional Unsteady Flow around Oscillating Wings
T. Bratanow and A. Ecer
American Institute of Aeronautics and Astronautics, Aerospace Sciences Meeting, 12th, Washington, D.C., Jan. 30 - Feb. 1, 1974, 14 p, 19 refs
Paper 74-184

A74-18734
The Supersonic Flow about Ducted Bodies with Subsonic Internal Boundaries
P. Bansod
American Institute of Aeronautics and Astronautics, Aerospace Sciences Meeting, 12th, Washington, D.C., Jan. 30 - Feb. 1, 1974, 10 p, 19 refs
Paper 74-18

A74-18731
A Simple Finite-Difference Method for Solving the Three-Dimensional Turbulent Boundary-Layer Equations
T.K. Fannelop and D.A. Humphreys
American Institute of Aeronautics and Astronautics, Aerospace Sciences Meeting, 12th, Washington, D.C., Jan. 3o - Feb. 1, 1974, 13 p, 36 refs
Paper 74-13

A74-18730
Study of Flow past Blunted Thick Plates with Separation and Shoulder Singularity Using Navier-Stokes Equations
U. Ghia and R.T. Davis
American Institute of Aeronautics and Astronautics, Aerospace Sciences Meeting, 12th, Washington, D.C., Jan. 30 - Feb. 1, 1974, 11 p, 11 refs
Paper 74-12

A74-18349
Applicability of Difference Methods in Solving the Navier-Stokes Equation for Large Values of the Reynolds Number
B.L. Rozhdestvenskii
Soviet Physics - Doklady, vol. 18, Jan. 1974, p 473-475

A74-16975
Numerical Solution of the Unsteady Navier-Stokes Equations in Curvilinear Coordinates - The Hypersonic Blunt Body Merged Layer Problem
K.J. Victoria and G.F. Widhopf
In: International Conference on Numerical Methods in Fluid Mechanics, 3rd, Paris, France, July 3-7, 1972, Proceedings, Volume 2, 1973, p 254-267, 8 refs

A74-16965
Calculation of Separated Flows at Subsonic and Transonic Speeds
M. Klineberg and J.L. Steger
In: International Conference on Numerical Methods in Fluid Mechanics, 3rd, Paris, France, July 3-7, 1972, Proceedings, Volume 2, 1973, p 161-168, 7 refs

A74-16962
Computational Problems in Three und Four Dimensional Boundary Layer Theory
H.A. Dwyer and W.J. McCroskey
In: International Conference on Numerical Methods in Fluid Mechanics, 3rd, Paris, France, July 3-7, 1972, Proceedings, Volume 2, 1973, p 138-145, 11 refs

A74-16956
Numerical Solutions of the Supersonic, Laminar Flow over a Two-Dimensional Compression Corner
J.E. Carter
In: International Conference on Numerical Methods in Fluid Mechanics, 3rd, Paris, France, July 3-7, 1972, Proceedings, Volume 2, 1973, p 69-78, 11 refs

A74-16952
Numerical Approach for Investigating Some Transonic Flows
O.M. Belotserkovskii and Iu. M. Davidov
In: International Conference on Numerical Methods in Fluid Mechanics, 3rd, Paris, France, July 3-7, 1972, Proceedings, Volume 2, 1973, p 25-32, 12 refs

A74-16947
A Predictor-Corrector Method for Three Coordinate Viscous Flows
S.G. Rubin
In: International Conference on Numerical Methods in Fluid Mechanics, 3rd, Paris, France, July 3-7, 1972, Proceedings, Volume 1, 1973, p 146-153, 8 refs

A74-16946
Finite Difference Methods for the Steady-State Navier-Stokes Equations
P.J. Roache
In: International Conference on Numerical Methods in Fluid Mechanics, 3rd, Paris, France, July 3-7, 1972, Proceedings, Volume 1, 1973, p 138-145, 10 refs

A74-16944
Numerical Experiments with the Compressible Navier-Stokes Equations
C.W. Kitchens, Jr.
In: International Conference on Numerical Methods in Fluid Mechanics, 3rd, Paris, France, July 3-7, 1972, Proceedings, Volume 1, 1973, p 120-129, 12 refs

A74-16937
Review of Methods for Solving the Navier-Stokes Equations
A.A. Dorodnitsyn
In: International Conference on Numerical Methods in Fluid Mechanics, 3rd, Paris, France, July 3-7, 1972, Proceedings, Volume 1, 1973, p 1-11

A74-16936
International Conference on Numerical Methods in Fluid Mechanics, 3rd, Université de Paris, France, July 3-7, 1972, Proceedings. Volume 1 - General Lectures, Fundamental Numerical Techniques, 1973, 195 p. Volume 2 - Problems of Fluid Mechanics, 1973, 284 p
Edited by H. Cabannes and R. Temam, Berlin and New York, Springer-Verlag

A74-15827
Flow of a Newtonian Fluid through a Sudden Contraction
J.S. Vrentas and J.L. Duda
Applied Scientific Research, vol. 28, Nov. 1973, p 241-260, 26 refs

A74-13902
Numerical Solution of the Navier-Stokes Equation of a Compressible Gas within a Wide Range of Reynolds Numbers
A.I. Tolstykh
Soviet Physics - Doklady, vol. 18, Nov. 1973, p 279-281

A74-13272
Similarity Solutions for the Interaction of a Potential Vortex with Free Stream Sink Flow and a Stationary Surface
J.A. Hoffmann
American Society of Mechanical Engineers, Winter Annual Meeting, Detroit, Mich., Nov. 11-15, 1973, 6 p, 20 refs
Paper 73-WA/FE-2

A74-13093
Three-Dimensional Periodic Boundary Layers
D.Y. Kasture
Ingenieur-Archiv, vol. 42, no. 6, 1973, p 411-415, 8 refs

A74-11960
Numerical Integration of the Time-Dependent Equations of Motion for Taylor Vortex Flow
C.V. Alonso and E.O. Macagno
Computers and Fluids, vol. 1, Sept. 1973, p 301-315, 19 refs

A74-11665
Finite Element Applications in Mathematical Physics
J.T. Oden
In: The Mathematics of Finite Elements and Applications; Proceedings of the Conference, Uxbridge, Middx., England, April 18-20, 1972. London and New York, Academic Press, 1973, p 239-282, 31 refs

A74-11497
The Application of Difference Methods to the Calculation of Viscous Liquid and Gas Flows
L. Iu. Brailovskaia, T.V. Kuskova, B.M. Pavlov and L.A. Chudov
Heat Transfer - Soviet Research, vol. 5, Sept.-Oct. 1973, p 119-123, 14 refs

A74-11433
Finite Element Method for Transit Linear Viscous Flow Problems
C.H. Lee
University of Southampton, International Conference on Numerical Methods in Fluid Dynamics, Southampton, England, Sept. 26-28, 1973, Paper, 15 p, 5 refs

A73-44651
A Divergent Difference Scheme for Calculation of Steady Supersonic Flows with Complex Structures (Divergentnaia raznostnaia skhema dlia rascheta sverkhzvukovykh ustanovivshikhsia techenii slozhnoi struktury)
V.I. Kosarev and K.M. Magomedov
Zhurnal Vychislitel'noi Matematiki i Matematicheskoi Fiziki, vol. 13, July-Aug. 1973, p 923-937, 10 refs

A74-43588
Growth of Uncertainty in Decaying Isotropic Turbulence
J.R. Herring, J.J. Riley, G.S. Patterson, Jr. and R.H. Kraichnan
Journal of the Atmospheric Sciences, vol. 30, Sept. 1973, p 997-1006, 19 refs

A73-41686
Application of a General Finite-Difference Method to Boundary Layer Flows
S.D. Katotakis and J. Vlachopoulos
Canadian Society for Mechanical Engineering, Transactions, vol. 1, no. 3, 1972, p 146-152, 17 refs

A73-40248
Flow past an Impulsively Started Circular Cylinder
W.M. Collins and S.C.R. Dennis
Journal of Fluid Mechanics, vol. 60, Aug. 21, 1973, p 105-127, 32 refs

A73-39225
A Method for Calculating Three-Dimensional Turbulent Boundary Layer by Using Streamline Co-Ordinates
T. Hotta
Japanese Journal of Applied Physics, vol. 12, June 1973, p 908-915, 12 refs

A73-39093
Viscous Flow over a Cone at Moderate Incidence. II - Supersonic Boundary Layer
T.C. Ling and S.G. Rubin
Journal of Fluid Mechanics, vol. 59, July 17, 1973, p 593-620, 38 refs

A73-38971
Numerical Study of Viscous Flow in a Cavity
J.D. Bozeman and C. Dalton
Journal of Computational Physics, vol. 12, July 1973, p 348-363, 16 refs

A73-38349
The Investigation on the Secondary Flow Induced by Jets
I.S. Kikkawa and K. Noto
JSME, Bulletin, vol. 16, Apr. 1973, p 724-732, 5 refs

A73-37852
Numerical Investigation of Unsteady Boundary-Layer Separation
D.P. Telionis, D.T. Tsahalis and M.J. Werle
Physics of Fluids, Vol. 16, July 1973, p 968-973, 16 refs

A73-36245
Supersonic Turbulent Boundary-Layer Flows with Tangentail Slot Injection
E.W. Miner and C.H. Lewis
American Institute of Aeronautics and Astronautics, Fluid and Plasma Dynamics Conference, 6th, Palm Springs, Calif., July 16-18, 1973, 25 p, 31 refs
Paper 73-696

A73-36235
The Response of Unsteady Boundary-Layer Separation to Impulsive Changes of Outer Flow
D.P. Telionis and D.T. Tsahalis
American Institute of Aeronautics and Astronautics, Fluid and Plasma Dynamics Conference, 6th, Palm Springs, Calif., July 16-18, 1973, 10 p, 27 refs
Paper 73-684

A73-36158
Computation of Three Dimensional Flows about Aircraft Configurations
F. Marconi and M. Salas
Computers and Fluids, vol. 1, June 1973, p 185-195, 13 refs

A73-36157
On the Solution of the Unsteady Navier-Stokes Equations Including Multicomponent Finite Rate Chemistry
G.F. Widhopf and K.J. Victoria
Computers and Fluids, vol. 1, June 1973, p 159-184, 18 refs

A73-36156
Finite-Difference Solution of the Incompressible Three-Dimensional Boundary Layer Equations for a Blunt Body
F.G. Blottner and M.A. Ellis
Computers and Fluids, vol. 1, June 1973, p 133-158, 23 refs

A73-35144
A Now Shock Capturing Numerical Method with Applications to Some Simple Supersonic Flow Fields
F. Walkden, G.T. Laws and P. Caine
In: Computational Fluid Dynamics Conference, Palm Springs, Calif., July 19, 20, 1973, Proceedings, 1973, p 173-181, 9 refs

A73-35142
Discrete Fluid Dynamics from the Union of Continuum Mechanics and Kinetic Theory
E.E. Blondeau, Jr.
In: Computational Fluid Dynamics Conference, Palm Springs, Calif., July 19, 20, 1973, Proceedings, 1973, p 150-152

A73-35141
Linearized Implicit Schemes for the Computation of Viscous Incompressible Flow - with Applications
A.A. Ganz, M.I. Dill and J.L. Liutermoza
In: Computational Fluid Dynamics Conference, Palm Springs, Calif., July 19, 20, 1973, Proceedings, 1973, p 141-149, 11 refs

A73-35139
Numerical Solution of the Three-Dimensional Navier-Stokes Equations in Integro-Differential Form - Flow about a Finite Body
J.F. Thompson, Jr., S.P. Shanks and J.C. Wu
In: Computational Fluid Dynamics Conference, Palm Springs, Calif., July 19, 20, 1973, Proceedings, 1973, p 123-132, 5 refs

A73-35138
Computational Considerations in Application of the Finite Element Method for Analysis of Unsteady Flow around Airfoils
T. Bratanow and A. Ecer
In: Computational Fluid Dynamics Conference, Palm Springs, Calif., July 19, 20, 1973, Proceedings, 1973, p 109-122, 17 refs

A73-35136
Fourth Order "Mehrstellen"-Integration for Three-Dimensional Turbulent Boundary Layers
E. Krause, W. Kordulla and E.H. Hirschel
In: Computational Fluid Dynamics Conference, Palm Springs, Calif., July 19, 2o, 1973, Proceedings, 1973, p 92-102, 26 refs

A73-35129
Numerical Calculation of the Three Dimensional Transonic Flow over a Yawed Wing
A. Jameson
In: Computational Fluid Dynamics Conference, Palm Springs, Calif., July 19, 20, 1973, Proceedings, 1973, p 18-26, 10 refs

A73-35126
Computational Fluid Dynamics Conference, Palm Springs, Calif., July 19, 20, 1973, Proceedings
Conference sponsored by the American Institute of Aeronautics and Astronautics. New York, American Institute of Aeronautics and Astronautics, Inc., 1973, 193 p

A73-35016
A Finite Difference Solution of the Two and Three-Dimensional Incompressible Turbulent Boundary Layer Equations
W.F. Klinksiek and F.J. Pierce
American Society of Mechanical Engineers, Applied Mechanics and Fluids Engineering Conference, Atlanta, Ga., June 20-22, 1973, 14 p, 62 refs
Paper 73-FE-20

A73-34830
The Finite Element Method in Fluid Mechanics
J.T. Oden
In: Finite Element Methods in Continuum Mechanics; Advanced Study Institute, Lisbon, Portugal, September 7-17, 1971, Lectures, 1973, p 151-186, 30 refs

A73-34178
Mathematical Formulation of Viscous-Inviscid Interaction Problems in Supersonic Flow
G. Miller
AIAA Journal, vol. 11, July 1973, p 938-942, 13 refs

A73-33261
The Numerical Integration of the Navier-Stokes Equations for the Two-Dimensional Incompressible Flow along a Planar Plate (Numerische Integration der Navier-Stokes-Gleichungen für die zweidimensionale, inkompressible Strömung längs einer ebenen Platte)
H. Fasel
Zeitschrift für angewandte Mathematik und Mechanik, vol. 53, Apr. 1973, p T 236-T 238

A73-32929
Numerical Solution for the Flow of a Fluid in a Heated Closed Cavity
D.H. Schultz
Quarterly Journal of Mechanics and Applied Mathematics, vol. 26, May 1973, p 173-192, 31 refs

A73-32816
Three-Dimensional Calculations of Hypersustentation (Calculs Tridimensionnels d'Hypersustentation)
P. Perrier and J.J. Deviers
Colloque d'Aérodynamique Appliquée, 9th, Saint-Cyr-l'Ecole, Yvelines and Paris, France, Nov. 8-10, 1972, Paper, 82 p, 116 refs

A73-29758
Study of a New Family of Solutions of Navier-Stokes Equations (Etude d'Une Nouvelle Famille de Solutions des Équations de Navier-Stokes)
J.C. Guilloud, J. Arnault and C. Dicrescenzo
Journal de Mécanique, vol. 12, Mar. 1973, p 47-74, 9 refs

A73-28608
A Numerical Method for Highly Accelerated Laminar Boundary-Layer Flows
R.C. Ackerberg and J.H. Phillips
SIAM Journal on Numerical Analysis, vol. 10, Mar. 1973, p 147-160, 9 refs

A73-28090
On the Numerical Treatment of the Navier-Stokes Equations for an Incompressible Fluid
G. Marshall and E. van Spiegel
Journal of Engineering Mathematics, vol. 7, Apr. 1973, p 173-188, 11 refs

A73-25710
A Simple Model of Normal Shock Wave and Turbulent Boundary-Layer Interaction
E. Lumsdaine
ASME, Transactions, Series E - Journal of Applied Mechanics, vol. 40, Mar. 1973, p 294-296

A73-25213
Numerical Study of a Viscous Flow through a Pipe Orifice
D. Zampaglione and M. Greppi
Meccanica, vol. 7, Sept. 1972, p 151-164, 14 refs

A73-25116
A Numerical Solution of the Navier-Stokes Equations Using the Finite Element Technique
C. Taylor and P. Hood
Computers and Fluids, vol. 1, Jan. 1973, p 73-100, 44 refs

A73-25115
Viscous Flow past Circular Cylinders
F. Nieuwstadt and H.B. Keller
Computers and Fluids, vol. 1, Jan. 1973, p 59-71, 8 refs

A73-24834
On the Computation of Unsteady Turbulent Boundary Layers
T. Cebeci and H.B. Keller
In: Recent Research on Unsteady Boundary Layers; Symposium, Quebec, Canada, May 24-28, 1971, Proceedings, Volume 1. Quebec, Presses de l'Université Laval, 1972, p 1072-1105, 16 refs

A73-24810
On Unsteady Three-Dimensional Laminar Flow
I. Pop
In: Recent Research on Unsteady Boundary Layers; Symposium, Quebec, Canada, May 24-28, 1971, Proceedings, Volume 1. Quebec, Presses de l'Université Laval, 1972, p 302-322, 16 refs

A73-23766
Numerical Study of the Flow of a Viscous Incompressible Fluid around a Circular Cylinder (Etude Numérique de l'Écoulement d'un Fluide Visqueux Incompressible autour du Cylindre Circulaire)
T.P. Loc
Académie des Sciences (Paris), Comptes Rendus, Série A - Sciences Mathématiques, vol. 276, no. 7, Feb. 12, 1973, p 567-570, 10 refs

A73-21495
Flow in the Vicinity of a Trailing Edge (Ecoulement au Voisinage d'un Bord de Fuite)
J.-P. Guiraud
Académie des Sciences (Paris), Comptes Rendus, Série A - Sciences Mathématiques, vol. 276, no. 5, Jan. 29, 1973, p 399-401, 5 refs

A73-21008
Unsteady Boundary Layer Flows at General Three-Dimensional Stagnation Points
M. Katagiri
Physical Society of Japan, Journal, vol. 34, Jan. 1973, p 225-231, 8 refs

A73-20435
Spiral Flows in Finite Rotating Annular Tubes
T.-K. Hung
American Society of Civil Engineers, Engineering Mechanics Division, Journal, vol. 99, Feb. 1973, p 13-29, 14 refs

A73-19953
Analysis of Flow of Viscous Fluids by the Finite-Element Method
J.T. Oden and L.C. Wellford, Jr.
AIAA Journal, vol. 10, Dec. 1972, p 1590-1599, 24 refs

A73-19501
Numerical Solution of the Navier-Stokes Equations by the Finite Element Method
R.T.-S. Cheng
Physics of Fluids, vol. 15, Dec. 1972, p 2098-2105, 10 refs

A73-19263
On a Finite-Difference Approach to Turbulence Problems
F.M. Galloway and R.J. Adler
Journal of Computational Physics, vol. 10, Dec. 1972, p 379-399, 10 refs

A73-16964
Shock Wave-Boundary Layer Interactions in Laminar Transonic Flow
H.M. Brilliant and T.C. Adamson, Jr.
American Institute of Aeronautics and Astronautics, Aerospace Sciences Meeting, 11th, Washington, D.C., Jan. 10-12, 1973, 10 p, 15 refs
Paper 73-239

N73-16545
On the Numerical Solution of Two-Dimensional, Laminar Compressible Flows with Imbedded Shock Waves
W.D. Goodrich, J.P. Lamb and J.J. Bertin
ASME, Transactions, Series D - Journal of Basic Engineering, vol. 94, Dec. 1972, p 765-769; Discussion, p 769, 770; Authors' Closure, p 770, 25 refs

A73-16526
Numerical Solutions of the Navier-Stokes Equations in Inlet Regions
J.W. McDonald, V.E. Denny and A.F. Mills
ASME, Transactions, Series E - Journal of Applied Mechanics, vol. 39, Dec. 1972, p 873-878, 15 refs

A73-16449
Numerical Solution of a Boundary Value Problem for the Navier-Stokes Equations (O chislennom reshenii kraevoi zadachi dlia uravnenii Nav'e-Stoksa)
K.I. Babenko and N.D. Vvedenskaia
Zhurmal Vychislitel'noi Matematiki i Matematicheskoi Fiziki, vol. 12, Sept.-Oct. 1972, p 1343-1349, 10 refs

A73-15093
Calculation Methods of Three-Dimensional Boundary Layers with and without Rotation of the Walls
C. Quemard and J. Cousteix
EUROMECH, Colloque sur les Couches Limites Turbulentes Tridimensionnelles, Berlin, West Germay, Sept. 25-27, 1972, 13 p, 6 refs
ONERA-TP-1135

A73-15003
Two Numerical Methods for Three-Dimensional Boundary Layers
L.S. Caretto, R.M. Curr and D.B. Spalding
Computer Methods in Applied Mechanics and Engineering, vol. 1, June 1972, p 39-57, 12 refs

A73-11670
An Explicit Difference Method for Steady Supersonic Flow (Ein explizites Differenzverfahren für die stationäre Überschallströmung)
K. Förster
Deutsche Gesellschaft für Luft- und Raumfahrt, Jahrestagung, 5th, Berlin, West Germany, Oct. 4-6, 1972, 17 p, 18 refs
Paper 72-066

A72-45781
Explicit Numerical Solution of the Three-Dimensional Incompressible Turbulent Boundary-Layer Equations
J.L. East, Jr. and F.J. Pierce
AIAA Journal, vol. 10, Sept. 1972, p 1216-1223, 28 refs

A72-41639
The Understanding and Prediction of Turbulent Flow /Sixth Reynolds-Prandtl Lecture
P. Bradshaw
Aeronautical Journal, vol. 76, July 1972, p 403-418, 57 refs

A72-41162
Computation of Three-Dimensional Non-Equilibrium Supersonic Flows
P.I. Chuskin
International Council of the Aeronautical Sciences, Congress, 8th, Amsterdam, Netherlands, Aug. 28 - Sept. 2, 1972, 13 p, 13 refs
Paper 72-37

A72-35479
Transonic Viscous Flow around Lifting Two-Dimensional Airfoils
J. Erdos, P. Baronti and S. Elzweig
American Institute of Aeronautics and Astronautics, Fluid and Plasma Dynamics, Conference, 5th, Boston, Mass., June 26-28, 1972, 27 p, 10 refs
Paper 72-678

A72-34646
Solution of the Two-Dimensional, Unsteady, Compressible Navier-Stokes Equations Using a Second-Order Accurate Numerical Scheme
D.J. Palumbo and E.L. Rubin
Journal of Computational Physics, vol. 9, June 1972, p 466-495, 26 refs

A72-34063
Numerical Calculation of Transonic Flow about Swept Wings
W.F. Ballhaus and F.R. Bailey
American Institute of Aeronautics and Astronautics, Fluid and Plasma Dynamics Conference, 5th, Boston, Mass., June 26-28, 1972, 11 p, 13 refs
Paper 72-677

A72-34042
Numerical Computation of Multishocked, Three-Dimensional Supersonic Flow Fields with Real Gas Effects
P. Kutler, W.A. Reinhardt and R.F. Warming
American Institute of Aeronautics and Astronautics, Fluid and Plasma Dynamics Conference, 5th, Boston, Mass., June 26-28, 1972, 18 p, 23 refs
Paper 72-702

A72-34040
Three Dimensional Nozzle-Exhaust Flow Field Analysis by a Reference Plane Technique
S.M. Dash and P.D. del Guidice
American Institute of Aeronautics and Astronautics, Fluid and Plasma Dynamics Conference, 5th, Boston, Mass., June 26-28, 1972, 13 p, 7 refs
Paper 72-704

A72-31446
Difference Method for Solving the Equations of an Incompressible Viscous Fluid in Cylindrical Coordinates (Raznostnyi metod resheniia uravnenii viazkoi neszhimaemoi zhidkosti v tsilindricheskikh koordinatakh)
K.B. Dzhakupov
Izvestiia, Seriia Fiziko-Matematicheskaia, vol. 10, Jan.-Feb. 1972, p 31-40, 9 refs

A72-28422
A Numerical Method for Three-Dimensional Viscous Flow - Application to the Hypersonic Leading Edge
S.G. Rubin and T.C. Lin
Journal of Computational Physics, vol. 9, Apr. 1972, p 339-364, 17 refs

A72-27183
Two-Dimensional Vortex Motion and "Negative Temperatures"
D. Montgomery
Physics Letters, vol. 39A, Apr. 10, 1972, p 8, 7, 11 refs

A72-24291
Numerical Solution of the Navier-Stokes Equations for Symmetric Laminar Incompressible Flow past a Parabola
R.T. Davis
Journal of Fluid Mechanics, vol. 51, Feb. 8, 1972, p 417-433, 17 refs

A72-20355
Numerical Simulation of Turbulent Flows
D.G. Fox and D.K. Lilly
In: Summer Computer Simulation Conference, Boston, Mass., July 19-21, 1971, Proceedings, Volume 2. Denver Colo., Board of Simulation Conferences; Montvale, N.J., American Federation of Information Processing Societies, 1971, p 834-841, 31 refs

A72-20077
Review of the Studies on Navier-Stokes Equations at the Computing Center of Academy of Sciences USSR, Moscow
A.A. Dorodnitsyn, S.A. Lulka and N.A. Meller
In: Symposium on Advanced Problems and Methods in Fluid Mechanics, 10th, Rynia, Poland, September 6-11, 1971, Proceedings, Part 2. Warsaw, Państwowe Wydawnictwo Naukowe, 1972, p 131-133

A72-19170
A Numerical Method for Solving the Navier-Stokes Equations for the Two-Dimensional, Incompressible, Steady Flow past a Thin Plate (Eine numerische Methode zur Lösung der Navier-Stokesschen Gleichungen für die zweidimensionale, inkompressible, stationäre Strömung längs einer dünnen Platte)
S. Loer
Ingenieur-Archiv, vol. 41, no. 1, 1971, p 28-40, 11 refs

A72-18526
Numerical Solution of the Navier-Stokes Equations for Flows in the Disk-Cylinder System
H.P. Pao
Physics of Fluids, vol. 15, Jan. 1972, p 4-11, 18 refs

A72-18189
Flow and Heat Transfer in a Rotating Enclosure with Axial Throughflow
D.K. Hennecke, E.M. Sparrow and E.R.G. Eckert
Wärme- und Stoffübertragung, vol. 4, no. 4, 1971, p 222-235, 8 refs

A72-18132
On Convergent Finite Differences Schemes for Initial-Boundary Value Problems for Navier-Stokes Equations
O.A. Ladyzhenskaia
In: Symposium on Advanced Problems and Methods in Fluid Mechanics, 9th, Kazimierz, Poland, September 1-7, 1969, Transactions, Part 2. Warsaw, Państwowe Wydawnictwo Naukowe, 1971, p 125-134, 6 refs

A72-18112
Some Unsolved Analytical Problems in Fluid Dynamics
M.Z. Krzywoblocki
In: Symposium on Advanced Problems and Methods in Fluid Mechanics, 9th, Kazimierz, Poland, September 1-7, 1969, Transactions, Part 1. Warsaw, Państwowe Wydawnictwo Naukowe, 1971, p 145-176, 102 refs

A72-17006
The Stability of Unsteady Axisymmetric Incompressible Pipe Flow Close to a Piston. I - Numerical Analysis. II - Experimental Investigation and Comparison with Computation
M.D. Hughes and J.H. Gerrard
Journal of Fluid Mechanics, vol. 50, Dec. 29, 1971, p 625-655, 18 refs

A72-16901
Subsonic and Transonic Potential Flow over Helicopter Rotor Blades
F.X. Caradonna and M.P. Isom
American Institute of Aeronautics and Astronautics, Aerospace Sciences Meeting, 10th, San Diego, Calif., Jan. 17-19, 1972, 16 p
Paper 72-39

A72-16860
Calculation of Viscous Drag of Two-Dimensional and Axisymmetric Bodies in Incompressible Flows
T. Cebeci, G.J. Mosinskis and A.M. Smith
American Institute of Aeronautics and Astronautics, Aerospace Sciences Meeting, 10th, San Diego, Calif., Jan. 17-19, 1972, 11 p, 24 refs
Paper 72-1

A72-16847
A Complete Numerical Technique for the Calculation of Three-Dimensional Inviscid Supersonic Flows
G. Moretti, B. Grossman and F. Marconi, Jr.
American Institute of Aeronautics and Astronautics, Aerospace Sciences Meeting, 10th, San Diego, Calif., Jan. 17-19, 1972, 11 p, 17 refs
Paper 72-192

A72-16843
Relaxation Techniques for Three-Dimensional Transonic Flow about Wings
F.R. Bailey and J.L. Steger
American Institute of Aeronautics and Astronautics, Aerospace Sciences Meeting, 10th, San Diego, Calif., Jan. 17-19, 1972, 15 p, 17 refs
Paper 72-189

A72-16841
Finite-Difference Analysis of the Three-Dimensional Turbulent Boundary Layer on a Sharp Cone at Angle of Attack in a Supersonic Flow
J.C. Adams, Jr.
American Institute of Aeronautics and Astronautics, Aerospace Sciences Meeting, 10th, San Diego, Calif., Jan. 17-19, 1972, 17 p, 52 refs
Paper 72-186

A72-16820
Navier-Stokes Solutions for Laminar Incompressible Flow over Yawed Spinning Bodies of Revolution
B.L. Clark
American Institute of Aeronautics and Astronautics, Aerospace Sciences Meeting, 10th, San Diego, Calif., Jan. 17-19, 1972, 15 p, 22 refs
Paper 72-112

A72-16817
Finite Element Computational Theory for Three-Dimensional Boundary Layer Flow
A.J. Baker
American Institute of Aeronautics and Astronautics, Aerospace Sciences Meeting, 10th, San Diego, Calif., Jan. 17-19, 1972, 13 p, 19 refs
Paper 72-108

A72-16685
Numerical Simulation of Three-Dimensional Homogeneous Isotropic Turbulence
S.A. Orszag and G.S. Patterson, Jr.
Physical Review Letters, vol. 28, Jan. 10, 1972, p 76-79, 16 refs

A72-15644
Computer Simulation of a Viscous Channel Flow
M. Greppi and C. Cercignani
Meccanica, vol. 6, Sept. 1971, p 125-131, 16 refs

A72-15245
Calculation of Two-Dimensional Unsteady Boundary Layers with Allowance for Unstable Effects (Zur Berechnung zweidimensionaler, instationärer Grenzschichten unter Einschluß von instabilen Vorgängen)
S. Loer
Dissertation, Universität Stuttgart, 1970, 114 p, 9 refs

A72-11587
Application of the Differential Equation for Turbulent Viscosity to the Analysis of Plane Nonself-Similar Flows (Primenenie differentsial'nogo uravneniia dlia turbulentnoi viazkosti k analizu ploskikh neavtomodel'nykh techenii)
A.N. Sekundov
Akademiia Nauk SSSR, Izvestiia, Mekhanika Zhidkosti i Gaza, Sept.-Oct. 1971, p 114-127
33 refs

A72-11395
The Three-Dimensional Turbulent Boundary Layer on an Infinite Yawed Wing
J.F. Nash and R.R. Tseng
Aeronautical Quarterly, vol. 22, 1971, p 346-362, 10 refs

A72-10226
A Numerical Fluid Dynamics Calculation Method for all Flow Speeds
F.H. Harlow and A.A. Amsden
Journal of Computational Physics, vol. 8, Oct. 1971, p 197-213, 6 refs

A71-44617
Generalized Finite-Element Method for Compressible Viscous Flow
Wen-Hwa Chu
AIAA-Journal, vol. 9, Nov. 1971, p 2275-2276

A71-37089
Supersonic Viscous Gas Flow past Blunt Bodies (Sverkhzvukovoe obtekanie zatuplennykh tel viazkim gazom)
I.M. Breev
PMTF - Zhurmal Prikladnoi Mekhaniki i Tekhnicheskoi Fiziki, May-June 1971, p 134-136, 9 refs

A71-36325
Solution of the Transonic Potential Equation Using a Mixed Finite Difference System
E.M. Murman and J.A. Krupp
In: International Conference on Numerical Methods in Fluid Dynamics, 2nd, University of California, Berkeley, Calif., September 15-19, 1970, Proceedings.
Edited by Maurice Holt. Berlin and New York, Springer-Verlag, Lecture Notes in Physics. Volume 8, 1971, p 199-206, 11 refs

A71-36323
Time-Dependent Calculation Method for Transonic Nozzle Flows
Pierre Laval
In: International Conference on Numerical Methods in Fluid Dynamics, 2nd, University of California, Berkeley, Calif., September 15-19, 1970, Proceedings.
Edited by Maurice Holt. Berlin and New York, Springer-Verlag, Lecture Notes in Physics, Volume 8, 1971, p 187-192, 15 refs

A71-36313
Accurate Numerical Methods for Boundary Layer Flows. I - Two-Dimensional Laminar Flows
Herbert B. Keller and Tuncer Cebeci
In: International Conference on Numerical Methods in Fluid Dynamics, 2nd, University of California, Berkeley, Calif., September 15-19, 1970, Proceedings.
Edited by Maurice Holt. Berlin and New York, Springer-Verlag, Lecture Notes in Physics, Volume 8, 1971, p 92-100, 8 refs

A71-34165
A Numerical Study of Laminar Separation Bubbles Using the Navier-Stokes Equations
W. Roger Briley
Journal of Fluid Mechanics, vol. 47, June 29, 1971, p 713-736, 12 refs

A71-33098
Numerical Solution for the Analysis of Unsteady Viscous Flow around an Oscillating Cylinder
Atsushi Okajima
In: Recent Advances in Matrix Methods of Structural Analysis and Design; U.S. National Science Foundation and Japan Society for the Promotion of Science, Seminar, Tokyo, Japan, August 25-30, 1969, Proceedings.
Edited by R.N. Gallagher, Y. Yamada and J.T. Oden. University, University of Alabama Press, 1971, p 809-834; Discussion, p 834, 835, 7 refs

A71-32996
Unstable Flows in Two Dimensions - Comparison of Laboratory Experiments with Numerical Simulation
N.J. Zabusky and G.S. Deem
In: Instability of Continuous Systems; International Union of Theoretical and Applied Mechanics, Symposium, Herrenalb, West Germany, September 8-12, 1969, Proceedings.
Edited by Horst Leipholz. Berlin, Springer-Verlag, 1971, p 151-157

A71-31542
Finite Element Analysis of General Fluid Flow Problems
Wallace W. Bowley and Julian F. Prince
American Institute of Aeronautics and Astronautics, Fluid and Plasma Dynamics Conference, 4th, Palo Alto, Calif., June 21-23, 1971, 12 p, 19 refs
Paper 71-602

A71-30409
Dynamical Evolution of Two-Dimensional Unstable Shear Flows
N.J. Zabusky and G.S. Deem
Journal of Fluid Mechanics, vol. 47, May 31, 1971, p 353-379, 22 refs

A71-29280
An Extended Numerical Method of Calculating Two-Dimensional or Axisymmetric Heated Flows Allowing for Dissipation
E.G. Broadbent
Ingenieur-Archiv, vol. 40, no. 2, 1971, p 81-95

A71-28982
A Numerical Solution for Natural Convection in Cylindrical Annuli
R.E. Powe, C.T. Carley and S.L. Carruth
ASME, Transactions, Series C - Journal of Heat Transfer, vol. 93, May 1971, p 210-220, 15 refs

A71-18554
A Systematic Development of the Supersonic Flow Fields over and behind Wings and Wing-Body Configurations Using a Shock-Capturing Finite-Difference Approach
Paul Kutler and Harvard Lomax
American Institute of Aeronautics and Astronautics, Aerospace Sciences Meeting, 9th, New York, N.Y., Jan. 25-27, 1971, 12 p, 27 refs
Paper 71-99

A71-18553
Application of the Method of Integral Relations to Transonic Airfoil Problems
Tsze C. Tai
American Institute of Aeronautics and Astronautics, Aerospace Sciences Meeting, 9th, New York, N.Y., Jan. 25-27, 1971, 9 p, 13 refs
Paper 71-98

A71-17564
Numerical Solution of Incompressible Flow Problems
Alexandre Joel Chorin
In: Numerical Solutions of Nonlinear Problems; Society for Industrial and Applied Mathematics, Symposium, Philadelphia, Pa., October 21-23, 1968, Proceedings. Edited by J.M. Ortega and W.C. Rheinboldt, Philadelphia, Society for Industrial and Applied Mathematics (Studies in Numerical Analysis, No. 2) 1970, p 64-71, 14 refs

A71-17552
Conservation Properties of Convection Difference Schemes
Steve A. Piacsek and Gareth P. Williams
Journal of Computational Physics, vol. 6, Dec. 1970, p 392-405, 12 refs

A71-15551
A Network Method of Solving the Navier-Stokes Equations in Cylindrical Coordinates (Setochnyi metod resheniia uravnenii Nav'e-Stokas v tsilindricheskikh koordinatakh)
K.P. Ivanov, O.A. Ladyzhenskaia and V.Ia. Rivkind
Vestnik, Matematika, Mekhanika, Astronomiia, vol. 25, July 1970, p 37-41, 6 refs

A71-14175
A Method for the Numerical Solution of the Navier-Stokes Equations (Une Méthode de Résolution Numérique des Équations de Navier-Stokes)
P. Jamet, P. Lascaux and P.-A. Raviart
Numerische Mathematik, vol. 16, no. 2, 1970, p 93-114, 14 refs

A71-14127
A Numerical Study of the Flow in the Vortex Angular-Rate Sensor
Charles Gilbert Richards
American Society of Mechanical Engineers, Winter Annual Meeting, New York, N.Y., Nov. 29 - Dec. 3, 1970, 11 p, 10 refs
Paper 70-WA/FE-5

A71-13426
Numerical Integration of Navier-Stokes Equations
S.I. Cheng
AIAA Journal, vol. 8, Dec. 1970, p 2115-2122, 32 refs

A71-11160
Transonic Flows past a Circular Cylinder
Czeslaw P. Kentzer
Journal of Computational Physics, vol. 6, Oct. 1970, p 168-182, 6 refs

A70-40611
Calculation of Transonic Flows past Bodies of Revolution (O raschete obtekaniia tel vrashcheniia transzvukovym potokom)
Iu. M. Lipnitskii and Iu. B. Lifshits
Prikladnaia Matematika i Mekhanika, vol. 34, May-June 1970, p 508-513, 5 refs

A70-26849
Stability Analysis of a Difference Scheme for the Navier-Stokes Equations
N.G. Campbell
Numerische Mathematik, vol. 14, no. 5, 1970, p 435-447

A70-24106
Stability of Finite Difference Methods for Time Dependent Navier-Stokes Equations
Cz. P. Kentzer
In: Polska Akademia Nauk, Instytut Podstawowych Problemów Techniki, Symposium on Advanced Problems and Methods in Fluid Dynamics, 8th, Tarda, Poland, September 18-25, 1967, Proceedings. Edited by W. Fiszdon, P. Kucharczyk and W.J. Prosnak, Warsaw, Państwowe Wydawnictwo Naukowe (Fluid Dynamics Transactions, Volume 4), 1969, p 45-51, 7 refs

A70-23176
Numerical Solutions of the Compressible Navier-Stokes Equations for the Laminar near Wake
J.S. Allen and S.I. Cheng
Physics of Fluids, vol. 13, Jan. 1970, p 37-52, 25 refs

A70-18349
On the Hypersonic Leading-Edge Problem in the Merged-Layer Regime
H.K. Cheng, S.Y. Chen, R. Mobly and C. Huber
In: Rarefied Gas Dynamics; Proceedings of the Sixth International Symposium, Massachusetts Institute of Technology, Cambridge, Mass., July 22-26, 1968, Volume 1
Edited by Leon Trilling and H.Y. Wachman, New York, Academic Press, Inc. (Advances in Applied Mechanics, Supplement 5), 1969, p 451-463, 21 refs

A70-18170
A Time-Dependent Approach to Fluid Mechanical Phenomenology
E. Eugene Callens, Jr.
American Institute of Aeronautics and Astronautics, Aerospace Sciences Meeting, 8th, New York, N.Y., Jan. 19-21, 1970, 10 p, 16 refs
Paper 70-46

A70-18113
Numerical Integration of Navier-Stokes Equations
S.I. Cheng
American Institute of Aeronautics and Astronautics, Aerospace Sciences Meeting, 8th, New York, N.Y., Jan. 19-21, 1970, 15 p, 53 refs
Paper 70-2

A70-14606
Numerical Calculation of the Supersonic Flow of a Viscous Perfect Gas past a Sphere (Chislennyi raschet sverkhzvukovogo obtekaniia sfery potokom viazkogo sovershennogo gaza)
V.K. Molodtsov
Zhurnal Vychislitel'noi Matematiki i Matematicheskoi Fiziki, vol. 9, Sept.-Oct. 1969, p 1211-1217, 6 refs

A70-12376
Role and Performance of Computers in the Numerical Integration of the Navier-Stokes Equations (Le Role et les Performances des Calculateurs dans l'Integration Numerique des Equations Navier-Stokes)
D. Dumitrescu, M.D. Cazacu, G. Martin and H. Oprica
Bulletin Mathématique, vol. 12, no. 3, 1968, p 17-25

A70-11909
Viscous Fluid Flow along a Flat Plate at Low Reynolds Numbers (Miscarea fluidului viscous in lungul unei placi plane la numere Reynolds mici)
D. Dumitrescu and C.I. Craciun
Studii si Cercetari de Mecanica Aplicata, vol. 28, no. 3, 1969, p 497-506, 7 refs

REPORT DOCUMENTATION PAGE			
1. Recipient's Reference	2. Originator's Reference AGARD-LS-73	3. Further Reference	4. Security Classification of Document UNCLASSIFIED
5. Originator	Advisory Group for Aerospace Research and Development North Atlantic Treaty Organization 7 rue Ancelle, 92200 Neuilly sur Seine, France		
6. Title	Computational Methods for Inviscid and Viscous Two-and-Three-Dimensional Flow Fields		
7. Presented at	The von Kármán Institute, Brussels, Belgium.		
8. Author(s) Various			9. Date February 1975
10. Author's Address Various			11. Pages 204
12. Distribution Statement	This document is distributed in accordance with AGARD policies and regulations, which are outlined on the Outside Back Covers of all AGARD publications.		
13. Keywords/Descriptors			14. UDC
Navier-Stokes equations Mathematical models Finite difference theory	Fluid flow Turbulence Viscous flow	Inviscid flow Boundary layer Computation	532.516:532.526.4

15. Abstract

The material in this book has been assembled to support a Lecture Series presented by the authors at the von Kármán Institute, Brussels, 17–22 February 1975.

This Lecture Series, sponsored by the Fluid Dynamics Panel and the von Kármán Institute, presents the recent developments in the numerical approach of fluid flow problems. Particular emphasis will be placed on numerical techniques for the solution of the compressible Navier-Stokes equations and the implementation of turbulence models, the computational techniques for boundary layers, hyperbolic partial differential equations, numerical stability of finite difference methods, numerical solutions of the Navier-Stokes equations for compressible fluids, and finite elements.

U168841

DISTRIBUTION OF UNCLASSIFIED AGARD PUBLICATIONS

NOTE: Initial distributions of AGARD unclassified publications are made to NATO Member Nations through the following National Distribution Centres. Further copies are sometimes available from these Centres, but if not may be purchased in Microfiche or photocopy form from the Purchase Agencies listed below. THE UNITED STATES NATIONAL DISTRIBUTION CENTRE (NASA) DOES NOT HOLD STOCKS OF AGARD PUBLICATIONS, AND APPLICATIONS FOR FURTHER COPIES SHOULD BE MADE DIRECT TO THE APPROPRIATE PURCHASE AGENCY (NTIS).

NATIONAL DISTRIBUTION CENTRES

BELGIUM
Coordonnateur AGARD – VSL
Etat-Major de la Force Aérienne
Caserne Prince Baudouin
Place Dailly, 1030 Bruxelles

CANADA
Defence Scientific Information Service
Department of National Defence
Ottawa, Ontario K1A OZ3

DENMARK
Danish Defence Research E
Østerbrogades Kaserne
Copenhagen Ø

FRANCE
O.N.E.R.A. (Direction)
29, Avenue de la Division
92, Châtillon sous Bagneu

GERMANY
Zentralstelle für Luftfahrt
und Information
8 München 86
Postfach 860881

GREECE
Hellenic Armed Forces C
D Branch, Athens

ICELAND
Director of Aviation
c/o Flugrad
Reykjavik

ITALY
Aeronautica Militare
Ufficio del Delegato Nazionale all'AGARD
3, Piazzale Adenauer
Roma/EUR

LUXEMBOURG
See Belgium

NETHERLANDS

National Aeronautics and Space Administration
WASHINGTON, D. C. 20546

OFFICIAL BUSINESS
Penalty For Private Use, $300.00

POSTAGE AND FEES PAID
NATIONAL AERONAUTICS AND
SPACE ADMINISTRATION
NASA-451

SPECIAL FOURTH CLASS MAIL
BOOK

872 001 C4 B 04 750822 S02276DS
DEPT OF THE NAVY
NAVAL POSTGRADUATE SCHOOL
ATTN: LIBRARY CODE 2124
MONTEREY CA 93940

St. Mary Cray
Orpington, Kent BR5 3RE

UNITED STATES
National Aeronautics and Space Administration (NASA)
Langley Field, Virginia 23365
Attn: Report Distribution and Storage Unit
(See Note above)

PURCHASE AGENCIES

Microfiche or Photocopy
National Technical
Information Service (NTIS)
5285 Port Royal Road
Springfield
Virginia 22151, USA

Microfiche
ESRO/ELDO Space
Documentation Service
European Space
Research Organization
114, Avenue Charles de Gaulle
92200 Neuilly sur Seine, France

Microfiche
Technology Reports
Centre (DTI)
Station Square House
St. Mary Cray
Orpington, Kent BR5 3RF
England

Requests for microfiche or photocopies of AGARD documents should include the AGARD serial number, title, author or editor, and publication date. Requests to NTIS should include the NASA accession report number.

* * *

Full bibliographical references and abstracts of AGARD publications are given in the following bi-monthly abstract journals:

Scientific and Technical Aerospace Reports (STAR),
published by NASA,
Scientific and Technical Information Facility
P.O. Box 33, College Park
Maryland 20740, USA

Government Reports Announcements (GRA),
published by the National Technical
Information Services, Springfield
Virginia 22151, USA

Printed by Technical Editing and Reproduction Ltd
Harford House, 7-9 Charlotte St, London. W1P 1HD